AD-A167 044 LITTORAL ZONE SEDIMENTS SAN DIEGO REGION OCTOBER 1983-JUNE 1984(U) UNIVERSITY OF SOUTHERN CALIFORNIA LOS ANGELES DEPT OF GEOLOGICAL SCIENCES DEC 85 1/2

UNCLASSIFIED USC-GEOL-CCSTWS-85-11 F/G 8/3 NL

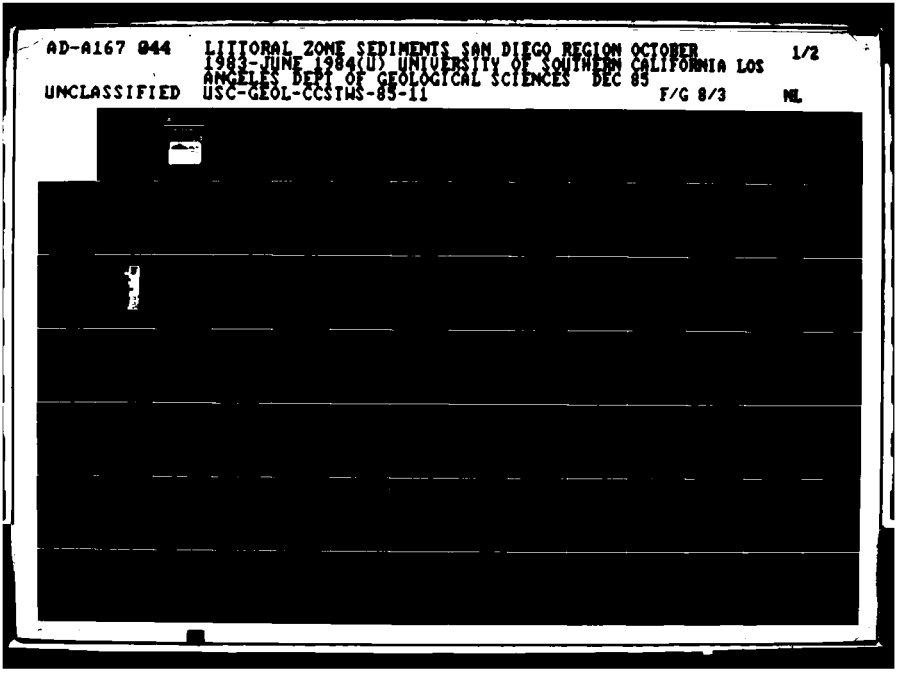

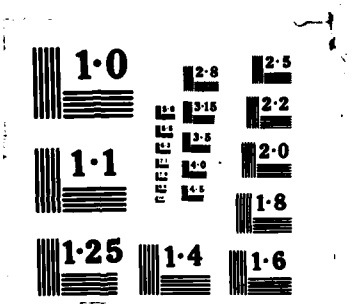
1·0
1·1
1·25
1·4
1·6
1·8
2·0
2·2
2·5
2·8
3·15

US Army Corps of Engineers
Los Angeles District

COAST OF CALIFORNIA
STORM AND TIDAL WAVES STUDY

LITTORAL ZONE SEDIMENTS
SAN DIEGO REGION
OCT 83 - JUN 84

REPORT DOCUMENTATION PAGE		READ INSTRUCTIONS BEFORE COMPLETING FORM
1. REPORT NUMBER CCSTWS 85-11	2. GOVT ACCESSION NO. AD A167044	3. RECIPIENT'S CATALOG NUMBER
4. TITLE (and Subtitle) LITTORAL ZONE SEDIMENTS SAN DIEGO REGION OCT 83-JUN 84		5. TYPE OF REPORT & PERIOD COVERED INTERIM DATA REPORT OCT 83- JUN 84 6. PERFORMING ORG. REPORT NUMBER
7. AUTHOR(s) UNIVERSITY OF SOUTHERN CALIFORNIA DEPARTMENT OF GEOLOGICAL SCIENCES		8. CONTRACT OR GRANT NUMBER(s)
9. PERFORMING ORGANIZATION NAME AND ADDRESS DEPARTMENT OF GEOLOGICAL SCIENCES UNIVERSITY OF SOUTHERN CALIFORNIA LOS ANGELES, CA.		10. PROGRAM ELEMENT, PROJECT, TASK AREA & WORK UNIT NUMBERS
11. CONTROLLING OFFICE NAME AND ADDRESS US ARMY CORPS OF ENGINEERS/LA DISTRICT P.O. BOX 2711/ ATTN: SPLPD-C L.A., CA. 90053-2325		12. REPORT DATE DECEMBER 1985 13. NUMBER OF PAGES 145
14. MONITORING AGENCY NAME & ADDRESS(if different from Controlling Office)		15. SECURITY CLASS. (of this report) UNCLASSIFIED 15a. DECLASSIFICATION/DOWNGRADING SCHEDULE

16. DISTRIBUTION STATEMENT (of this Report)

APPROVED FOR PUBLIC RELEASE; DISTRIBUTION UNLIMITED

17. DISTRIBUTION STATEMENT (of the abstract entered in Block 20, if different from Report)

18. SUPPLEMENTARY NOTES

COPIES ALSO OBTAINABLE FROM THE NATIONAL TECHNICAL INFORMATION SERVICE, SPRINGFIELD, VA. 22151

19. KEY WORDS (Continue on reverse side if necessary and identify by block number)

COASTAL PROCESSES, COAST OF CALIFORNIA STORM AND TIDAL WAVES STUDY, LITTORAL ZONE SEDIMENTS, SAN DIEGO REGION

20. ABSTRACT (Continue on reverse side if necessary and identify by block number)

THIS TECHNICAL REPORT INCLUDES THE REDUCTION AND INTERPRETATION OF MINERALOGIC AND GRAIN-SIZE DATA COLLECTED IN CONJUNCTION WITH TASK 1D, SEDIMENT SAMPLING, COAST OF CALIFORNIA STORM AND TIDAL WAVES STUDY. THE SAMPLES WERE COLLECTED BY PERSONNEL FROM SCRIPPS INSTITUTE OF OCEANOGRAPHY (SIO) AT RANGE LINE LOCATIONS SELECTED BY SIO AND THE LOS ANGELES DISTRICT, U.S. ARMY CORPS OF ENGINEERS. THE DATA ON WHICH THIS REPORT IS BASED IS FROM THE TASK'S SECOND SAMPLE SET; WHICH INCLUDES A LATE SUMMER SUBSET COLLECTED

DD FORM 1 JAN 73 1473 EDITION OF 1 NOV 65 IS OBSOLETE

SECURITY CLASSIFICATION OF THIS PAGE (When Data Entered)

FROM 10/83 INTO 1/84, AND A WINTER SUBSET COLLECTED FROM 2/84 TO 5/84. MINERALOGIC AND GRAIN-SIZE DATA WERE SUPPLIED TO THE SEDIMENTARY PETROLOGY LABORATORY (SPL) AT THE UNIVERSITY OF SOUTHERN CALIFORNIA (USC) BY PERSONNEL FROM THE SOUTH PACIFIC DIVISION (SPD) LABORATORY AND THE LOS ANGELES DISTRICT OF THE US ARMY CORPS OF ENGINEERS. THESE DATA WERE ENTERED INTO A DIGITAL DATA BASE, WHICH IS COMPATIBLE WITH A DIGITAL EQUIPMENT CORPORTATION VAX-11/780 COMPUTING SYSTEM. ALL DATA SUPPLIED TO THE SPL WERE PROCESSED ON THIS COMPUTING SYSTEM.

12

LITTORAL ZONE SEDIMENTS
SAN DIEGO REGION, DANA POINT TO MEXICAN BORDER
(October 1983 - June 1984)
Ref. No. CCSTWS 85-11

Coast of California Storm and Tidal Waves Study

Interim Data Report

U.S. Army Corps of Engineers
Los Angeles District, Planning Division
Coastal Resources Branch
P.O. Box 2711
Los Angeles, California 90053

DECEMBER 1985

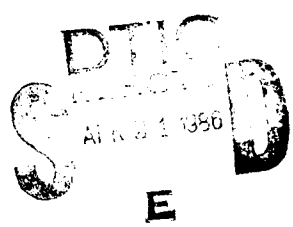

prepared by

University of Southern California
Department of Geological Sciences
Los Angeles, California

SYLLABUS

This technical report includes the reduction and interpretation of mineralogic and grain-size data collected in conjunction with Task 1D, Sediment Sampling, Coast of California Storm and Tidal Wave Study. The samples were collected by personnel from Scripps Institute of Oceanography (SIO) at range line locations selected by SIO and the Los Angeles District, U.S. Army Corps of Engineers. The data on which this report is based is from the Task's second sample set which includes a late-summer subset collected from October 1983 into January 1984, and a winter subset collected from February to June 1984. Mineralogic and grain-size data were supplied to the Sedimentary Petrology Laboratory ~~(SPL)~~ at the University of Southern California (USC) by personnel from the SPD Laboratory and the Los Angeles District of the U.S. Army Corps of Engineers. These data were entered into a Digital Data Base, which is compatible with a Digital Equipment Corporation VAX-11/780 Computing System. All data supplied to the SPL were processed on this computing system.

CONTENTS

FIGURES

TABLES

APPENDICES

1. INTRODUCTION

Objectives

1.01 This report has two major objectives, which will serve to better define sediment source areas, sand transport paths and transport mechanisms in the littoral zone extending from Dana Point to the United States-Mexico border. The first objective is to use available mineralogic data to define littoral segments along this portion of the southern California coast. The second is to examine grain-size fining-trends (1) to define the most likely transport direction within each littoral segment (or part thereof) during the sampling period, and (2) to better document the complexity of littoral transport paths as a function of elevation (bathymetry). Recommendations for future work concerning sand sources and transport paths are provided.

Purpose and Scope

1.02 The purpose of the Coast of California Storm and Tidal Waves Study is to collect, reduce and interpret oceanographic, meteorologic, hydrologic, geologic and sedimentologic information. Task 1D includes the collection, analysis and interpretation of sedimentologic data from the littoral zone. Results of Task 1D will be integrated with Task 1F, River Sediment Discharge Study, and Task 1G, Bluff Sediment Study to locate ultimate and local source areas and to determine the volumetric contribution of each potential source area to each beach segment.

Authority

1.03 This storm and tidal wave study is being undertaken pursuant to Section 208, of the Flood Control Act of 1965, Public Law 89-298.

Report Preparation

1.04 This report was prepared by Dr. Robert Osborne, Department of Geological Sciences, University of Southern California. The Research Assistants were E. Bomer, T. Fogarty, K. Kronenfeld Beratan and C. Sheehan.

1.4 The study was initially funded by the House Appropriation Committee in its Report No. 97-177, 97th Congress, 1st Session (page 23). The Corps of Engineers has been directed to concentrate on the Dana Point to Mexican border segment of the study (House Report No. 97-177, page 23).

Prior Reports

1.05 The following are related reports prepared by the Los Angeles District which contain significant data on littoral zone sediments.

Title	Date
Beach Erosion Control Report on Cooperative Study of San Diego County, California, Appendix, Phase 2.	March, 1960
Beach Erosion Control Report Cooperative Research and Data Collection Program of Southern California, Cape San Martin to Mexican Boundary. Three Year Report 1964-1966.	March, 1969
Three Year Report, 1967-1969 Cooperative Research and Data Collection Program, Coast of California.	December, 1970
Geomorphic Framework Report, Dana Point to the Mexican Border, Coast of California Storm and Tidal Waves Study.	September, 1984
Sediment Sampling, Dana Point to the Mexican Border (Task 1D, Nov-83 to Jan-84) CCSTWS 84-5.	November, 1984

Methods

1.06 The mineralogical data supplied was divided into two sets. The first set reflected the total light and heavy mineral composition of each sample, and contained quartz, potassium feldspar, plagioclase feldspar, and the total heavy mineral suite. The second set contained only the heavy mineral fraction of each sample, and included the following minerals: biotite, opaque minerals, pyroxene (other than augite), augite, hornblende, garnet, zircon, sphene, rutile, piedmontite, clinozoisite-epidote, actinolite-tremolite, glaucophane, and glaucophane schist (a rock fragment). Each of these data sets was recast to sum to 100 percent. The following minerals were deleted prior to recasting, because of their infrequent occurrence and small concentrations in the obtained samples: andalusite, apatite, beryl, corundum, muscovite, olivine, sillimanite, topaz, tourmaline, wollastonite, and the category "doubtful determination".

1.07 Grain-size data supplied by the Army Corps of Engineers representing the weight percent of sediment passing through a given sieve was recomputed to the weight percent of sediment retained on a given sieve. The conventional moment measures (mean, standard deviation, skewness and kurtosis) were computed using the phi scale.

1.08 The reader is referred to the First Year-End Report for Task 1D, Sediment Sampling, CCSTWS for the location of range lines employed in this report.

2. GENERAL SEDIMENTOLOGIC CONSIDERATIONS

2.01 Emery (1960) and Inman and Chamberlain (1960) identified a series of littoral cells along the southern California coast. These cells are based on the concept of longshore transport of dominantly fluvially-derived sediment, which is entrapped either by submarine canyon heads or by points of land which extend seaward from the general position of the coastline. Three major coastal divisions are present in this study area. The Oceanside Littoral Cell extends from Dana Point to Point La Jolla, and this cell may be further subdivided by Carlsbad Submarine Canyon. The second division is the coastal lowland in the Pacific and Mission Beach area, which occurs on the former delta of the San Diego River. Alluvium from the San Diego River extends almost to Crystal Pier at Pacific Beach, where it changes to a natural barrier (spit) extending across most of Mission Bay. The jetties constructed at the mouth of Mission Bay have interrupted the transport of sand from Mission Beach to Ocean Beach (Kuhn and Shepard, 1984), therefore, Ocean Beach is treated as a pocket beach in the present study. The coastal segment from the entrance to San Diego Bay to the United States-Mexico border comprises the Silver Strand Littoral Cell.

2.02 Assuming temperate drought conditions, which are temporally dominant in historic records for southern California (Inman, 1981), winter waves generally have a net energy flux component to the south due to their generation by northern Pacific storms passing close to southern California, whereas summer waves often show a net energy flux to the north due to their generation from more distant storms, either southwest of Acapulco or from Antarctica. As such, littoral sediment transport is commonly bidirectional in the short term, and many palimpsest grain-size fining-trends occur at different elevations in the littoral zone. Palimpsest trends do not reflect conditions present during

the sampling period, but may be subject to reworking under different hydraulic conditions. From a longer-term perspective, net longshore sediment transport appears to be south for the Oceanside Littoral Cell and the Mission Bay area, and north for the Silver Strand Littoral Cell. Inasmuch as comparatively small sediment volumes may produce observable longshore transport features such as spits and fillets, considerable effort must be expended to quantitatively evaluate the magnitude of the longshore vectorial component with respect to the onshore-offshore (shore-normal) vectorial component by means of slope array SXY guages, beach profiles, and studies of sediment sources and transport paths.

2.03 Although wave statistics and associated nearshore current measurements are most useful in documenting relatively short-term longshore transport directions, net transport direction and magnitude over significantly longer periods (hundreds to perhaps thousands of years) may be approached using geomorphologic and sedimentologic data. The following lines of geologic evidence have proven useful in defining the net transport direction, particularly where there is a point source for the entrained sediment and relatively high mechanical-energy conditions prevail within each littoral segment: (1) a reduction of mean grain size in the direction of transport, (2) a reduction in the volume of petrologic or shape-distinctive sediment in the direction of transport, (3) a decrease in the abundance of heavy minerals in the direction of transport, (4) a reduction of the prominence of sea cliffs in the direction of transport, (5) an increase in beach width in the direction of transport, (6) stream mouth diversion in the direction of transport, (7) spit elongation in the direction of transport, and (8) sand buildups (fillets) on the upcurrent sides of groins and jetties. One might also consider the asymmetry of petrologic-and/or shape-distinctive light-and/or heavy-mineral

assemblages adjacent to known point sources, because the areal extent of each such assemblage should be greater in the net transport direction.

2.04 At present, the interpretation of petrologic and grain-size trends is confounded by two major factors. Additional samples are needed adjacent to suspected point sources, namely stream mouths and beach nourishment projects, to document their importance and to determine the net transport direction associated with each such point source. These addition samples are necessary, because the present samples were collected too far from these points sources to make the evaluations required. Secondly, there is a paucity of information concerning potential lithologic and grain-size trends present in the sedimentary strata in areas with contributing sea cliffs (Osborne and Pipkin, 1983). For example, Osborne and others (1985) have documented that there is a strong correlation ($r^2 = 0.81$, where r is the multiple correlation coefficient) between longshore fining trends observed in cliff-backshore and corresponding foreshore samples within the five littoral segments at Lake Tahoe which show the most persistent grain-size fining trends. The value for the multiple correlation coefficient would be even higher if the fines washed from the foreshore samples were considered in the calculations. This correlation suggests that the observed longshore fining trends largely are inherited from backshore erosion, and therefore have little to do with net longshore sediment transport direction. Such relationships may exist for parts of the southern California coastline where littoral grain size and petrologic trends may reflect at least partial inheritance from adjacent sedimentary strata. Clearly the strength of this association cannot be evaluated until a systematic study of the sedimentary structure of the coastal sea cliffs and bluffs is performed, particularly in areas where contributing cliffs and bluffs occur.

3. SEDIMENT SOURCES

3.01 Inasmuch as all mineralogic materials in sediment and sedimentary strata are directly or indirectly derived from crystalline rocks of the earth's crust, it is necessary to consider (1) the ultimate crystalline source rocks and (2) the local fluvial and cliff sediment sources.

3.02 The 5 to 10 percent of the earth's surface that is mountainous supplies at least 80 percent of the siliciclastic sediment to modern depositional basins. Furthermore, rates of denudation are directly proportional to relief, and, in general, it appears that streams draining areas of highest relief have the highest proportion of bedload (Blatt and others, 1980, p. 24-26). It is therefore appropriate to consider the crystalline terrains exposed at higher elevations as the dominant ultimate source rocks for the obtained sample set.

3.03 The Geologic Map of the Corona, Elsinore, and San Luis Rey Quadrangles, California (Larsen, 1948) shows that the basement complex consists of two principal units: (1) the Late Jurassic (Portlandian) Santiago Peak Volcanics and (2) the mid-Cretaceous plutonic rocks assigned to the southern California batholith, which intrudes the Santiago Peak Volcanics. The Santiago Peak Volcanics occur as an elongate belt of low-rank metamorphosed volcanic, volcaniclastic and sedimentary rocks that crop out from the southern edge of the Los Angeles basin southward into Mexico (Gray and others, 1971). Compositionally these rocks range from basalt to rhyolite, but are predominantly dacite and andesite. A number of low-rank metamorphosed, small gabbroic plutons, which were probably feeders for the volcanic strata, are included in the Santiago Peak Volcanics.

3.04 Plutonic rocks of the southern California batholith are generally quartz diorite and gabbro. The quartz diorite contains large phenocrysts of plagioclase and potassium feldspar, and hornblende and biotite are present in minor amounts. The gabbroic units are compositionally variable, but consist mostly of calcic feldspar and pyroxene, with minor amounts of quartz and biotite. Larsen (1948) named the principal units in the southern California batholith the Woodson Mountain Granodiorite, the Bonsall Tonalite, and the San Marcos Gabbro. Table 1 summarizes the modal mineralogic composition for the regional sample set and the principal source rocks. The compositional data for the Woodson Mountain Granodiorite, Bonsall Tonalite and San Marcos Gabbro are from Larsen (1948). It is clear from Table 1 that crystalline rocks in the southern California batholith are capable of producing the major mineral assemblages present in the sample set. Available time does not permit an exhaustive literature search to document the presence of minor accessory minerals in these crystalline rocks; however, zircon, sphene and rutile commonly are associated with acid plutonic rocks; piedmontite and clinozoisite-epidote are associated with mafic igneous rocks; and actinolite-tremolite is a high-rank metamorphic mineral and may be a constituent of some glaucophane schist.

3.05 The occurrence of glaucophane, glaucophane schist and actinolite-tremolite reflects ultimate derivation from the Mesozoic metamorphic age (110 m.y.b.p.) Catalina Schist terrane, which consists of a glaucophane-rich, blueschist. Stuart (1979, p. 36) reports a diverse set of clast types, which occur in the San Onofre Breccia. These include clasts of (1) the blueschist facies, which is rich in glaucophane and contains quartz, albite and chlorite;

Table 1. Modal mineralogic composition of sample set and principal source rocks.

Principal Detrital Minerals Identified in Sample Set	Regional Sample Set (%)	Woodson Mountain Granodiorite (%)	Bonsall Tonalite (%)	San Marcos Gabbro (%)
Quartz	42	33 (30-40)	20-25	4 (0-10)
Potassium Feldspar	11	20 (10-30)	4-15	Tr
Plagioclase Feldspar	25	41 (30-55)	55-60	59 (47-66)
Biotite	1	5 (1-8)	5-15	3 (0-6)
Opaque Minerals	2	Tr	Tr	3
Pyroxene	Tr	Tr	Tr	8 (0-28)
Augite		Tr	Tr	7 (0-17)
Hornblende	13	1 (0-2)	10	
Garnet	Tr		Tr	13 (1-42)
Zircon	Tr			
Sphene	1			
Rutile	Tr			
Piedmontite	Tr			
Clinozoisite-Epidote	3			
Actinolite-Tremolite	Tr			
Glaucophane	Tr			
Glaucophane Schist	1			

(2) the glaucophanic greenschist facies, which is rich in epidote and contains albite; (3) the greenschist facies, which is rich in actinolite and contains epidote, albite and chlorite; (4) the quartz schist facies, which consists of foliated quartz with greenschist and abundant glaucophane; (5) the saussurite gabbro facies, which contains actinolite, zoisite, clinozoisite and albite; (6) the amphibolite facies which contains amphibole, zoisite and garnet; and (7) the serpentinite facies, which contains calcite, tremolite, chlorite and actinolite. Such terranes are exposed on Santa Catalina Island and the Palos Verdes Hills, and occur in the subsurface of the Los Angeles basin, but are not known to occur within the uplands associated with the southern California batholith. The San Onofre Breccia (Miocene) is the most extensive deposit containing Catalina Schist detritus (Stuart, 1979). Scattered exposures of this unit occur from Santa Cruz Island southeastwrd to the Laguna Beach-Oceanside area, and then again south of Tijuana. The San Onofre Breccia is exposed as a strike ridge extending from San Onofre Mountain near Dana Point almost to Oceanside, and this exposure as well as younger sedimentary strata exposed along the coastal cliffs may have served as the local source for the glacophane, glaucophane schist and perhaps the actinolite-tremolite grains present in the sample set.

4. LITTORAL SEGMENTS: DANA POINT TO THE UNITED STATES-MEXICO BORDER

4.01 Given the occurrence of the Oceanside, Mission Beach and Silver Strand littoral divisions, each may be subdivided into segments defined either by (1) distinctive mineralogic assemblages due to natural or man-influenced processes (especially beach nourishment programs), or (2) by known natural or man-made barriers (jetties and breakwaters) to littoral sand transport. Fourteen littoral segments tentatively may be identified using these criteria. It must be stressed that the petrologic data base used to define these segments is marginal. Eight of the fourteen segments identified consist of only one sample, which is usually associated with an apparent point source - either the mouth of a river or estuary or the site of one or more beach nourishment programs. Additional sampling is required in the lower reaches (above the zone of tidal influence) of each such river to establish the river as the primary sand source - if, in fact, this presumed relationship is true. Furthermore, closely-spaced ($\cong$ 1 km) samples should be taken along the beach both upcoast and downcoast of such point sources. Such sampling would permit the determination of the net transport direction by means of the reduction of petrologically distinct light and heavy mineral assemblages in the direction of transport as well as the areal asymmetry (elongated in the net transport direction) of such petrofacies.

4.02 The longshore changes in total lithology and heavy mineralogy are illustrated in Figures 1 and 2, respectively; and the average total lithology and heavy mineralogy by segment are shown in Figures 3 and 4, respectively.

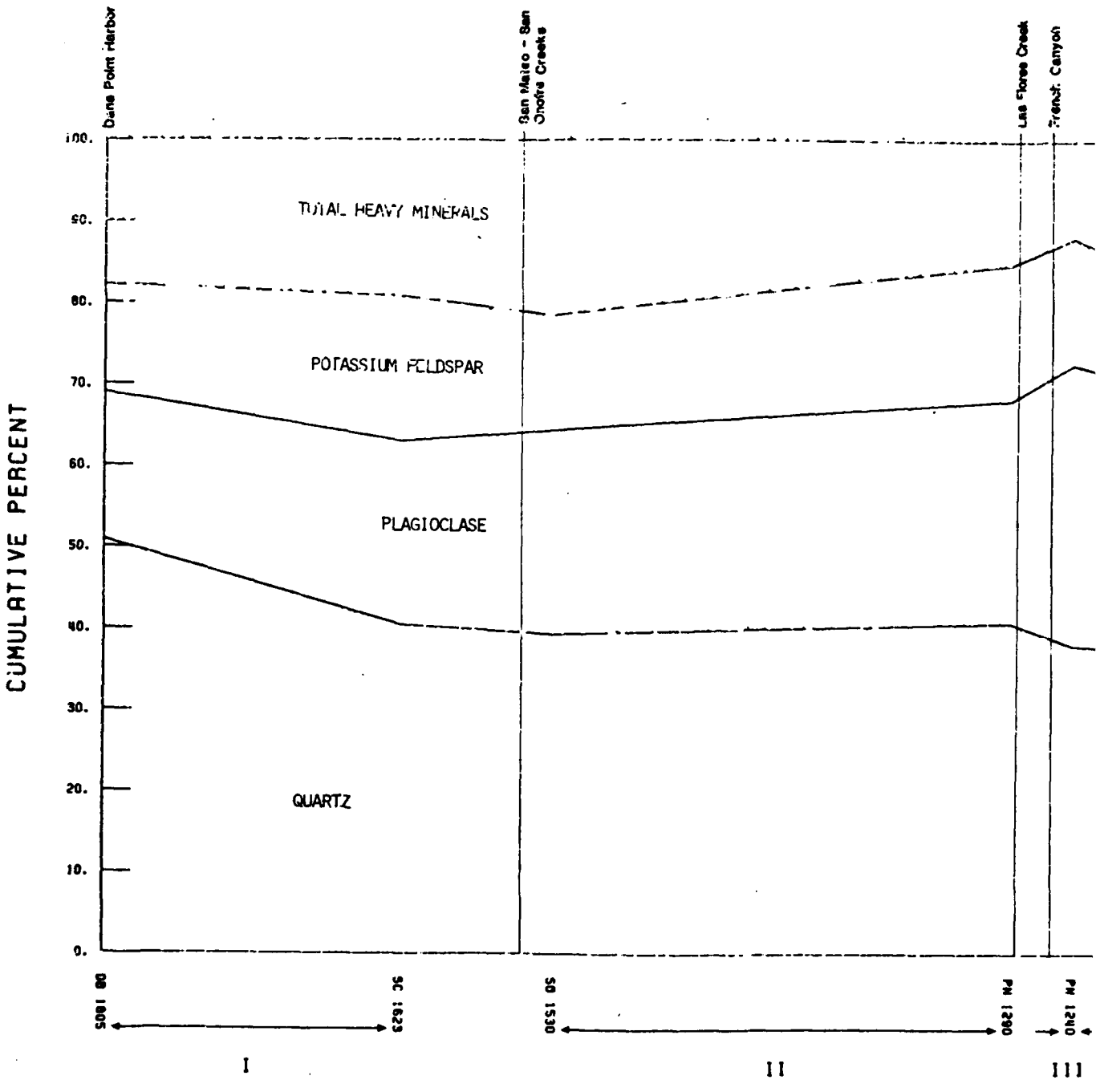
Dana Point Harbor
San Mateo - San Onofre Creeks
Las Flores Creek
Trench Canyon
100.
90.
80.
70.
60.
50.
40.
30.
20.
10.
0.
TOTAL HEAVY MINERALS
POTASSIUM FELDSPAR
PLAGIOCLASE
QUARTZ
CUMULATIVE PERCENT
DB 1805
SC 1823
SD 1530
PN 1280
PN 1240
I
II
III

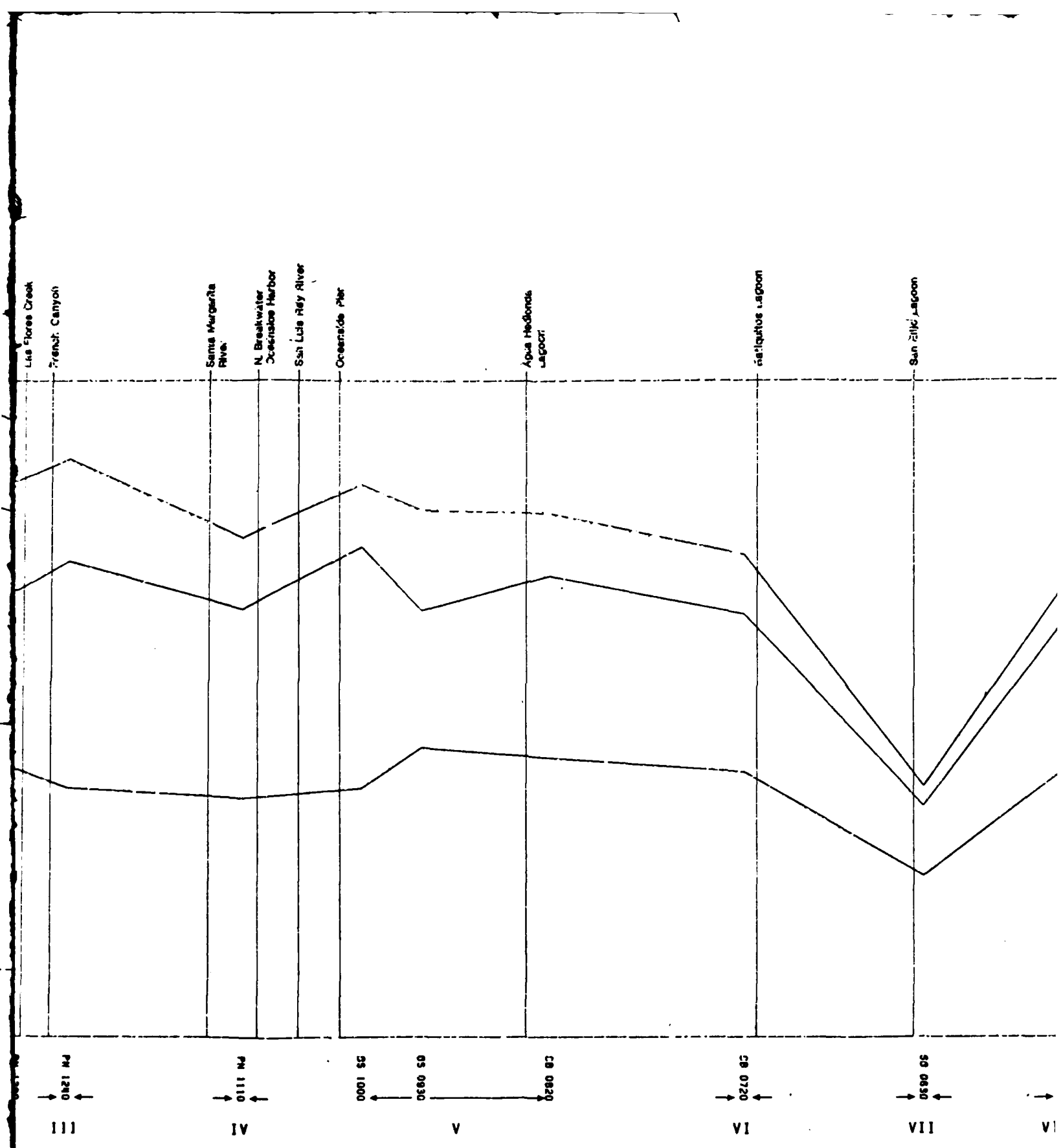

FIG. 1 - MINERAL COMPOSITION OF SEDIMENT SAMPLES FROM THE END-OF-WINTER

(0 METERS, MLLW) 1 INCH = 2.0 MILES

2

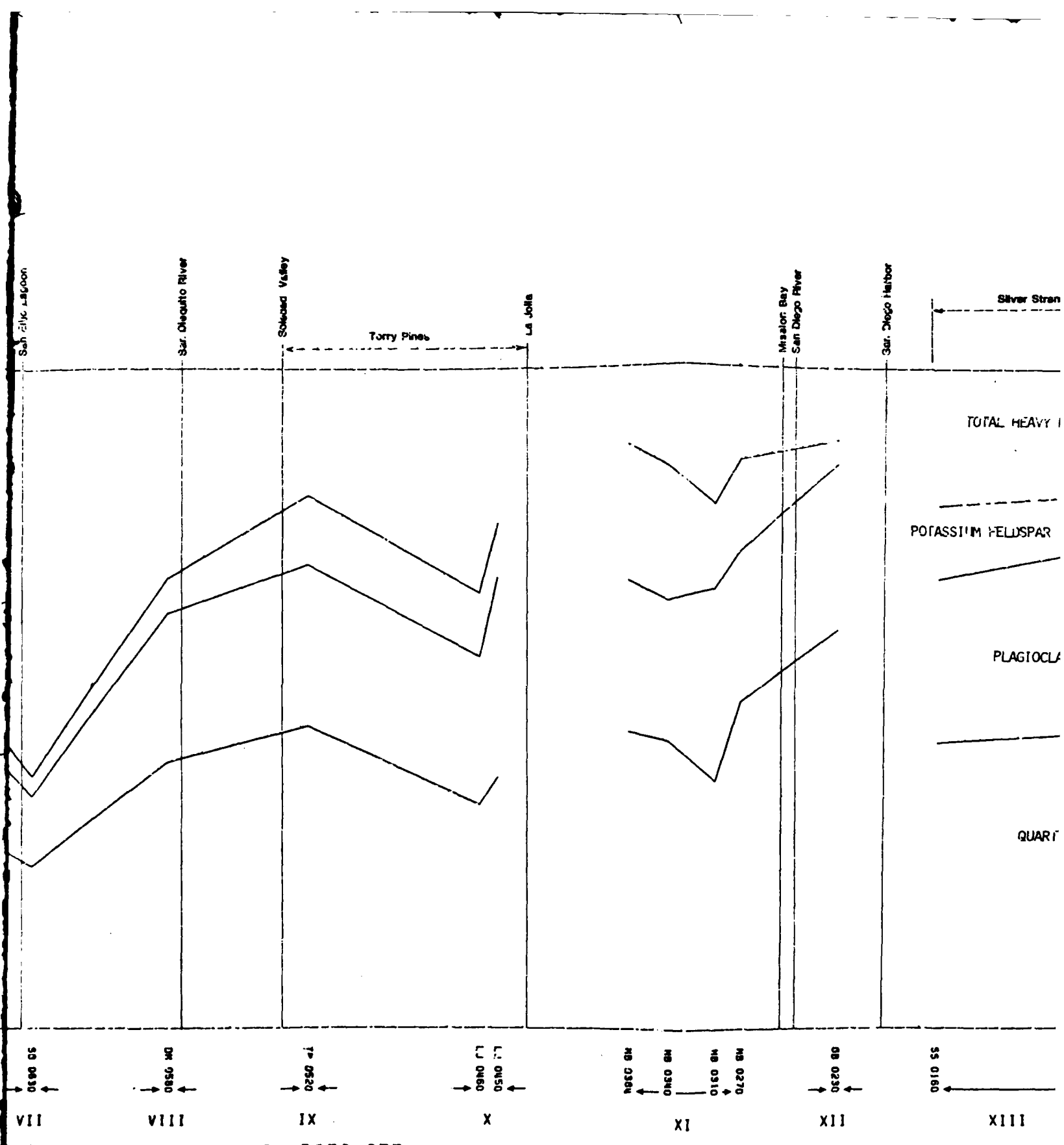

END-OF-WINTER REGIONAL DATA SET

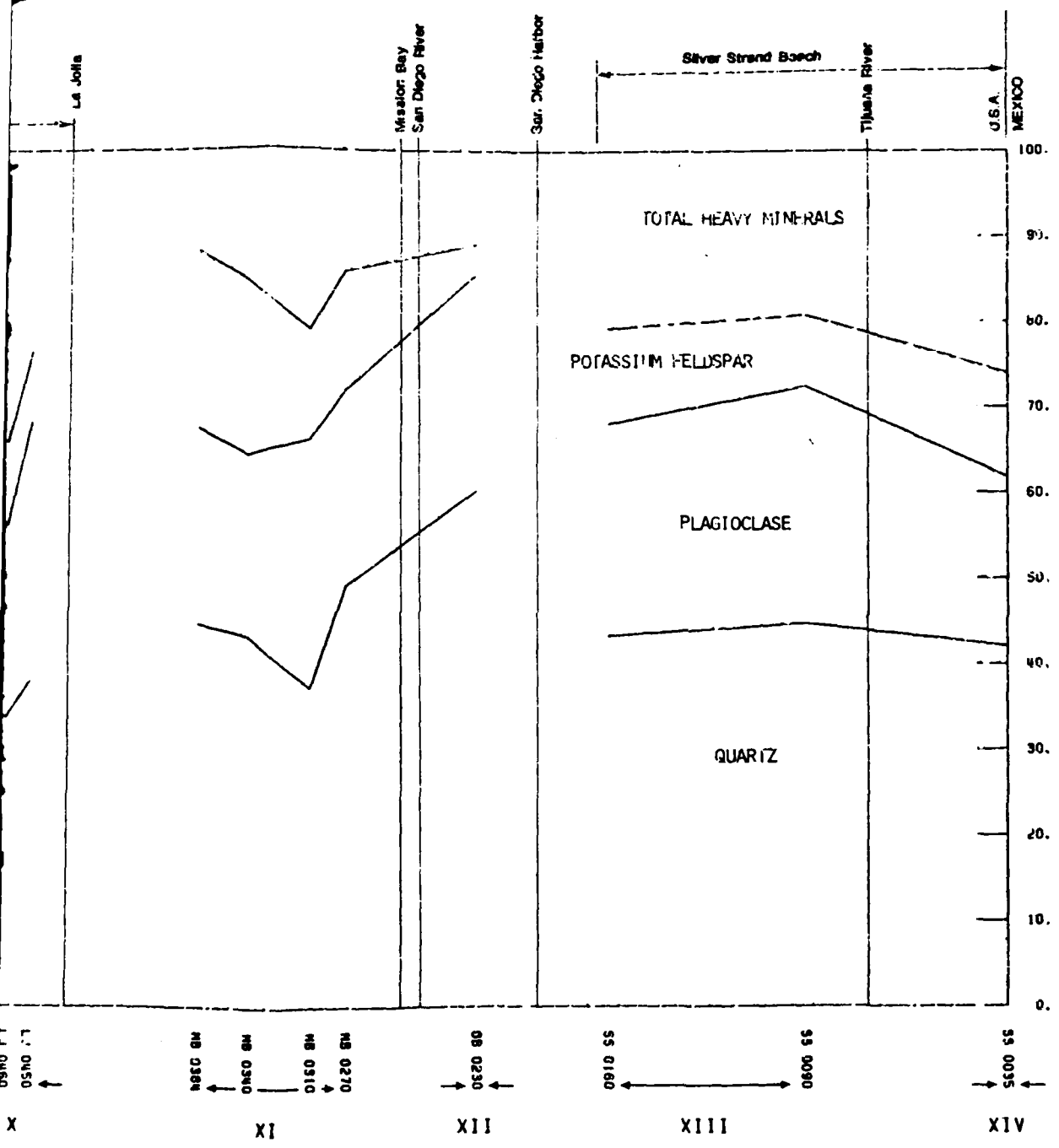
La Jolla
Mission Bay
San Diego River
San Diego Harbor
Silver Strand Beach
Tijuana River
U.S.A.
MEXICO
TOTAL HEAVY MINERALS
POTASSIUM FELDSPAR
PLAGIOCLASE
QUARTZ
100.
90.
80.
70.
60.
50.
40.
30.
20.
10.
0.
X
XI
XII
XIII
XIV

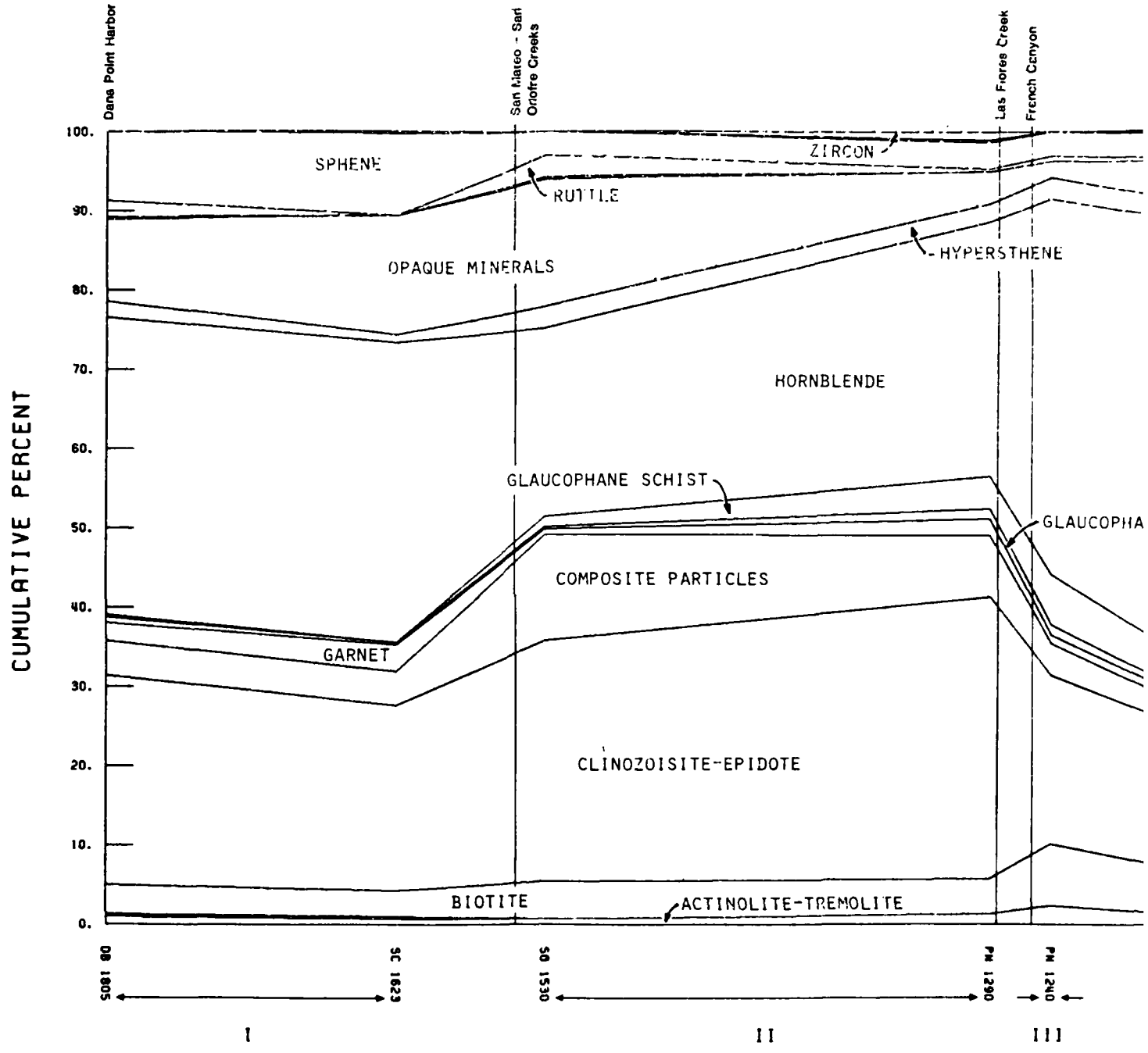
Dana Point Harbor
San Mateo - San Onofre Creeks
Las Flores Creek
French Canyon
CUMULATIVE PERCENT
100.
90.
80.
70.
60.
50.
40.
30.
20.
10.
0.
SPHENE
ZIRCON
RUTILE
OPAQUE MINERALS
HYPERSTHENE
HORNBLENDE
GLAUCOPHANE SCHIST
GLAUCOPHA
COMPOSITE PARTICLES
GARNET
CLINOZOISITE-EPIDOTE
BIOTITE
ACTINOLITE-TREMOLITE
DB 1805
SC 1823
SD 1530
PN 1290
PN 1240
I
II
III

FIG.

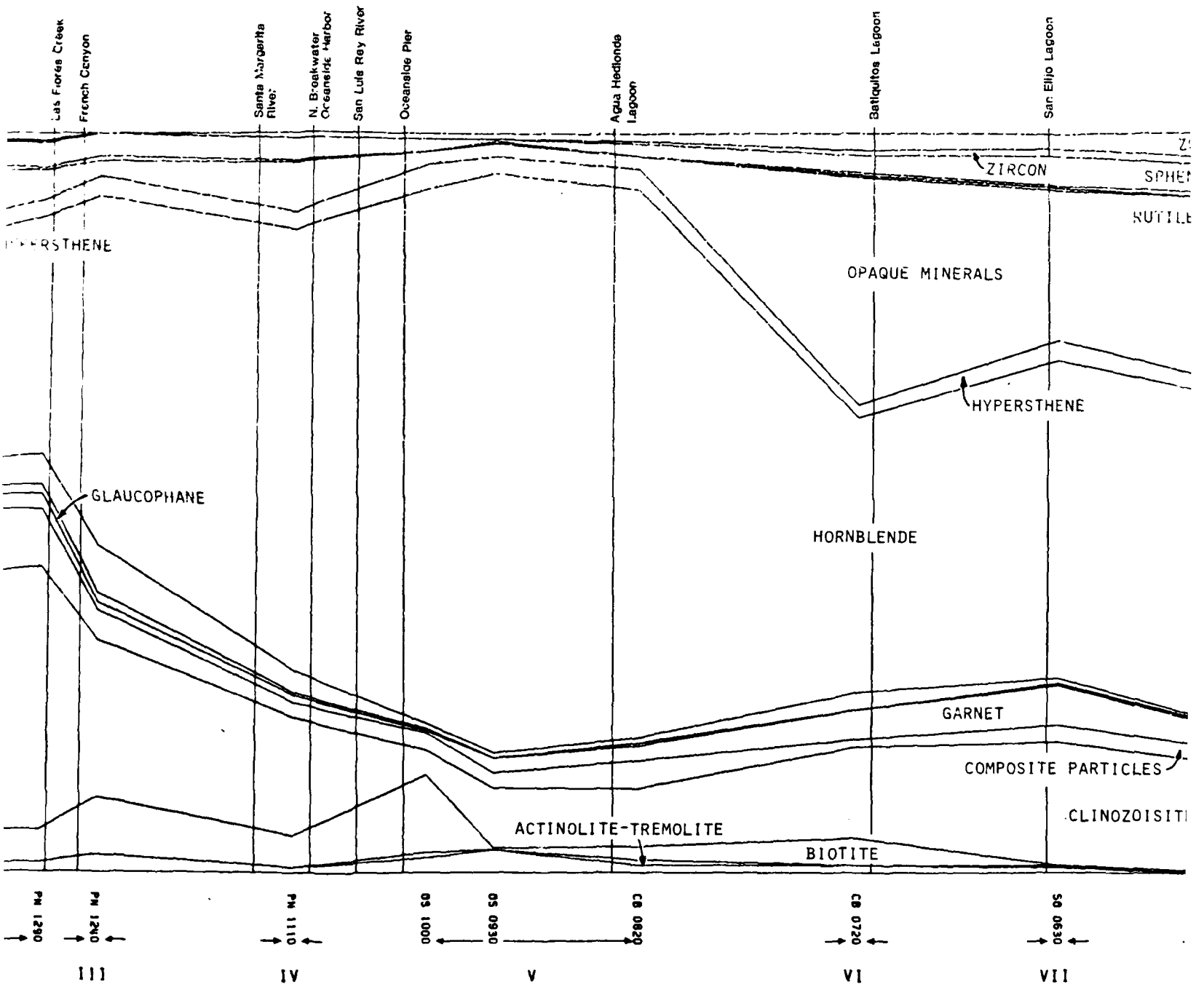

FIG. 2 - HEAVY MINERAL COMPOSITION OF SEDIMENT SAMPLES FROM THE END-OF-WI

(0 METERS, MLLW) 1 INCH = 2.0 MILES

2

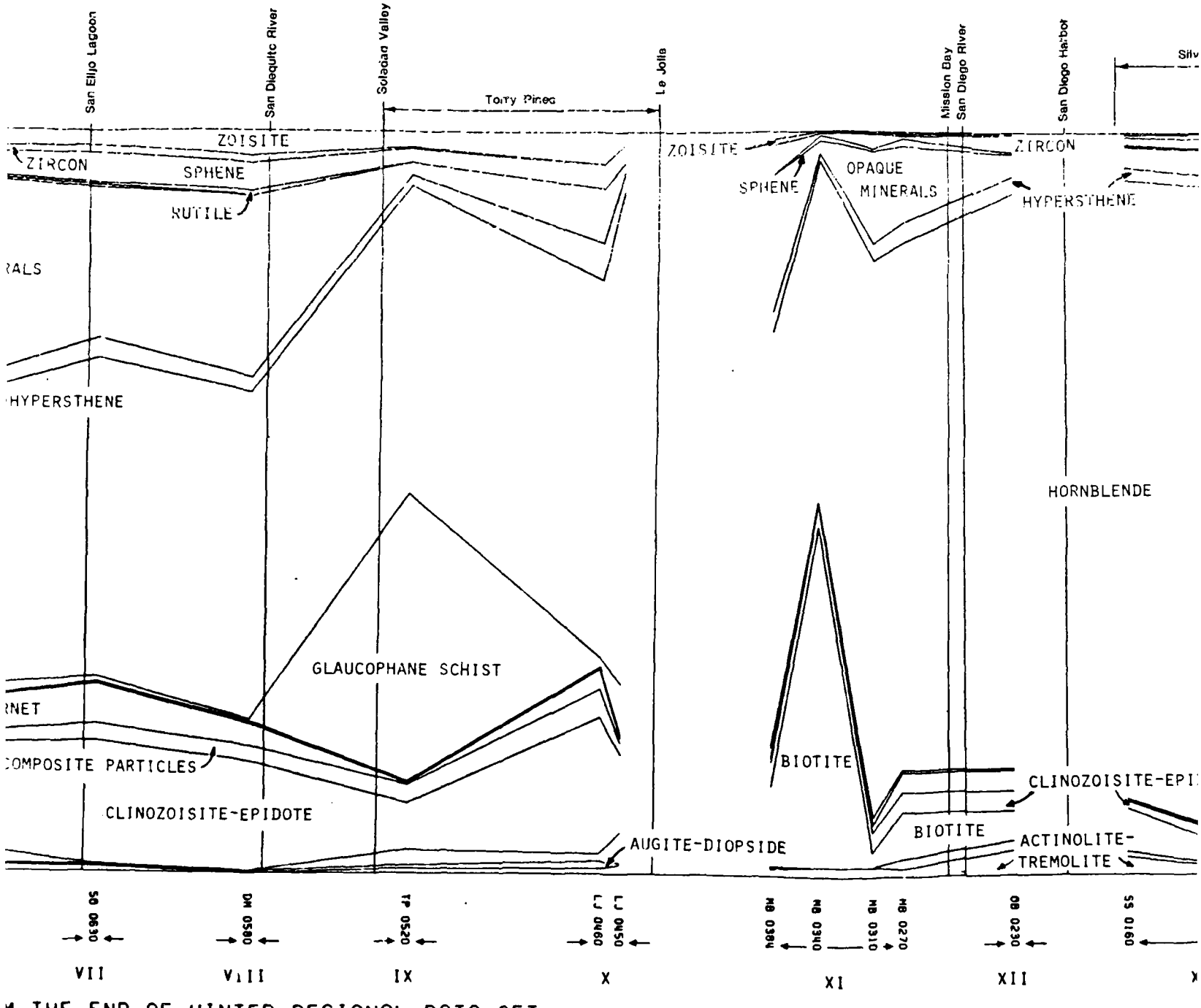

M THE END-OF-WINTER REGIONAL DATA SET.

ILES

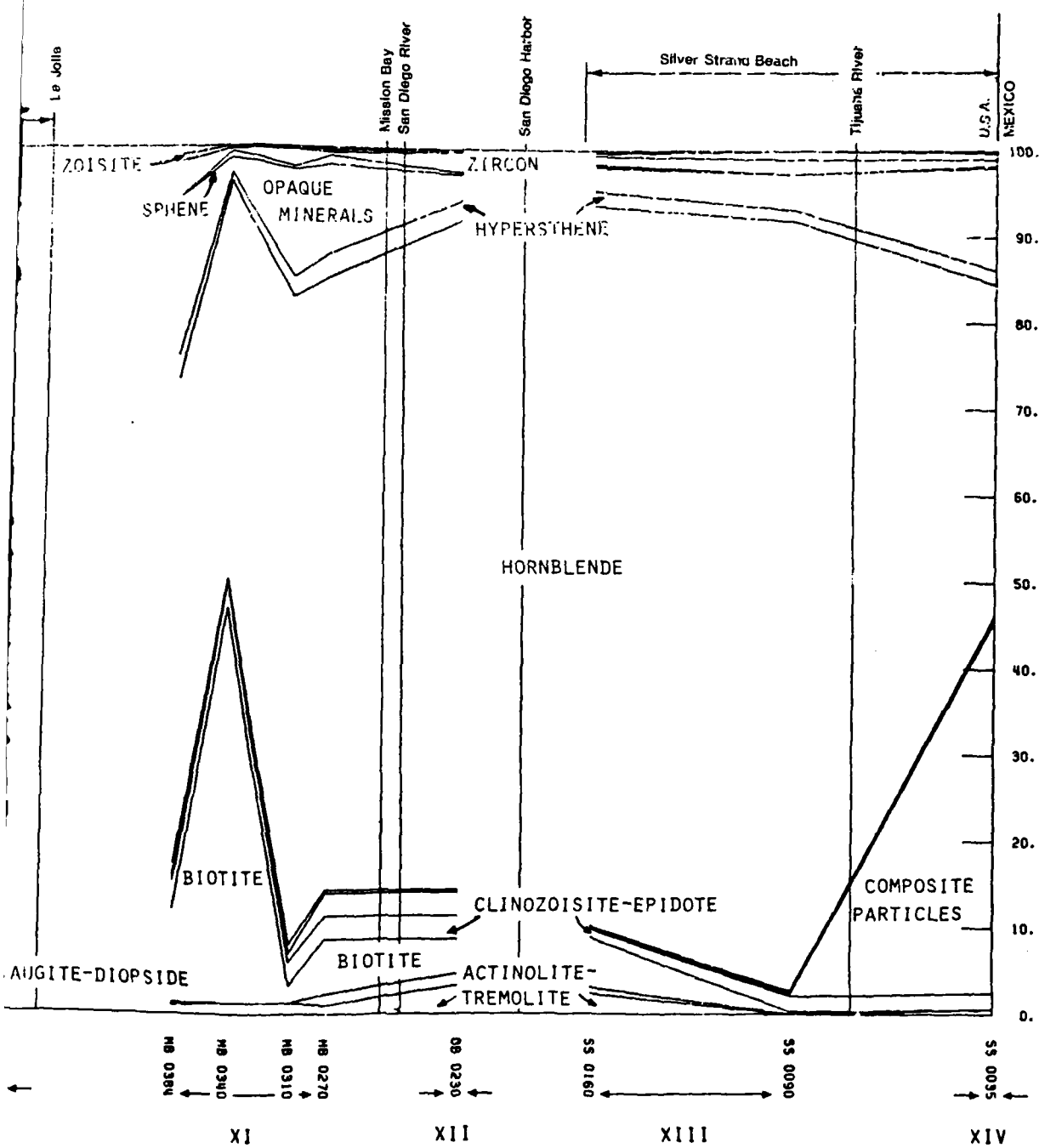
La Jolla
Mission Bay
San Diego River
San Diego Harbor
Silver Strand Beach
Tijuana River
U.S.A.
MEXICO
ZOISITE
ZIRCON
SPHENE
OPAQUE MINERALS
HYPERSTHENE
HORNBLENDE
BIOTITE
CLINOZOISITE-EPIDOTE
COMPOSITE PARTICLES
AUGITE-DIOPSIDE
BIOTITE
ACTINOLITE-TREMOLITE
100.
90.
80.
70.
60.
50.
40.
30.
20.
10.
0.
MB 0360
MB 0340
MB 0310
MB 0270
BB 0230
SS 0160
SS 0090
SS 0035
XI
XII
XIII
XIV

4

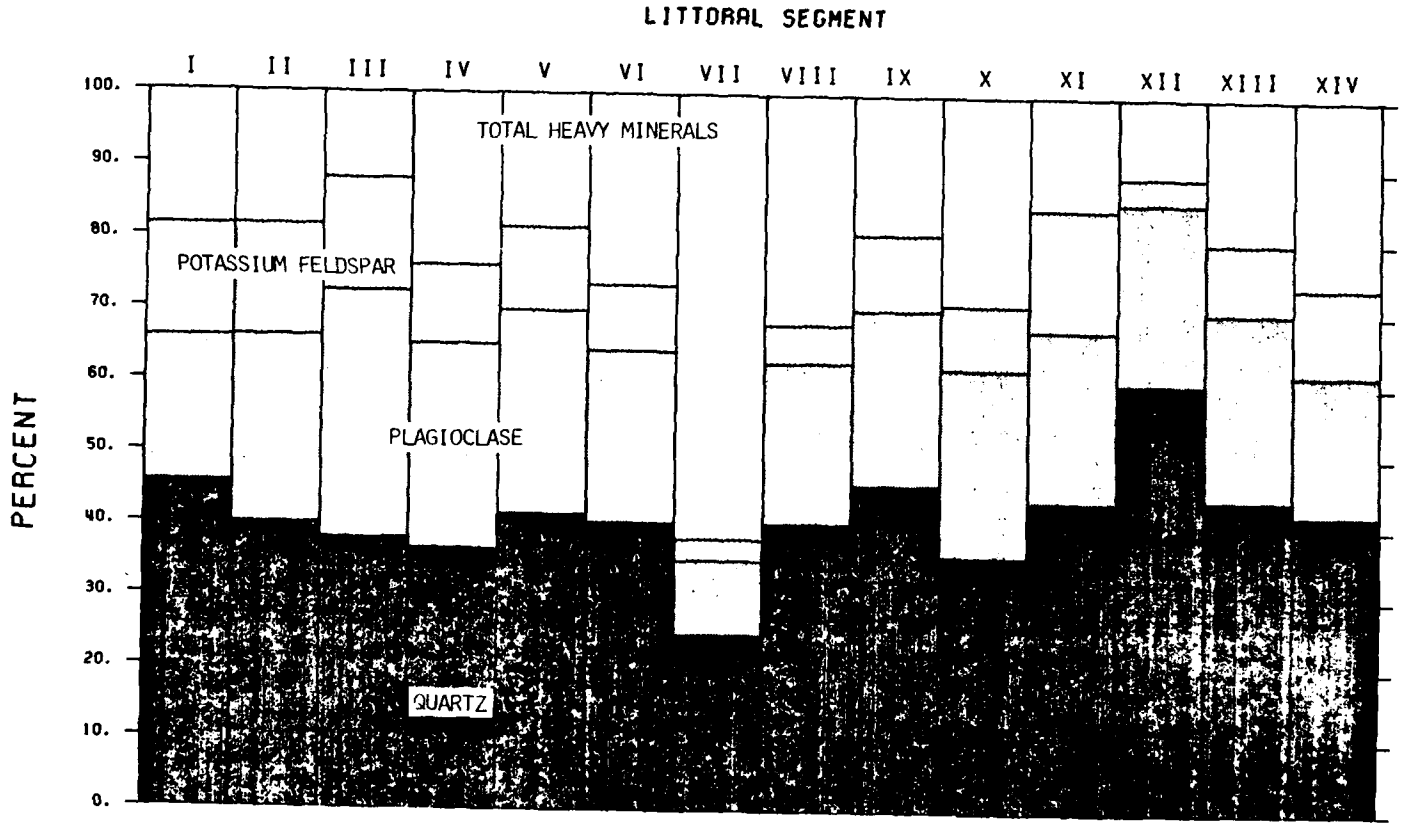

FIG. 3 - AVERAGE MINERAL COMPOSITION OF SEDIMENT SAMPLES BY SEGMENT FROM THE END-OF-WINTER REGIONAL DATA SET.

Fig. 4. Average heavy mineral composition of sediment samples by segment from the end-of-winter regional data: 1=actinolite-tremolite; 2=auqite-diopside; 3=biotite; 4=clinozoisite-epidote; 5=composite particles; 6=garnet; 7=glaucophane; 8=glaucophane schist; 9=hornblende; 10=hypersthene; 11=opaque minerals; 12=piedmontite; 13=rutile; 14=sphene; 15=zircon; and 16=zoisite.

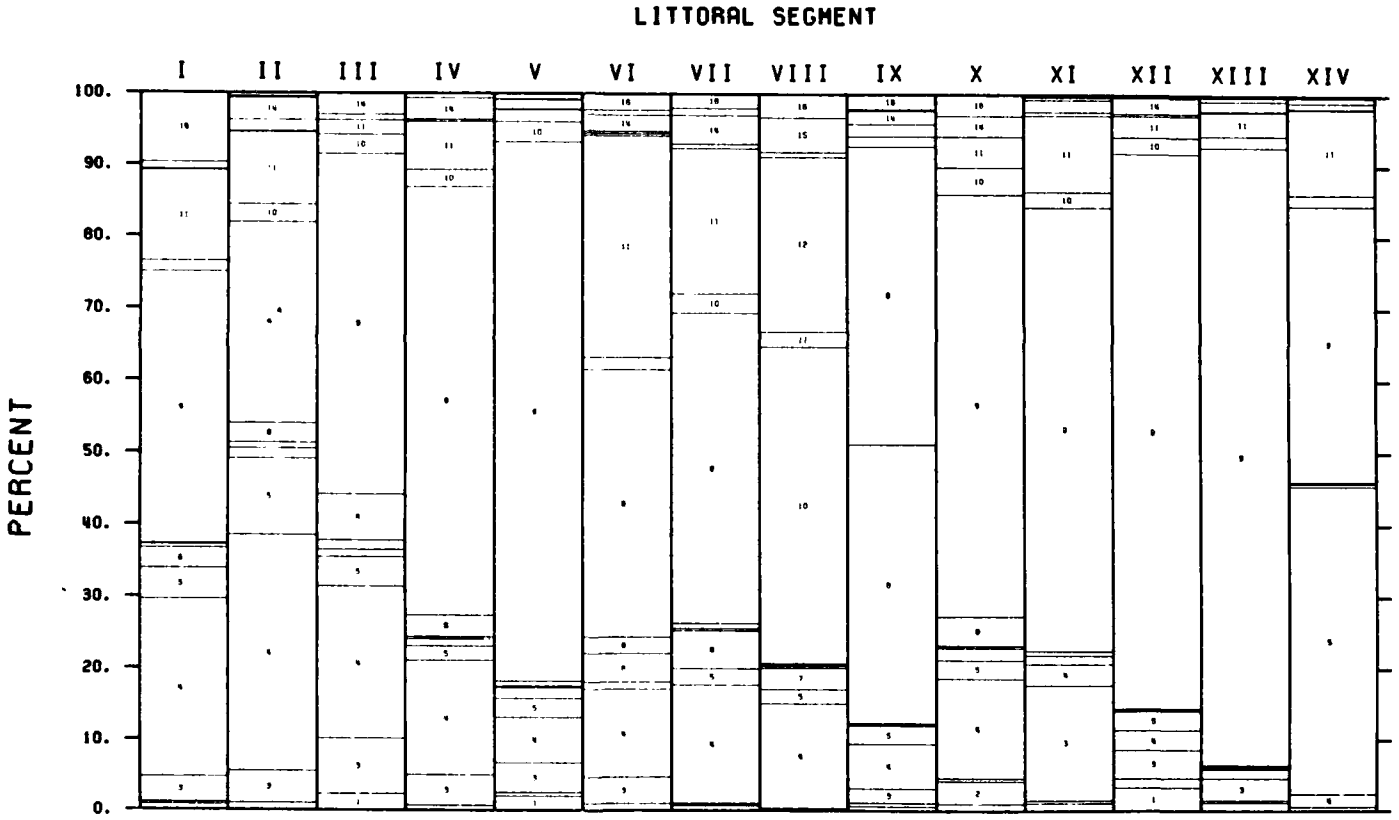

FIG. 4 - AVERAGE HEAVY MINERAL COMPOSITION OF SEDIMENT SAMPLES BY SEGMENT FROM THE END-OF-WINTER REGIONAL DATA SET.

Littoral Segment I. Stations DB-1805 through SC-1623

4.03 Segment I is backed by non-contributing cliffs. Figures 1 and 2 show a slight downcoast decrease in quartz with corresponding increases in plagioclase and potassium feldspar and a relatively consistent set of heavy minerals, given an error range on the order of ± 5 percent.

4.04 The boundary between segments I and II occurs between stations SC-1623 and SO-1530. This area is backed by non-contributing cliffs, and includes the mouths of the San Mateo and San Onofre Rivers, which may serve as important sand contributors. Although there is a slight downcoast increase in plagioclase and total heavy minerals with a corresponding decrease in quartz and potassium feldspar, there is no substantive downcoast change in the total lithology (Fig. 1). There is, however, a major decrease in hornblende and sphene, with associated increases in clinozoisite-epidote and composite grains (Fig. 2).

4.05 The enrichment of hornblende at SC-1623 may reflect upcoast transport from sediment input through the San Mateo River. There is a slight upcoast decrease in heavy minerals, which may reflect net upcoast transport, but this argument cannot be substantiated with the available data.

Littoral Segment II. Stations SO-1530 through PN-1290

4.06 Segment II is backed by contributing cliffs. There is a downcoast decrease in total heavy minerals with associated slight increases in plagioclase and potassium feldspar (Fig. 1). Figure 2 shows a notable decrease in opaque minerals with corresponding increases in clinozoisite-epidote, glaucophane schist and hornblende. The occurrence of glaucophane schist is interesting, because it reflects the reworking of grains that

were ultimately derived from the Catalina Schist terrane. In this area, the most likely local source for the grains of glaucophane schist is the San Onofre Breccia.

4.07 The boundary between segments II and III occurs between stations PN-1290 and PN-1240, which includes contributing cliffs and Los Flores Creek. There is a downcoast decrease in quartz and total heavy minerals with an associated increase in plagioclase (Fig. 1). Inasmuch as PN-1290 is coarser-grained ($\bar{x}$ = 0.39 mm, where $\bar{x}$ is the mean grain size) than PN=1240 ($\bar{x}$ = 0.22 mm), a downcoast increase in total heavy minerals might be expected, so the observed downcoast decrease is particularly significant. There is an important downcoast increase in hornblende, and minor increases in biotite and perhaps glaucophane schist, with a corresponding decrease in clinozoisite-epidote. This change most likely reflects sediment input from Los Flores Creek.

Littoral Segment III. Station PN-1240

4.08 Segment III is backed by contributing cliffs, and occurs upcoast of the mouth of the Santa Margarita River. Inasmuch as this segment contains only one sample, no downcoast trends within this segment can be discerned.

4.09 The boundary between segments III and IV occurs between stations PN-1240 and PN-1110, which is backed by contributing cliffs and contains the mouth of the Santa Margarita River. There is a marked downcoast increase in the volume of total heavy minerals between these two stations, with corresponding decreases in plagioclase and potassium feldspar. There is also a dramatic downcoast increase in hornblende and biotite, and a corresponding decrease in clinozoisite-epidote. These mineralogic trends most likely are associated with input from the Santa Margarita River, but additional samples are needed to demonstrate this relationship.

Littoral Segment IV. Station PN-1110

4.10 Segment IV occurs south of the mouth of the Santa Margarita River, and probably is bounded downcoast by the north jetty at the Camp Pendleton Boat Basin and Oceanside Harbor. There are no contributing cliffs in this area. As this segment contains only one sample, no trends within this coastal zone can be described.

4.11 The boundary between segments IV and V occurs between stations PN-1110 and OS-1000. There are no contributing cliffs in this area, but the Santa Margarita River and beach nourishment programs are important local sand sources. Unfortunately no grain-size or mineralogic data is available for the end-of-winter data set at station OS-1070, which is located immediately downcoast of the south jetty at Oceanside Harbor. Acquisition of data at this location would have been most helpful in defining mineralogic and grain-size trends adjacent to the jetties on either side of the harbor. There is a downcoast decrease in total heavy minerals with a corresponding increase in plagioclase (Fig. 1). Figure 2 shows a marked increase in hornblende and to a lesser degree biotite, with corresponding decreases in clinozoisite-epidote and opaque minerals.

Littoral Segment V. Stations OS-1000 through CB-820

4.12 Segment V is partially backed by contributing cliffs (south of CB-880 almost to CB-120), has been affected by beach nourishment programs (OS-1000 through at least OS-930), and includes a possible estuarine source through outflow from Buena Vista Lagoon (CB-880) and Aqua Hedionda Lagoon (CB-820). This segment also includes the head of Carlsbad Submarine Canyon, which may serve to divide the Oceanside Littoral Cell.

4.13 A modest downcoast increase in quartz, potassium feldspar and total heavy minerals occurs from station OS-1000 to OS-930, and there is a minor increase in plagioclase and decrease in potassium feldspar from OS-930 to OS-820 (Fig. 1). The heavy mineral data (Fig. 2) display an increase in hornblende and clinozoisite-epidote and a marked decrease in biotite from OS-1000 to OS-930, and are rather consistent to CB-820. No major mineralogical changes coincide with the position of the head of the Carlsbad Submarine Canyon.

4.14 The boundary between segments V and VI is between stations CB-820 and CB-720, which occurs immediately south of the mouth of Bataquitos Lagoon. This area is backed by contributing cliffs. There is a modest downcoast increase in the volume of total heavy minerals, with minor decreases in quartz and plagioclase (Fig. 1). Figure 2 shows a marked downcoast increase in opaque minerals and a modest increase of clinozoisite-epidote, and a major reduction in the volume of hornblende. It is suspected that these mineral assemblages are related to episodic flushing of Bataquitos Lagoon, but this relationship cannot be established with the available data.

Littoral Segment VI. Station CB-720

4.15 Segment VI consists only of station CB-720, and is likely to contain cliff-derived sediment as well as sediment periodically flushed from Bataquitos Lagoon.

4.16 The boundary between segments VI and VII occurs between stations CB-720 and SD-630, which occurs at Cardiff State Beach immediately downcoast of the San Elijo River. There is a tremendous downcoast increase in the volume of total heavy minerals from CB-720 to SD-630 with associated decreases in quartz, plagioclase and potassium feldspar (Fig. 1). Interestingly enough,

there is a modest downcoast increase in clinozoisite-epidote, but all other heavy minerals remain in relatively constant proportions between these two stations (Fig. 2).

Littoral Segment VII. Station SD-630

4.17 Segment VII consists only of station SD-630, and may receive sediment from contributing cliffs as well as the San Elijo River.

4.18 Station SD-630 is located immediately south of the San Elijo Lagoon, and is characterized by an anomalously high value for total heavy minerals (Fig. 1). This concentration of heavy minerals is most likely related to episodic flushing of the San Elijo Lagoon, and subsequent wave reworking in the swash zone.

4.19 The boundary between stations VII and VIII occurs between stations SD-630 and DM-580, which is backed by contributing cliffs. Figure 1 indicates there is a major downcoast decrease in total heavy mineral content, modest increases in quartz and potassium feldspar, and a minor increase in plagioclase. There is a small downcoast increase in the volume of total opaque minerals, but the proportions of the other heavy minerals remain relatively constant (Fig. 2).

Littoral Segment VIII. Station DM-580

4.20 Station DM-580 is located immediately south of the mouth of the San Diequito River, and may receive fluvial sediment from this local source as well as from contributing cliffs.

4.21 The boundary between segments VIII and IX occurs between sample stations DM-580 and TP-520, and this area may receive sediment from contributing cliffs and Soledad Creek. There is a downcoast decrease in the

volume of total heavy minerals, with associated increases in quartz, plagioclase and potassium feldspar (Fig. 1). Figure 2 shows a tremendous increase in the volume of glaucophane schist at TP-520, with a corresponding decrease in opaque minerals, and a modest reduction in clinozoisite-epidote and garnet.

Littoral Segment IX. Station TP-520

4.22 Station TP-520 occurs near the mouth of Soledad Creek, and therefore may receive episodic fluvial as well as cliff-derived sediment.

4.23 The sample from station TP-520 is highly enriched in glaucophane schist. The occurrence of glaucophane schist grains indicates that these particles were ultimately derived from the Catalina Schist terrane. Inasmuch as no crystalline Catalina Schist terrane is exposed in the study area, the presence of these grains implies that they have been reworked from older sedimentary strata such as the Miocene San Onofre Breccia or the Monterey Formation. Since the most extensive exposure of the San Onofre Breccia occurs between Dana Point (San Onofre Mountains) and Oceanside (Stuart, 1979), it is not clear why this highly enriched sediment occurs as far south as Torrey Pines. Sampling may have to be performed to determine if such material is being derived from strata exposed in the adjacent contributing cliffs.

4.24 The boundary between IX and X occurs between stations TP-520 and LJ-460. There is a major downcoast increase in total heavy minerals, and an associated increase in quartz (Fig. 1). There is a major downcoast reduction in glaucophane schist, with corresponding increases in clinozoisite-epidote, opaque minerals, and a minor increase in hypersthene.

Littoral Segment X. Stations LJ-460 through LJ-450

4.25 Stations LJ-460 and LJ-450 are located betwen Scripps and La Jolla Submarine Canyons, and are backed by contributing cliffs.

4.26 There is a substantial downcoast decrease in total heavy minerals and a minor decrease in potassium feldspar from stations LJ-460 to LJ-450, with corresponding increases in quartz and plagioclase (Fig. 1). Heavy minerals also show marked changes between these two stations (Fig. 2). There is a substantial downcoast increase in hornblende, and modest increases in biotite and glaucophane schist. These changes are coupled with a notable downcoast decrease in clinozoisite-epidote, and moderate downcoast decreases in opaque minerals and zoisite. The observed variability in relatively closely-spaced samples may be related to the complex littoral wave and current system between the heads of Scripps and La Jolla Submarine Canyons (Shepard, 1950), or such trends may be partly inherited from cliff-derived sediment.

4.27 The Oceanside Littoral Cell is terminated at the submarine canyon complex associated with Point La Jolla.

Littoral Segment XI. Stations MB-384 through MB-270

4.28 Stations MB-384 through MB-270 occur along a downcoast-directed spit which extends most of the way across the mouth of Mission Bay. The San Diego River enters Mission Bay, where it has deposited a considerable volume of sediment, and the coastal lowland occupied by Pacific and Mission Beaches occurs on older deltaic sediment deposited by the San Diego River. Such fluvial sediment extends almost to Crystal Pier at Pacific Beach, where the character of the sediment changes and extends downcoast as a spit. The

sediment comprising Mission Beach presumably was derived by the reworking of older San Diego River alluvium combined with downcoast littoral drift. No beach nourishment programs have been performed between these two stations.

4.29 From samples MB-384 through MB-310, there is a downcoast increase in the total heavy minerals and plagioclase, with associated decreases in quartz and potassium feldspar (Fig. 1). From MB-310 to MB-270, there is a downcoast decrease in total heavy minerals and plagioclase, and a corresponding increase in quartz. From MB-384 to MB-340, there is a tremendous downcoast increase in biotite, with noteworthy decreases in hornblende and opaque minerals (Fig. 2). From MB-340 to MB-310, there is a dramatic downcoast reduction in biotite, and appreciable increases in the amount of hornblende and opaque minerals. From MB-310 to MB-270, there is a downcoast increase in biotite, and a decrease in opaque minerals. The increases in the amount of biotite may be due to the acquisition of samples in areas characterized by low mechanical-energy during or before the sampling period.

4.30 Littoral segment XI is bounded downcoast by the north jetty at the entrance to Mission Bay.

Littoral Segment XII. Station OB-230

4.31 Station OB-230 is located at Ocean Beach, which is a pocket beach extending from the south San Diego River jetty to Sunset Cliffs. Damming of the San Diego River considerably reduced the volume of sand received by Ocean Beach, and the three jetties constructed at the mouth of Mission Bay have terminated the sand supply received from Mission Beach. As a result, the cliffs at Ocean Beach have receded considerably, and sand obtained from north of the Mission Bay jetties was placed along Ocean Beach to reduce the rate of

cliff erosion (Kuhn and Shepard, 1984). Fill placed in 1950 migrated upcoast to form a spit across the mouth of the San Diego River, and downcoast erosion was initiated. Additional fill dredged from Mission Bay was placed in 1955, and was contained by a groin at Cape May Avenue. Although the sample from OB-230 may be a combination of cliff-derived and beach fill, it most likely represents sand supplied by beach nourishment.

4.32 As this segment is represented by only one sample, no trends within this pocket beach can be defined. However, when compared to MB-270, the sample from OB-230 is significantly enriched in quartz, moderately enriched in plagioclase, moderately reduced in potassium feldspar, and slightly reduced in total heavy minerals (Fig. 1). Figure 2 shows that the heavy mineral suites are similar; however, OB-230 is enriched in hornblende and depleted in total opaque minerals.

4.33 Littoral Segment XII is bounded downcoast by Sunset Cliffs.

Littoral Segment XIII. Stations SS-160 through SS-90

4.34 Stations SS-160 through SS-90 occur within the Silver Strand Littoral Cell. This cell extends from Zuniga jetty, which forms the southern boundary of the entrance to San Diego Bay, to the border between the United States and Mexico. The principle natural sediment source for this cell is the Tijuana River, which was particularly important prior to damming. Beach nourishment programs have been performed at Imperial Beach and in the area adjacent to Hotel del Coronado (Kuhn and Shepard, 1984). The Silver Strand Littoral Cell consists of a long, upcoast-directed spit, which extends from the embayment associated with the Sweetwater and Tijuana Rivers. Inman (1976) has documented that the primary zone of net accretion is at and directly offshore

of Zuniga Shoal by comparing isolines of sand accretion obtained from surveys carried out in 1923 and 1934. Unfortunately there is no petrographic data for stations SS-200 and SS-180, so it is not possible to determine whether or not the upcoast portion of this spit is compositionally similar to segment XIII. Although beach nourishment has occurred near Hotel del Coronado, the sand in the foreshore zone may be dominated by sand derived from the area of Imperial Beach, therefore meaningful compositional trends might be obtained by sampling the upcoast part of this spit.

4.35 From SS-160 to SS-90, there is a slight downcoast decrease in total heavy minerals and potassium feldspar, with corresponding minor increases in quartz and plagioclase (Fig. 1). There is a downcoast increase in hornblende, and an associated decrease in biotite between these two stations (Fig. 2).

4.36 The boundary between segments XIII and IV occurs between stations SS-90 and SS-35. There is a moderate downcoast increase in heavy minerals and a minor increase in potassium feldspar, which is associated with a reduction in the amount of plagioclase (Fig. 1). More dramatic changes are recorded in the heavy mineral assemblages (Fig. 2). Substantial downcoast increases occur in the volume of composite grains and total opaques, with an associated decrease in hornblende.

Littoral Segment XIV. Station SS-35

4.37 Station SS-35 is located about 1.25 miles north of the mouth of the Tijuana River, and sand obtained from this area most likely represents some mixture of sediment derived from the Tijuana River as well as by beach nourishment programs. There is a possibility that some sand may have been derived from the contributing cliffs south of the Tijuana River.

5. LONGSHORE GRAIN-SIZE FINING TRENDS

5.01 Examination of Figures 5 and 6 shows considerable variability in the direction of fining-trends between adjacent sample stations, with water depth, and, where possible, by season. Data concerning the directional aspects of fining-trends were partitioned into the following sets: (1) Oceanside Cell, end of summer, (2) Oceanside Cell, end of winter, (3) Mission Beach, end-of-winter, (4) Silver Strand Cell, end-of-winter, and (5) Mission Beach plus Silver Strand Cell, end-of-winter. The end-of-summer data sets for the Mission Beach and Silver Strand area were too inadequate with regard to sample spacing and bathymetry to include in this analysis. The data for the Mission Beach and Silver Strand segments were pooled because of the need to roughly balance the sample size (n) between cells to facilitate comparisons among sample sets. The fact that both Mission Beach and Silver Strand are spits and are thus similar in a general sedimentologic sense provides additional justification for pooling these data.

5.02 Table 2 summarizes the percentage of <u>similar</u> directions of longshore grain-size trends as a function of bathymetry as well as the sample size (n). The percentage of opposing trends is 100 percent minus the tabulated value. Although the sample size (n) for each littoral segment is marginal to meager from a stochastic viewpoint, the observed finding-trends suggest some interesting but tentative areal and bathymetric relationships. Such relationships should be integrated and evaluated in terms of the wave statistics and the knowledge of nearshore seafloor topography during the sampling period.

5.03 The Oceanside, end-of-summer set shows good agreement in the direction of fining between the +1 and 0m data and the -3 to -6m data. In contrast, the +1 and -1m, 0 and -1m, and -1 and -3m data show strong dissimilarity. There

Cara Point Harbor
San Mateo - San Onofre Creeks
Las Flores Creek
French Canyon
ELEVATION (METERS)
3
1
0
-1
-3
-6
SC 1685
SC 1720
SC 1823
SO 1530
SO 1470
PN 1390
PN 1290
PN 1240
I
II
III

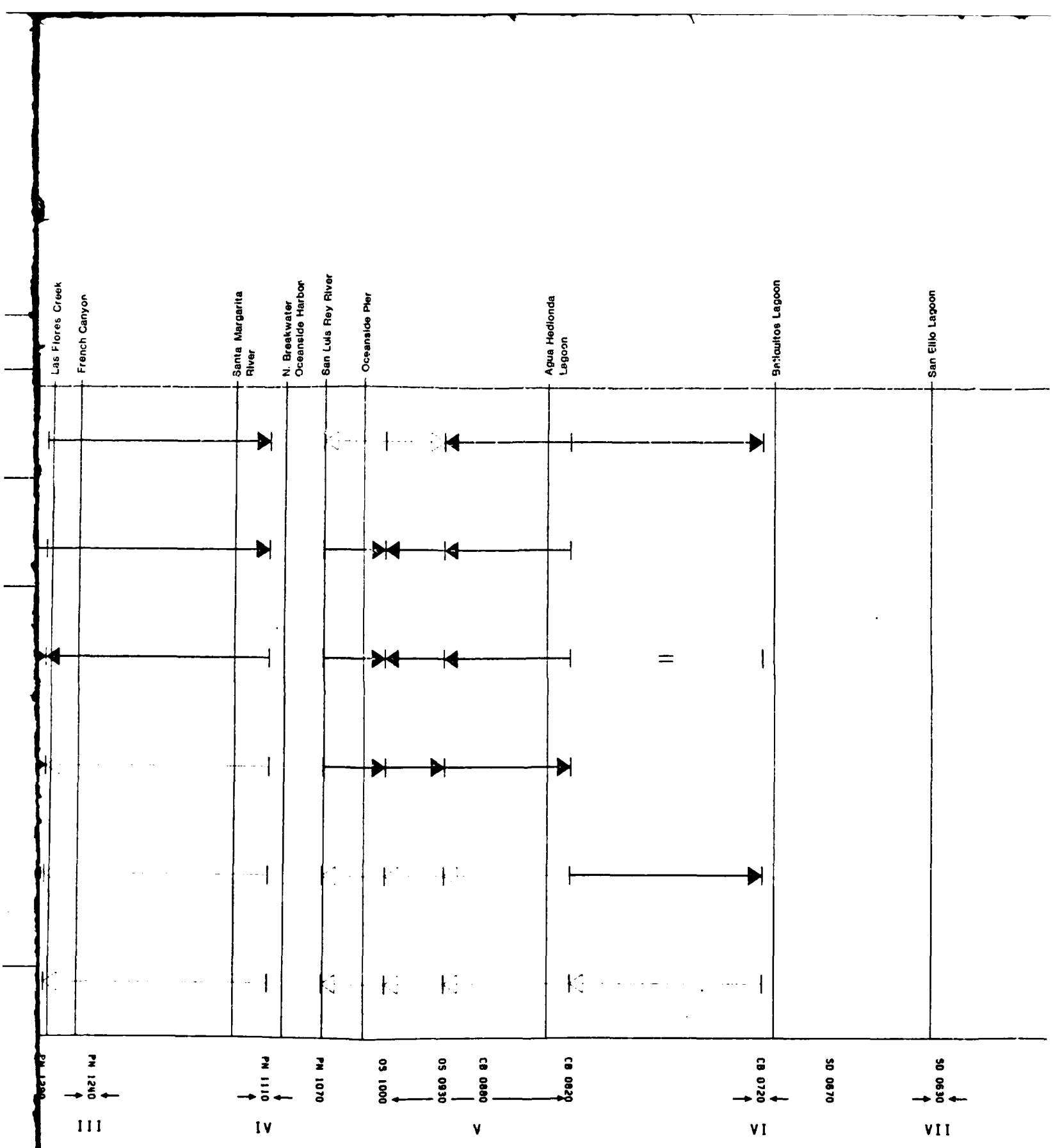

FIG. 5 - SUMMARY OF GRAIN-SIZE FINING TRENDS FOR THE END-OF-SUMMER

POSSIBLE PALIMPSEST TRENDS SHOWN BY THIN ARROWS.

2

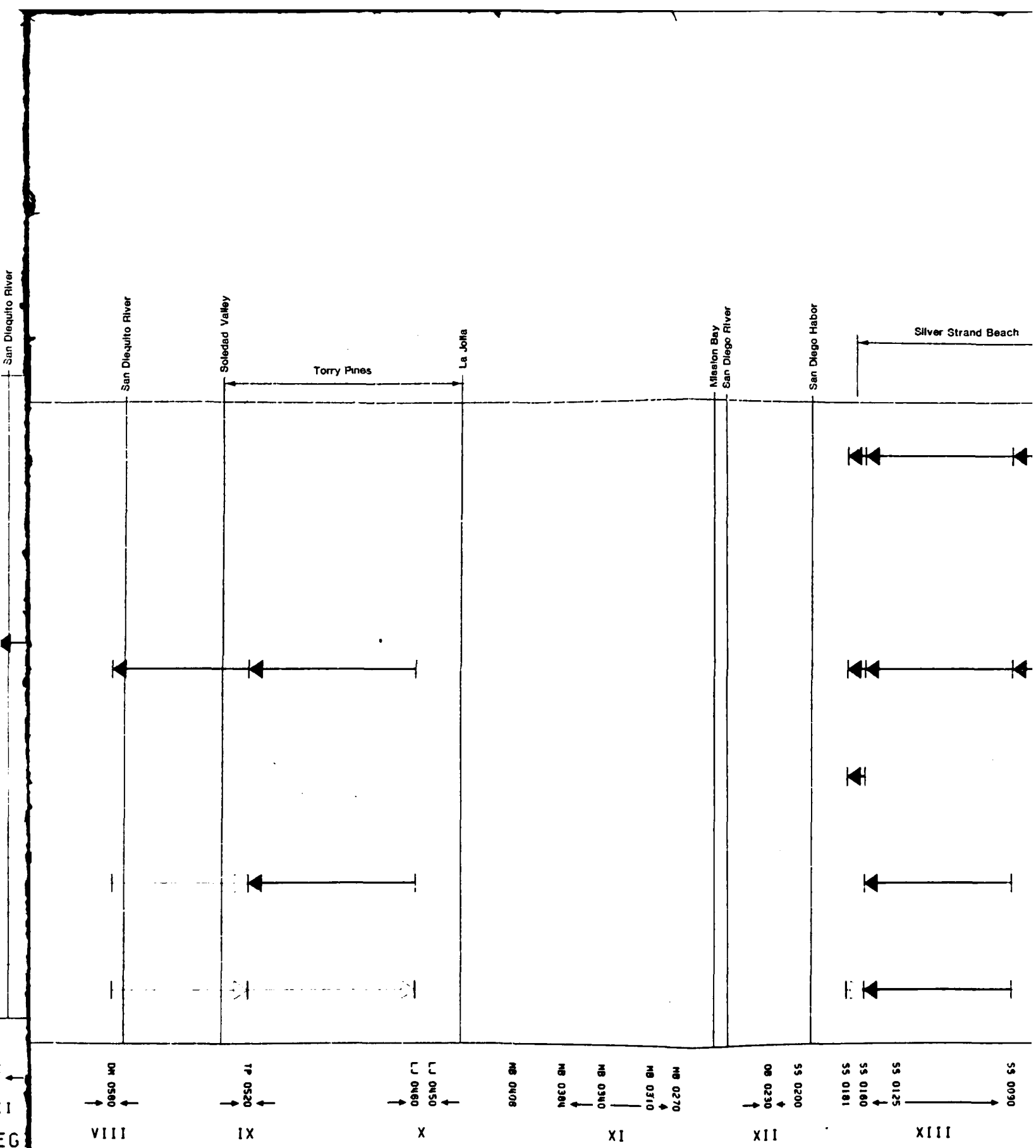

MMER REGIONAL DATA SET.

Mission Bay
San Diego River
San Diego Habor
Silver Strand Beach
Tijuana River
U.S.A.
MEXICO
3
1
0
-1
-3
-6
MB 0270
MB 0510
MB 0960
MB 0360
SS 0020
OB 0230
SS 0090
SS 0125
SS 0180
SS 0181
SS 0070
SS 0035
SS 0015
XI
XII
XIII
XIV

4

Davis Point Harbor
San Mateo - San Dieguito Stream
Las Flores Creek
Pierson Canyon
ELEVATION (METERS)
3
1
0
-1
-3
-6
08 1805
SC 1720
SC 1823
SO 1530
SO 1870
PM 1900
PM 1230
I
II
I

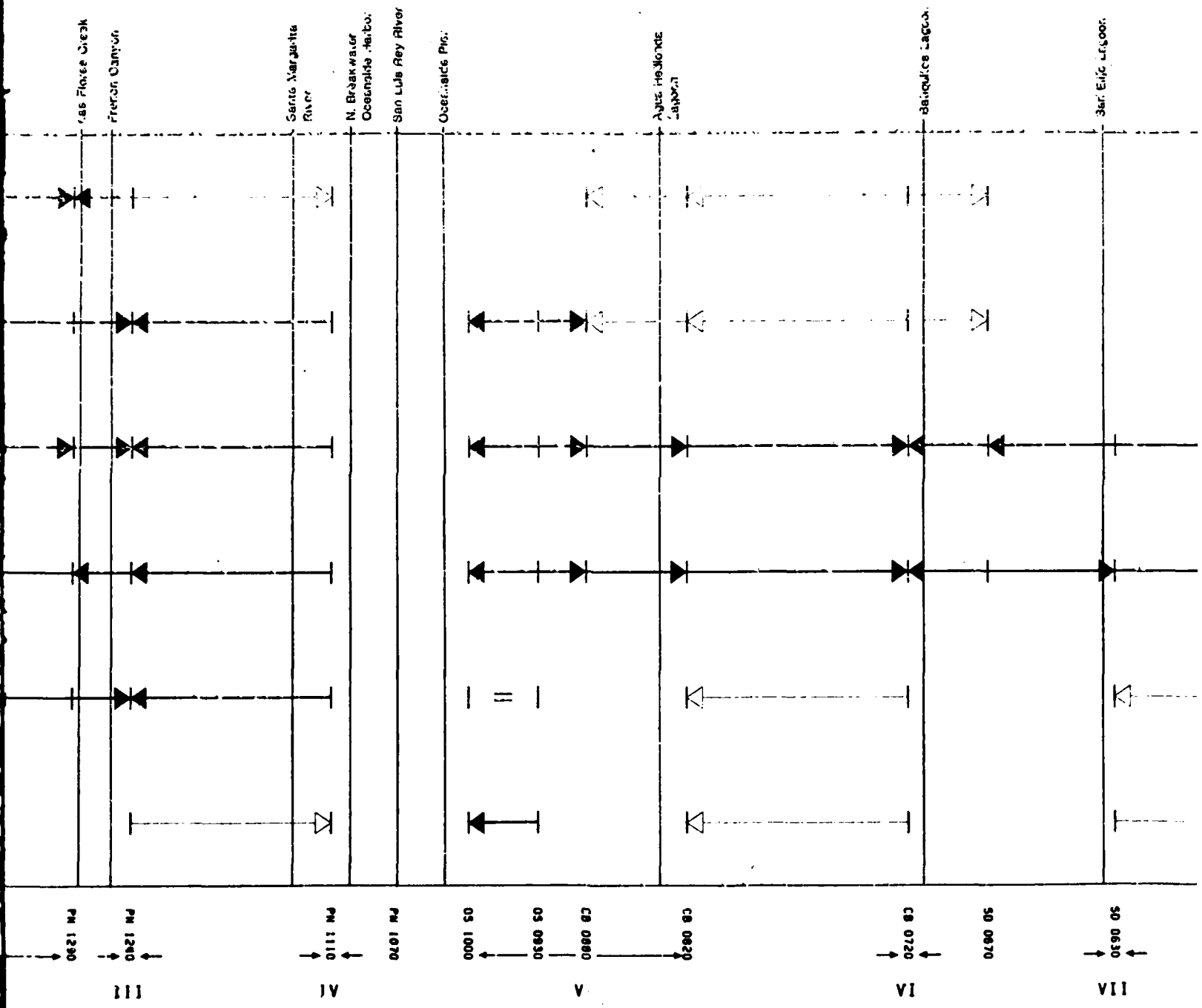

FIG. 6 - SUMMARY OF GRAIN-SIZE FINING TRENDS FOR THE END-OF-WIN

POSSIBLE PALIMPSEST TRENDS SHOWN BY THIN ARROWS.

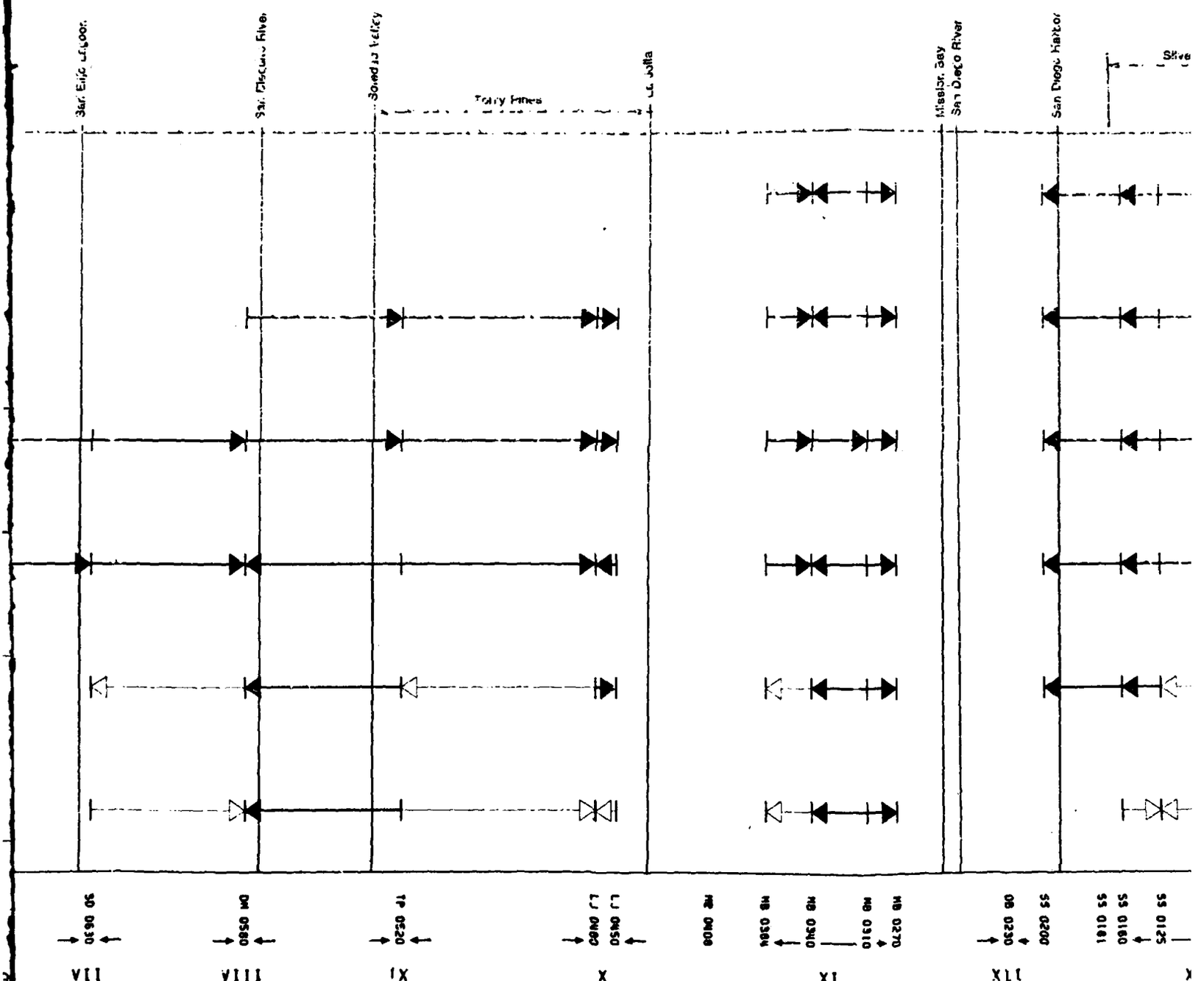

END-OF-WINTER REGIONAL DATA SET.

IN ARROWS.

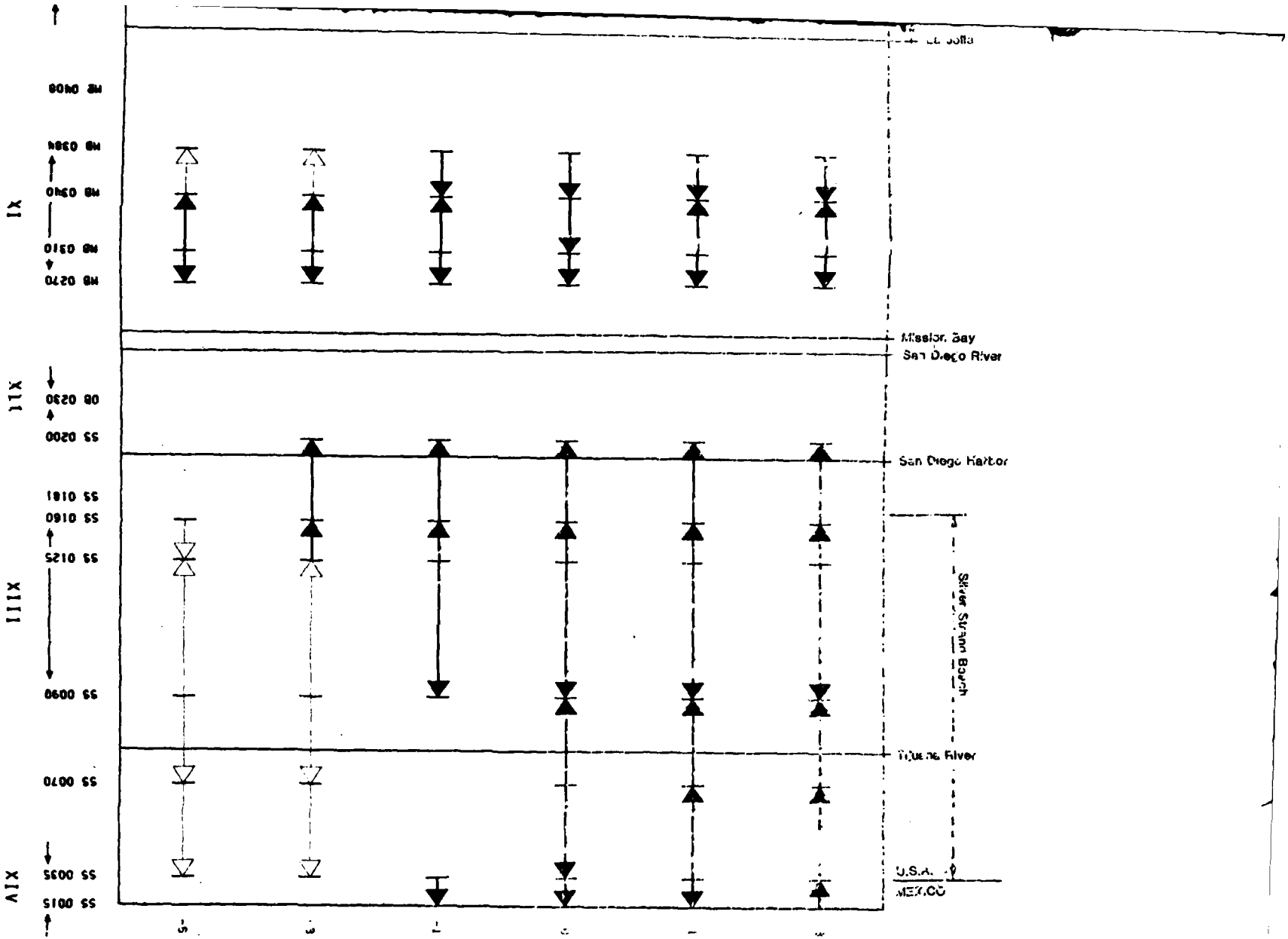
La Jolla
Mission Bay
San Diego River
San Diego Harbor
Silver Strand Beach
Tijuana River
U.S.A.
MEXICO
IX
XI
XII
XIII
XIV

Table 2. Percentage of similar directions of longshore grain-size fining trends for major littoral segments. Important values are underlined.

Bathymetry (m) datum MLLW	Oceanside Cell end-of-summer		Oceanside Cell end-of-winter		Mission Beach Cell end-of-winter		Silver Strand Cell end-of-winter		Mission Beach plus Silver Strand Cell end-of-winter	
	%	n	%	n	%	n	%	n	%	n
+3 and +1	50	8	50	10	100	3	83	6	89	9
+3 and 0	50	8	44	9	67	3	67	6	67	9
+3 and -1	38	8	30	10	67	3	75	4	71	7
+3 and -3	43	7	50	6	67	3	40	5	50	8
+3 and -6	29	7	100	4	67	3	0	4	29	7
+1 and 0	75	8	53	15	67	3	83	6	78	9
+1 and -1	13	8	47	15	67	3	100	4	86	7
+1 and -3	67	6	62	8	67	3	40	5	50	8
+1 and -6	67	6	50	6	67	3	0	4	27	7
0 and -1	38	8	56	18	67	3	100	4	86	7
0 and -3	67	6	33	9	33	3	60	5	50	8
0 and -6	67	6	38	8	33	3	25	4	27	7
-1 and -3	17	6	44	9	67	3	67	3	67	6
-1 and -6	17	6	63	8	67	3	0	1	50	4
-3 and -6	86	7	57	7	67	3	75	4	86	7

seems to be a transition zone within the 0 to -3m bathymetric range, where opposing fining-trends are relatively common.

5.04 The Oceanside, end-of-winter set shows no strong associations with the possible exception of the -3 to -6m samples (57 percent agreement). The value of 100 percent between the +3 and -6m samples is highly questionable, as n only equals 4.

5.05 The end-of-winter data for Mission Beach and Silver Strand show similar relationships, and therefore will be discussed in terms of the pooled data set. The direction of the grain-size fining-trends is rather consistent for the +3 through -1m samples, and for the -3 through -6m samples. The -1 to -3m bathymetric zone seems to be less consistent, but even in this zone there is a consistency of 67 percent.

Littoral Transport Directions, Oceanside Cell

End-of-Summer Sample Set

5.06 The end-of-summer Oceanside data set (Fig. 7) is highly variable with respect to the direction of grain-size fining both in an areal as well as a bathymetric sense. In general, the -3 and -6m fining trends may be interpreted as palimpsest, whereas the +3 m trends may be either palimpsest or in apparent equilibrium with the littoral wave and current regime characteristic of the sampling period. Excluding consideration of the +3m trends, the transition from "active" littoral transport to palimpsest conditions appears to occur from elevations of 0 to -1m to an elevation of about -3m.

5.07 Samples DB-1805 and SC-1623 were collected on November 17 and November 5, 1983, respectively. The +3, +1 and Om samples show downcoast fining, whereas the -1m samples fine upcoast. From SC-1623 to SO-1530 (November 10, 1983), the +3, +1, and Om samples fine upcoast, and the -1m samples fine

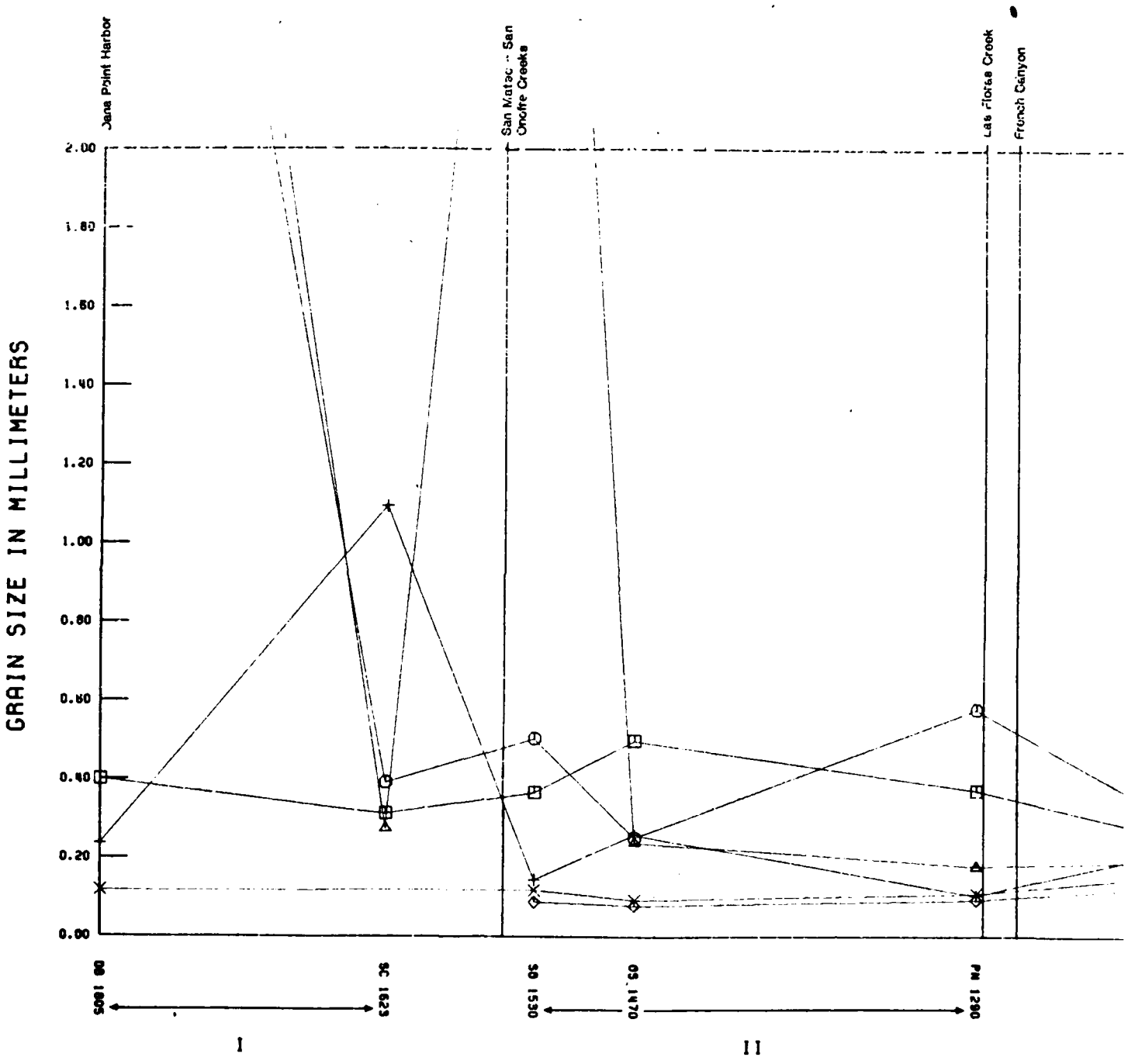
GRAIN SIZE IN MILLIMETERS
2.00
1.80
1.60
1.40
1.20
1.00
0.80
0.60
0.40
0.20
0.00
Dana Point Harbor
San Mateo - San Onofre Creeks
Las Flores Creek
French Canyon
I
II

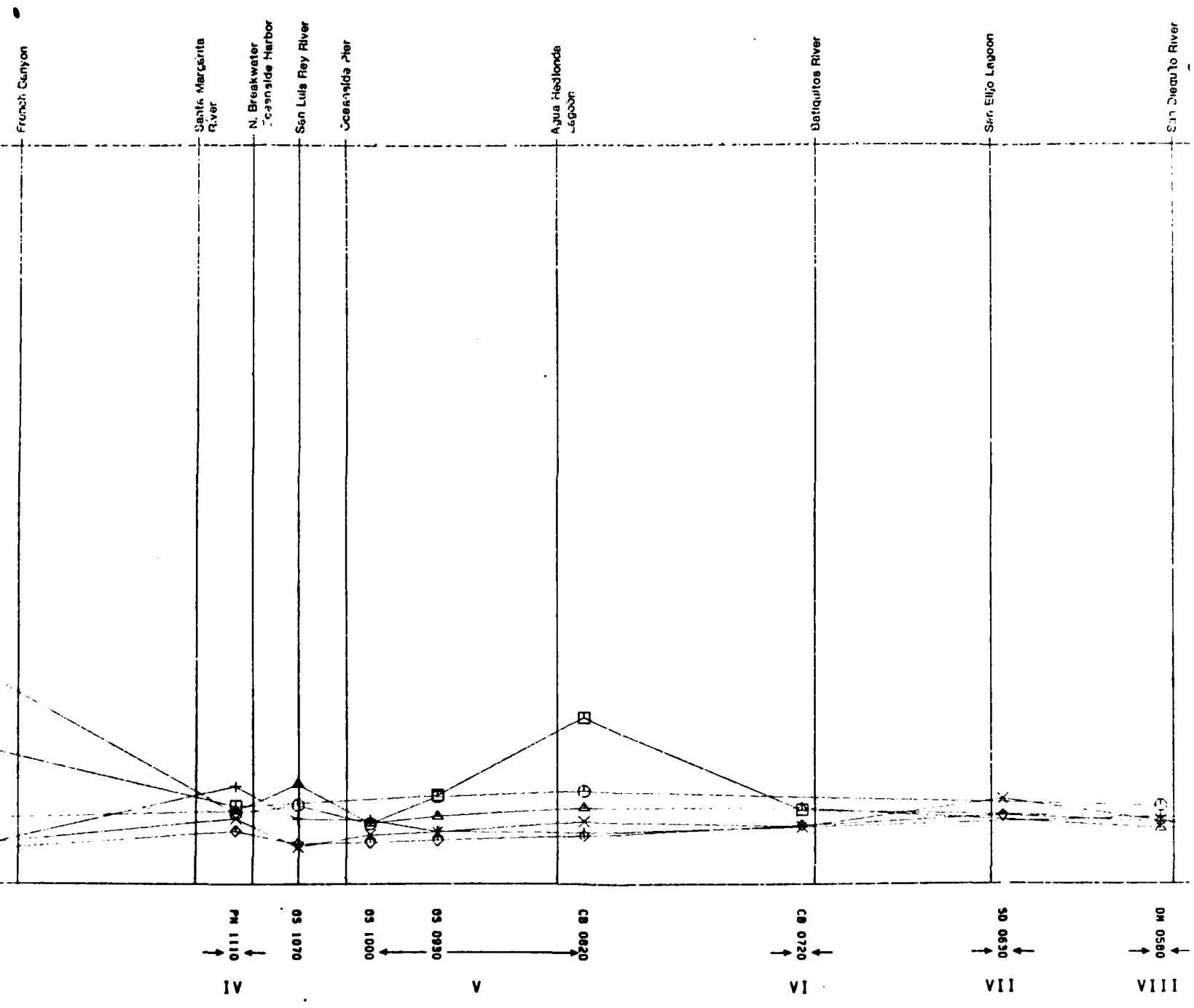

FIG. 7 - GRAIN-SIZE FINING TRENDS FOR THE END-OF-SUMMER REGIONAL

1 INCH = 2.0 MILES

2

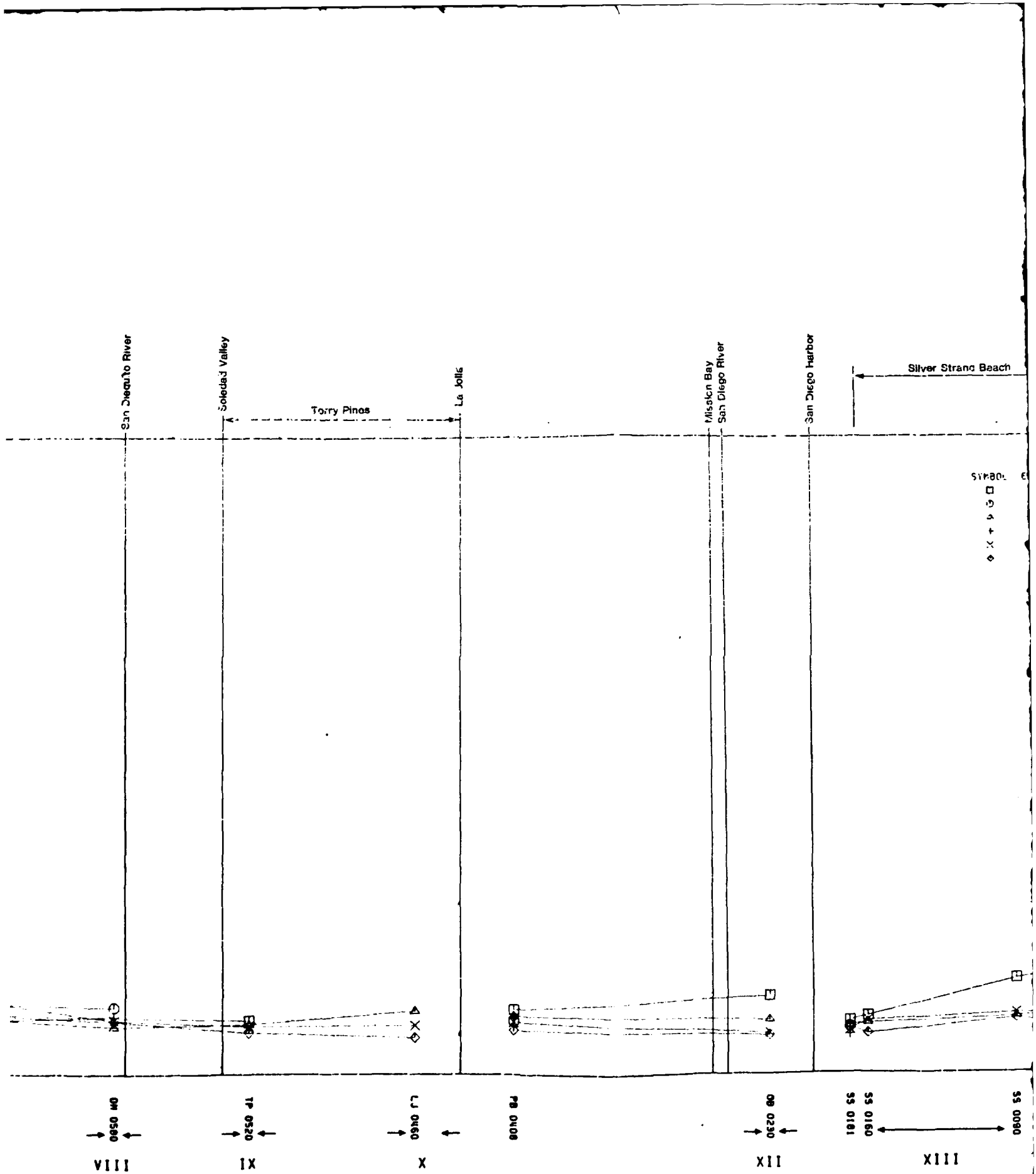

REGIONAL DATA SET

3

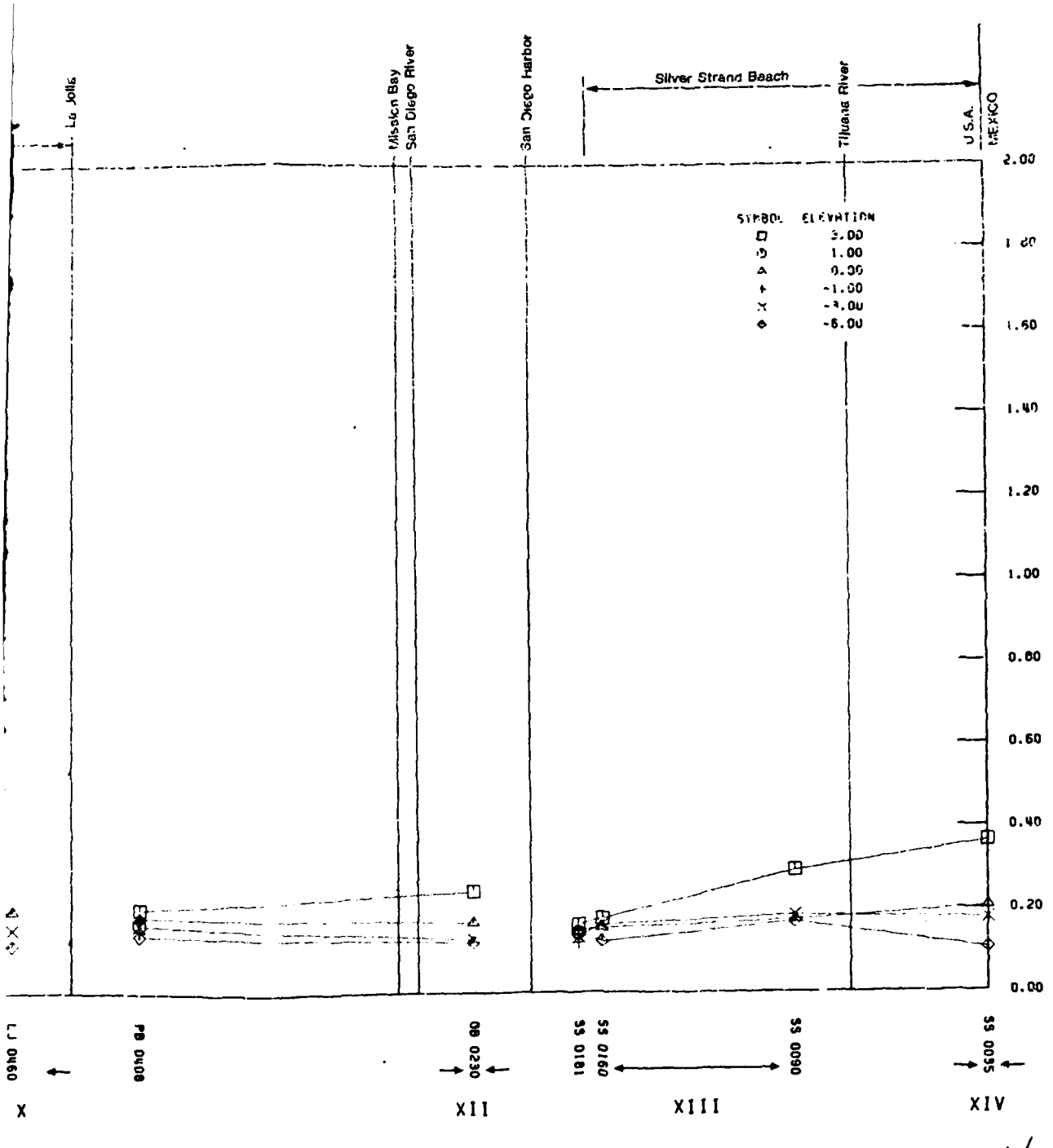
La Jolla
Mission Bay
San Diego River
San Diego Harbor
Silver Strand Beach
Tijuana River
U.S.A.
MEXICO
SYMBOL ELEVATION
5.00
1.00
0.00
-1.00
-3.00
-5.00
2.00
1.80
1.60
1.40
1.20
1.00
0.80
0.60
0.40
0.20
0.00
LJ 0060
PB 0108
08 0230
SS 0181
SS 0160
SS 0090
SS 0035
X
XII
XIII
XIV

4

downcoast. In both of these sets, the -1m samples seem to represent palimpsest fining trends, which are opposed to the trend direction indicated by samples collected at higher elevations.

5.08 The interpretation for fining trends between SO-1530 (November 10, 1983) and SO-1470 (November 27, 1983) is confusing. The +3 and -1m samples fine upcoast, whereas the 1, 0, -3, and -6m samples fine downcoast. The +3 and -1m as well as the -3 and -6m sets may represent palimpsest trends. A transition in fining direction appears to occur at an elevation between -1 and -3m.

5.09 From SO-1470 (November 27, 1983) to PN-1290 (January 8, 1984), the +3, 0 and -1m samples all fine downcoast, and the +1, -3 and -6m samples fine upcoast. The +3m trend as well as the -3 and -6m trends may be palimpsest, with a transition between the -1 and -3 sample sets. The opposition of the trends in the +1 and -3m interval is difficult to explain without additional information.

5.10 From PN-1290 (January 8, 1984) to PN-1110 (January 7, 1984), the +3 and +1m samples fine downcoast, whereas the 0, -1, -3 and -6m samples fine upcoast. The transition from the "active" littoral zone to palimpsest sediment appears to occur between 0 and -1m.

5.11 From OS-1070 (October 26, 1983) to OS-1000 (October 27, 1983), the +3, -3 and -6m samples apparently display palimpsest upcoast fining trends. The +1, 0m and -1m, samples fine downcoast. The transition from the "active" littoral transport zone to palimpsest fining trends appears to occur from -1 to -3m.

5.12 From OS-1000 (October 27, 1983) to OS-930 (October 26, 1983), the +3 and -1m samples fine downcoast, whereas the +1, 0, -3 and -6m samples fine upcoast. Again, the +3, -3 and -6m trends may be palimpsest, but the opposed directions in the +1 to -1m interval is difficult to explain.

5.13 From OS-930 (October 26, 1983) to CB-820 (October 26, 1983), the +3, +1 and 0m samples fine upcoast, the -1m samples fine downcoast, and the -3 and -6m samples display probably palimpsest upcoast fining.

5.14 From CB-820 (October 26, 1983) to CB-720 (October 18, 1983), the +3 and -3m samples fine downcoast, whereas the -6m samples show a palimpsest upcoast fining trend.

5.15 From DM-580 (October 28, 1983) to TP-520 (October 17, 1983), the 0m samples fine upcoast, the -3m samples fine downcoast, and the -6m samples show no trend. The transition in the direction of fining appears to occur between 0 and -3 m.

5.16 From TP-520 (October 17, 1983) to LJ-460 (October 17, 1983), the 0m samples fine upcoast, the -3m samples show no longshore trend, and the -6m samples display palimpsest downcoast fining.

End-of-Winter Sample Set

5.17 The end-of-winter Oceanside data set (Fig. 8) shows considerable variability with regard to both geographic location and bathymetry. The -3 and -6m fining trends usually may be interpreted as palimpsest, whereas the +3m trends may either represent the littoral wave and current system characteristic of the sampling period of may be palimpsest. The +3 and +1m samples from stations CB-880 through CB-720 display very consistent trends, which may represent reworking of higher elevation sediment into the +1m sample set. Excluding the +3m trends, the transition from the "active" to palimpsest part of the littoral zone often appears to occur between the +1 and 0m sample sets, but sometimes occurs between the -1 and -3m sets.

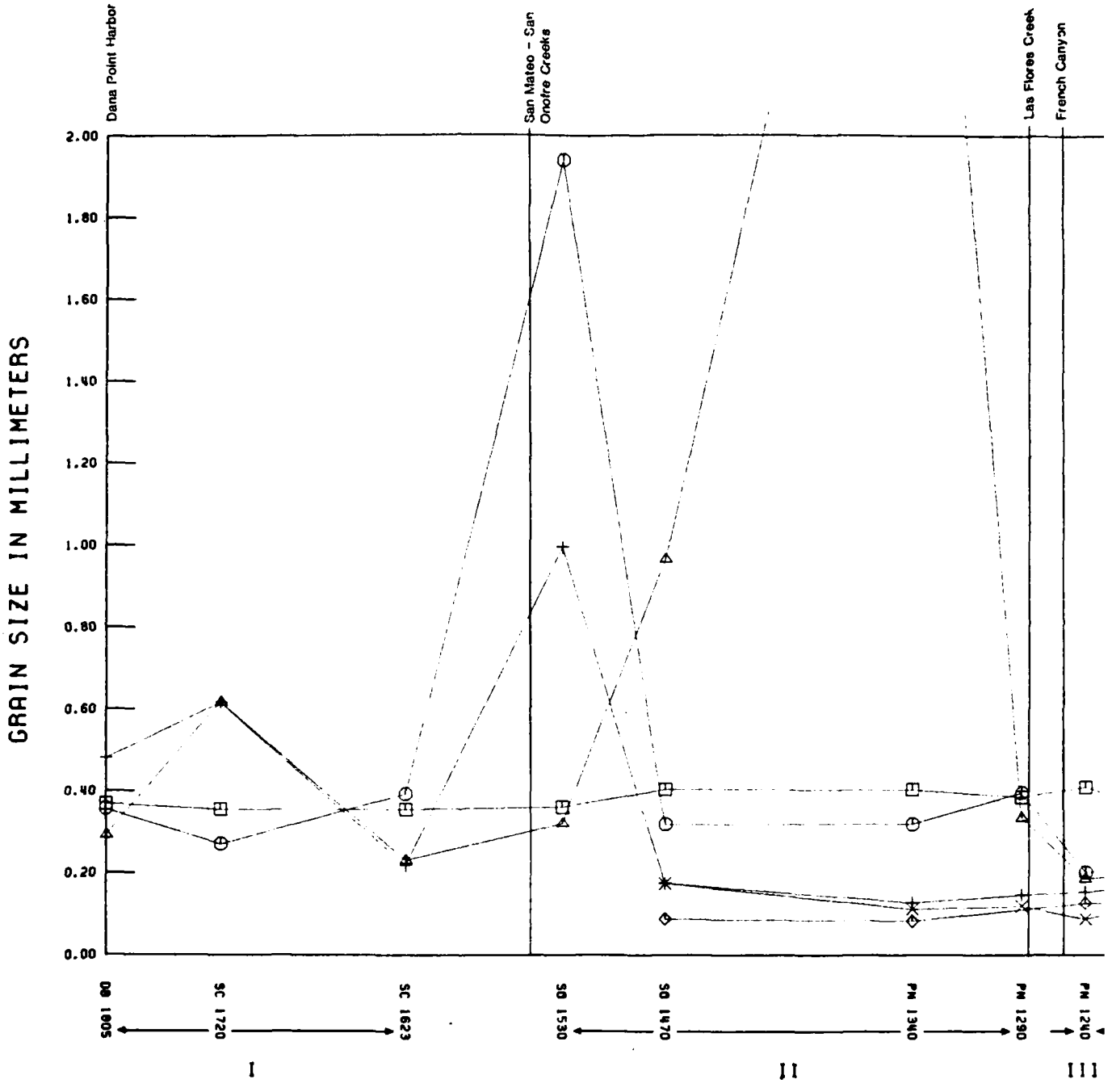
GRAIN SIZE IN MILLIMETERS
2.00
1.80
1.60
1.40
1.20
1.00
0.80
0.60
0.40
0.20
0.00
Dana Point Harbor
San Mateo - San Onofre Creeks
Las Flores Creek
French Canyon
DB 1005
SC 1720
SC 1623
SD 1530
SD 1470
PN 1390
PN 1290
PN 1240
I
II
III

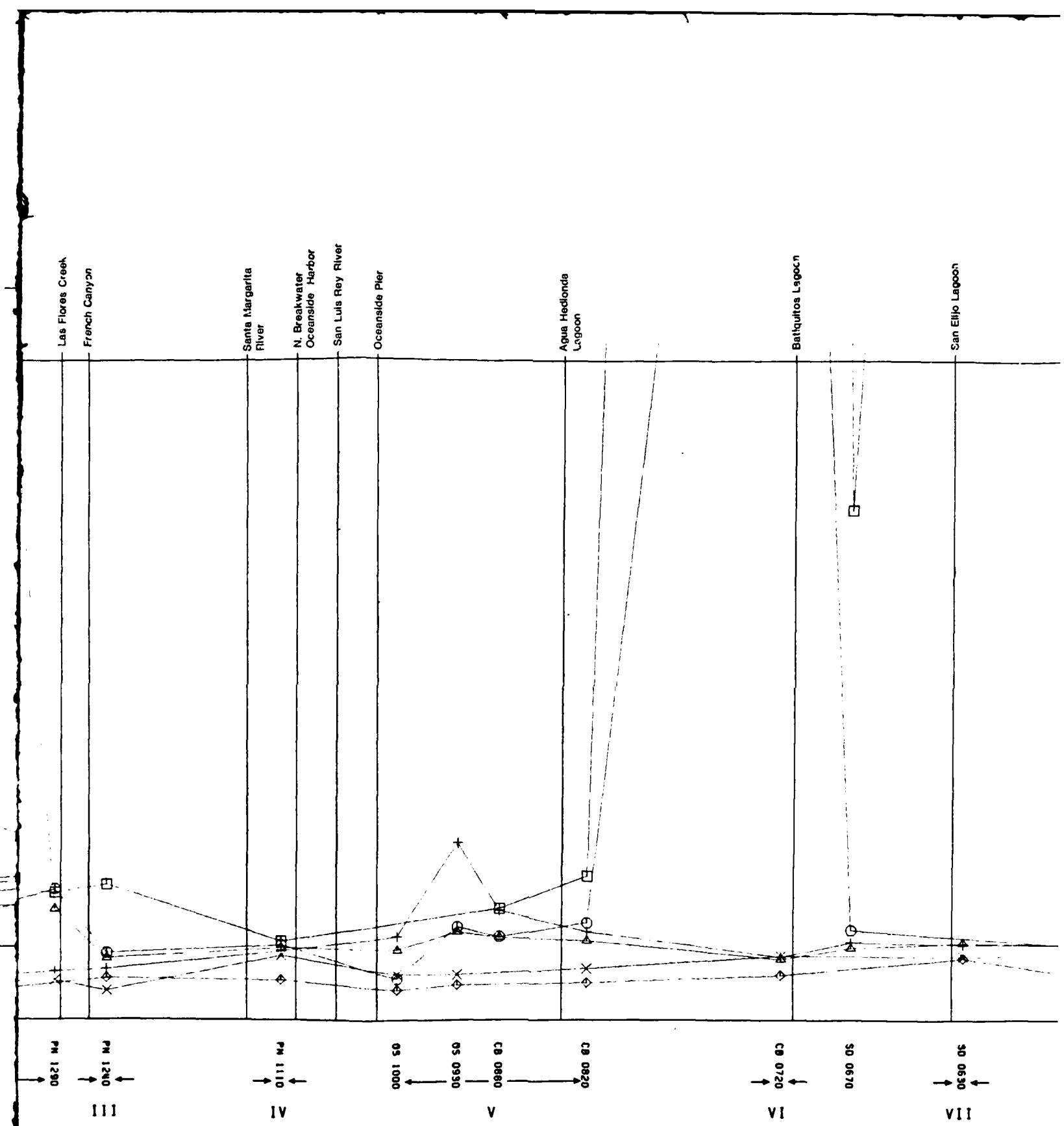

FIG. 8 - GRAIN-SIZE FINING TRENDS FOR THE END-OF-WINTER REG

1 INCH = 2.0 MILES

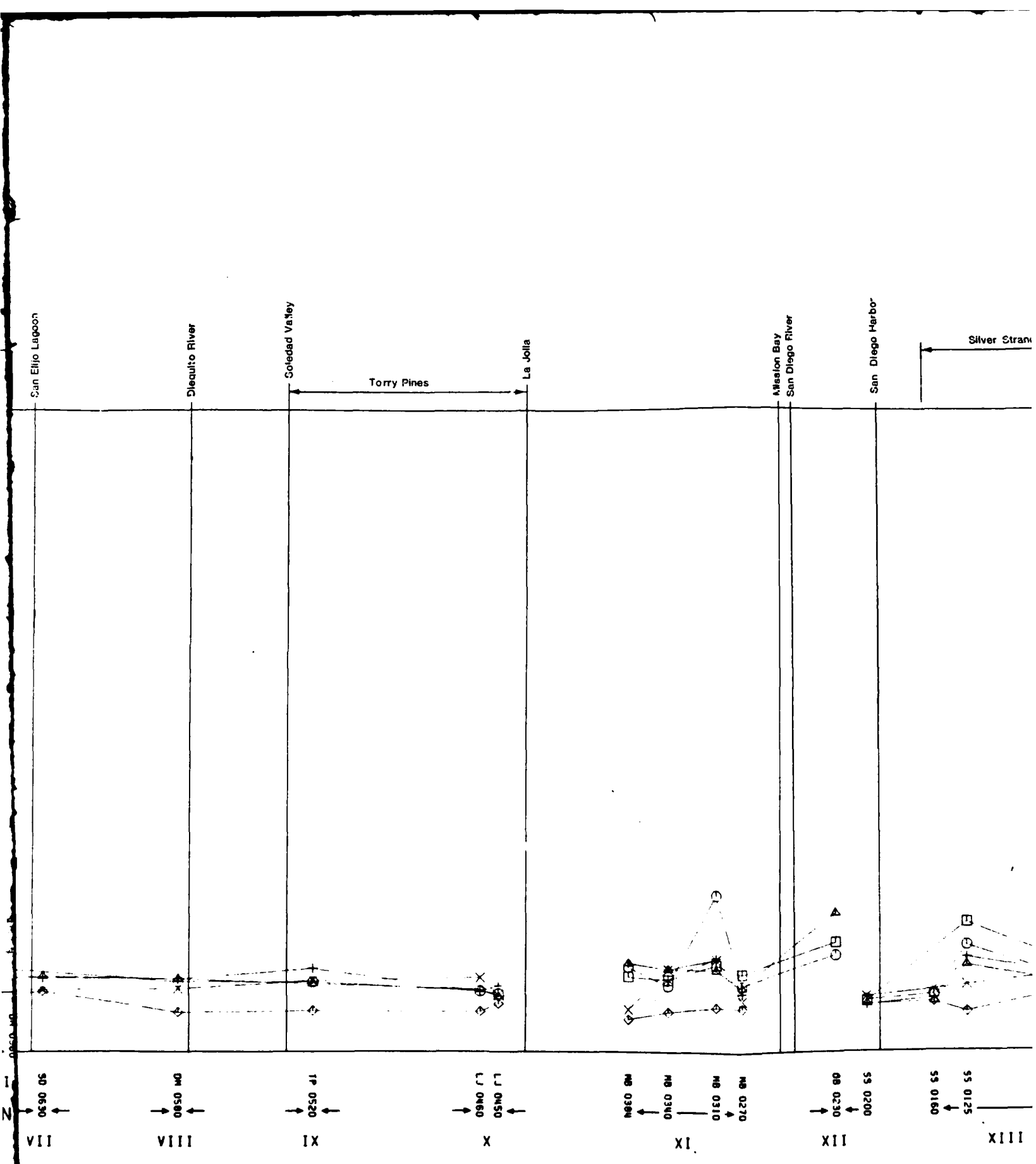

INTER REGIONAL DATA SET

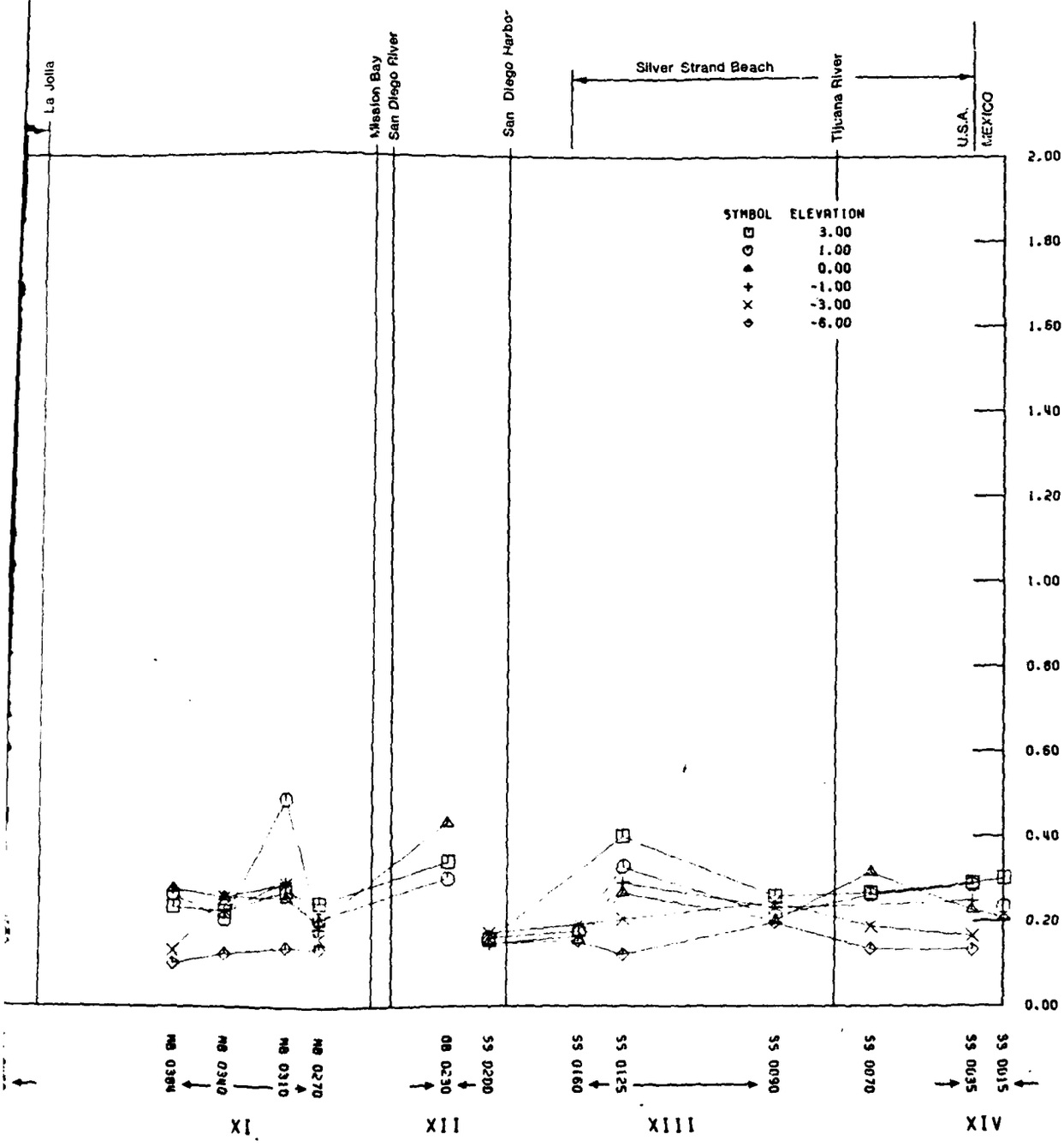
La Jolla
Mission Bay
San Diego River
San Diego Harbor
Silver Strand Beach
Tijuana River
U.S.A.
MEXICO
SYMBOL ELEVATION
3.00
1.00
0.00
-1.00
-3.00
-6.00
2.00
1.80
1.60
1.40
1.20
1.00
0.80
0.60
0.40
0.20
0.00
XI
XII
XIII
XIV

5.18 From DB-1805 (June 8, 1984) to SC-1720 (June 28, 1984), the +3 and +1m samples fine downcoast, whereas the 0 and -1m samples fine upcoast. The similarity in trend between the +3 and +1 samples may represent an inherited trend in the +1m samples through sediment reworking, and the downcoast-fining trend displayed by the 0 and -1m samples may reflect the true transport direction during the sampling period.

5.19 The transport direction from SC-1720 (June 28, 1984) to SC-1623 (June 7, 1984) is indeterminate. The 0 and -1m samples fine downcoast, whereas the +1m sample slightly fines upcoast. It is more tempting to argue for downcoast transport during the sampling period, but the opposed direction for the +1m sample set is disturbing.

5.20 The +3, +1, 0 and -1m samples all fine upcoast from station SC-1623 (June 7, 1984) to SC-1530 (June 7, 1984). The consistency of these upcoast longshore trends may reflect the sheltering of station SC-1530 from winter storms by San Mateo Point, finer-grained sediment input through the San Mateo River, or persistent longshore transport in the upcoast direction.

5.21 From SC-1530 (June 7, 1984) to SO-1470 (June 6, 1984), the +3 and 0m samples fine upcoast, whereas the +1 and -1m samples fine downcoast. The reason for these opposed trends is not apparent from the available information.

5.22 From SO-1470 (June 6, 1984) to PN-1340 (June 9, 1984), the +1m samples show no longshore fining trend, the 0m samples fine upcoast, and the -3 to -6m samples display palimpsest downcoast fining trends.

5.23 The transport direction from stations PN-1340 (June 9, 1984) to PN-1290 (June 2, 1984) is not apparent. The +3 and 0m samples fine downcoast, whereas the +1, -1 and -3m samples fine upcoast.

5.24 The sample set from PN-1290 (June 2, 1984) to PN-1240 (June 2, 1984) is equally perplexing. The +3 and -1m samples fine upcoast, whereas the +1, 0 and -3m samples fine downcoast.

5.25 From PN-1240 (June 2, 1984) to PN-1110 (May 31, 1984), the +3 and -6m samples record palimpsest downcoast fining trends, whereas the +1, 0, -1 and -3m samples all fine upcoast.

5.26 A strong fining trend is shown from station OS-1000 (May 23, 1984) to OS-930 (May 24, 1984). The +1, 0, -1 and -6m samples all fine upcoast.

5.27 From OS-930 (May 24, 1984) to CB-880 (May 25, 1984), the +1, 0 and -1m samples fine downcoast, and the -3 and -6m samples record a palimpsest upcoast fining trend.

5.28 From CB-880 (May 25, 1984) to CB-820 (May 22, 1984), and from CB-820 through CB-720 (May 21, 1984), the +3 and +1m as well as the -3 to -6m samples all display palimpsest upcoast fining trends. The +1m trends may well have been derived by reworking of sediment at higher elevation (+3m). The 0 and -1m samples fine downcoast, and probably represent the sediment transport direction at the time of sampling. The transition from the higher-level palimpsest trends to the "active" portion of the littoral zone appears to have been from +1 to 0m, and the transition to the lower palimpsest tends from -1 to -3m.

5.29 A similar relationship exists from CB-720 (May 21, 1984) to SD-670 (May 10, 1984). The +3 and +1m samples both fine downcoast and the +1m trend is largely inherited through reworking; however, the 0 and -1m samples fine upcoast between these two stations.

5.30 The sediment transport direction is indeterminate between stations SD-670 (May 10, 1984) and SD-630 (May 18, 1984). The 0m samples fine upcoast, but the -1m samples slightly fine downcoast.

5.31 From SD-630 (May 18, 1984) to DM-580 (May 9, 1984), the 0, -1 and -6m samples fine downcoast, whereas the -3m samples fine upcoast. The downcoast trends shown by the 0 and -1m samples probably reflect the transport direction during the sampling period, and the -3 and -6m trends probably are palimpsest.

5.32 The transport direction from DM-580 (May 9, 1984) to TP-520 (May 9, 1984) is indeterminate. The +1 and 0m samples fine downcoast, and the -1, -3, and -6m samples fine upcoast. The opposition of the 0 and -1m samples is difficult to reconcile with the available data.

5.33 From TP-520 (May 9, 1984) to LJ-460 (April 23, 1984), the +1, 0, -1 and -6m samples fine downcoast, whereas the -3m samples fine upcoast. The -3 and -6m samples may reflect palimpsest trends, which would suggest downcoast transport during the sample period, with a transition from "active" littoral to palimpsest trends from -1 to -3m.

5.34 From LJ-460 (April 23, 1984) to LJ-450 (May 3, 1984), the +1, 0 and -3m samples fine downcoast, and the -1 and -6m samples fine upcoast. Although the -3 and -6m trends may be palimpsest, the opposition of the 0 and -1m trends is difficult to explain with the available information.

Littoral Transport Directions, Mission Beach Cell

End-of-Summer Sample Set

5.35 Only two samples were taken for this set (PB-408 and OB-230), which occur on opposite sides of the Mission Bay jetties (Fig. 7). No meaningful longshore transport trends can be obtained from these data, because of the interference of the jetties.

End-of-Winter Sample Set

5.36 Samples MB-384 through MB-310 were collected from April 30 through May 2, 1984, but MB-270 was not collected until June 27, 1984. If available, wave statistics for this interval should be reviewed to determine whether or not important changes occurred.

5.37 From MB-384 to MB-340, the +3 through -1m sample sets fine downcoast (Fig. 8), whereas the -3 and -6m samples display a palimpsest upcoast fining trend. From MB-340 to MB-310, samples from +3 to -6m generally fine upcoast, but the 0m samples show very little change. It is not known whether this represents a palimpsest summer condition or if it reflects wave patterns affected by the Mission Bay jetties. From MB-310 to MB-270, all samples from +3m to -6m fine downcoast.

5.38 Inasmuch as Mission Beach is a spit elongated downcoast, the longterm net transport direction has been downcoast.

Littoral Transport Directions, Silver Strand Cell

End-of-Summer Sample Set

5.39 Although the sample spacing and depths of the end-of-summer sample set is unsystematic as compared with the associated winter set (Fig. 7), the summer set was collected over a short time interval (October 20 through 24, 1983). The -6m samples from SS-180 to SS-160 and the -3 and -6m samples from SS-090 to SS-035 show downcoast fining trends indicative of winter swell, whereas all other sample pairs show upcoast fining indicative of summer swell conditions. This data may be interpreted as reflecting a normal summer pattern with upcoast sediment transport with the -3 and -6m trends representing palimpsest conditions from an earlier winter swell.

End-of-Winter Sample Set

5.40 Although the sample spacing and bathymetric control is acceptable for this set (Fig. 8), the samples were taken over a period extending from February 29 through May 17, 1984. Unless there is wave data to justify this extended sampling interval, any interpretation of the associated longshore grain-size trends may range from wishful thinking to contrived. From stations SS-200 to SS-125, all samples from +3 to -3m show upcoast fining, which probably reflects the sheltering of this area from winter storms by Point Loma. From SS-125 to SS-90, the +3 to -1m samples reflect expected downcoast fining, whereas the -3 to -6m sample sets reflect palimpsest upcoast fining trends. From SS-90 to SS-15, +3 to +1 or 0m samples generally show upcoast fining, but deeper samples usually show palimpsest downcoast fining.

5.41 The fact that the Silver Strand is a spit elongated upcoast argues convincingly for net longterm upcoast transport.

6. BIVARIATE PLOTS OF GRAIN-SIZE PARAMETERS

6.01 Bivariate plots were constructed using the combinations of mean phi, phi standard deviation, phi skewness and kurtosis (Tables 3 and 4) for each sediment sample. Although these plots were prepared for each littoral segment (Appendices A through F), they were pooled for interpretative purposes due to the small number of samples present in many of the littoral segments. The fields shown in Figures 9 through 14 are based on the areas with the greatest concentration of points, and the mean values for the mean phi and phi standard deviation are shown by dots on the appropriate bars in Figures 9 through 14. Data values considered as statistical outliers are included in the computations for the mean phi and phi standard deviations, therefore the dots may not be centered on the bars.

Phi Standard Deviation Versus Mean Phi

6.02 Figure 9 shows the bivariate plot of phi standard deviation versus mean phi for the end-of-summer sample set. The +3 and +1m samples show similar ranges with mean phi values from 0.75 to 2.75. The 0m samples are finer grained with a much smaller range of values (1.80 to 2.80 phi), which may reflect the presence of a slightly coarser-grained lag deposit on the upper shoreface. The samples from -1 through -6m show progressive fining, and a similar range of associated mean phi values of about 1.40 phi units.

6.03 The range of values for the phi standard deviation decreases from 0.63 at +3m to 0.56 at +1m, which most likely represents progressive sorting by nearshore waves and currents. The range of values then increases to 0.72 at -1m and 0.68 at -3m, and then decreases to 0.55 at -6m; which may reflect sediment mixing in the -1 to -3m zone, followed by settling from low-energy currents or suspension at -6m. The samples all range from moderately well-sorted to very well-sorted (Folk, 1974), as might be expected from sediment deposited in a high-energy littoral zone.

TABLE 3.

SUMMARY OF GRAIN-SIZE PARAMETERS FOR THE END-OF-SUMMER REGIONAL SET

SAMPLE	ELEVATION	PHI	MM	SD	SKEW	KURT
DB 1305	3.00M0	1.3225	0.3998	0.5704	-0.2680	3.4046
DB 1305	1.00M1	-2.1100	4.3169	1.6535	1.0451	2.5211
DB 1305	0.00M2	-2.3238	5.0063	1.3811	1.1864	3.0527
DB 1305	-1.00M3	2.0838	0.2359	1.1569	-1.9467	8.0881
DB 1305	-3.00M4	3.0850	0.1178	1.0754	-1.6508	4.7178
SC 1623	3.00M0	1.6825	0.3115	0.9484	0.1102	3.1957
SC 1623	1.00M1	1.3563	0.3906	0.6438	-2.0642	10.5658
SC 1623	0.00M2	1.8700	0.2736	0.5868	-1.1741	7.2179
SC 1623	-1.00M3	-0.1275	1.0924	2.0678	-0.2051	1.6194
SO 1530	3.00M0	1.4500	0.3660	0.5958	-0.1702	2.5848
SO 1530	1.00M1	0.9900	0.5035	0.6547	-0.3773	2.7746
SO 1530	0.00M2	-2.0750	4.2134	1.8162	0.8850	2.7424
SO 1530	-1.00M3	2.7875	0.1448	0.7869	-1.7188	7.9628
SO 1530	-3.00M4	3.0800	0.1183	0.5724	-1.1320	5.2604
SO 1530	-6.00M5	3.5062	0.0880	0.5164	-1.8745	7.5442
OS 1470	3.00M0	1.0875	0.4974	0.6647	-0.1568	2.8781
OS 1470	1.00M1	1.9950	0.2509	0.4555	0.2280	3.2507
OS 1470	0.00M2	2.0650	0.2398	0.5033	-0.8579	5.3435
OS 1470	-1.00M3	1.9550	0.2579	0.8539	-0.9874	3.4717
OS 1470	-3.00M4	3.4200	0.0934	0.4396	-0.7936	4.2817
OS 1470	-6.00M5	3.6688	0.0786	0.4067	-2.6128	14.6344
OS 1470	3.00M0	1.2325	0.4256	0.5434	-0.0036	3.8063
OS 1470	1.00M1	1.7425	0.2989	0.5080	-0.6815	6.6126
OS 1470	0.00M2	2.0600	0.2398	0.4460	-0.1947	4.9604
OS 1470	-1.00M3	2.4500	0.1830	0.4743	-0.8011	6.1541
OS 1470	-3.00M4	2.6225	0.1624	0.6080	-0.1171	2.2714
PN 1290	3.00M0	1.4300	0.3711	0.6296	-0.2537	4.0545
PN 1290	1.00M1	0.7925	0.5773	0.9118	0.3967	2.4552
PN 1290	0.00M2	2.4887	0.1782	0.6996	-2.9044	16.7593
PN 1290	-1.00M3	3.2550	0.1047	0.5291	-3.5322	21.3626
PN 1290	-3.00M4	3.2000	0.1088	0.7226	-4.7398	31.4201
PN 1290	-6.00M5	3.4262	0.0930	0.4985	-1.9106	10.5857
PN 1110	3.00M0	2.2500	0.2102	0.5099	-0.4526	4.7337
PN 1110	1.00M1	2.3875	0.1911	0.6074	-0.3595	3.5624
PN 1110	0.00M2	2.3387	0.1977	0.6771	-0.8311	3.8168
PN 1110	-1.00M3	1.9162	0.2649	0.7636	-0.3389	3.1878
PN 1110	-3.00M4	2.4950	0.1774	0.6640	-1.4807	7.1640
PN 1110	-6.00M5	2.8063	0.1430	0.6542	-0.1893	3.0076
OS 1070	2.10M0	2.2475	0.2106	0.6607	-1.3327	7.8619
OS 1070	1.00M1	2.2287	0.2133	0.5108	-0.0271	3.7131
OS 1070	0.00M2	1.8850	0.2707	0.5695	0.0675	3.1916
OS 1070	-1.00M3	2.5038	0.1763	0.9183	-1.4406	6.2322
OS 1070	-3.00M4	3.3200	0.1001	0.4695	-1.1116	6.5819
OS 1070	-6.00M5	3.2000	0.1088	0.5405	-1.1119	5.0189
OS 1000	2.10M0	1.7925	0.2887	0.5799	-0.4902	5.3998
OS 1000	1.00M1	2.6225	0.1624	0.4433	-0.3224	3.6194
OS 1000	0.00M2	2.6063	0.1642	0.5122	-0.6983	3.9706
OS 1000	-1.00M3	2.5338	0.1727	0.6339	-1.5601	8.3427
OS 1000	-3.00M4	2.9100	0.1330	0.9828	-1.5063	5.6991
OS 1000	-6.00M5	3.1512	0.1126	0.4580	-1.1070	6.2244
OS 0930	3.00M0	2.0650	0.2390	0.5082	-0.5834	5.2807
OS 0930	1.00M1	2.0875	0.2353	0.7717	-1.3805	5.2939
OS 0930	0.00M2	2.4550	0.1824	1.0852	-1.4253	4.1857
OS 0930	-1.00M3	2.8200	0.1416	0.7682	-1.4754	6.3668
OS 0930	-3.00M4	2.8438	0.1393	0.7904	-1.8411	8.3209
OS 0930	-6.00M5	3.0825	0.1181	0.5605	-0.7769	3.7992

TABLE 3. (cont.)

CB	0820	3.00M0	1.1525	0.4498	0.8485	0.3348	2.4591
CB	0820	1.00M1	1.9950	0.2509	0.4387	-0.1471	5.5303
CB	0820	0.00M2	2.2775	0.2063	0.5675	-0.2303	4.0822
CB	0820	-1.00M3	2.8488	0.1388	0.5914	-1.7500	8.7913
CB	0820	-3.00M4	2.5650	0.1690	0.7129	-0.6110	3.9727
CB	0820	-6.00M5	2.9400	0.1303	0.6446	-0.6000	3.0707
CB	0720	3.00M0	2.3200	0.2003	0.3743	0.1952	3.4003
CB	0720	0.00M2	2.2775	0.2063	0.7727	-1.1301	6.0208
CB	0720	-3.00M4	2.6837	0.1556	0.6112	-0.0820	2.5532
CB	0720	-6.00M5	2.6537	0.1589	0.5422	-0.3652	3.3456
SO	0630	-3.00M4	2.1250	0.2293	0.5847	-0.4057	3.9916
SO	0630	-6.00M5	2.4288	0.1857	0.7728	-0.1424	2.8854
DM	0580	1.00M1	2.2513	0.2100	0.6674	-1.2558	7.7091
DM	0580	0.00M2	2.7413	0.1496	0.4477	-0.3165	3.0101
DM	0580	-1.00M3	2.4750	0.1799	0.6483	-1.3664	7.2179
DM	0580	-3.00M4	2.5550	0.1702	0.6924	-0.5630	4.2642
DM	0580	-6.00M5	2.5787	0.1674	0.6549	0.0294	2.8704
TP	0520	3.00M0	2.5625	0.1693	0.4502	-0.0796	3.3581
TP	0520	0.00M3	2.6737	0.1567	0.4175	-0.2641	3.1915
TP	0520	-3.00M4	2.7287	0.1509	0.4476	-0.2506	3.3634
TP	0520	-6.00M5	2.9337	0.1309	0.5042	-0.5625	3.5438
LJ	0460	2.00M0	2.5850	0.1667	0.6548	-2.9415	17.2770
LJ	0460	0.00M2	2.3363	0.1980	0.6120	-0.5746	4.6596
LJ	0460	-3.00M4	2.7062	0.1532	0.7938	-1.9597	8.8618
LJ	0460	-6.00M5	3.1175	0.1152	0.4301	-0.3204	2.9023
PB	0408	3.00M0	2.2950	0.2038	0.4642	-0.2542	3.3132
PB	0408	1.00M1	2.5775	0.1675	0.5689	-0.1679	2.5250
PB	0408	0.00M2	2.4425	0.1840	0.5859	-0.4083	2.9931
PB	0408	-1.00M3	2.7325	0.1505	0.4664	-0.6548	3.5892
PB	0408	-3.00M4	2.5950	0.1655	0.6835	0.0907	2.4345
PB	0408	-6.00M5	2.8438	0.1393	0.6961	-0.8158	4.3222
OB	0230	3.00M0	2.0300	0.2449	0.4082	0.3030	4.0049
OB	0230	0.00M2	2.5538	0.1703	0.7069	-0.8129	3.3606
OB	0230	-3.00M4	2.9550	0.1290	0.6712	-1.0885	4.0424
OB	0230	-6.00M5	3.0350	0.1220	0.6065	-1.0686	4.8187
SS	0181	3.00M0	2.6163	0.1631	0.5292	-1.2321	7.0208
SS	0181	1.00M1	2.7963	0.1440	0.4072	-0.5258	4.0281
SS	0181	0.00M2	2.7562	0.1480	0.5930	-1.7798	8.9141
SS	0181	-1.00M3	3.0538	0.1284	0.5498	-1.5493	7.3007
SS	0181	-3.00M4	2.9063	0.1334	0.6153	-1.8988	9.1627
SS	0181	-6.00M5	2.8287	0.1408	0.5625	-0.6588	4.0671
SS	0160	3.00M0	2.4887	0.1782	0.4737	-0.2313	3.7206
SS	0160	0.00M2	2.6813	0.1559	0.5137	-0.0986	2.6011
SS	0160	-3.00M4	2.6063	0.1642	0.5977	-0.9849	4.8224
SS	0160	-6.00M5	3.0225	0.1231	0.4810	-1.1092	5.4728
SS	0090	3.00M0	1.7700	0.2932	0.5416	-1.4896	7.8605
SS	0090	0.00M2	2.5225	0.1740	0.4648	0.1382	2.7894
SS	0090	-3.00M4	2.4288	0.1857	0.6541	-1.2644	6.7235
SS	0090	-6.00M5	2.5612	0.1694	0.8931	-1.7049	7.2087
SS	0035	3.00M0	1.4625	0.3629	0.7837	-0.8793	2.7693
SS	0035	0.00M2	2.2887	0.2047	0.5049	-0.2133	3.8025
SS	0035	-3.00M4	2.5813	0.1766	0.6726	-1.6715	8.8639
SS	0035	-6.00M5	3.2525	0.1049	0.6162	-1.4386	6.6526

TABLE 4.

SUMMARY OF GRAIN-SIZE PARAMETERS FOR THE END-OF-WINTER REGIONAL DATA SET

SAMPLE	ELEVATION	PHI	MM	SD	SKEW	KURT
DB 1005	3.00M0	1.4425	0.3679	0.5776	-0.4197	3.3749
DB 1005	1.00M1	1.4887	0.3563	0.5804	0.5001	3.7943
DB 1005	0.00M2	1.7750	0.2922	0.5540	-0.0987	3.5297
DB 1005	-1.00M3	1.0600	0.4796	0.8427	-0.2735	3.1753
SC 1720	3.00M0	1.4950	0.3548	0.5074	-0.4608	3.0099
SC 1720	1.00M1	1.8850	0.2707	0.4575	-1.0285	4.7226
SC 1720	0.00M2	0.6975	0.6166	2.4316	-1.5147	3.6506
SC 1720	-1.00M3	0.7013	0.6150	2.0050	-0.7705	2.3580
SC 1623	3.00M0	1.5000	0.3536	0.6010	-1.7271	7.9028
SC 1623	1.00M1	1.3525	0.3916	0.5778	-1.2092	4.4988
SC 1623	0.00M2	2.1150	0.2308	0.4942	-0.8685	5.6051
SC 1623	-1.00M3	2.1950	0.2184	0.3801	-0.2230	3.3081
SO 1530	3.00M0	1.4750	0.3597	0.3961	-0.3787	3.0614
SO 1530	1.00M1	-0.9550	1.9386	2.8021	-0.4429	1.2521
SO 1530	0.00M2	1.6450	0.3197	0.5258	0.0137	3.2615
SO 1530	-1.00M3	0.0088	0.9940	1.8660	-0.6667	2.0672
SO 1470	3.00M0	1.3125	0.4026	0.4865	-0.5489	3.8642
SO 1470	1.00M1	1.6550	0.3175	0.4566	-0.4042	3.0690
SO 1470	0.00M2	0.0538	0.9634	1.9547	-0.8898	2.5987
SO 1470	-1.00M3	2.5238	0.1739	0.3794	0.0869	3.0249
SO 1470	-3.00M4	2.5213	0.1742	0.4753	0.2399	3.2106
SO 1470	-6.00M5	3.5162	0.0874	0.5375	-2.0001	9.5233
PN 1340	3.00M0	1.3150	0.4019	0.5311	-0.7175	4.2696
PN 1340	1.00M1	1.6525	0.3181	0.8930	-1.7522	5.8792
PN 1340	0.00M2	-1.8587	3.6269	2.4861	0.5372	1.7140
PN 1340	-1.00M3	2.9750	0.1272	0.7927	-2.3574	10.0134
PN 1340	-3.00M4	3.1637	0.1116	0.3268	-0.5483	4.5019
PN 1340	-6.00M5	3.5963	0.0827	0.4596	-1.5746	6.6343
PN 1290	3.00M0	1.3800	0.3842	0.4776	-0.3319	2.6742
PN 1290	1.00M1	1.3425	0.3943	0.5891	-0.3458	2.7048
PN 1290	0.00M2	1.5825	0.3339	0.5821	-1.6949	6.4752
PN 1290	-1.00M3	2.7762	0.1460	0.6233	-2.3196	11.9823
PN 1290	-3.00M4	3.0687	0.1192	0.4075	-1.0060	5.9366
PN 1240	3.00M0	1.2925	0.4082	0.5185	-0.2543	3.3128
PN 1240	1.00M1	2.3150	0.2010	0.4102	-0.8958	4.5881
PN 1240	0.00M2	2.4325	0.1852	0.8046	-1.6963	5.5131
PN 1240	-1.00M3	2.7037	0.1535	0.4722	-1.0540	5.2644
PN 1240	-3.00M4	3.5162	0.0874	0.3613	-0.3682	3.2457
PN 1240	-6.00M5	2.9913	0.1258	0.4210	-2.9275	18.8159
PN 1110	3.00M0	2.0775	0.2369	0.5653	-1.4558	10.6947
PN 1110	1.00M1	2.1500	0.2253	0.4062	-0.0671	2.8264
PN 1110	0.00M2	2.2000	0.2176	0.4031	-0.0458	2.5830
PN 1110	-1.00M3	2.2750	0.2066	0.5804	-1.1714	4.8995
PN 1110	-3.00M4	2.3600	0.1948	0.4826	-0.9848	5.5841
PN 1110	-6.00M5	3.0563	0.1202	0.3506	-0.4351	3.4437
PN 1110	10.00M	-4.1312	17.5239	1.1842	4.5862	25.5774
PN 1110	15.00M	3.8012	0.0717	0.3231	-1.5503	4.5735
OS 1000	1.00M1	3.0113	0.1240	0.4265	-0.4938	3.6170
OS 1000	0.00M2	2.2450	0.2110	0.3122	0.2534	3.3695
OS 1000	-1.00M3	1.9950	0.2509	0.4769	0.2705	2.6589
OS 1000	-3.00M4	2.8700	0.1368	0.6031	-1.9286	11.3385
OS 1000	-6.00M5	3.4738	0.0900	0.4229	-0.6231	3.3621
OS 1000	10.00M	3.7162	0.0761	0.4224	-1.8649	7.3736
OS 1000	15.00M	3.8975	0.0671	0.2420	-2.4879	8.8324

TABLE 4. (cont.)

OS	0930	1.00M1	1.8300	0.2813	0.4512	-0.8912	3.6992
OS	0930	0.00M2	1.9100	0.2661	0.3992	-1.1095	4.9708
OS	0930	-1.00M3	0.9025	0.5350	1.0066	-1.0427	5.3874
OS	0930	-3.00M4	2.0663	0.1371	0.3902	-0.3315	3.3439
OS	0930	-6.00M5	3.2338	0.1063	0.4296	-0.4320	3.6422
CB	0880	3.00M0	1.5700	0.3368	0.4389	-0.5639	3.3951
CB	0880	1.00M1	1.8900	0.2517	0.4030	-0.2789	3.0553
CB	0880	0.00M2	2.0000	0.2500	0.3841	-0.3310	3.3108
CB	0880	-1.00M3	1.5950	0.3310	0.5324	0.0450	2.5467
CB	0820	3.00M0	1.2000	0.4353	0.9083	-0.0328	3.2441
CB	0820	1.00M1	1.7650	0.2942	0.3966	-0.4141	3.1620
CB	0820	0.00M2	2.0650	0.2406	0.3598	-0.8713	4.1296
CB	0820	-1.00M3	1.9050	0.2670	0.4566	-1.0444	4.2942
CB	0820	-3.00M4	2.6037	0.1556	0.6949	-1.5392	7.4463
CB	0820	-6.00M5	3.1450	0.1130	0.4849	-0.4542	4.1629
CB	0720	3.00M0	-4.4375	21.6681	0.2724	4.1295	18.0526
CB	0720	1.00M1	-2.4237	5.3656	1.9054	1.5498	4.2303
CB	0720	0.00M2	2.4400	0.1843	0.3223	0.1170	2.8452
CB	0720	-1.00M3	2.3000	0.1921	0.2968	-0.1551	4.3986
CB	0720	-3.00M4	2.3637	0.1943	0.6142	-1.1269	7.7097
CB	0720	-6.00M5	2.8737	0.1364	0.5152	-0.0828	2.5960
SD	0670	3.00M0	-0.6275	1.5449	2.7234	-0.0969	1.1086
SD	0670	1.00M1	1.8750	0.2726	0.3631	-0.2643	3.0531
SD	0670	0.00M2	2.1900	0.2192	0.2853	-0.0057	2.9350
SD	0670	-1.00M3	2.0850	0.2357	0.3940	-0.3252	3.9978
SD	0630	0.00M2	2.0900	0.2349	0.3072	-0.7100	3.5534
SD	0630	-1.00M3	2.1250	0.2293	0.3700	-1.4903	8.5304
SD	0630	-3.00M4	2.3725	0.1931	0.5274	-0.0116	3.5074
SD	0630	-6.00M5	2.4162	0.1873	0.5517	-0.3458	4.7762
DM	0580	1.00M1	2.1950	0.2184	0.3383	-0.0567	3.7625
DM	0580	0.00M2	2.1350	0.2277	0.3151	-0.4949	3.5972
DM	0580	-1.00M3	2.1400	0.2269	0.4098	-0.0111	3.2752
DM	0580	-3.00M4	2.3512	0.1960	0.5539	-1.1473	8.5616
DM	0580	-6.00M5	3.0213	0.1232	0.5394	-0.1475	2.6577
DM	0580	10.00M	3.2963	0.1018	0.5293	-0.4349	2.7101
DM	0580	15.00M	3.4150	0.0938	0.5364	-0.7271	3.0052
TP	0520	3.00M0	-4.2613	19.1763	0.5268	2.0555	6.5524
TP	0520	1.00M1	2.2050	0.2169	0.2924	-0.2849	3.7026
TP	0520	0.00M2	2.2400	0.2117	0.3807	-0.5104	4.5264
TP	0520	-1.00M3	1.9500	0.2588	0.5148	-0.3629	2.9640
TP	0520	-3.00M4	2.1750	0.2214	0.5117	-0.9843	4.7527
TP	0520	-6.00M5	2.9750	0.1272	0.4444	-0.2254	3.3354
LJ	0460	1.00M1	2.4100	0.1882	0.2990	-0.2622	2.3582
LJ	0460	0.00M2	2.3750	0.1928	0.3112	0.0155	2.7773
LJ	0460	-1.00M3	2.4150	0.1875	0.3045	-0.0158	2.6590
LJ	0460	-3.00M4	2.1250	0.2293	0.5166	-1.0098	5.3460
LJ	0460	-6.00M5	3.0075	0.1244	0.3605	-0.3977	2.8696
LJ	0460	10.00M	3.0100	0.1241	0.3928	-0.4877	3.5026
LJ	0460	15.00M	3.1125	0.1156	0.3664	-0.3591	3.4432
LJ	0450	1.00M1	2.4800	0.1792	0.3195	-0.0802	2.7293
LJ	0450	0.00M2	2.5450	0.1713	0.3098	-0.4718	2.9754
LJ	0450	-1.00M3	2.2950	0.2038	0.3008	0.2368	3.4648
LJ	0450	-3.00M4	2.5000	0.1768	0.4153	-0.3141	3.4499
LJ	0450	-6.00M5	2.7462	0.1490	0.3947	0.1095	3.2349
MB	0384	3.00M0	2.1000	0.2333	0.3282	-0.3200	3.1511
MB	0384	1.00M1	1.9250	0.2633	0.3897	-0.1917	3.0227
MB	0384	0.00M2	1.8600	0.2755	0.5412	-0.4920	3.5745
MB	0364	-1.00M3	2.0900	0.2349	0.4684	-0.2734	2.8339
MB	0384	-3.00M4	2.9313	0.1311	0.4317	-0.6604	4.6316
MB	0384	-6.00M5	3.3100	0.1008	0.4091	-0.1240	3.1197
MB	0340	3.00M0	2.1600	0.2238	0.2773	-0.3990	3.7006

TABLE 4. (cont.)

MB	0340	1.00M1	2.2850	0.2052	0.3623	-0.2644	3.2739
MB	0340	0.00M2	1.9600	0.2570	0.6212	-0.6461	3.2135
MB	0340	-1.00M3	2.1450	0.2261	0.4811	-0.1093	2.9876
MB	0340	-3.00M4	1.9600	0.2570	0.4959	0.0682	3.4482
MB	0340	-6.00M5	3.0113	0.1240	0.4366	-0.3583	3.2145
MB	0310	3.00M0	1.8800	0.2717	0.3976	-0.3795	3.0941
MB	0310	1.00M1	1.0375	0.4872	0.5931	-0.2012	2.9070
MB	0310	0.00M2	1.9700	0.2553	0.6013	-0.6521	3.1543
MB	0310	-1.00M3	1.7725	0.2927	0.4823	-1.1219	6.4688
MB	0310	-3.00M4	1.7925	0.2887	0.5304	-0.7446	5.2154
MB	0310	-6.00M5	2.8450	0.1392	0.4521	-1.4059	7.8974
MB	0270	3.00M0	2.0400	0.2432	0.3548	-0.7034	3.9965
MB	0270	1.00M1	2.2750	0.2066	0.3562	-0.0726	2.9028
MB	0270	0.00M2	2.3200	0.2003	0.3466	0.1666	2.8254
MB	0270	-1.00M3	2.4500	0.1830	0.4583	-1.1846	7.0680
MB	0270	-3.00M4	2.6450	0.1599	0.4318	-0.9792	5.5014
MB	0270	-6.00M5	2.8675	0.1370	0.4746	-0.9336	5.9467
OB	0230	3.00M0	1.5600	0.3392	0.4170	-0.5380	4.1789
OB	0230	1.00M1	1.7400	0.2994	0.4999	-0.3802	2.7694
OB	0230	0.00M2	1.2175	0.4300	0.6262	-0.4749	4.5491
SS	0200	3.00M0	2.6850	0.1555	0.2886	-0.3011	3.6576
SS	0200	1.00M1	2.6500	0.1593	0.3742	-0.6586	4.2194
SS	0200	0.00M2	2.7587	0.1478	0.4874	-1.8742	9.6263
SS	0200	-1.00M3	2.7850	0.1451	0.4327	-0.8397	6.8807
SS	0200	-2.80M	3.0575	0.1201	0.6145	-0.2938	3.7625
SS	0200	-3.00M4	2.5500	0.1708	0.5385	-1.1238	4.0832
SS	0160	2.69M0	2.3100	0.2017	0.3826	-0.7421	4.8664
SS	0160	1.00M1	2.5100	0.1756	0.3121	-0.4457	2.7686
SS	0160	0.00M2	2.7100	0.1528	0.2973	-0.2598	3.5903
SS	0160	-1.00M3	2.6000	0.1649	0.3354	-0.1590	2.9200
SS	0160	-3.00M4	2.3825	0.1918	0.5921	-0.8278	4.6339
SS	0160	-6.00M5	2.7175	0.1520	0.5273	-0.5570	4.3836
SS	0160	10.00M	2.4800	0.1792	0.5496	-1.1630	5.2894
SS	0125	3.00M0	1.3250	0.3991	0.5879	-0.5555	3.6184
SS	0125	1.00M1	1.6100	0.3276	0.5283	-1.2481	6.3287
SS	0125	0.00M2	1.9100	0.2661	0.4236	-0.7595	4.4267
SS	0125	-1.00M3	1.7875	0.2897	0.6740	-0.3677	3.2867
SS	0125	-3.00M4	2.2912	0.2043	0.7038	-1.0028	4.8131
SS	0125	-6.00M5	3.0475	0.1210	0.5171	-1.8470	9.1769
SS	0090	3.00M0	1.9550	0.2579	0.4588	-0.8990	4.1641
SS	0090	1.00M1	2.2350	0.2124	0.2780	-0.3617	4.4051
SS	0090	0.00M2	2.3150	0.2010	0.3135	-0.1035	4.0324
SS	0090	-1.00M3	2.1150	0.2308	0.4175	-0.6970	6.4650
SS	0090	-3.00M4	2.0375	0.2436	0.6426	-0.8058	4.5990
SS	0090	-6.00M5	2.3525	0.1958	0.5455	-0.1093	3.4046
SS	0070	3.00M0	1.9100	0.2661	0.3800	-0.4722	2.8174
SS	0070	1.00M1	1.9350	0.2615	0.4281	-0.9788	4.8348
SS	0070	0.00M2	1.6700	0.3143	0.6990	-0.8776	4.8445
SS	0070	-3.00M4	2.4100	0.1882	0.4576	-0.5960	3.9906
SS	0070	-6.00M5	2.8900	0.1349	0.4691	-0.8178	6.3557
SS	0035	3.00M0	1.7925	0.2887	0.6215	-1.7679	8.8188
SS	0035	1.00M1	1.8075	0.2857	0.4385	-1.5090	9.4084
SS	0035	0.00M2	2.1450	0.2261	0.3626	-0.6016	5.1928
SS	0035	-1.00M3	2.0150	0.2474	0.5622	-1.9851	9.4828
SS	0035	-3.00M4	2.6050	0.1644	0.6499	-2.2274	14.0017
SS	0035	-6.00M5	2.9188	0.1322	0.5409	-0.8541	5.1983

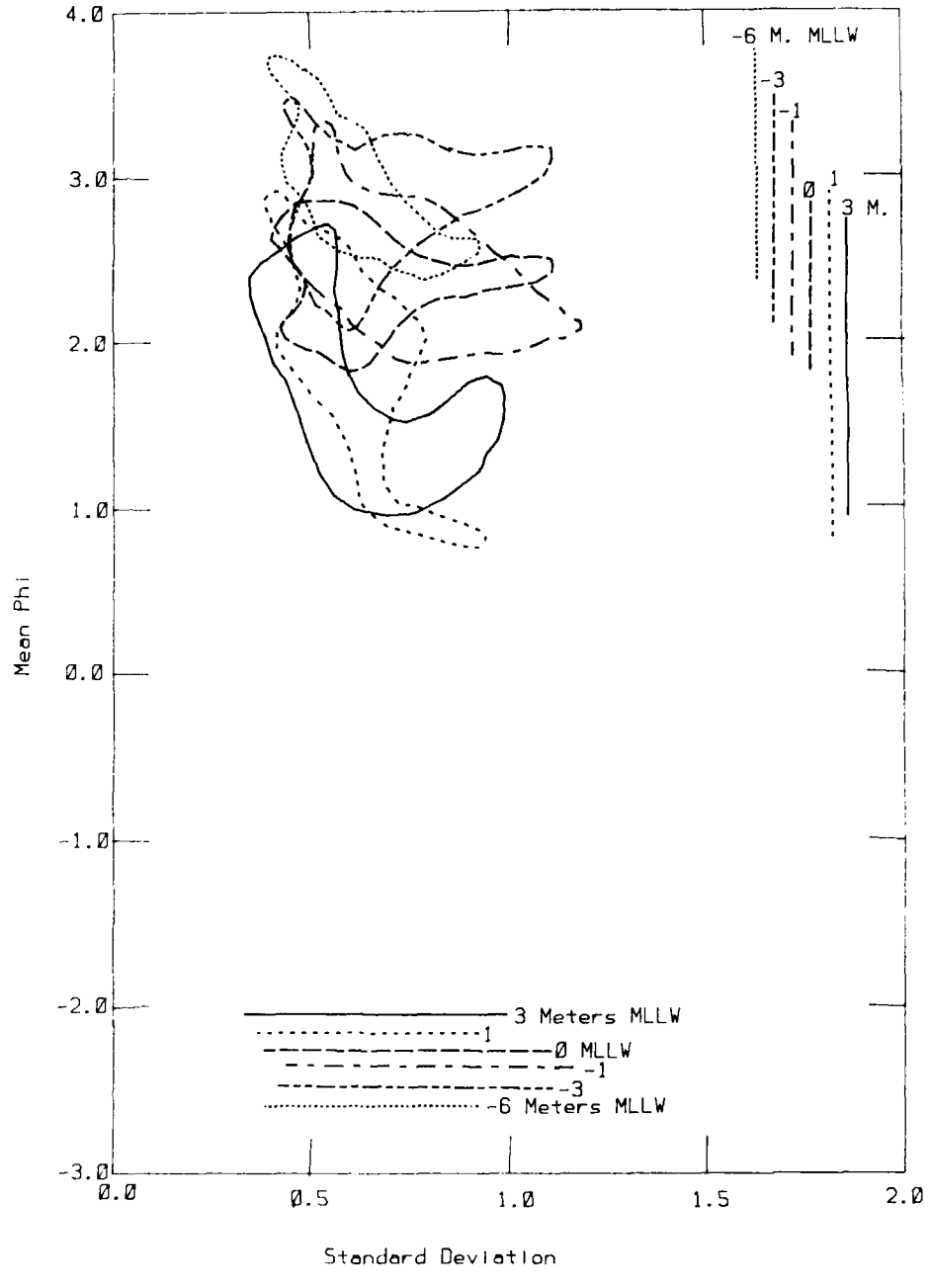

Figure 9. Bivariate plot of phi standard deviation versus mean phi for the end-of-summer data set. Dots on bars indicate mean values.

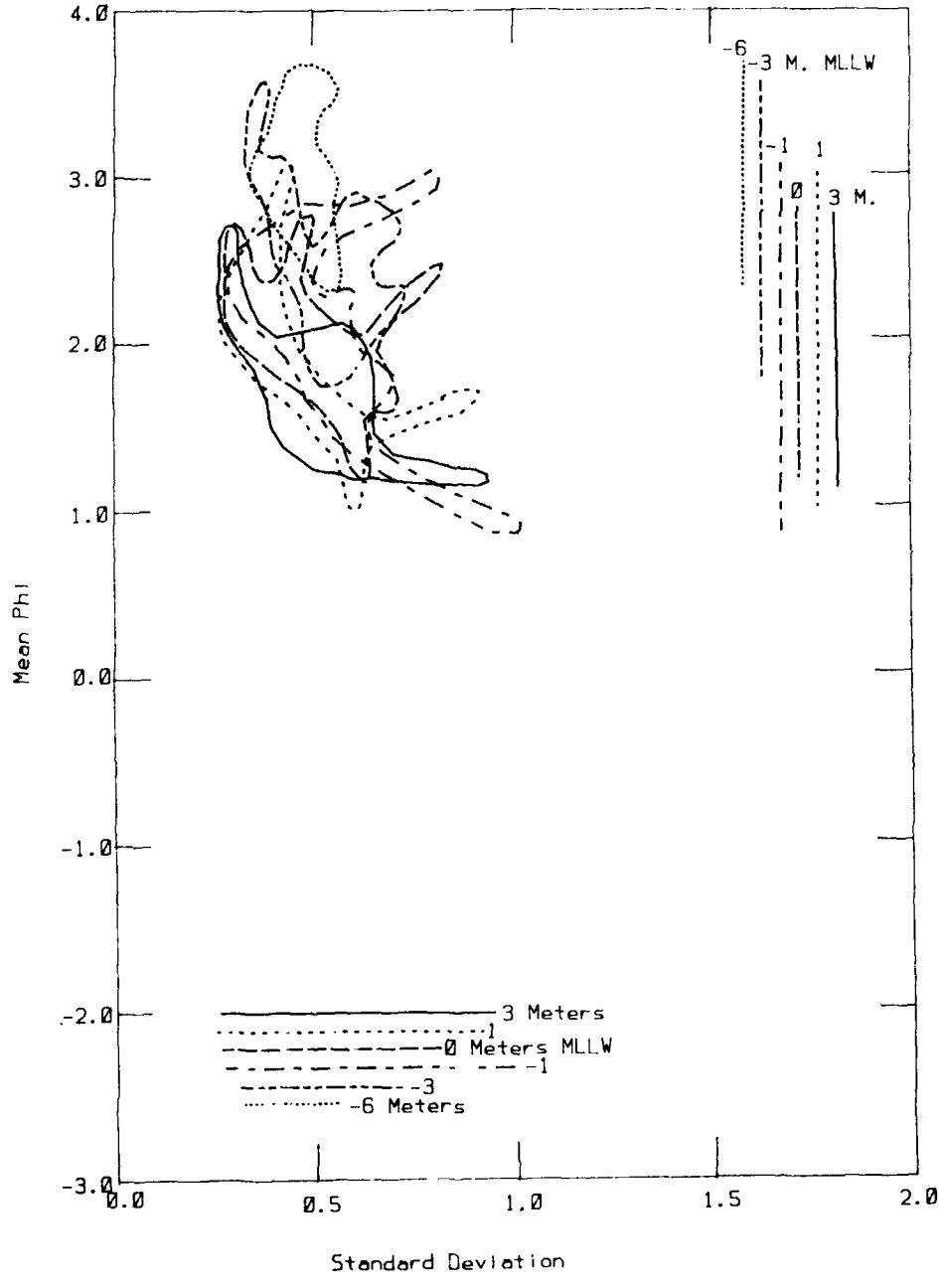

Figure 10. Bivariate plot of mean phi versus phi standard deviation for the end-of-winter data set. Dots on bars indicate mean values.

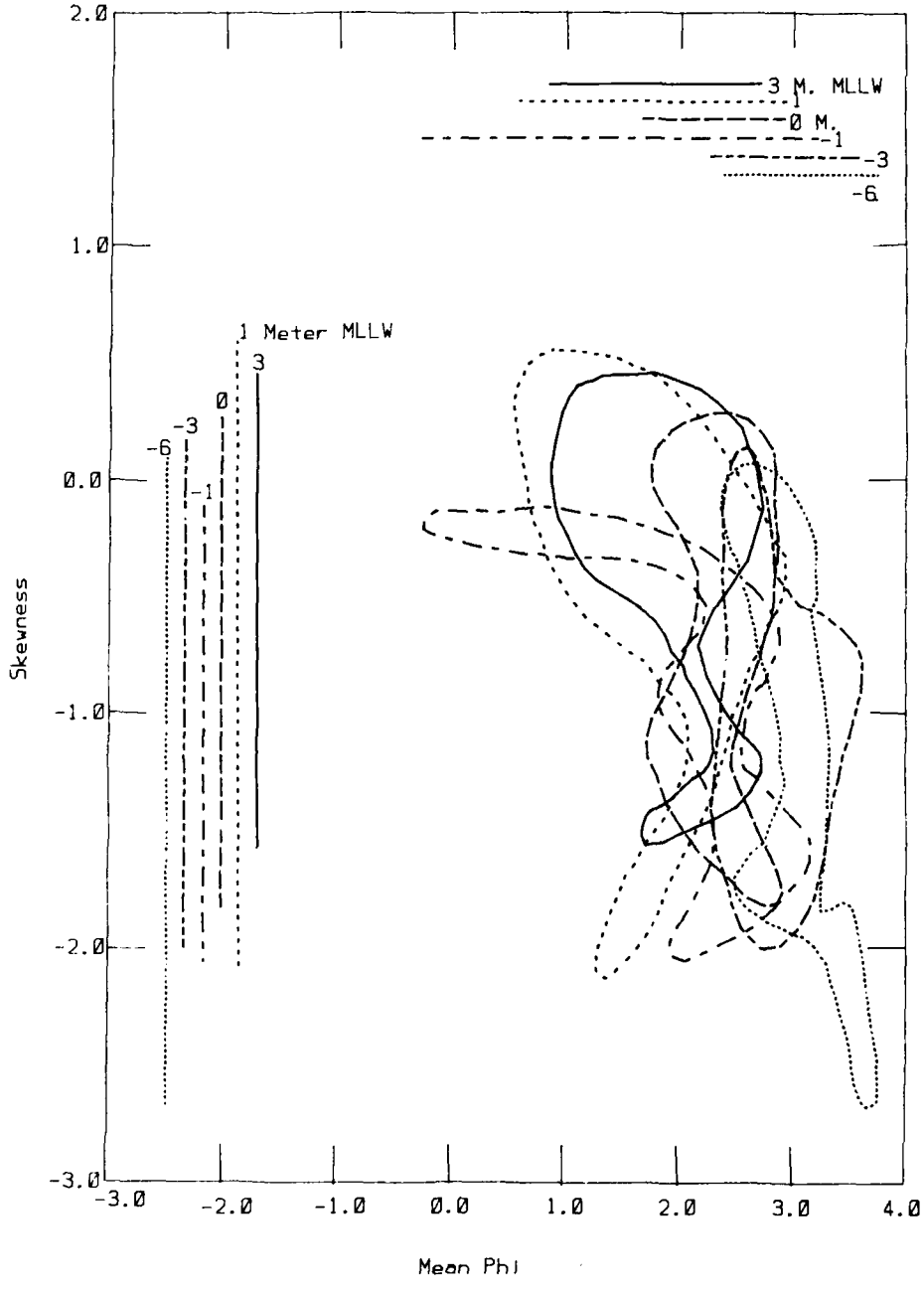

Figure 11. Bivariate plot of mean phi skewness for the end-of-summer data set. Dots on bars indicate mean values.

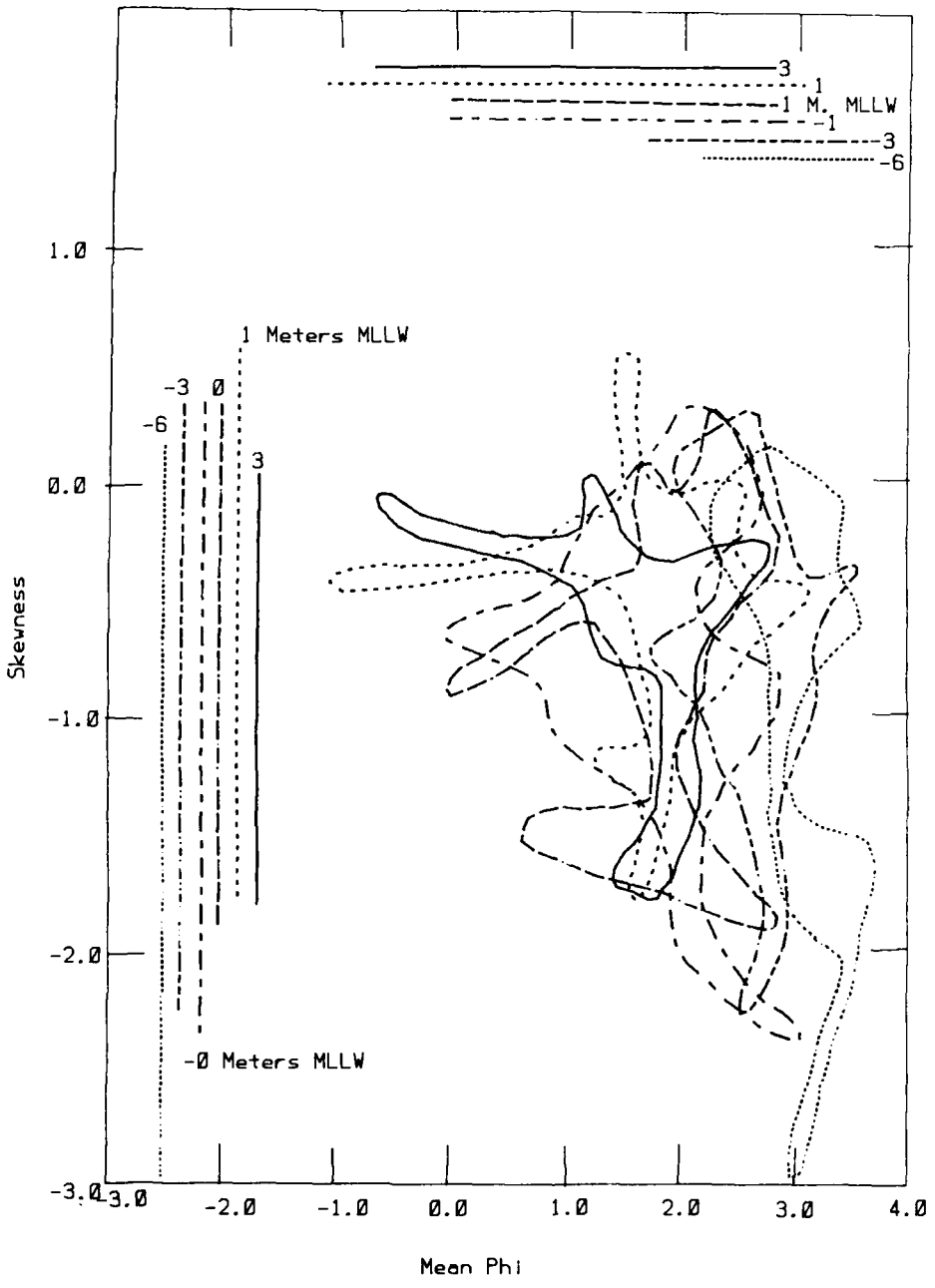

Figure 12. Bivariate plot of mean phi versus phi skewness for the end-of-winter data set. Dots on bars indicate mean values.

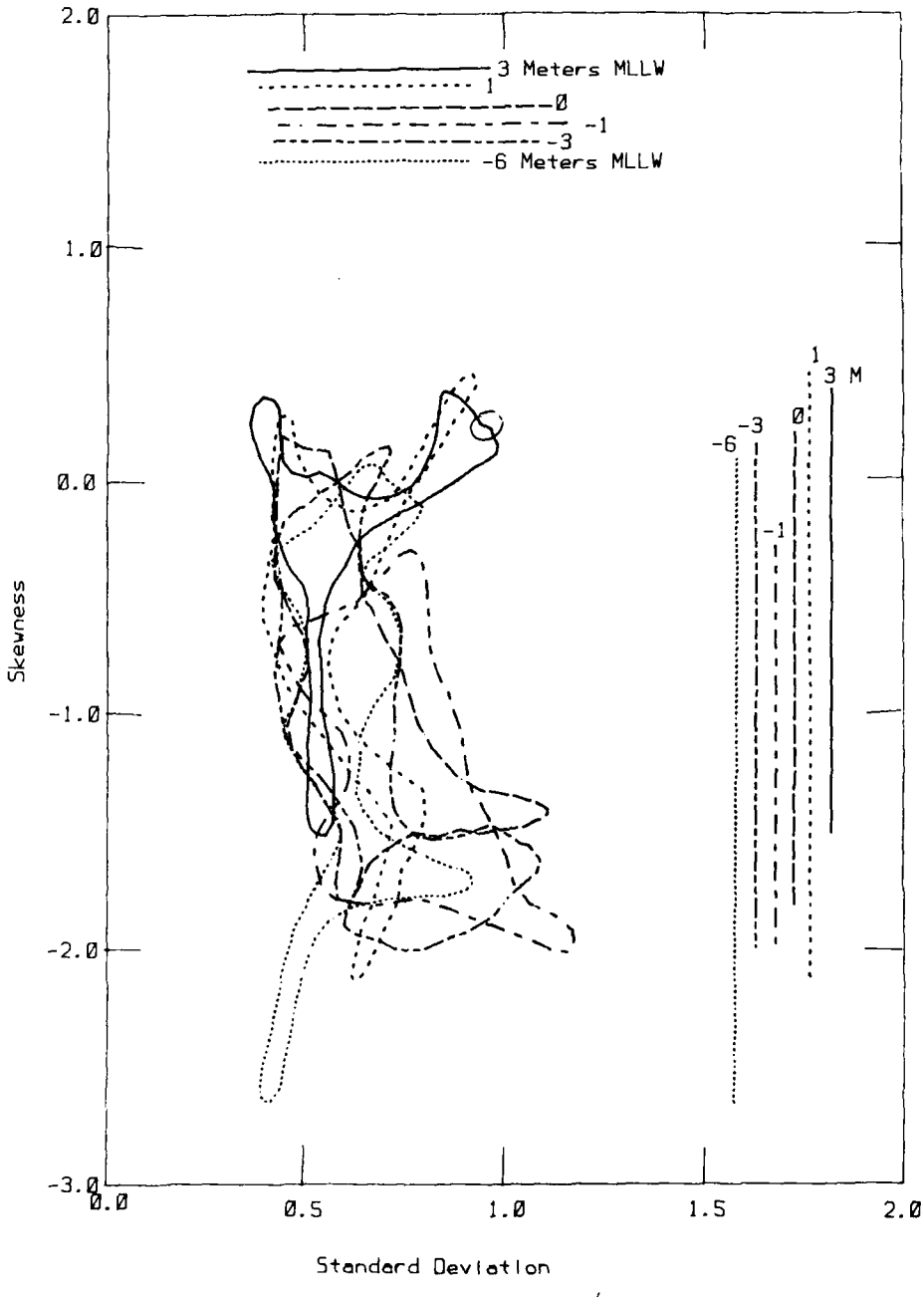

Figure 13. Bivariate plot of standard deviation versus phi skewness for the end-of-summer data set. Dots on bars indicate mean values.

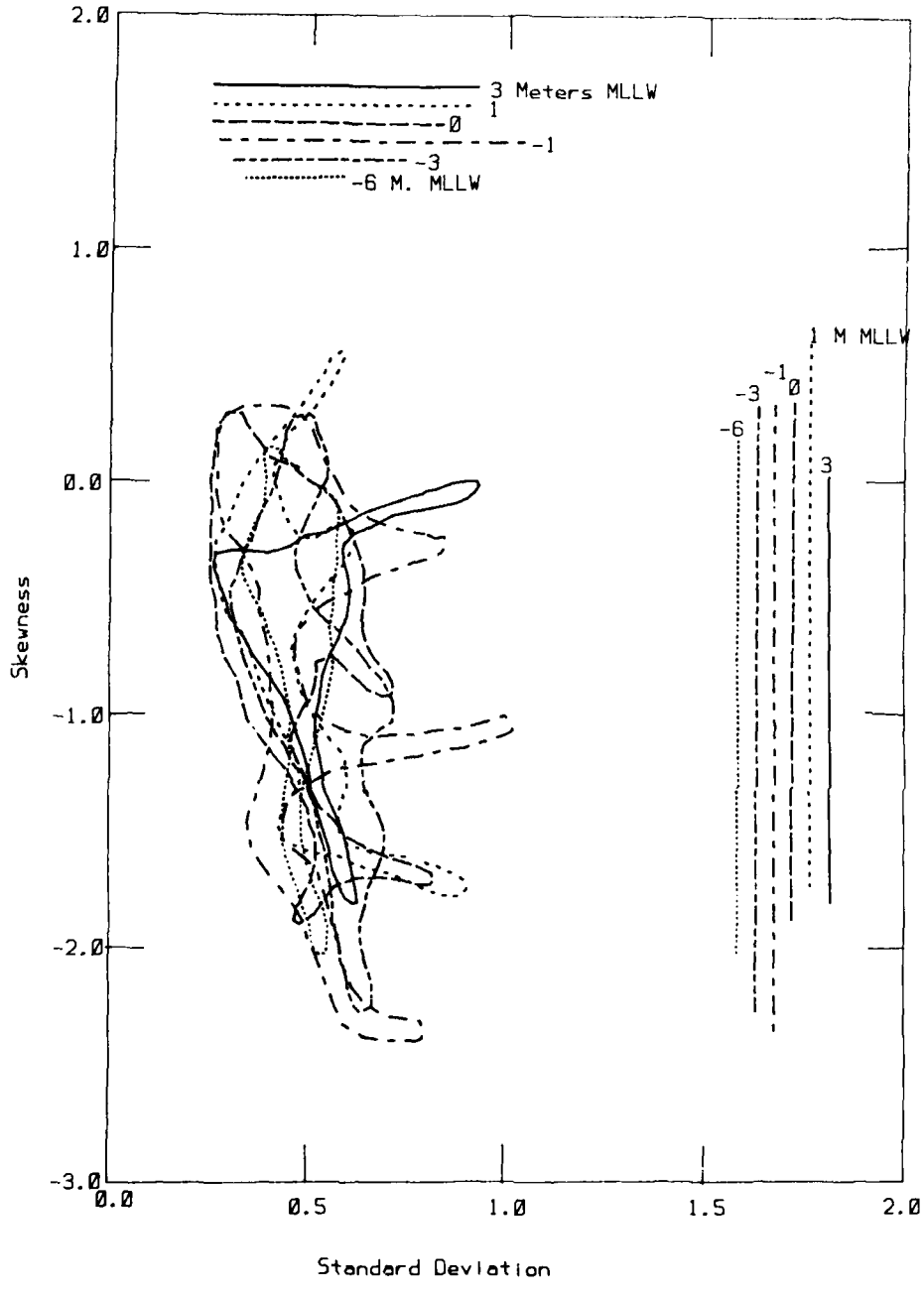

Figure 14. Bivariate plot of phi standard deviation versus phi skewness for the end-of-winter data set. Dots on bars indicate mean values.

6.04 The mean phi values for the end-of-winter sample set (Fig. 10) display a similar range from 1.0 to 3.00 for the +3, +1 and 0m samples, whereas progressive fining occurs from -1 through -6m. It should be noted that the range of mean phi values at the +3, +1 and 0m elevations is greater for the winter sample set, the -1m range is quite similar for both seasonal sets, and the range for the +1 and -6m samples are greater for the summer set.

6.05 The range of values for the phi standard deviation decrease from 0.69 at +3m, to 0.67 at +1m and 0.56 at 0m, increases to 0.74 at -1m, and progressively decreases to 0.42 and 0.25 at -3 and -6m, respectively. Again, the change from +3 to 0m probably reflects sorting along the shoreface, the change to -3m reflects sediment mixing, and the change from -3 to -6m reflects deposition from weak littoral currents or from suspension. The winter samples are moderately well-sorted to very well-sorted (Folk, 1974).

6.06 Figures 9 and 10 show that the summer and winter sample sets overlap considerably, therefore, this sample set shows no major seasonal change.

Mean Phi Versus Phi Skewness

6.07 Figure 11 shows the bivariate plot for mean values versus phi skewness for the summer sample set. The grain-size trends (mean phi values) for both the summer and winter sets have been discussed in the previous section.

6.08 Except for the +3m sample set, which ranges from -1.60 to +0.45 phi skewness units, the remainder of the values range from approximately -2.00 units to +0.55 at +1m, +0.25 at 0m, -0.15 at -1m, -0.20 at -3m, and +0.10 at -6m. Using Folk's (1974) classification, the samples range from very strongly coarse-skewed to strongly fine-skewed, but generally range from coarse-skewed to strongly coarse-skewed (-0.10 to -1.00), which is characteristic of many beach sands. The most prominent trends are an increase in the range of phi

skewness values from +3 to +1m, a decrease to -1m, and another increase from -1 to -3m.

6.09 The values for the winter sample set (Fig. 12) show much the same trends. There is an increase in the range of phi skewness values from +3 to +1m, a decrease to the 0m sample elevation, and another increase to the -1, -3 and -6m elevations. These trends also are related to sorting along the upper shoreface, mixing in the lower shoreface, and nearshore deposition.

6.10 The end-of-summer and end-of-winter sample sets show considerable overlap, which suggests no important seasonal variation during the sampling interval.

Phi Standard Deviation Versus Phi Skewness

6.11 The trends observed for the phi standard deviation and phi skewness values as a function of sample elevation and season have been described. Figures 13 and 14, which is a plot of phi standard deviation versus phi skewness, provides little additional information, but is presented for completeness. Here again, the fields show considerable overlap, which argues against pronounced seasonal changes.

7. RECOMMENDATIONS

7.01 Although sampling in the littoral zone may be difficult, every effort should be made to minimize the duration of the sampling period for each segment, so that resultant data can be better integrated with wave statistics and bathymetric profiles typical of the sampling period. Extended sampling periods tend to confound observed sedimentologic trends, and data interpretation is much less definitive.

7.02 Sampling should be replicated as closely as possible with regard to areal location and elevation (bathymetry). Failure to perform such replication produces a great deal of data, which cannot be integrated or compared with other data sets to discern systematic areal and/or temporal trends. Such data is obviously of very limited scientific value.

7.03 Inasmuch as the analysis of the regional data has produced a set of tentative littoral segments, attention should now be directed to the verification of these segments and the documentation of the sediment sources and transport paths within each segment. As the tentative temporal and spatial distribution of sediment in the proposed segments has been identified, site-specific sampling and other analytical methods should be performed to accomplish the objectives of this task. Additional sediment samples are needed adjacent to suspected point sources, particularly stream mouths and beach nourishment projects, to document their importance as sand contributors and to determine the net longshore transport direction associated with each such point source. Fluvial samples are needed near the mouth of streams above the effects of the tidal prism for the following localities: San Mateo River, San Onofre River, Los Flores Creek, Santa Margarita River, San Luis Rey River, Bataquitos Lagoon, San Elijo River, San Dequito Rivers, San Diego River and the Tia Juana River. Furthermore two samples at MLLW are needed at

approximately 0.5 mile intervals both upcoast and downcoast of each stream mouth named as well as at each placement site along the Oceanside and Imperial beaches to compare with the associated point-source samples to determine the longshore areal asymmetry of each distinct mineralogic assemblage. If storm-related and seasonal variations are to be assessed during the field data-collection phase of the CCSTW Study, it is necessary to collect sample sets within 2 to 3 weeks of major storm and runoff events as well as temporally restricted end-of-winter and end-of-summer sample sets at MLLW.

7.04 Cliff and bluff sampling (Task 1G) should be instituted in areas of contributing cliffs to evaluate the character and volume of sediment that might be delivered to each associated littoral segment. The most cost-effective sampling mechanism (Osborne and Pipkin, 1983) is to measure approximately thirty stratigraphic sections and apply a weighted-average sampling technique to characterize the grain-size and mineralogical content of each section. Aerial and ground-based photographs as well as maps showing changes in the coastline through time should be used to estimate average rates of cliff retreat, from which volumetric determinations might be computed. Although more difficult, the role of gullying also must be evaluated, perhaps through detailed photogrammetric analysis.

7.05 Inasmuch as one of the major objectives of Task 1D (littoral sediment), Task 1F (fluvial sediment) and Task 1G (bluff sediment) is to determine the volumetric contribution of each potential local source area to the associated littoral segment, it is highly recommended that studies using the Fourier grain-shape analysis of quartz grains be initiated following the collection of these samples. No other technique will permit a sample to be quantitatively partitioned into its component parts, each of which reflects the volumetric contribution of local sources. Fourier grain-shape analysis, often coupled

with quartz grain-surface microtextural analysis using scanning electron microscopy, has evolved into a standard sedimentologic technique. Most discussion concerns methods to improve the resolution of this technique even more, rather than on whether or not meaningful sedimentologic information is derived. Fourier grain-shape analysis has been applied to a wide variety of natural tracer and petrofacies problems, and the interested reader is referred to the following papers: Brown and others (1980), Ehrlich and others (1974), Ehrlich and Chin (1980), Ehrlich and Weinberg (1970), Ehrlich and others (1980), Hudson and Ehrlich (1980), Mazzullo and Ehrlich (1980, 1983), Mrakovitch and others (1976), Riester and others (1982), Van Nieuwenhuise and others (1978), and Young (1980). Grain-shape studies completed in California include Bloom (1979), Clark and Osborne (1982), Ehrlich and others (1974), Gaynor (1984), Porter and others (1979), and Osborne and others (1985). Such analyses could be performed on 100 gram splits of samples collected for Tasks 1D, 1F and 1G, so no additional sampling expense would be incurred.

8. REFERENCES

Blatt, H., Middleton, G. V., and Murray, 1972, Origin of sedimentary rocks: Englewood Cliffs, New Jersey, Prentice-Hall, Inc., 634 p.

Bloom, L., 1979, The relationships among river, beach and submarine canyon sands in the southern Santa Barbara littoral cell, Ventura County, California: Fourier grain-shape analysis: unpubl. Master's thesis, Univ. of Southern California, Los Angeles, California, 115 p.

Brown, P. J., Ehrlich, R., and Colquhoun, D. J., 1980, Origin of patterns of quartz sand types on the southeastern United States continental shelf and implications on contemporary shelf sedimentation - Fourier grain shape analysis: Jour. Sed. Petrology, v. 50, p. 1095-1100.

Clark, R. A., and Osborne, R. H., 1982, Contribution of Salinas River sand to the beaches of Monterey Bay, California, during the 1978 flood period: Fourier grain-shape analysis: Jour. Sed. Petrology, v. 52, p. 807-822.

Ehrlich, R., and Weinberg, B., 1970, An exact method for characterization of grain shape: Jour. Sed. Petrology, v. 40, p. 205-212.

Ehrlich, R., Orzeck, J. J., and Weinberg, B., 1974, Detrital quartz as a natural tracer - Fourier grain shape analysis: Jour. Sed. Petrology, v. 44, p. 145-150.

Ehrlich, R., and Chin, M., 1980, Fourier grain-shape analysis: A new tool for sourcing and tracking abyssal silts: Marine Geol., v. 38, p. 219-232.

Ehrlich, R., Brown, P. J., Yarus, J. M., and Przygocki, R., 1980, The origin of shape frequency distributions and the relationship between size and shape: Jour. Sed. Petrology, v. 50, p. 475-484.

Emery, K. O., 1960, The sea off southern California: A modern habitat of petroleum: New York, John Wiley and Sons, 366 p.

Folk, R. L., 1974, Petrology of sedimentary rocks: Austin, Texas, Hemphill's Bookstore, 182 p.

Gaynor, J. M., 1984, Sources and transport of sand in the littoral zone of Lake Tahoe, California and Nevada: Fourier grain-shape analysis: unpubl. Master's thesis, University of Southern California, Los Angeles, California, 112 p.

Gray, C. H., Jr., Kennedy, M. P., and Morton, P. K., 1971, Petroleum potential of southern coastal and mountain area, California: American Association of Petroleum Geologists, Memoir 15, p. 372-383.

Hudson, C. B., and Ehrlich, R., 1980, Determination of relative provenance contributions in samples of quartz sand using Q-mode factor analysis of Fourier grain shape data: Jour. Sed. Petrology, v. 50, p. 1101-1110.

Inman, D. L., 1976, Summary report of man's impact on the California coastal zone: Technical Report, State of California Department of Navigation and Ocean Development, 150 p.

Inman, D. L., 1981, Evaluation of the budget of waves and sand, Oceanside littoral cell and recommendations for monitoring and sand bypassing: Technical Report, U.S. Army Corps of Engineers, Los Angeles District, 24 p.

Inman, D. L., and Chamberlain, T. K., 1960, Littoral sand budget along the southern California coast: Report of the Twenty-first International Geological Congress, Copenhagen, Volume of Abstracts, p. 245-246.

Kuhn, G. G., and Shepard, F. P., 1984, Sea cliffs, beaches and coastal valleys of San Diego County: Berkeley, University of California Press, 193 p.

Larsen, E. S., 1948, Batholith of Corona, Elsinore, and San Luis Rey quadrangles, southern California: Geological Society of America Memoir 29, 182 p.

Mazzullo, J. M., and Ehrlich, R., 1980, A vertical variation in the St. Peter Sandstone - Fourier grain shape analysis: Jour. Sed. Petrology, v. 50, p. 63-70.

Mazzullo, J. M., and Ehrlich, R., 19893, Grain sahpe variation in the St. Peter Sandstone: A record of eolian and fluvial sedimentation of an early Paleozoic cratonic sheet sand: Jour. Sed. Petrology, v. 53, p. 105-119.

Osborne, R. H., and Pipkin, B. W., 1983, Shorezone contribution of cliff-derived sediment, Dana Point to the United States-Mexico border, San Diego County, California: Technical Report, Los Angeles District, U.S. Army Corps of Engineers, 27 p.

Osborne, R. H., Edelman, M. C., Gaynor, J. M., and Waldron, J. M., 1985, Sedimentology of the littoral zone in Lake Tahoe, California-Nevada: Technical Report, California State Lands Commission, 88 p.

Porter, G. A., Ehrlich, R., Osborne, R. H., and Combellick, R. A., 1979, Sources and nonsources of beach sand along southern Monterey Bay, California - Fourier shape analysis: Jour. Sed. Petrology, v. 49, p. 727-732.

Riester, D. D., Shipp, R. C., and Ehrlich, R., 1982, Patterns of quartz sand shape variation, Long Island littoral and shelf: Jour. Sed. Petrology, v. 52, p. 1307-1314.

Shepard, F. P., 1950, Longshore current observations in southern California: U.S. Army Corps of Engineers Beach Erosion Board Technical Mem. No. 13, 54 p.

Stuart, C. J., 1979, Lithofacies and origin of the San Onofre Breccia, coastal southern California, in Stuart, C. J., ed., A guidebook to Miocene lithofacies and depositional environments, southern California and northwestern Baja California: Los Angeles, Pacific Section of the Society of Economic Paleontologists and Mineralogists, p. 25-42.

Van Nieuwenhuise, R., Yarus, J. M., Przygocki, R. S., and Ehrlich, R., 1978, Sources of shoaling in Charleston Harbor: Fourier grain shape analysis: Jour. Sed. Petrology, v. 48, p. 373-384.

Young, K., 1980, Fourier analysis of quartz grains, a new method of interpreting sediment movement: Marine Resource Bull., v. 12, no. 2, p. 4-5.

Appendix A Bivariate plots of phi standard deviation versus mean phi for the end-of-summer regional data set by littoral segment. Symbols are as follows: square is +3m, hexagon is +1m, triangle is 0m, vertical cross is -1m, diagonal cross is -3m, and diamond is -6m.

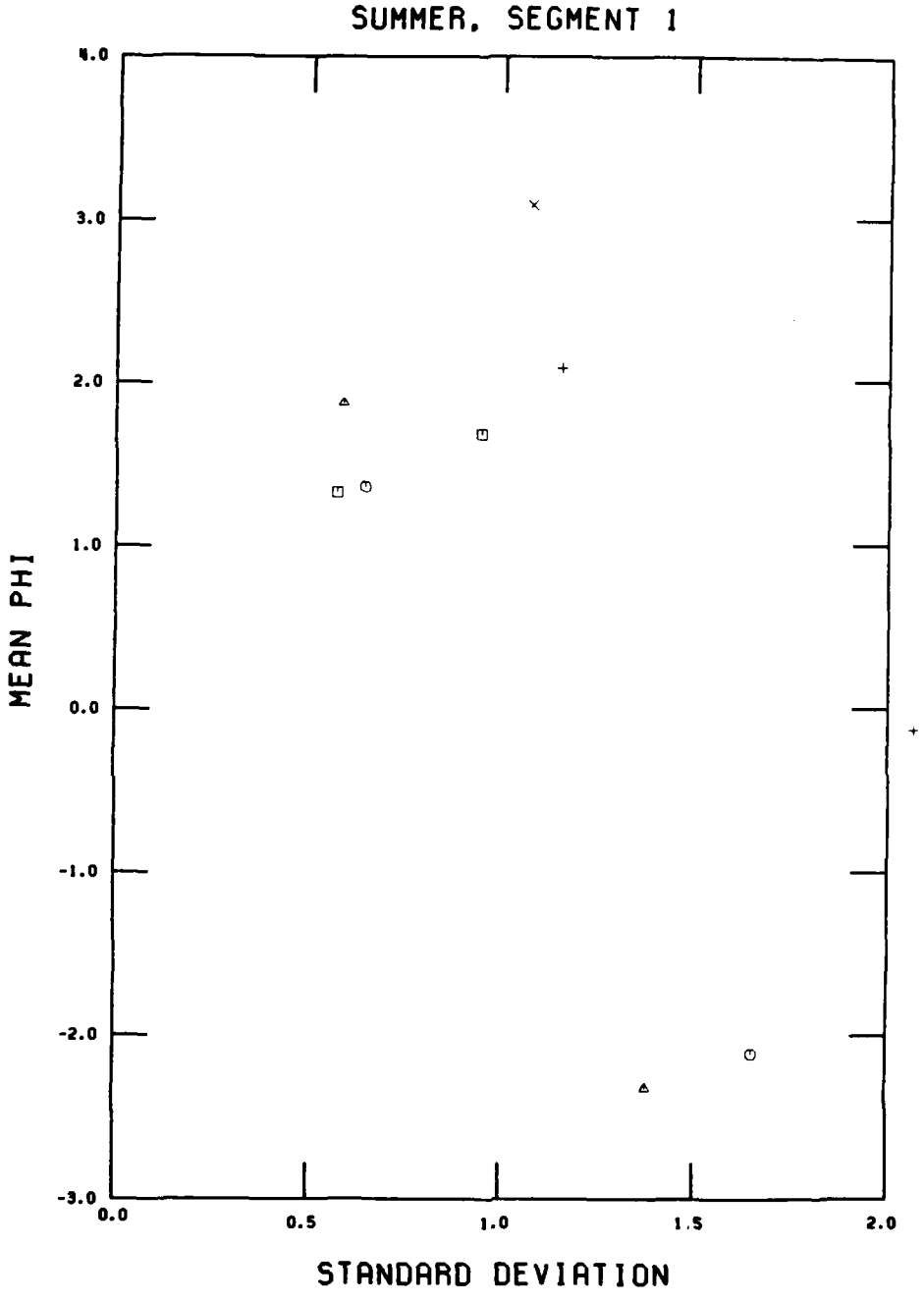
SUMMER, SEGMENT 1
4.0
3.0
2.0
1.0
0.0
-1.0
-2.0
-3.0
MEAN PHI
0.0
0.5
1.0
1.5
2.0
STANDARD DEVIATION

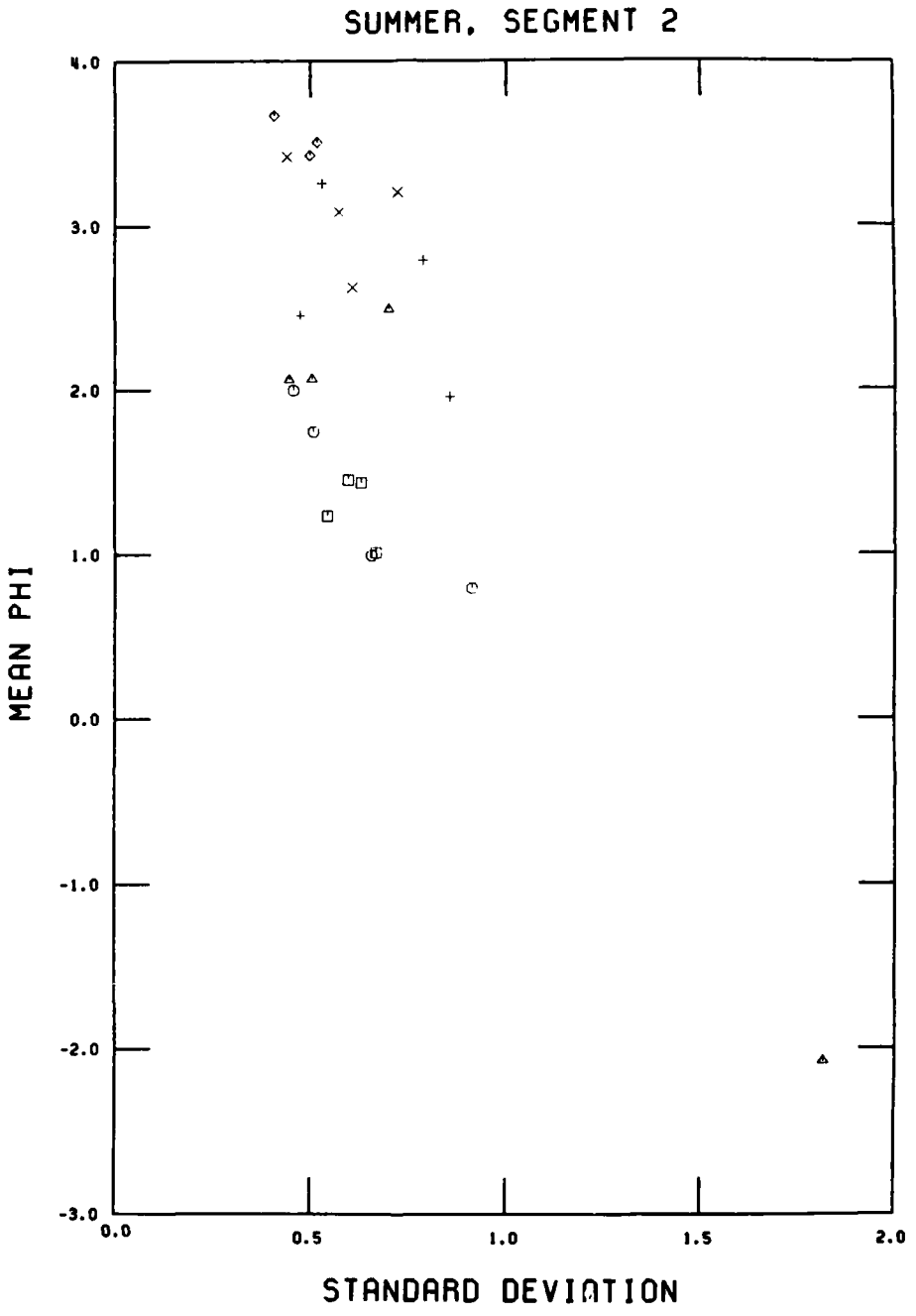
SUMMER, SEGMENT 2
4.0
3.0
2.0
1.0
0.0
-1.0
-2.0
-3.0
MEAN PHI
0.0
0.5
1.0
1.5
2.0
STANDARD DEVIATION

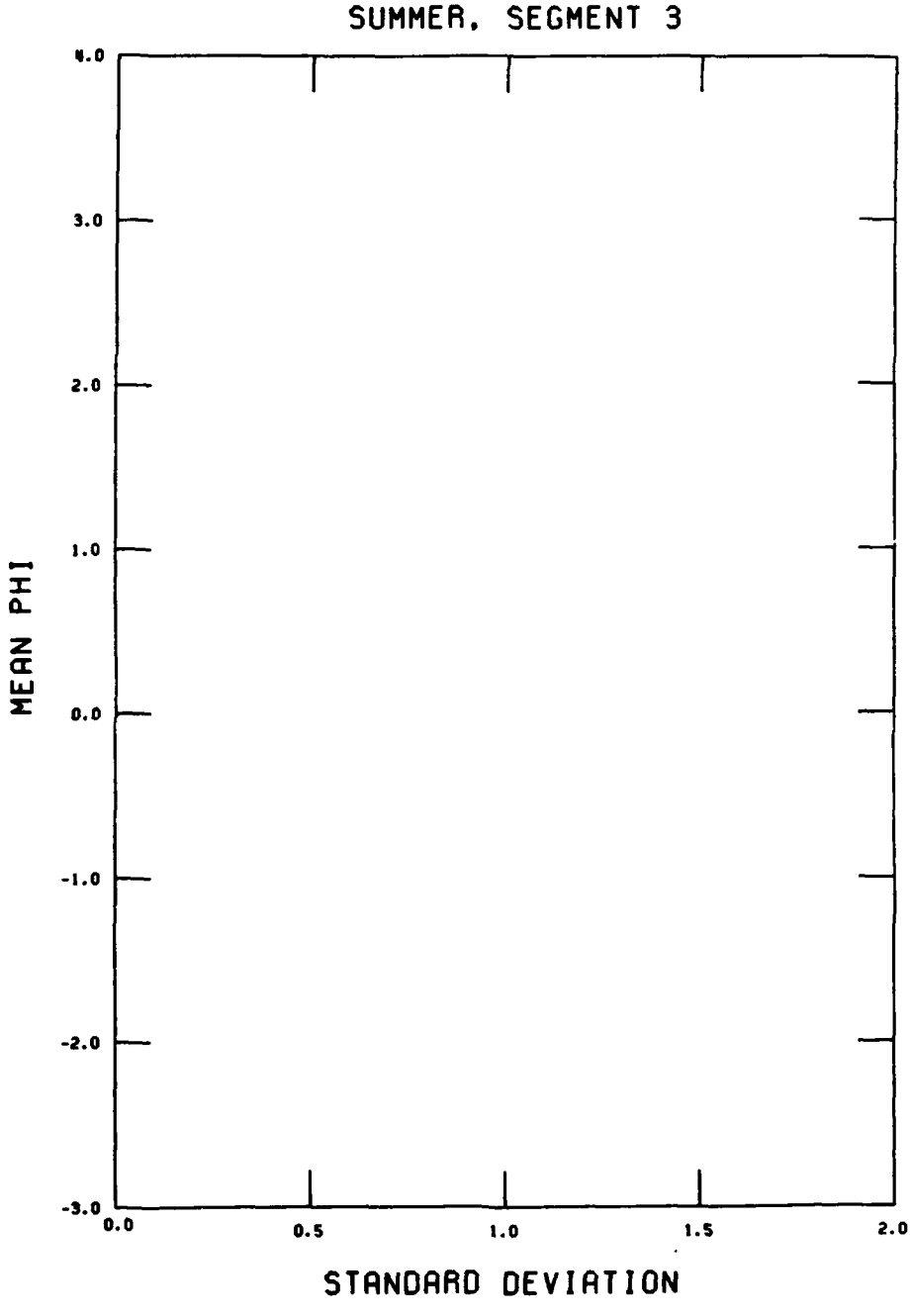
SUMMER, SEGMENT 3
MEAN PHI
6.0
3.0
2.0
1.0
0.0
-1.0
-2.0
-3.0
0.0
0.5
1.0
1.5
2.0
STANDARD DEVIATION

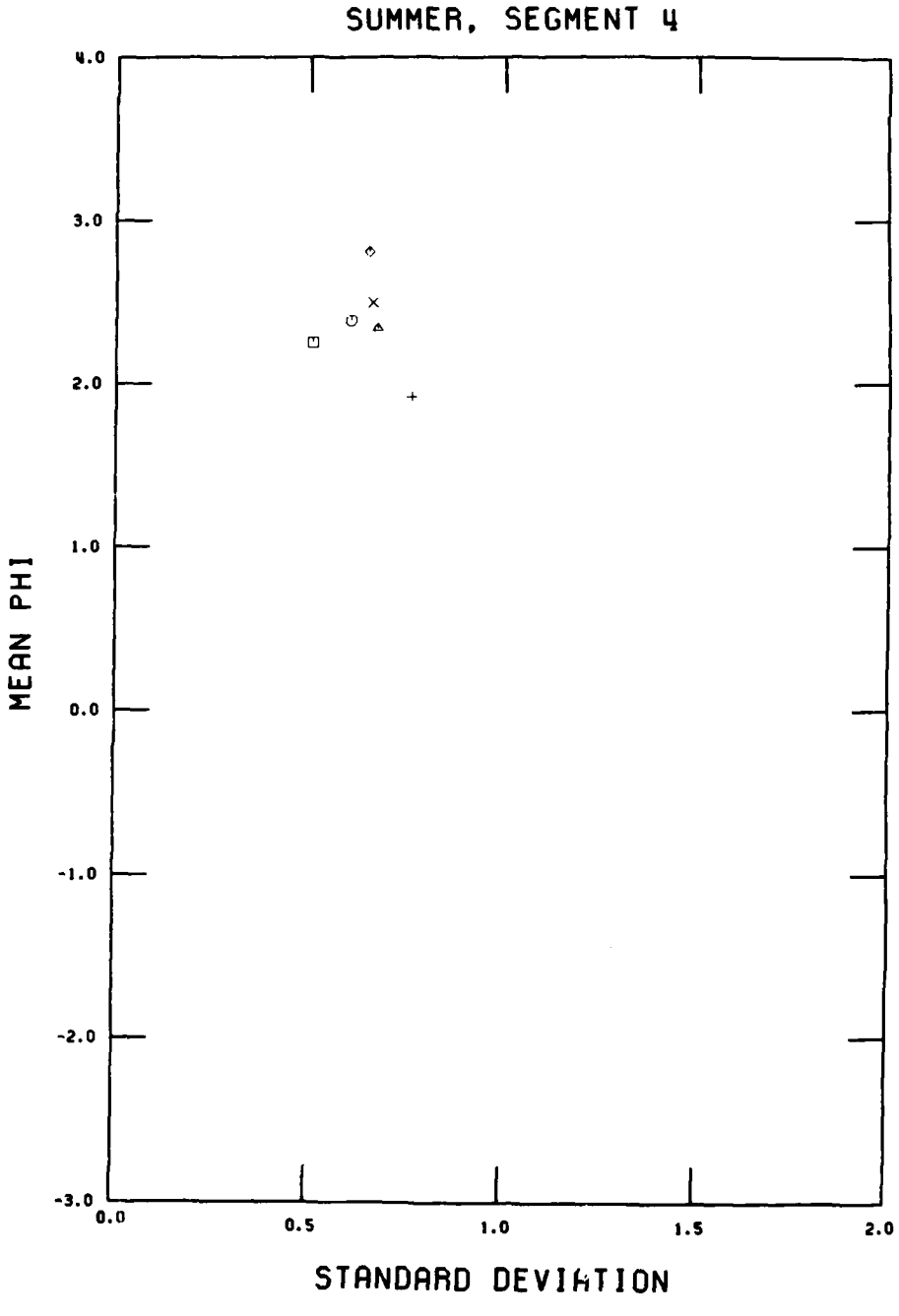
SUMMER, SEGMENT 4
4.0
3.0
2.0
1.0
0.0
-1.0
-2.0
-3.0
MEAN PHI
0.0
0.5
1.0
1.5
2.0
STANDARD DEVIATION

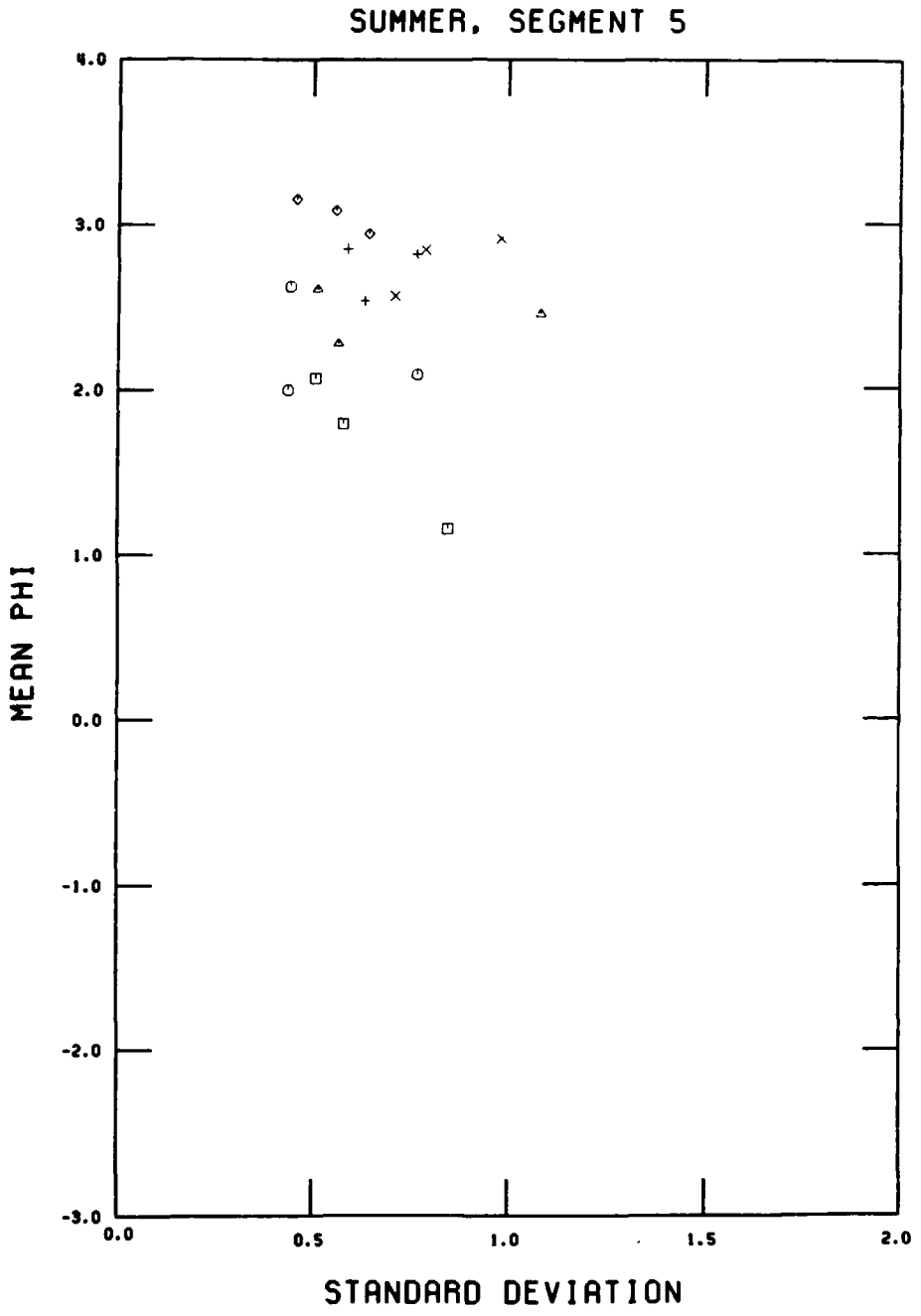
SUMMER, SEGMENT 5
4.0
3.0
2.0
1.0
0.0
-1.0
-2.0
-3.0
MEAN PHI
0.0
0.5
1.0
1.5
2.0
STANDARD DEVIATION

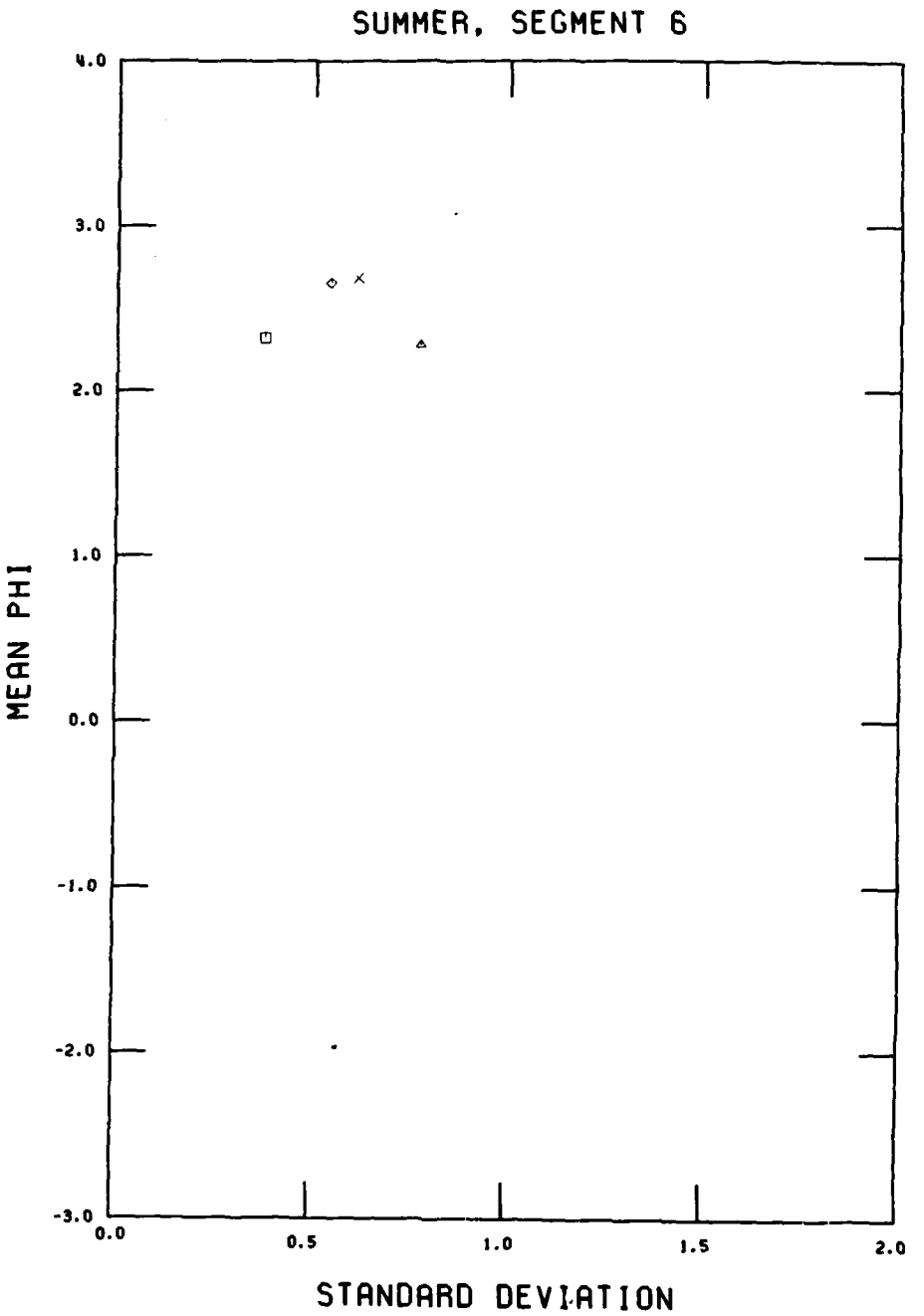
SUMMER, SEGMENT 6
4.0
3.0
2.0
1.0
0.0
-1.0
-2.0
-3.0
MEAN PHI
0.0
0.5
1.0
1.5
2.0
STANDARD DEVIATION

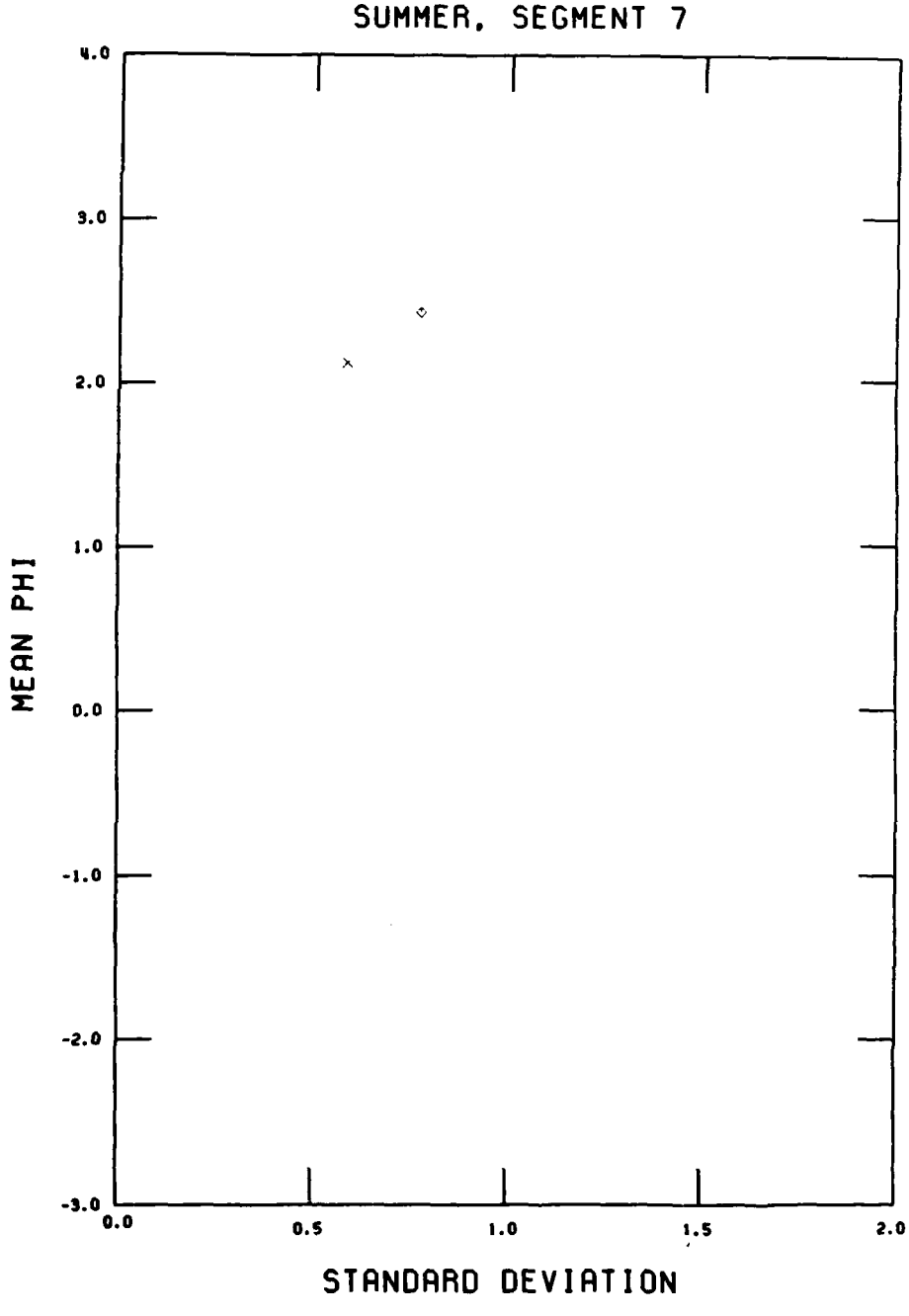
SUMMER, SEGMENT 7
4.0
3.0
2.0
1.0
0.0
-1.0
-2.0
-3.0
MEAN PHI
0.0
0.5
1.0
1.5
2.0
STANDARD DEVIATION

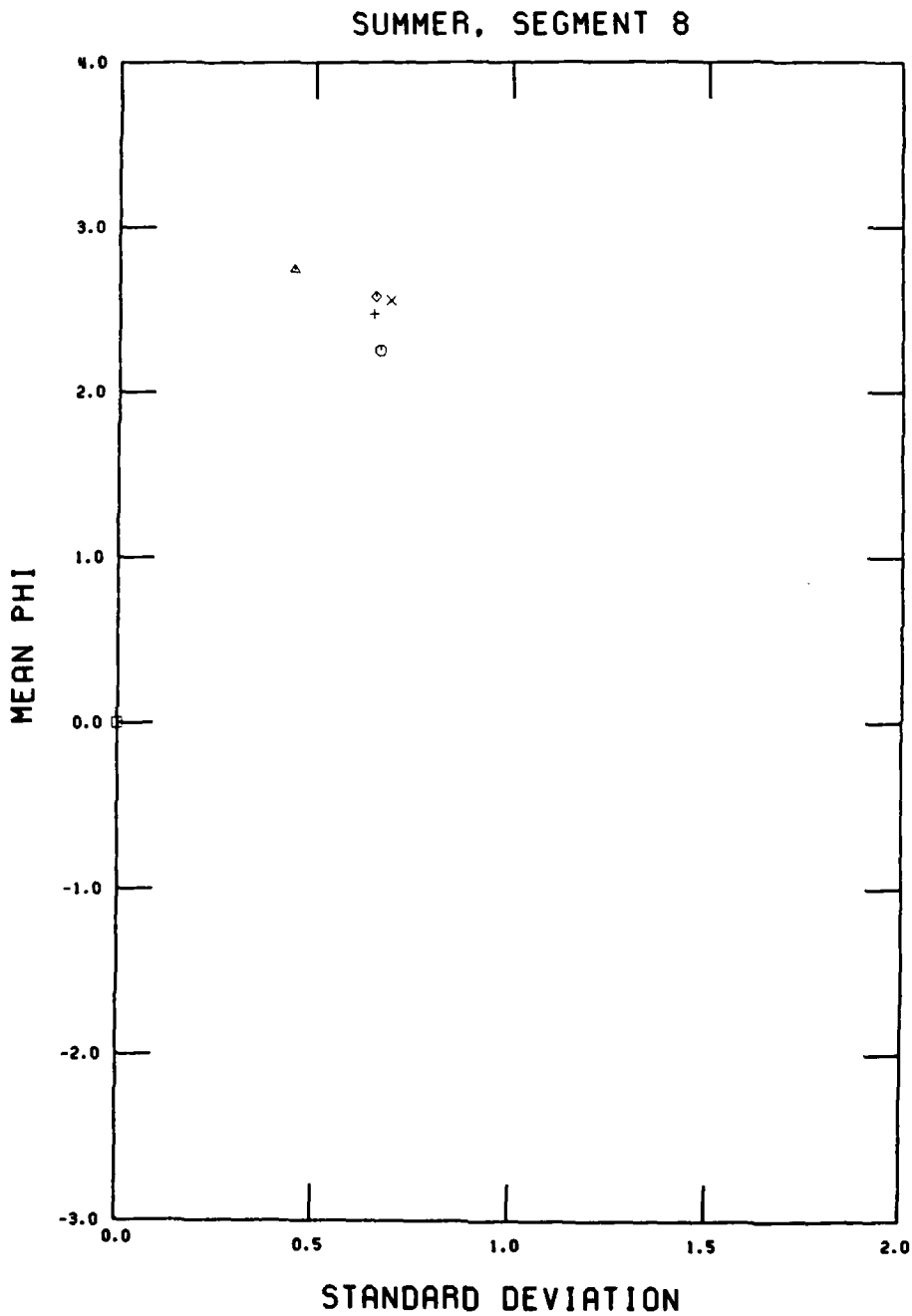
SUMMER, SEGMENT 8
4.0
3.0
2.0
1.0
0.0
-1.0
-2.0
-3.0
MEAN PHI
0.0
0.5
1.0
1.5
2.0
STANDARD DEVIATION

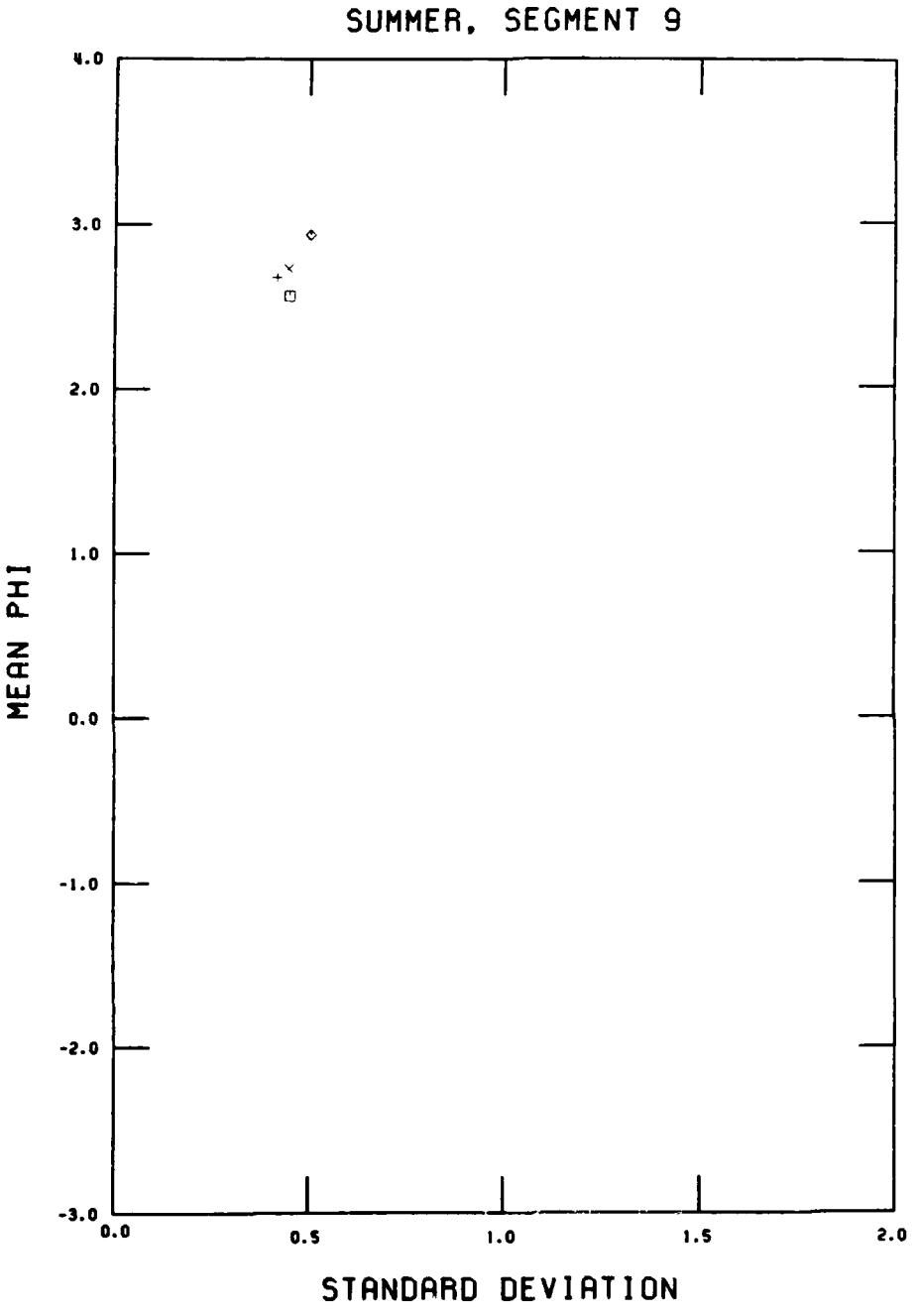
SUMMER, SEGMENT 9
4.0
3.0
2.0
1.0
0.0
-1.0
-2.0
-3.0
MEAN PHI
0.0
0.5
1.0
1.5
2.0
STANDARD DEVIATION

AD-A167 044 LITTORAL ZONE SEDIMENTS SAN DIEGO REGION OCTOBER 1983-JUNE 1984(U) UNIVERSITY OF SOUTHERN CALIFORNIA LOS ANGELES DEPT OF GEOLOGICAL SCIENCES DEC 85 2/2

UNCLASSIFIED USC-GEOL-CCSIWS-85-11 F/G 8/3 NL

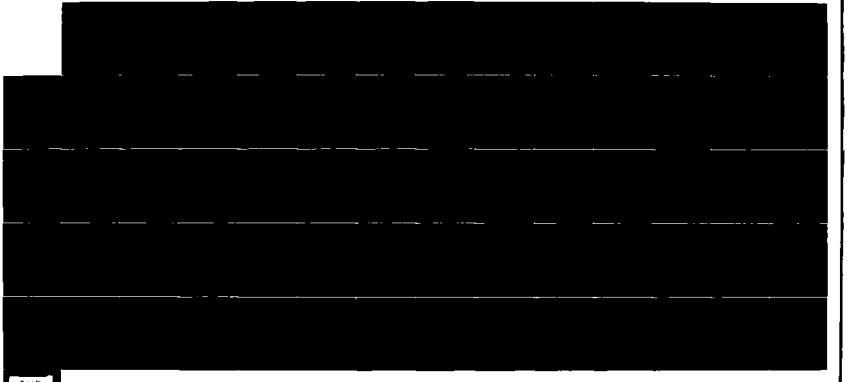

END
DATE FILMED
6-86
DT

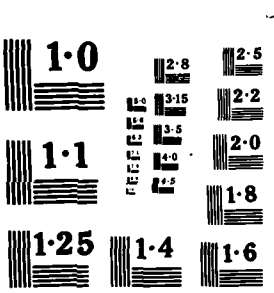
1·0
1·1
1·25
2·8
3·15
3·5
4·0
4·5
1·4
2·5
2·2
2·0
1·8
1·6

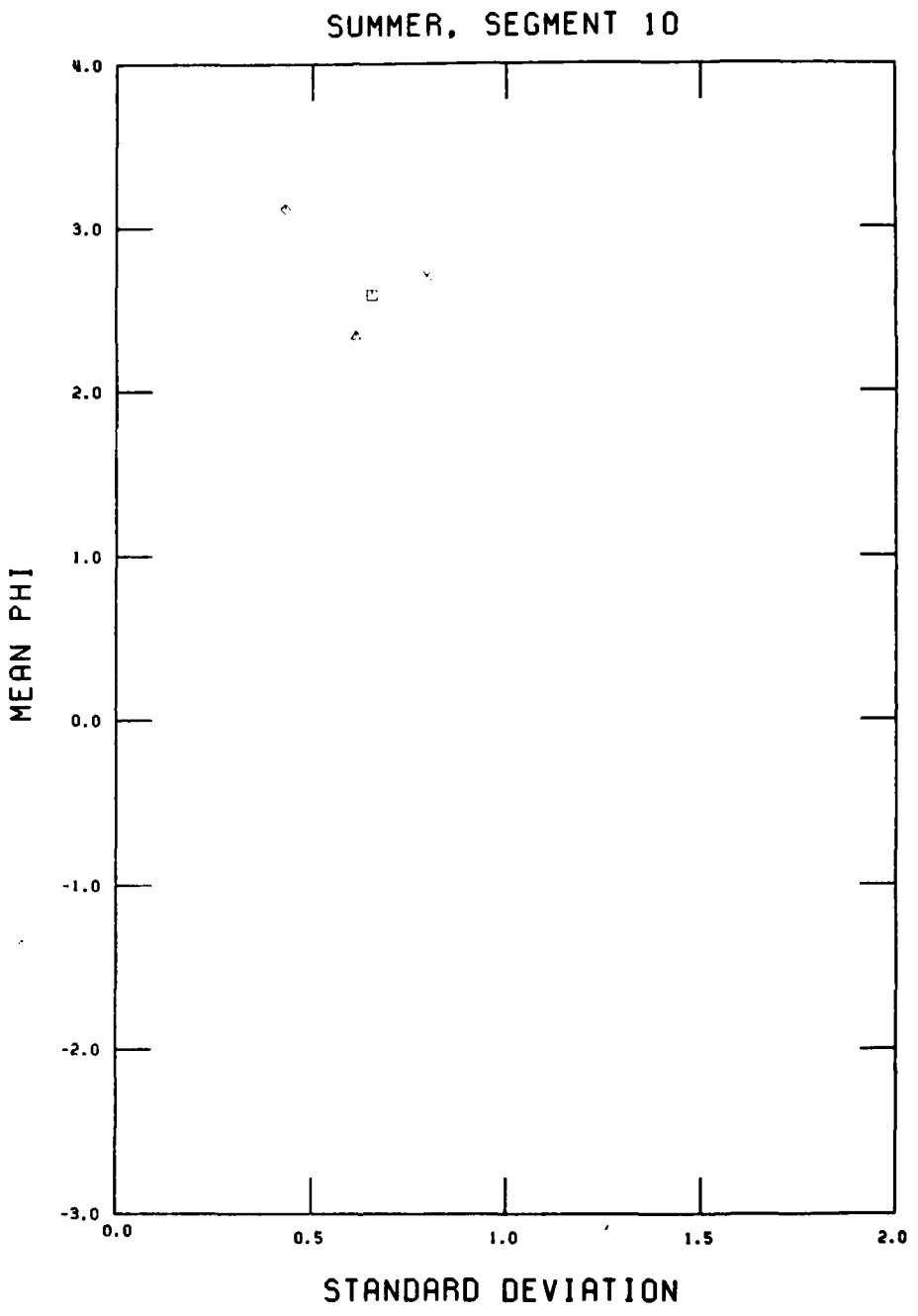
SUMMER, SEGMENT 10
4.0
3.0
2.0
1.0
0.0
-1.0
-2.0
-3.0
MEAN PHI
0.0
0.5
1.0
1.5
2.0
STANDARD DEVIATION

Appendix B Bivariate plots of mean phi versus phi skewness for the end-of-summer regional data set by littoral segment. Symbols are the same as for Appendix A.

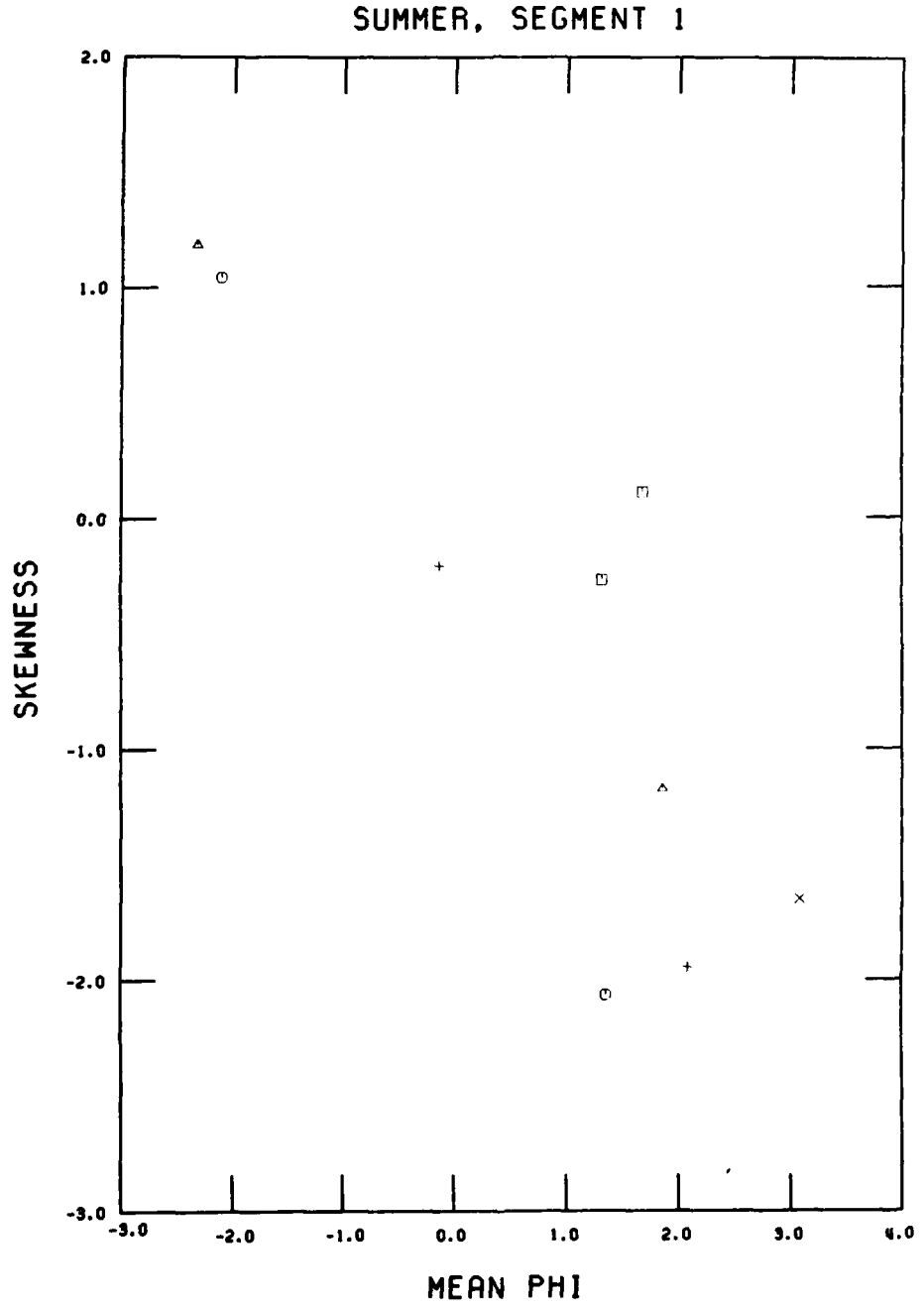
SUMMER, SEGMENT 1
2.0
1.0
0.0
-1.0
-2.0
-3.0
SKEWNESS
-3.0
-2.0
-1.0
0.0
1.0
2.0
3.0
4.0
MEAN PHI

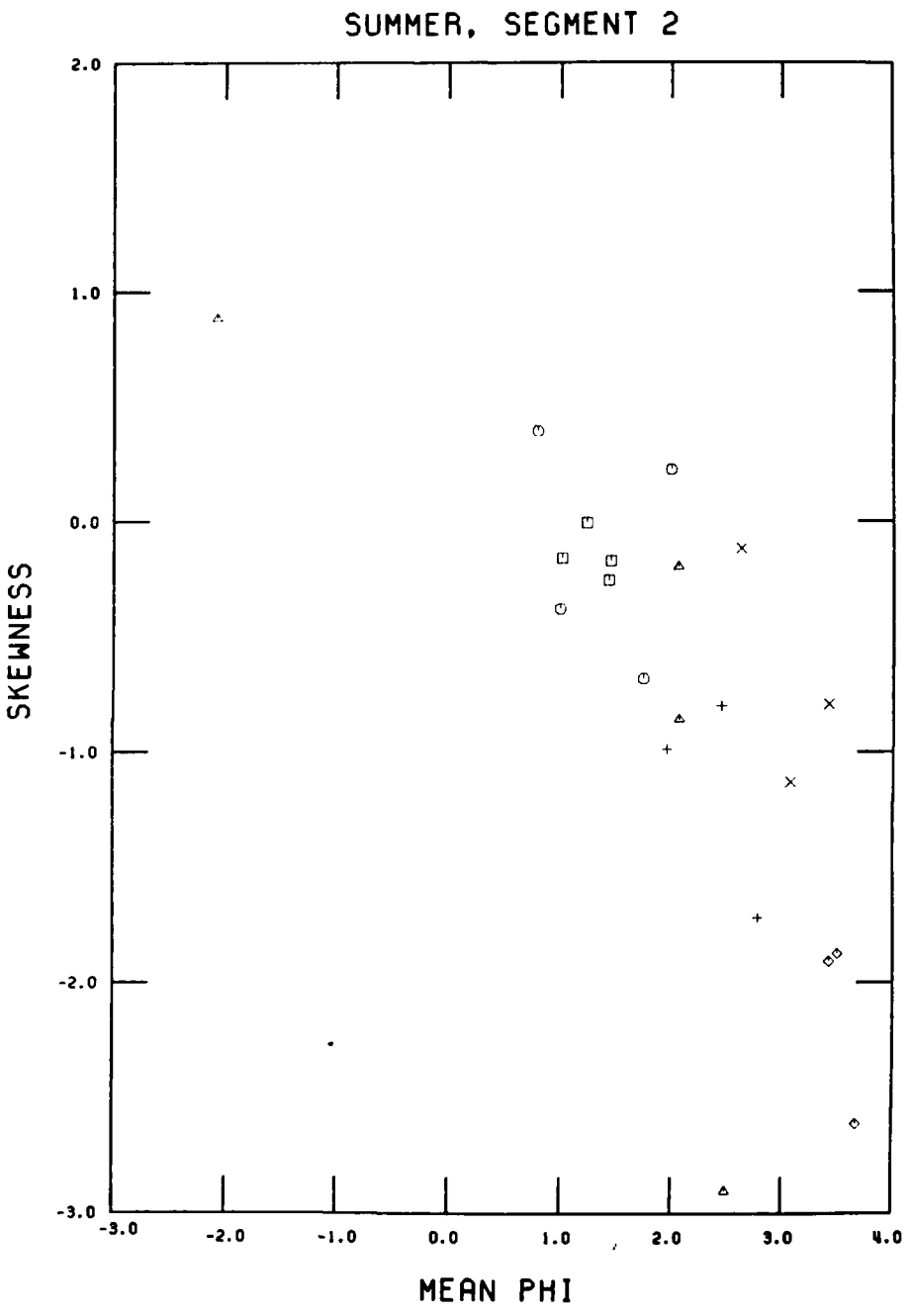
SUMMER, SEGMENT 2
SKEWNESS
MEAN PHI
2.0
1.0
0.0
-1.0
-2.0
-3.0
-3.0
-2.0
-1.0
0.0
1.0
2.0
3.0
4.0

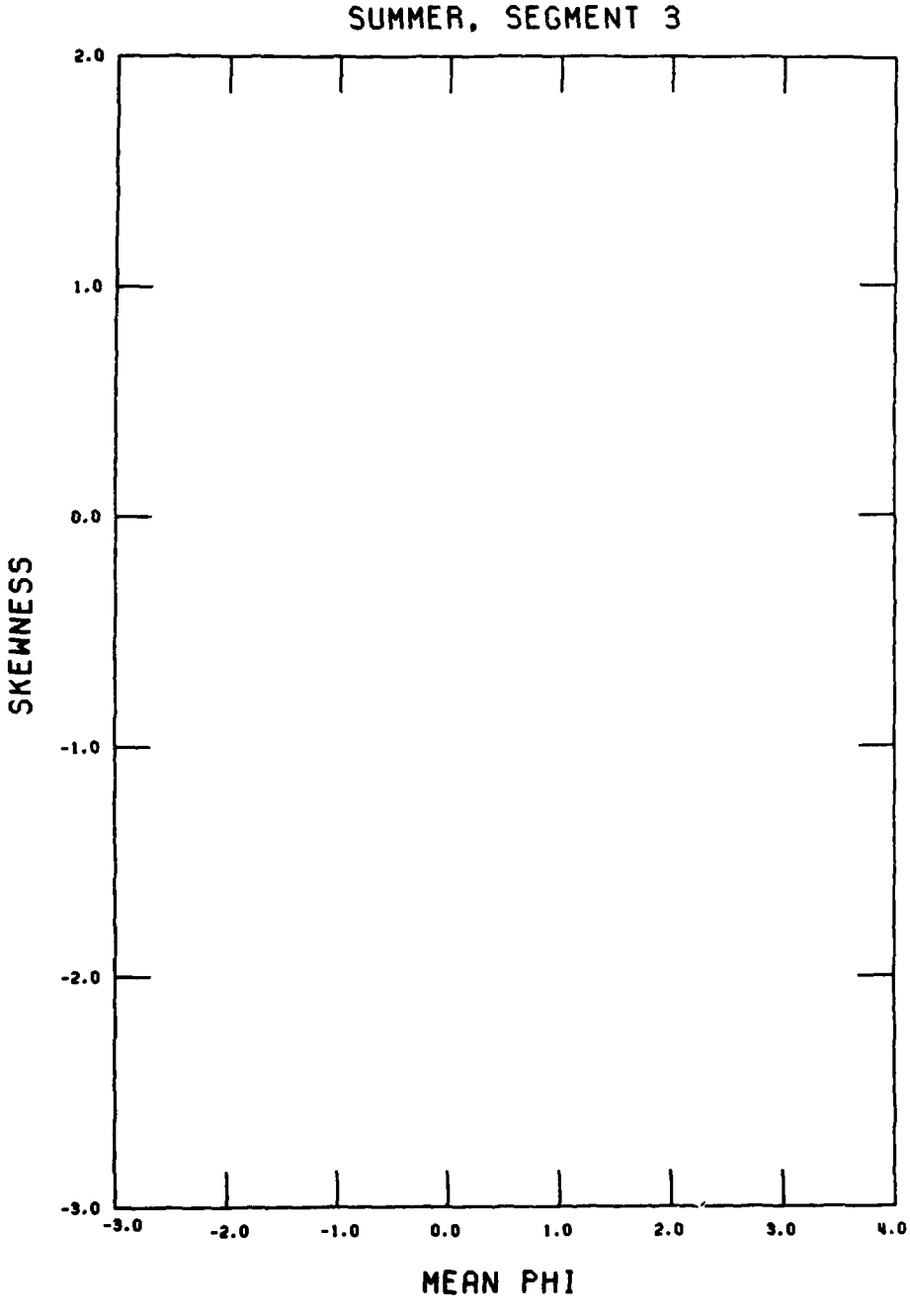
SUMMER, SEGMENT 3
2.0
1.0
0.0
-1.0
-2.0
-3.0
SKEWNESS
-3.0
-2.0
-1.0
0.0
1.0
2.0
3.0
4.0
MEAN PHI

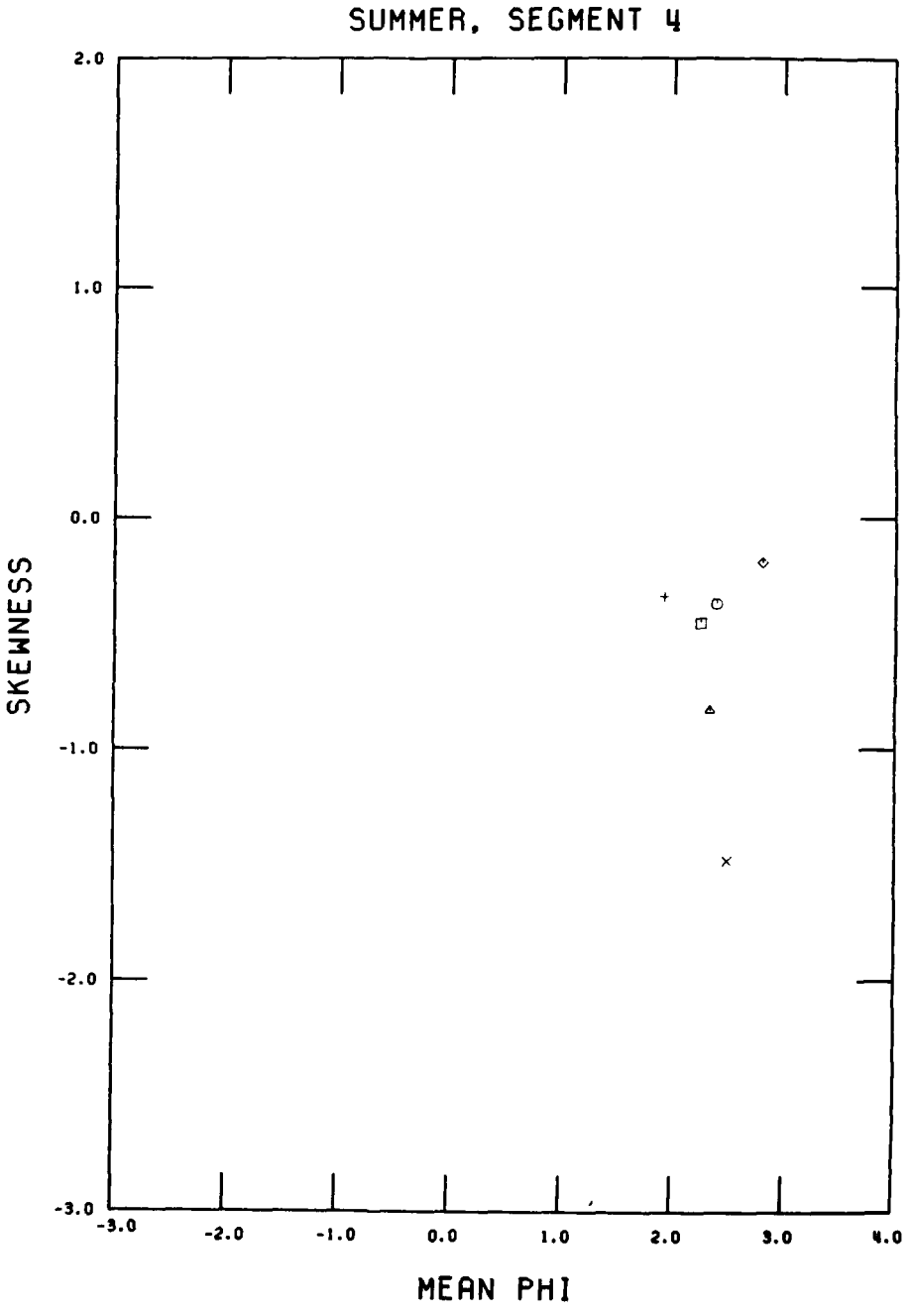
SUMMER, SEGMENT 4
SKEWNESS
MEAN PHI
2.0
1.0
0.0
-1.0
-2.0
-3.0
-3.0
-2.0
-1.0
0.0
1.0
2.0
3.0
4.0

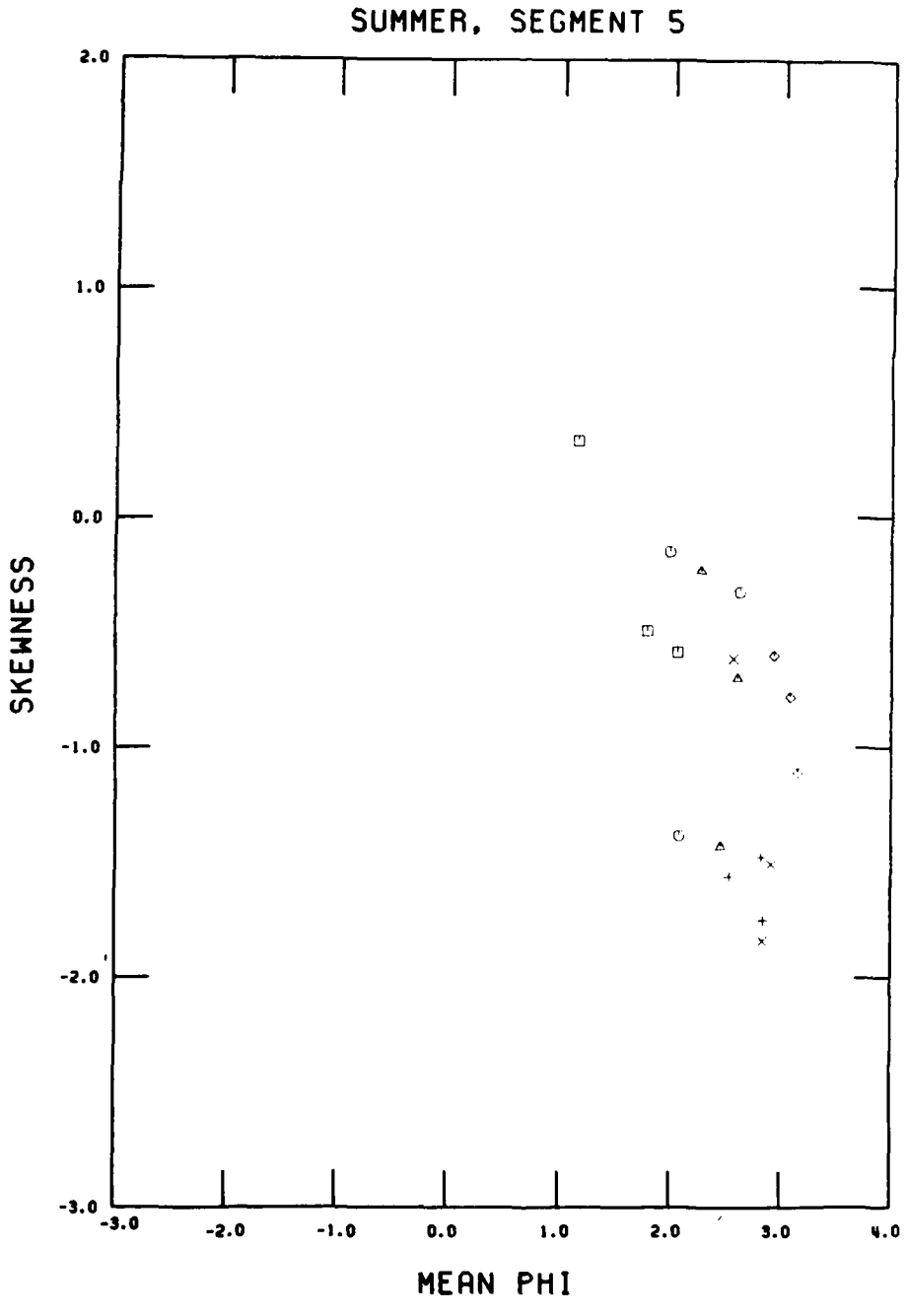
SUMMER, SEGMENT 5
SKEWNESS
MEAN PHI
2.0
1.0
0.0
-1.0
-2.0
-3.0
-3.0
-2.0
-1.0
0.0
1.0
2.0
3.0
4.0

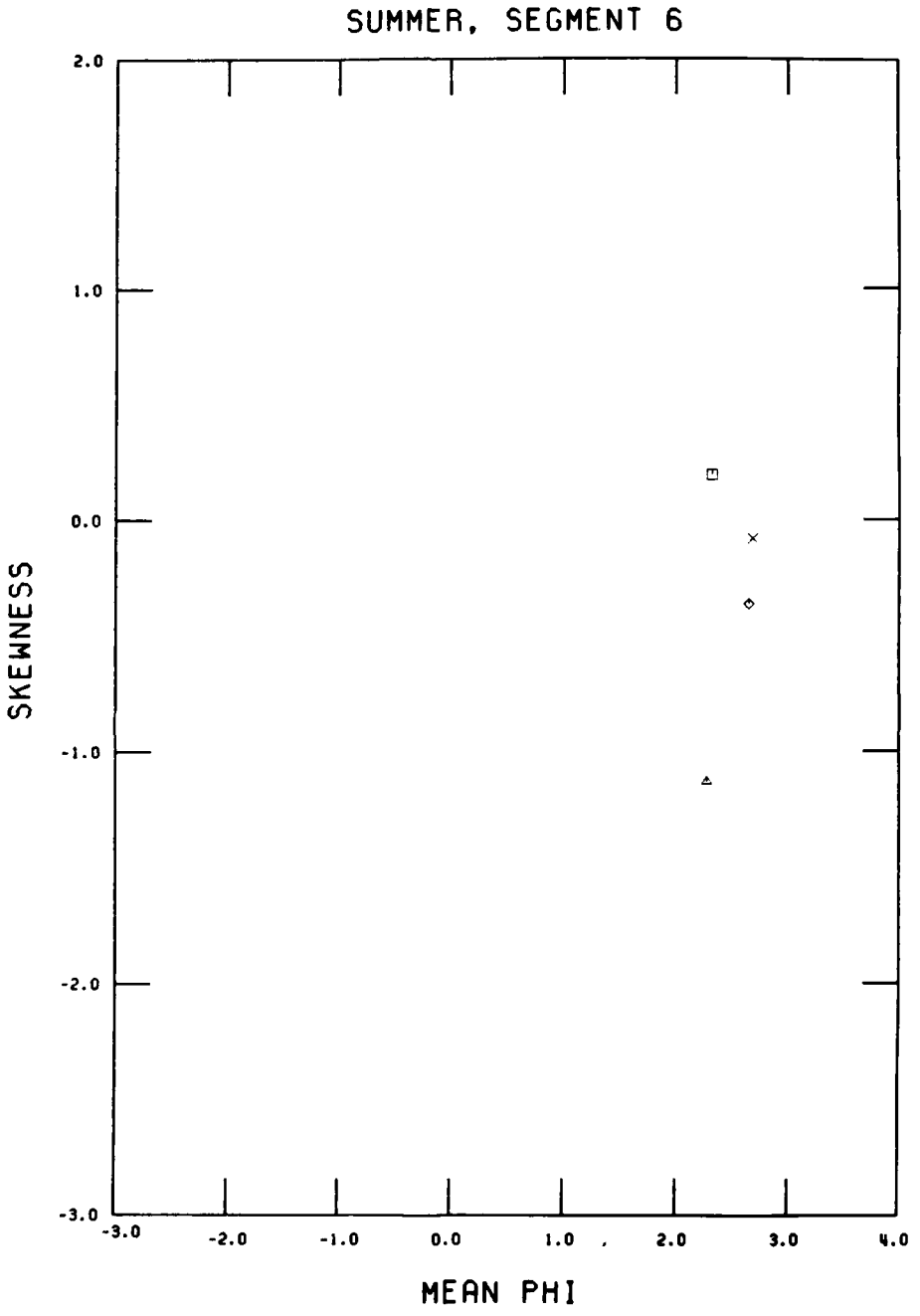
SUMMER, SEGMENT 6
SKEWNESS
MEAN PHI
2.0
1.0
0.0
-1.0
-2.0
-3.0
-3.0
-2.0
-1.0
0.0
1.0
2.0
3.0
4.0

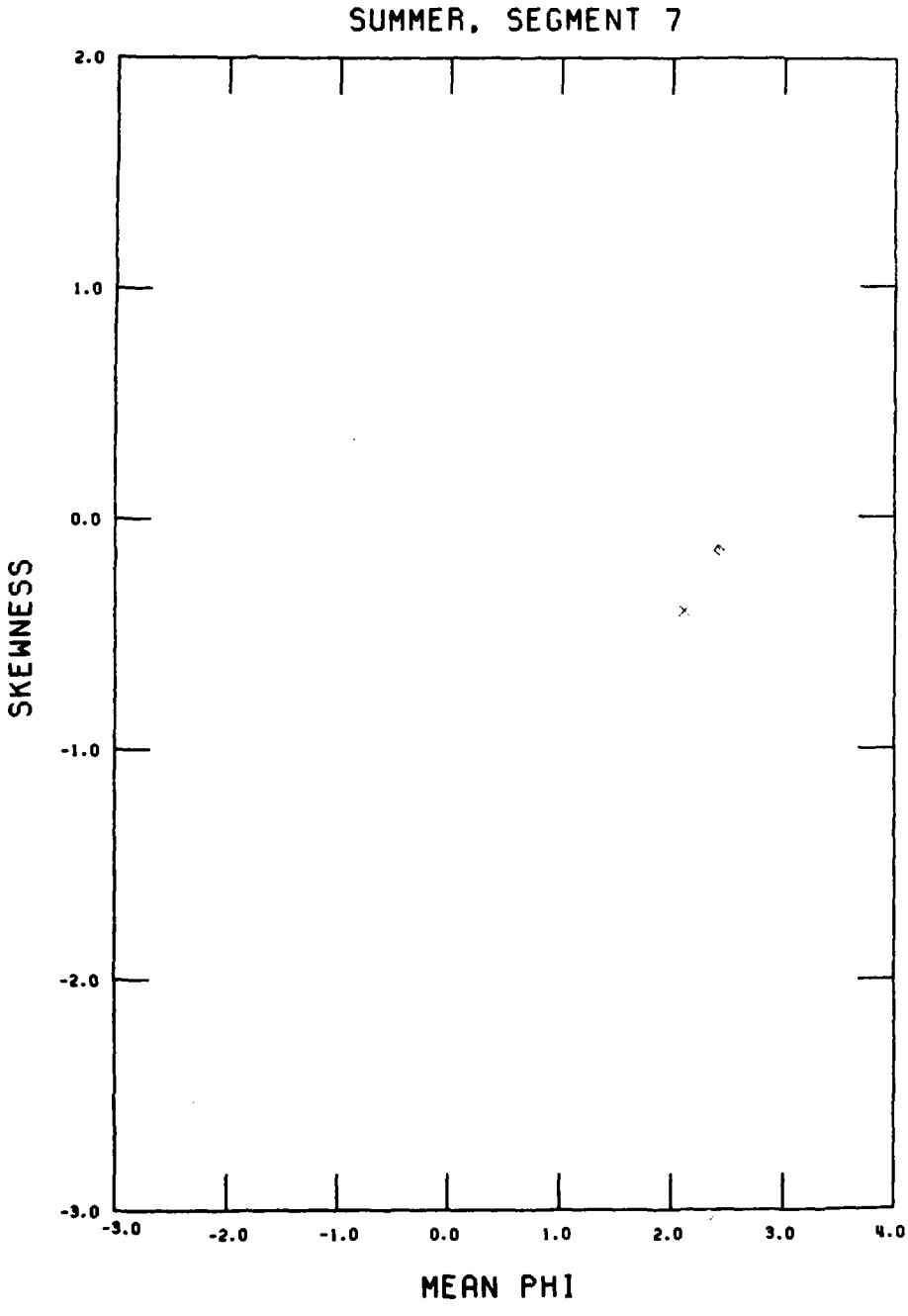
SUMMER, SEGMENT 7
2.0
1.0
0.0
-1.0
-2.0
-3.0
SKEWNESS
-3.0
-2.0
-1.0
0.0
1.0
2.0
3.0
4.0
MEAN PHI

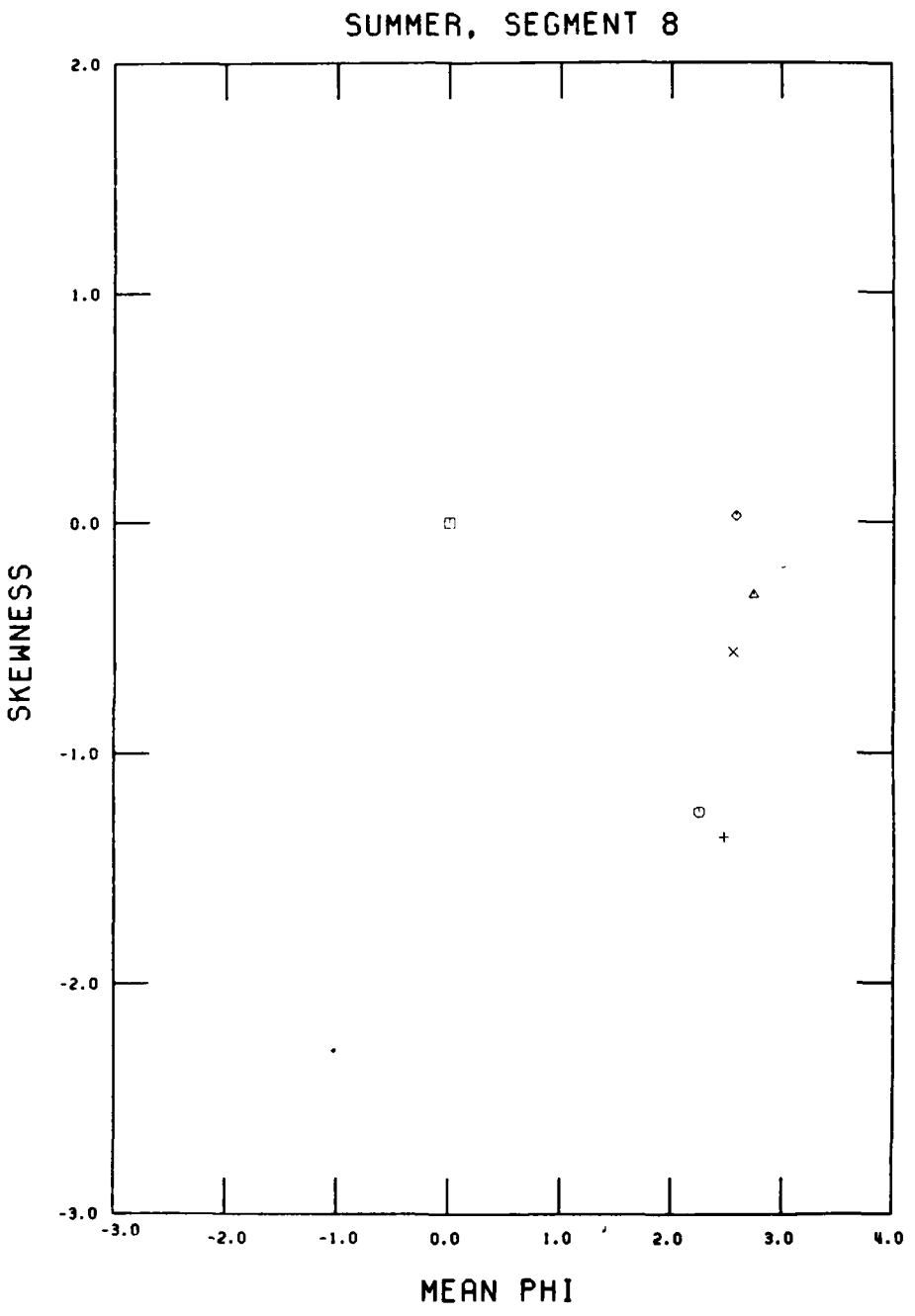
SUMMER, SEGMENT 8
SKEWNESS
MEAN PHI
2.0
1.0
0.0
-1.0
-2.0
-3.0
-3.0
-2.0
-1.0
0.0
1.0
2.0
3.0
4.0

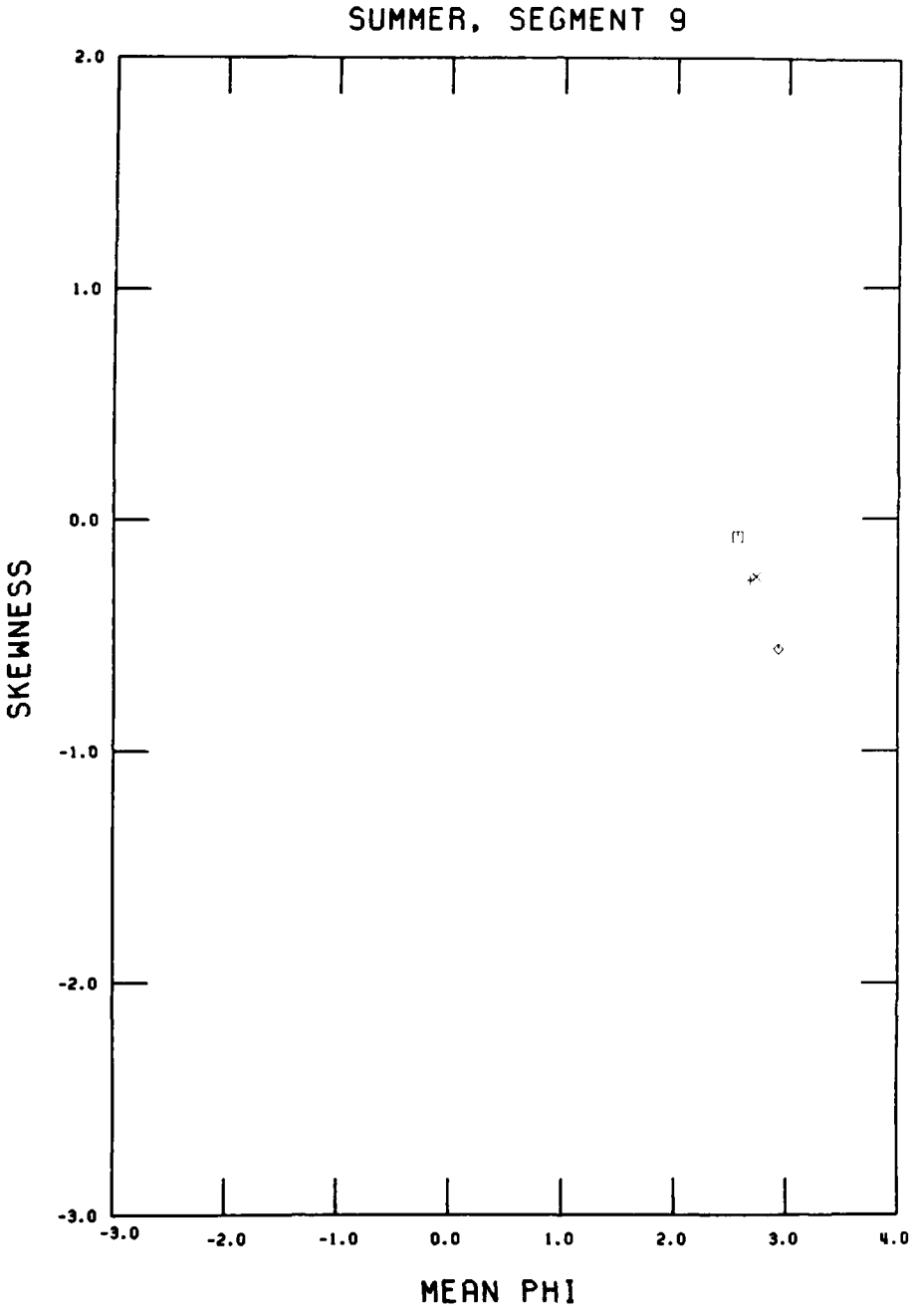
SUMMER, SEGMENT 9
2.0
1.0
0.0
-1.0
-2.0
-3.0
SKEWNESS
-3.0
-2.0
-1.0
0.0
1.0
2.0
3.0
4.0
MEAN PHI

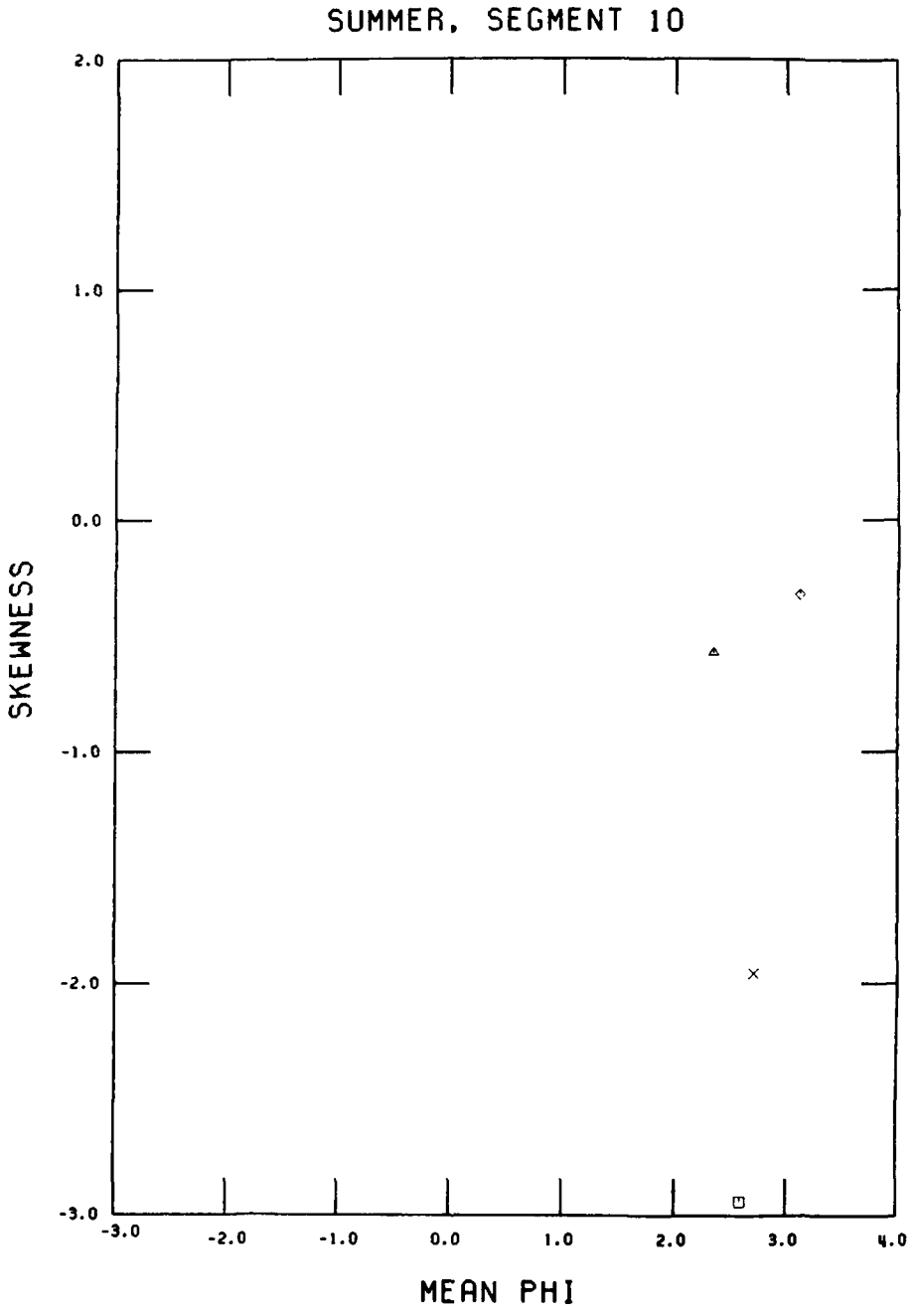
SUMMER, SEGMENT 10
SKEWNESS
MEAN PHI
2.0
1.0
0.0
-1.0
-2.0
-3.0
-3.0
-2.0
-1.0
0.0
1.0
2.0
3.0
4.0

Appendix C Bivariate plots of phi standard deviation versus phi skewness for the end-of-summer regional data set by littoral segment. Symbols are the same as for Appendix A.

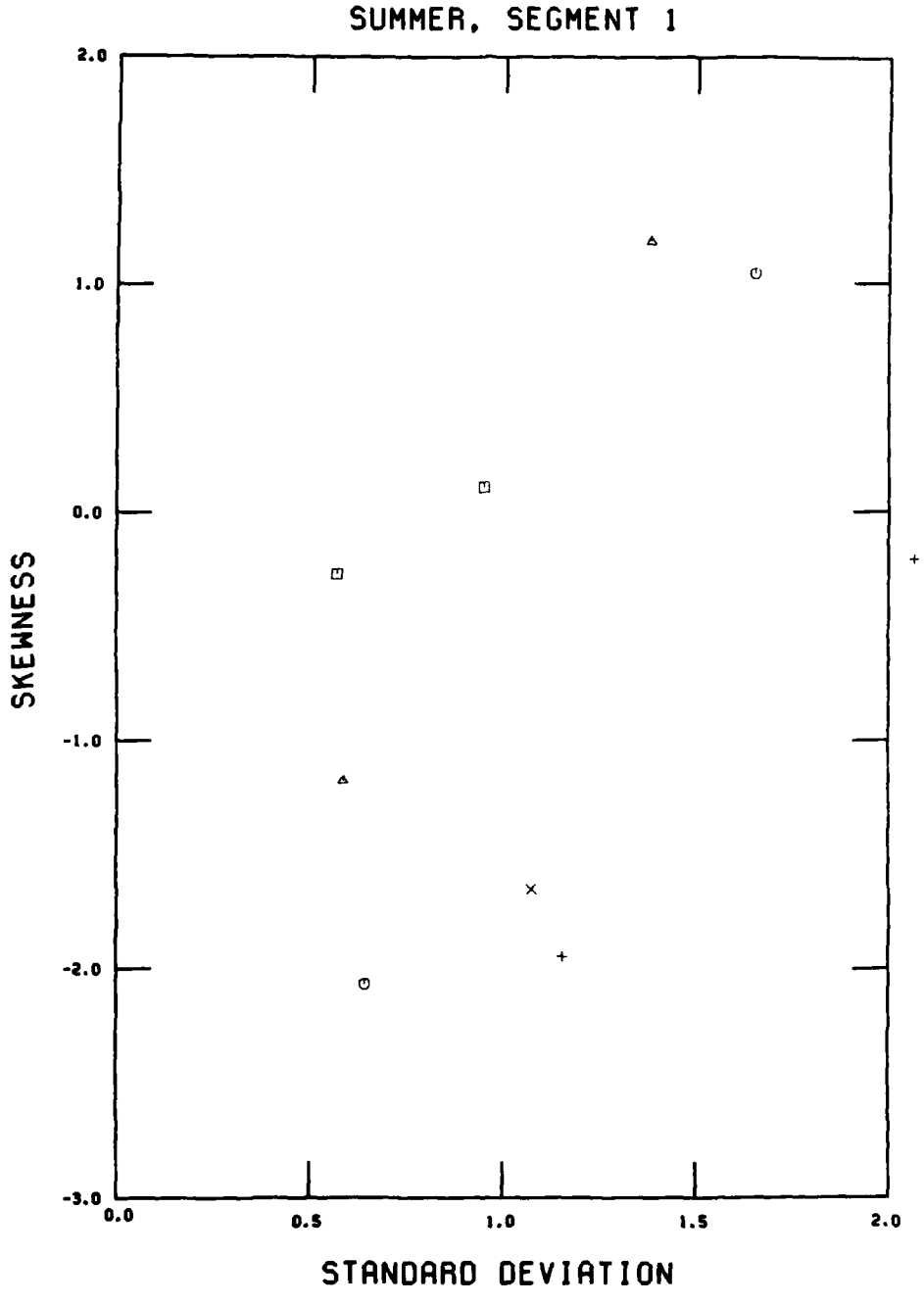
SUMMER, SEGMENT 1
2.0
1.0
0.0
-1.0
-2.0
-3.0
SKEWNESS
0.0
0.5
1.0
1.5
2.0
STANDARD DEVIATION

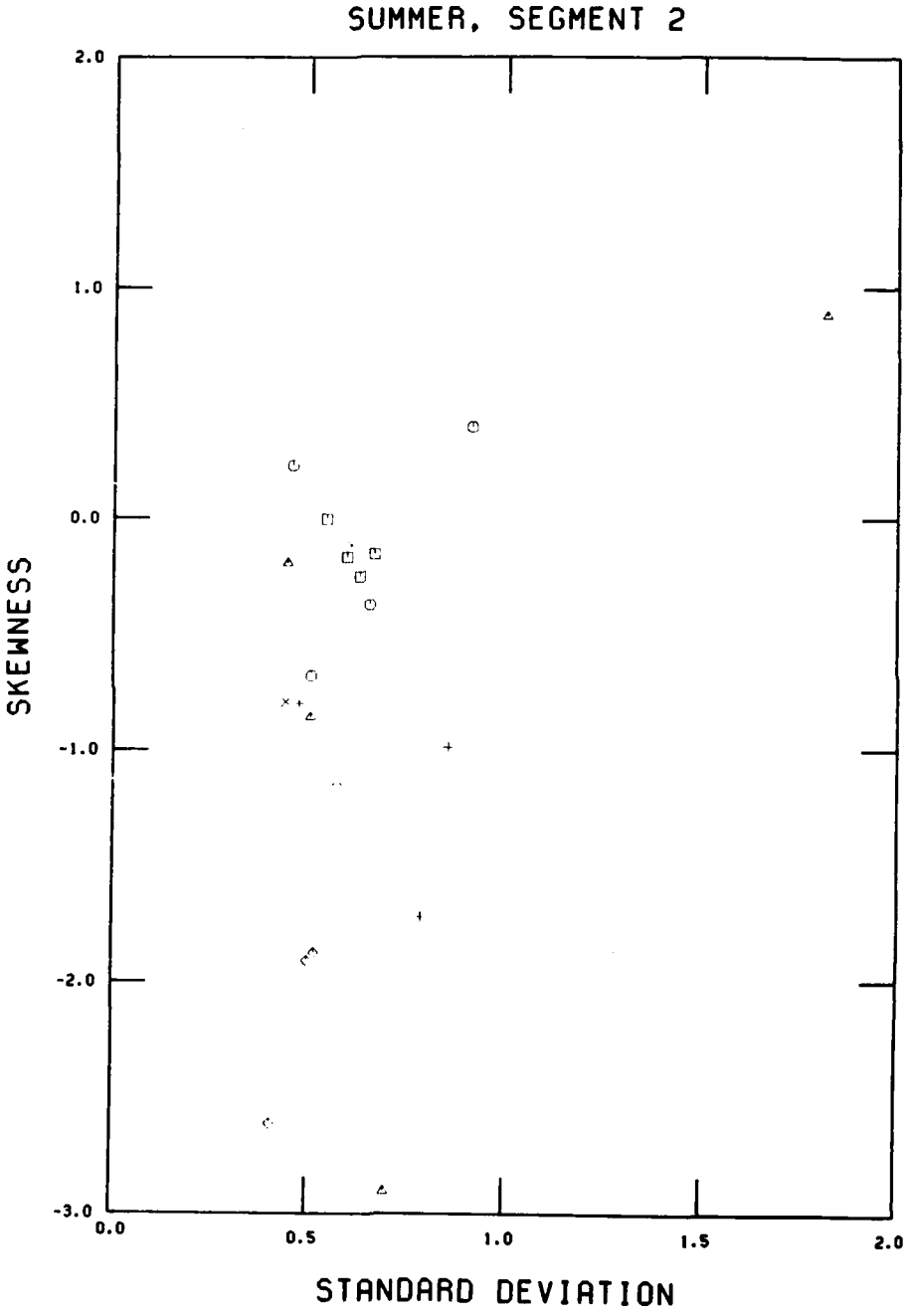
SUMMER, SEGMENT 2
2.0
1.0
0.0
-1.0
-2.0
-3.0
SKEWNESS
0.0
0.5
1.0
1.5
2.0
STANDARD DEVIATION

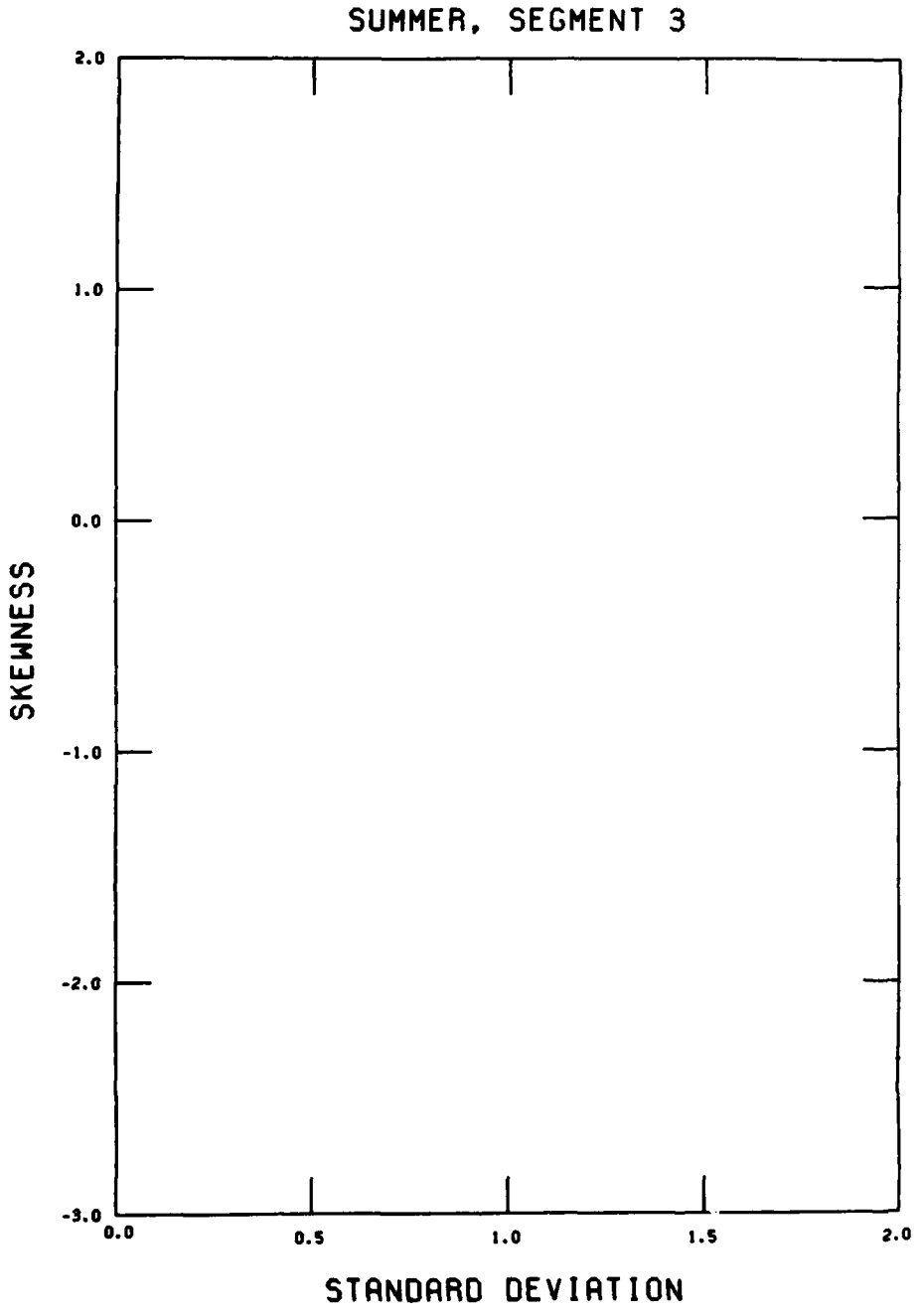
SUMMER, SEGMENT 3
2.0
1.0
0.0
-1.0
-2.0
-3.0
SKEWNESS
0.0
0.5
1.0
1.5
2.0
STANDARD DEVIATION

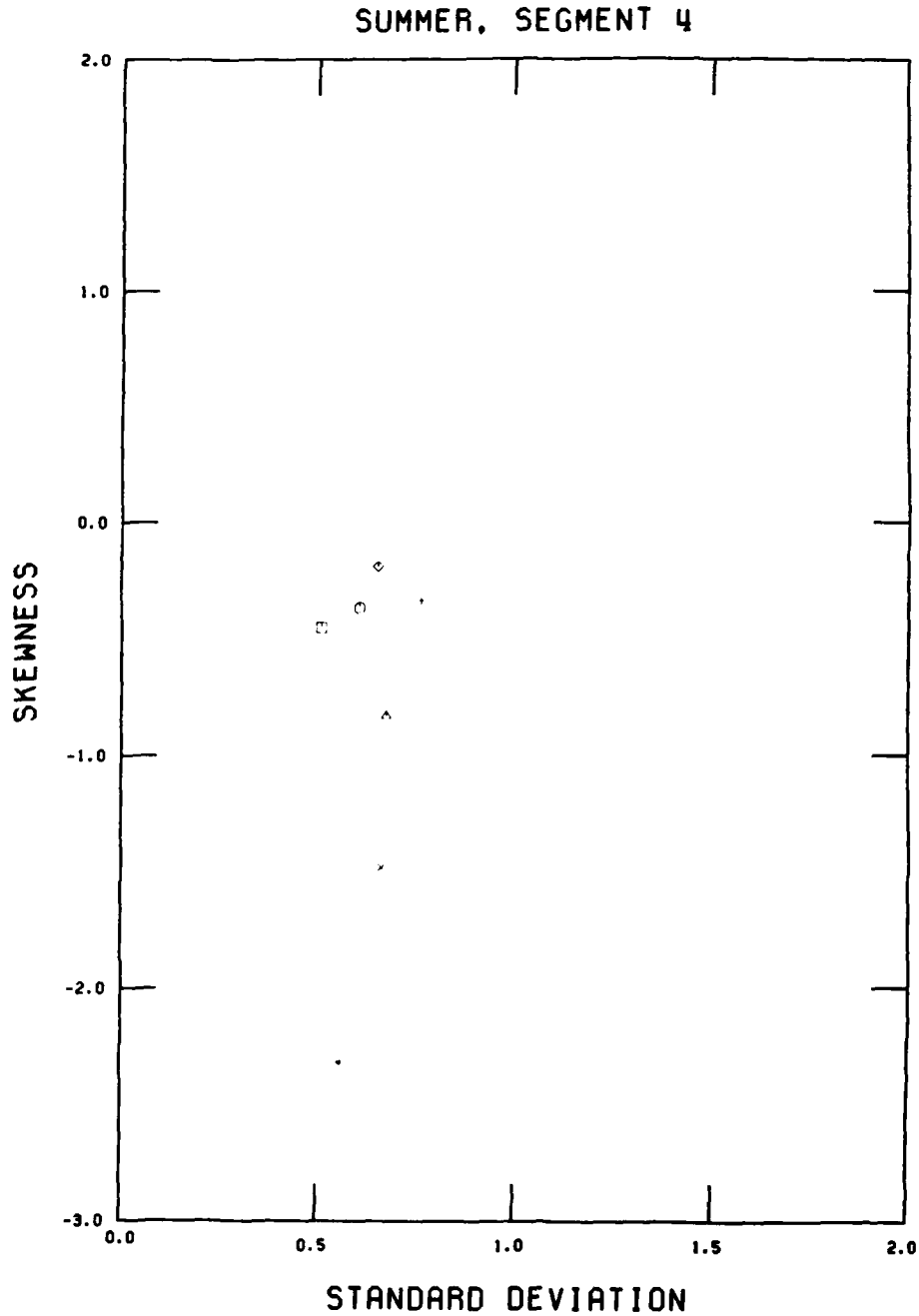
SUMMER, SEGMENT 4
2.0
1.0
0.0
-1.0
-2.0
-3.0
SKEWNESS
0.0
0.5
1.0
1.5
2.0
STANDARD DEVIATION

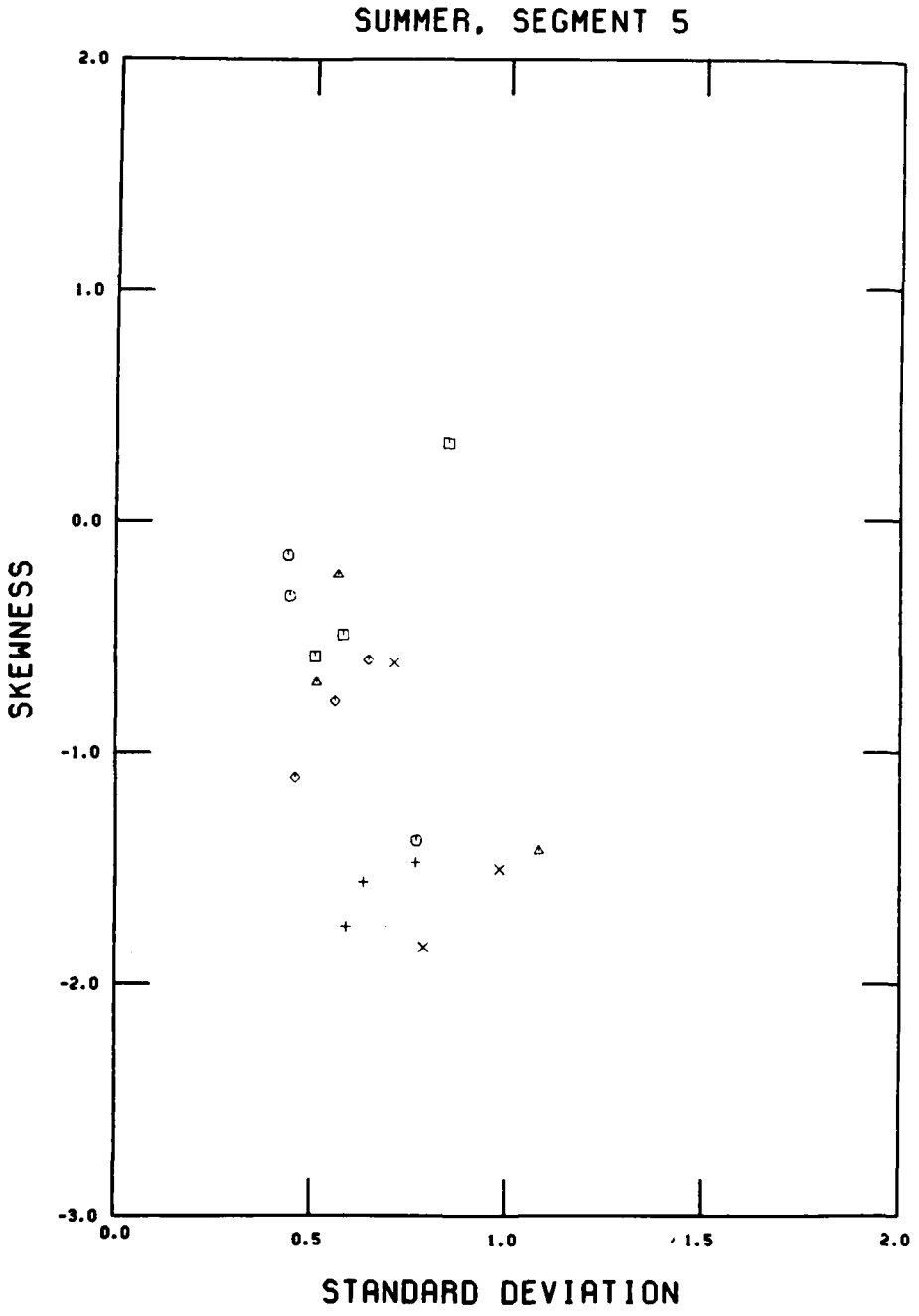
SUMMER, SEGMENT 5
2.0
1.0
0.0
-1.0
-2.0
-3.0
SKEWNESS
0.0
0.5
1.0
1.5
2.0
STANDARD DEVIATION

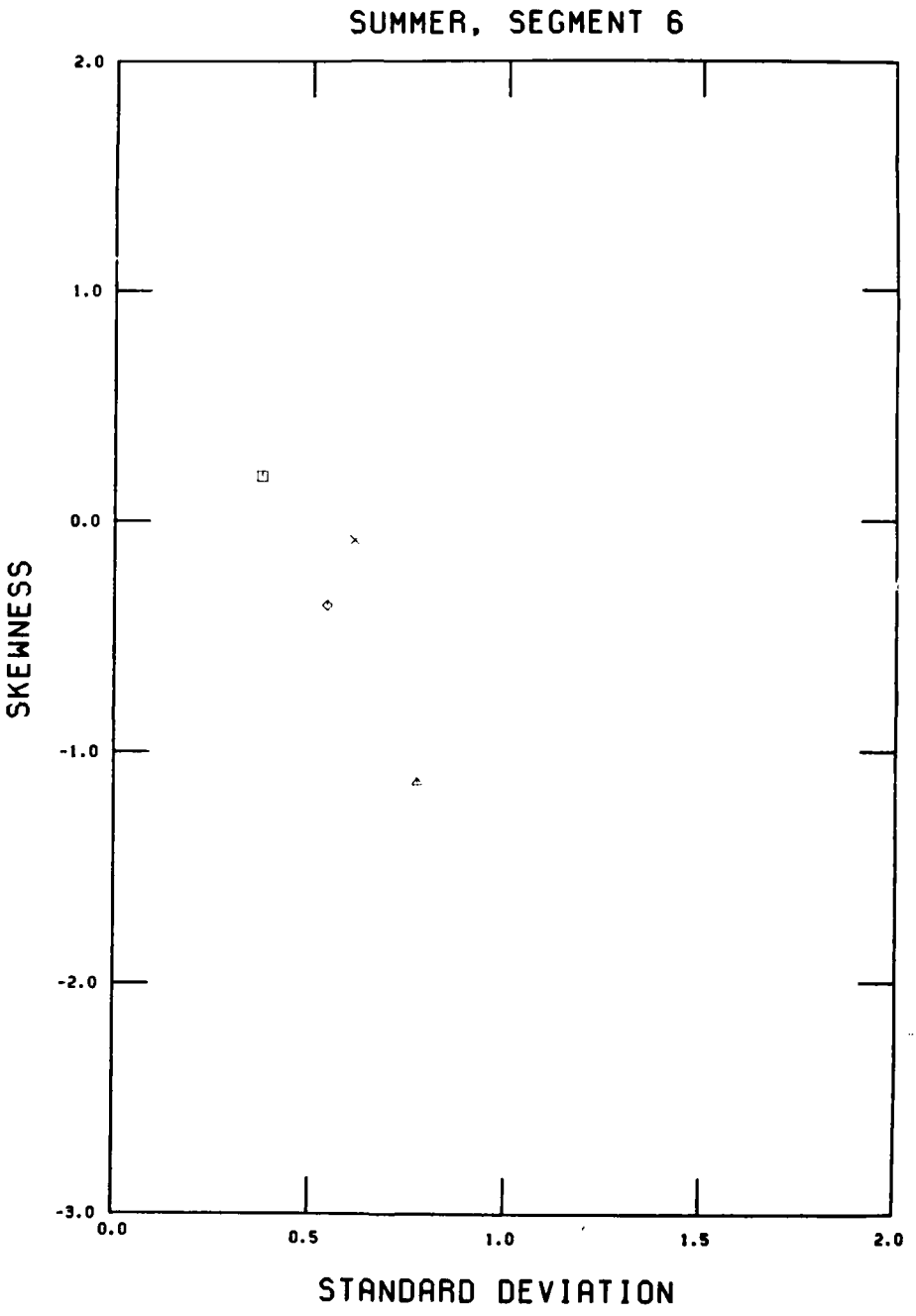
SUMMER, SEGMENT 6
2.0
1.0
0.0
-1.0
-2.0
-3.0
SKEWNESS
0.0
0.5
1.0
1.5
2.0
STANDARD DEVIATION

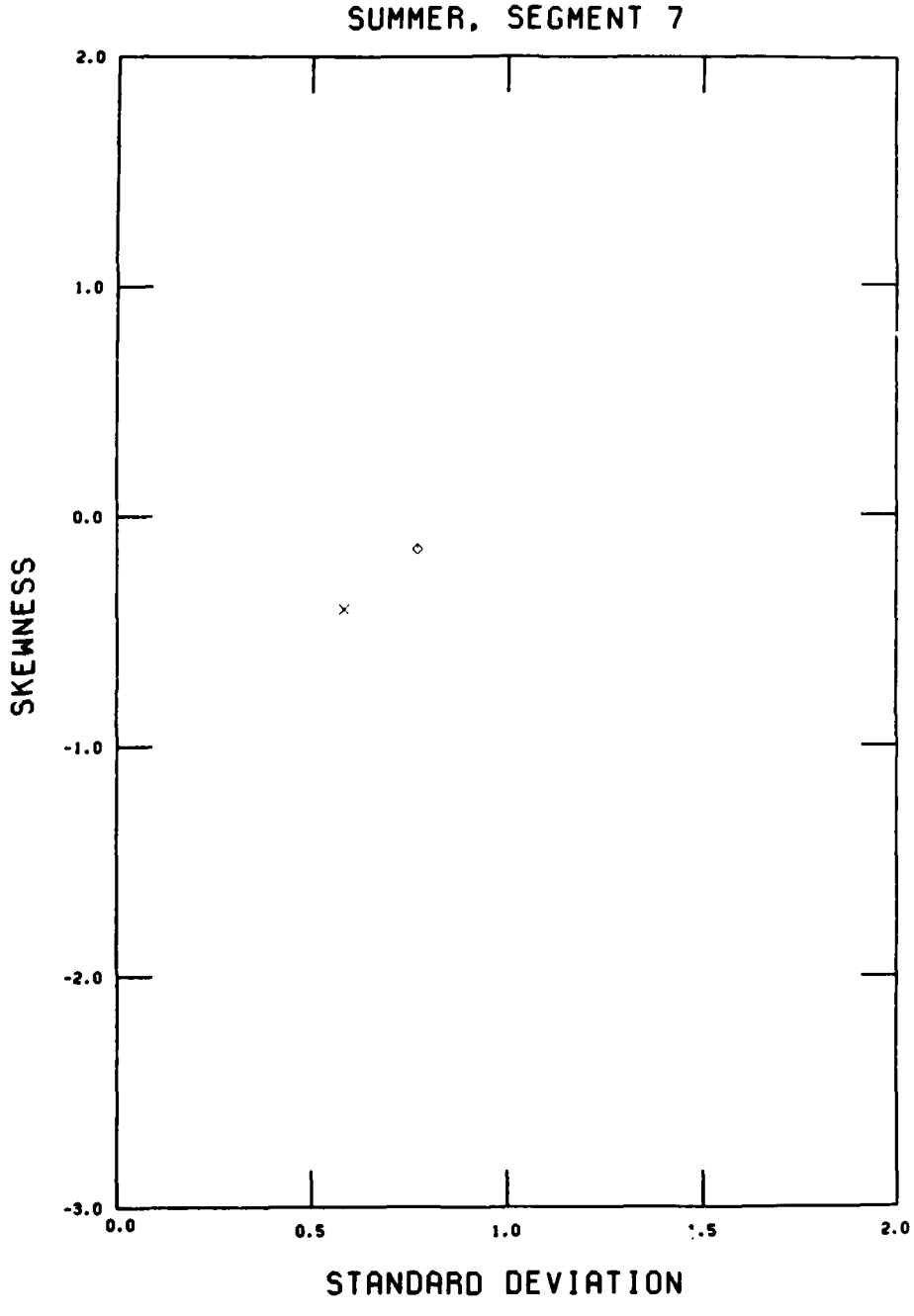
SUMMER, SEGMENT 7
2.0
1.0
0.0
-1.0
-2.0
-3.0
SKEWNESS
0.0
0.5
1.0
1.5
2.0
STANDARD DEVIATION

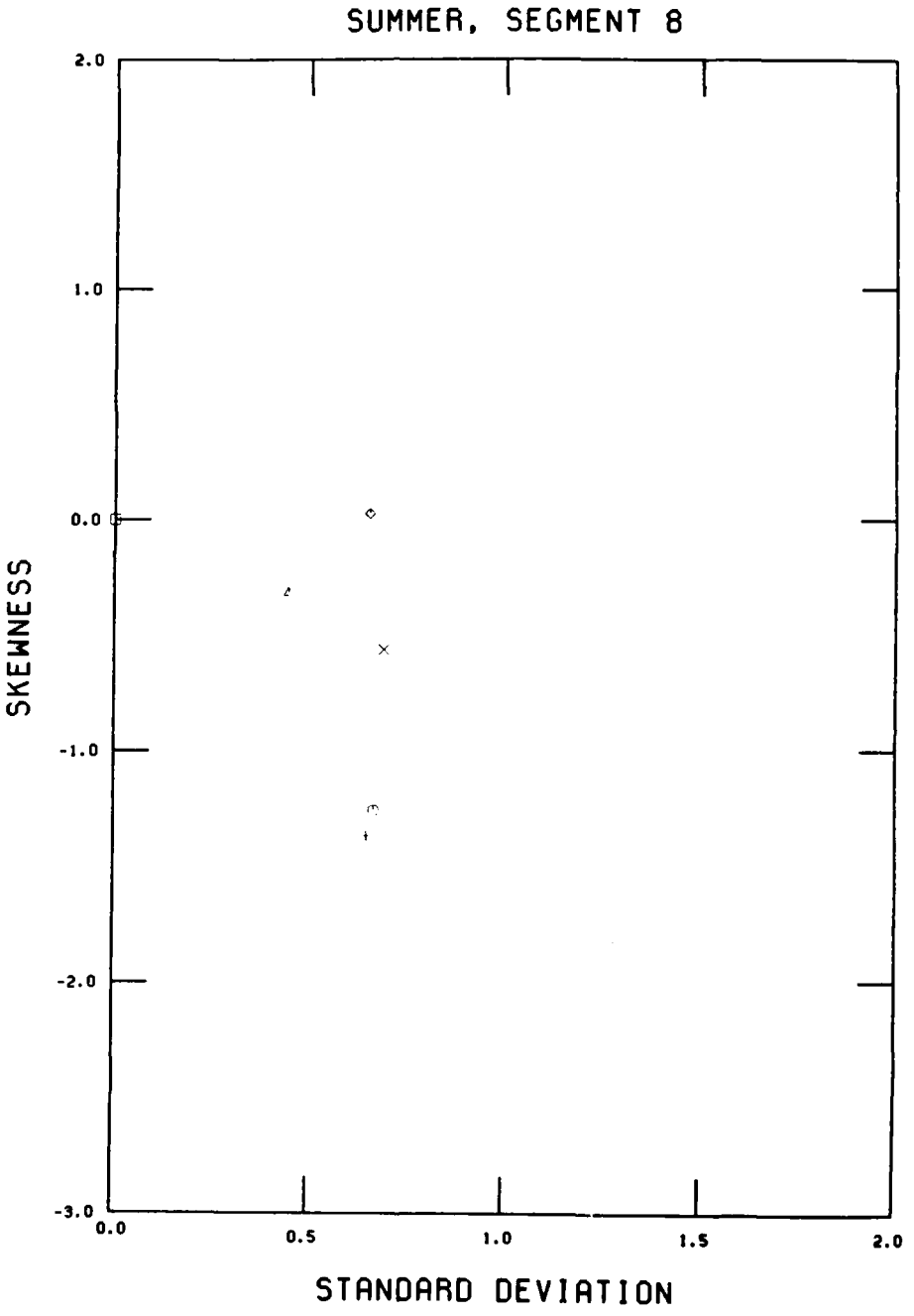
SUMMER, SEGMENT 8
2.0
1.0
0.0
-1.0
-2.0
-3.0
SKEWNESS
0.0
0.5
1.0
1.5
2.0
STANDARD DEVIATION

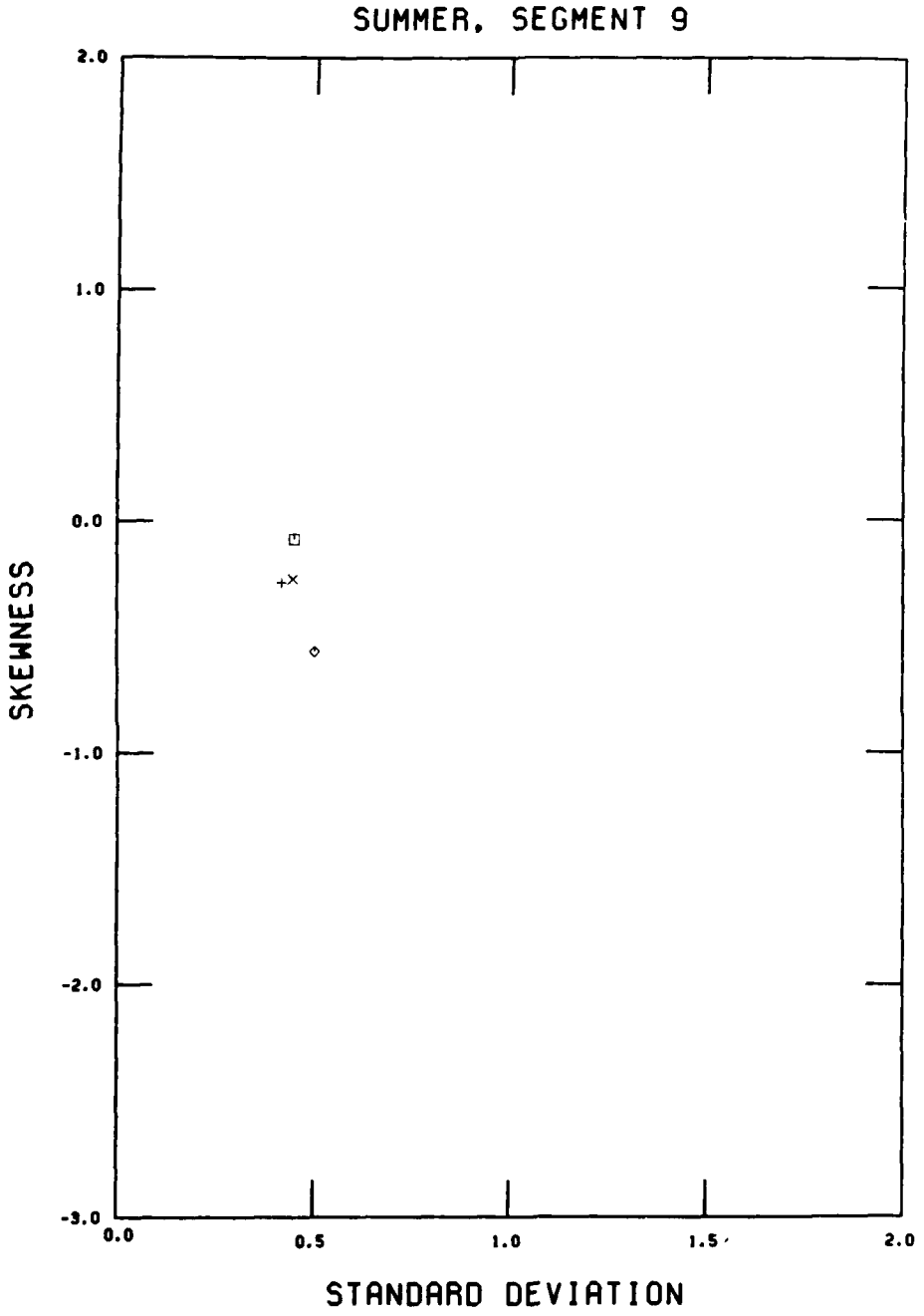
SUMMER, SEGMENT 9
2.0
1.0
0.0
-1.0
-2.0
-3.0
SKEWNESS
0.0
0.5
1.0
1.5
2.0
STANDARD DEVIATION

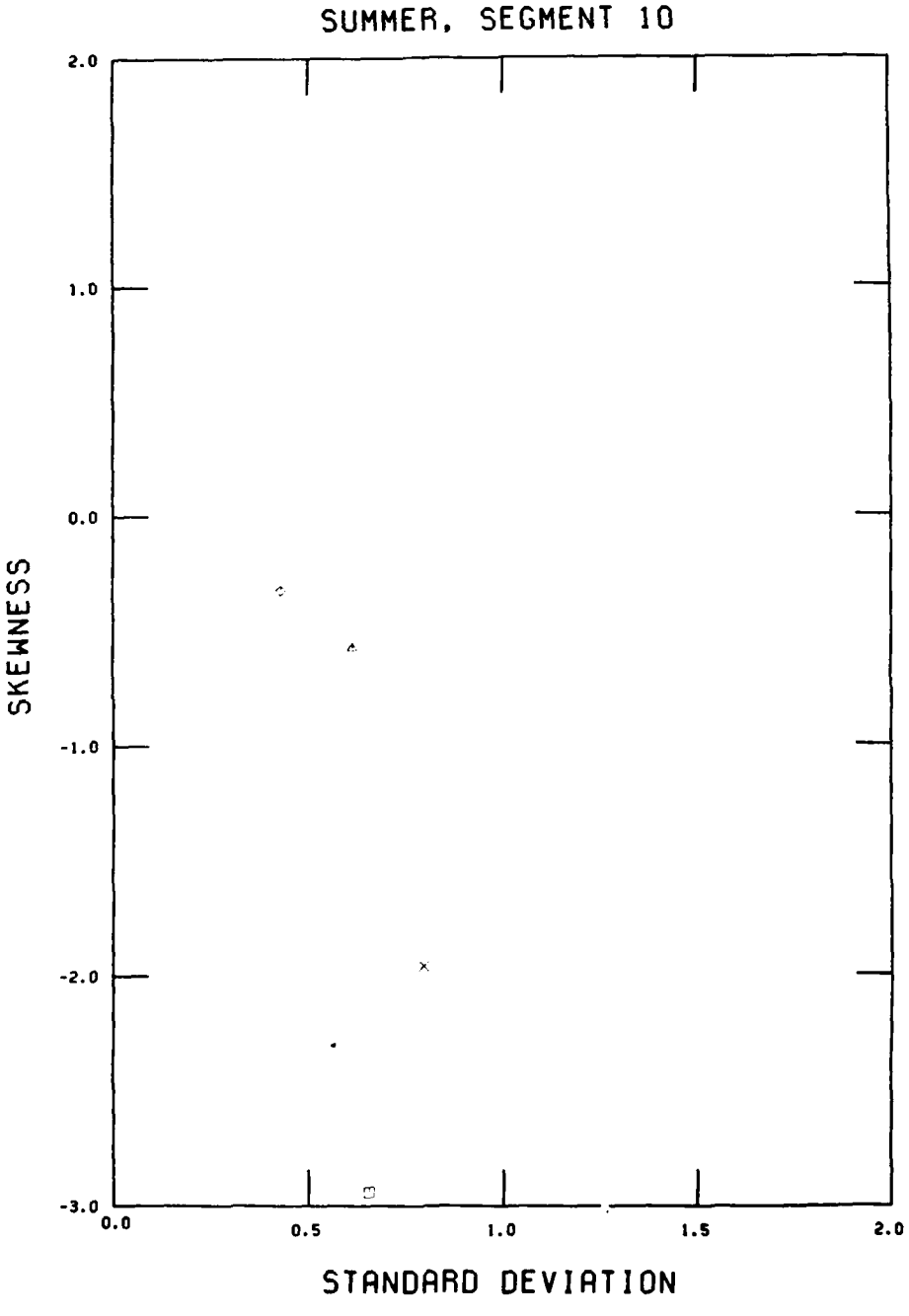
SUMMER, SEGMENT 10
2.0
1.0
0.0
-1.0
-2.0
-3.0
SKEWNESS
0.0
0.5
1.0
1.5
2.0
STANDARD DEVIATION

Appendix D Bivariate plots of phi standard deviation versus mean phi for the end-of-winter regional data set by littoral segment. Symbols are the same as for Appendix A.

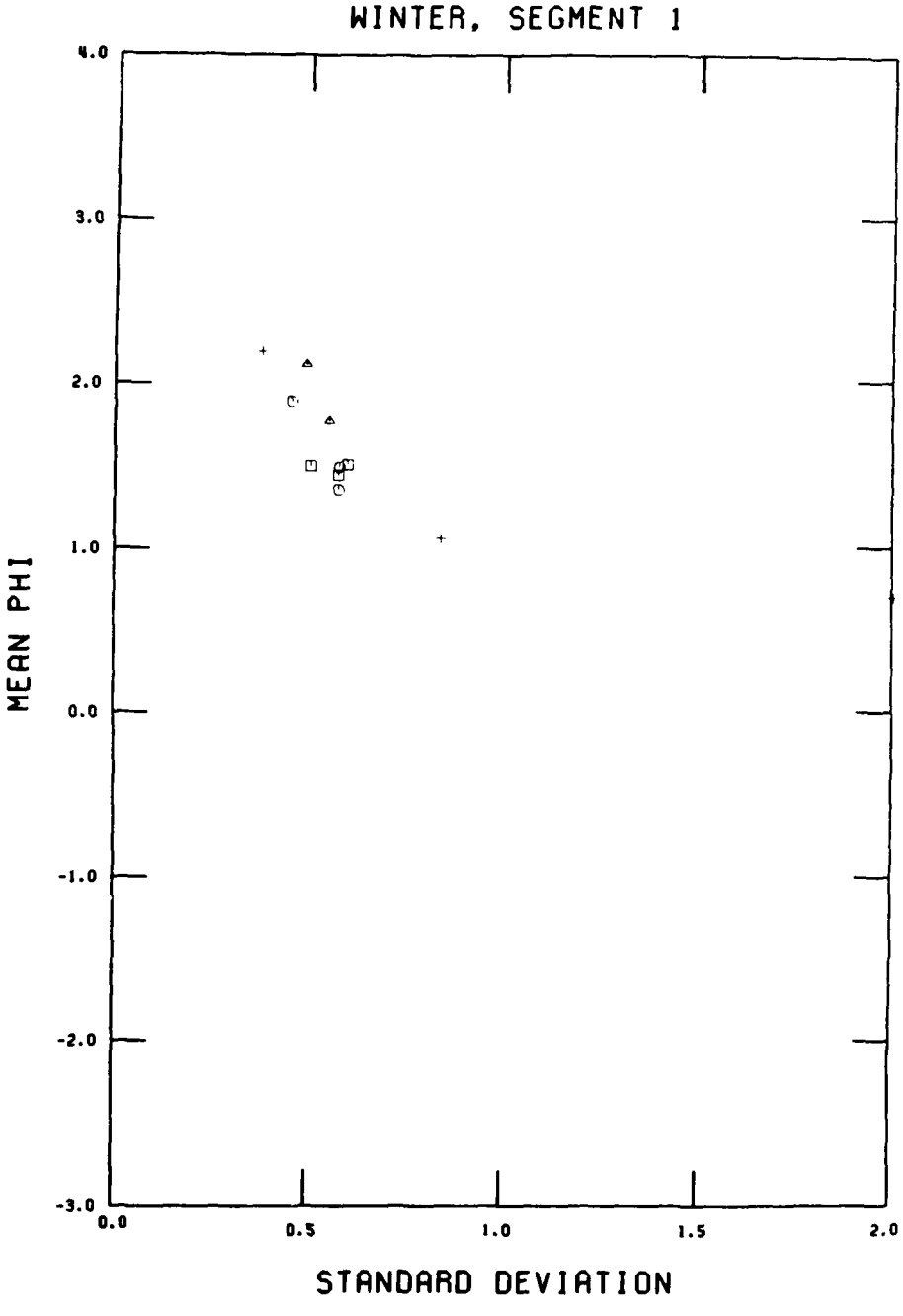
WINTER, SEGMENT 1
4.0
3.0
2.0
1.0
0.0
-1.0
-2.0
-3.0
MEAN PHI
0.0
0.5
1.0
1.5
2.0
STANDARD DEVIATION

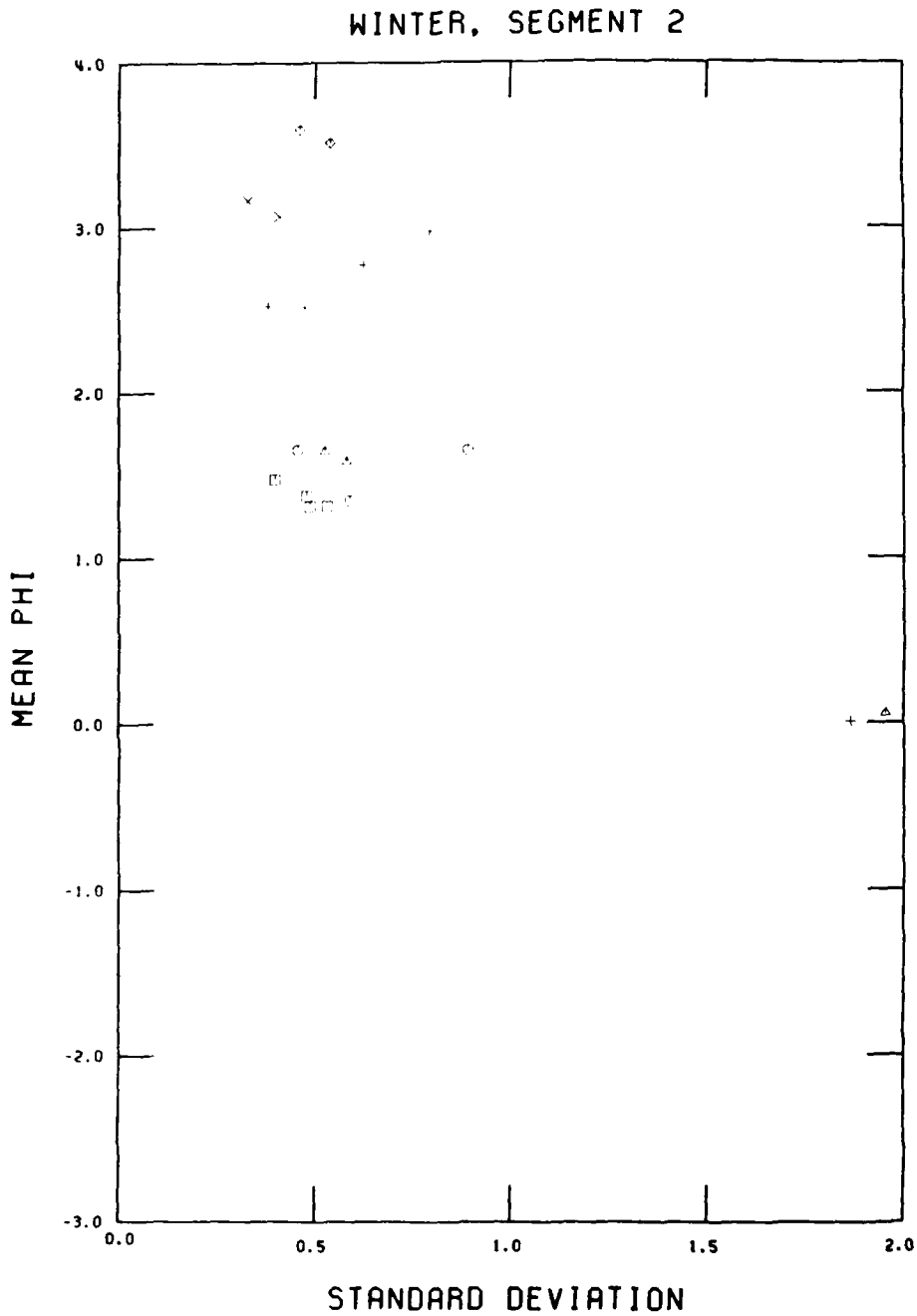
WINTER, SEGMENT 2
4.0
3.0
2.0
1.0
0.0
-1.0
-2.0
-3.0
MEAN PHI
0.0
0.5
1.0
1.5
2.0
STANDARD DEVIATION

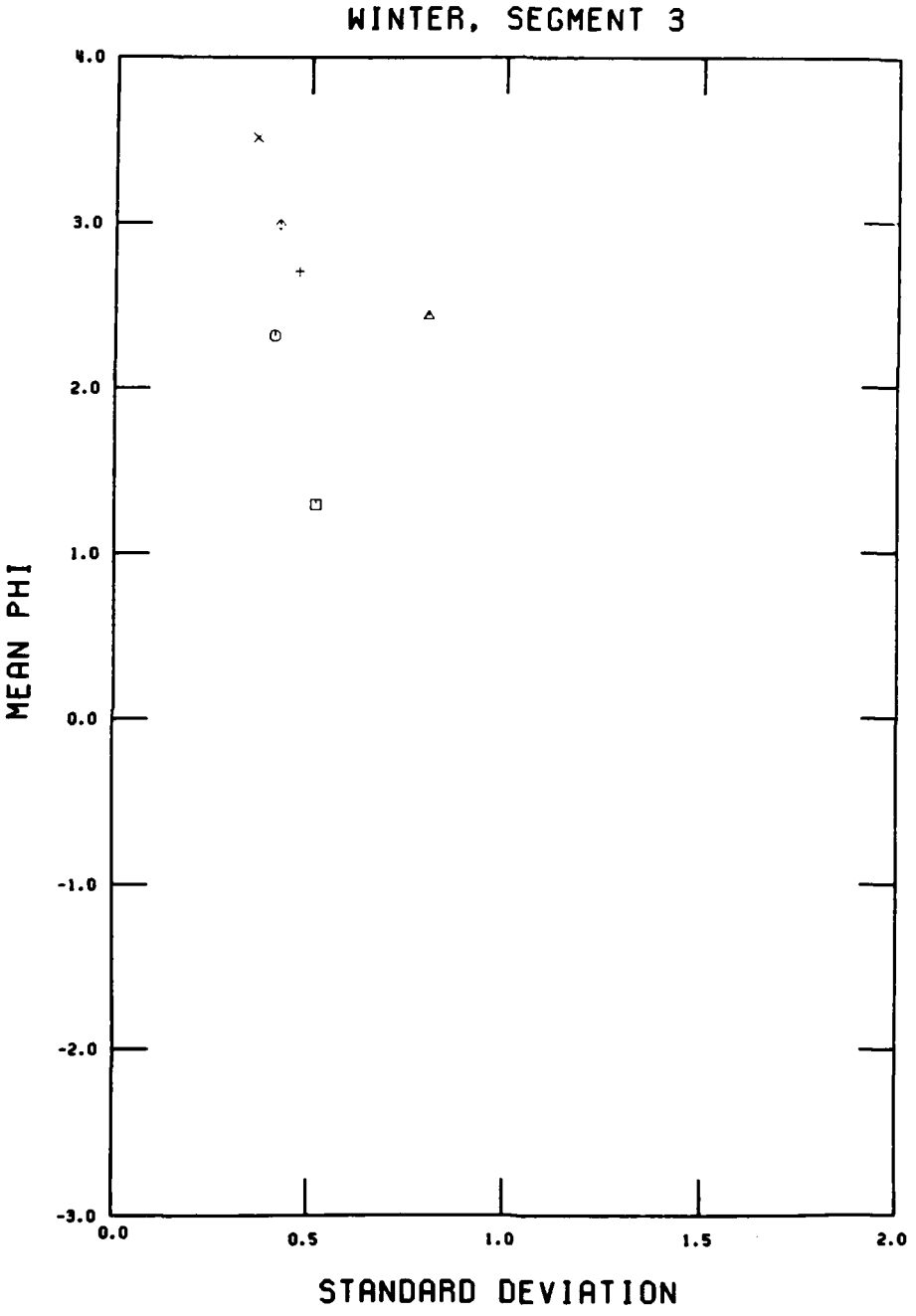
WINTER, SEGMENT 3
4.0
3.0
2.0
1.0
0.0
-1.0
-2.0
-3.0
MEAN PHI
0.0
0.5
1.0
1.5
2.0
STANDARD DEVIATION

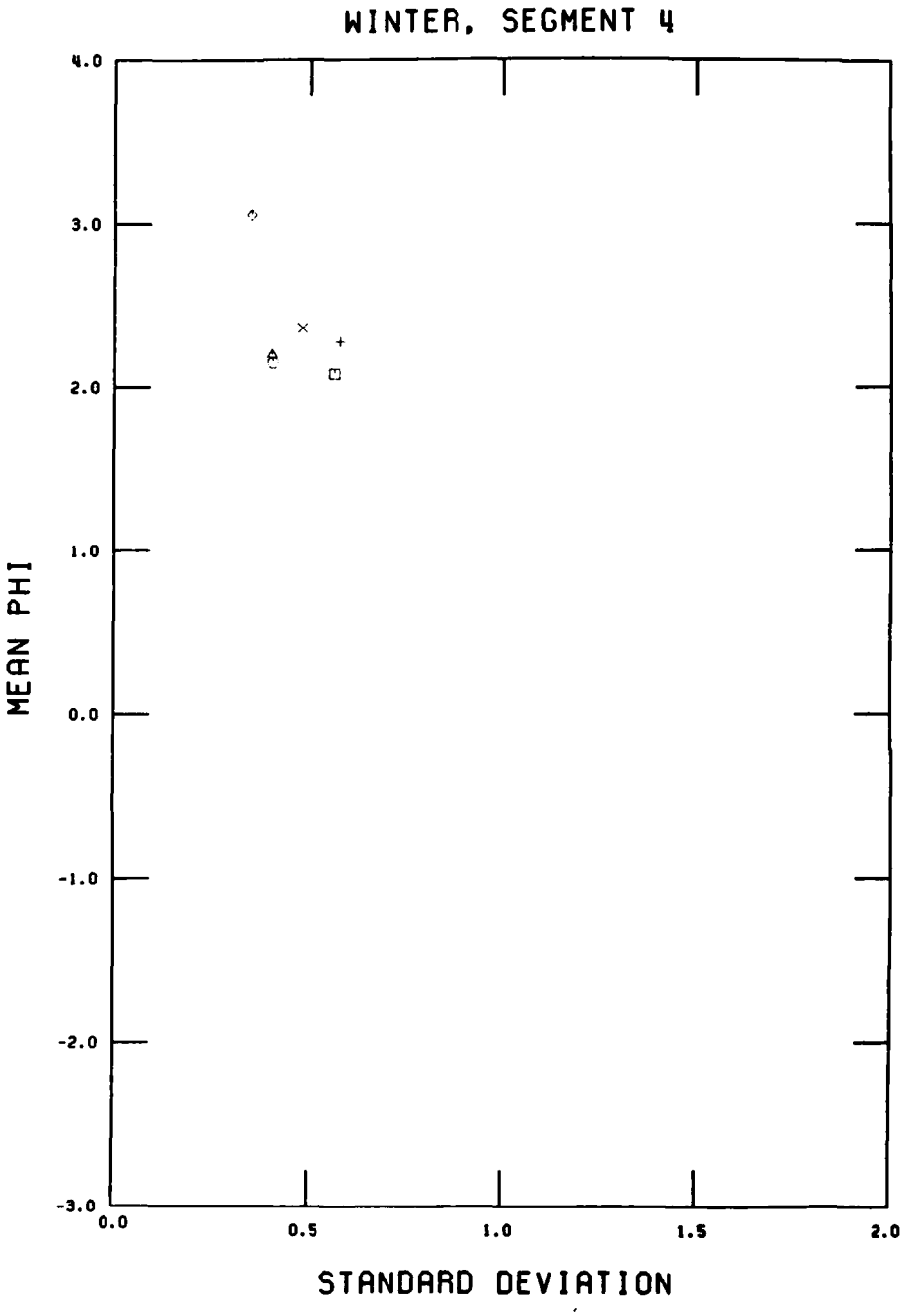
WINTER, SEGMENT 4
4.0
3.0
2.0
1.0
0.0
-1.0
-2.0
-3.0
MEAN PHI
0.0
0.5
1.0
1.5
2.0
STANDARD DEVIATION

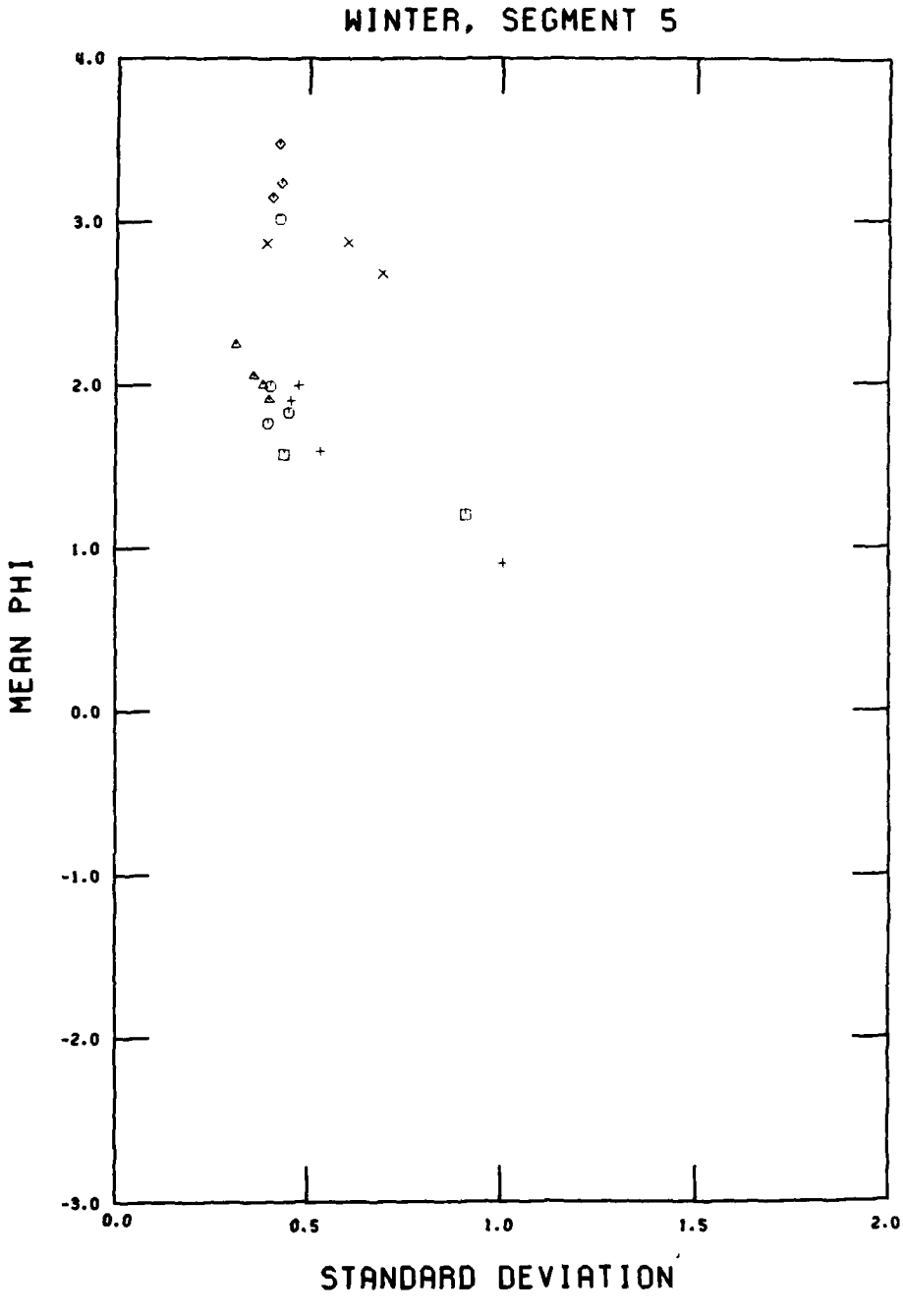
WINTER, SEGMENT 5
MEAN PHI
4.0
3.0
2.0
1.0
0.0
-1.0
-2.0
-3.0
0.0
0.5
1.0
1.5
2.0
STANDARD DEVIATION

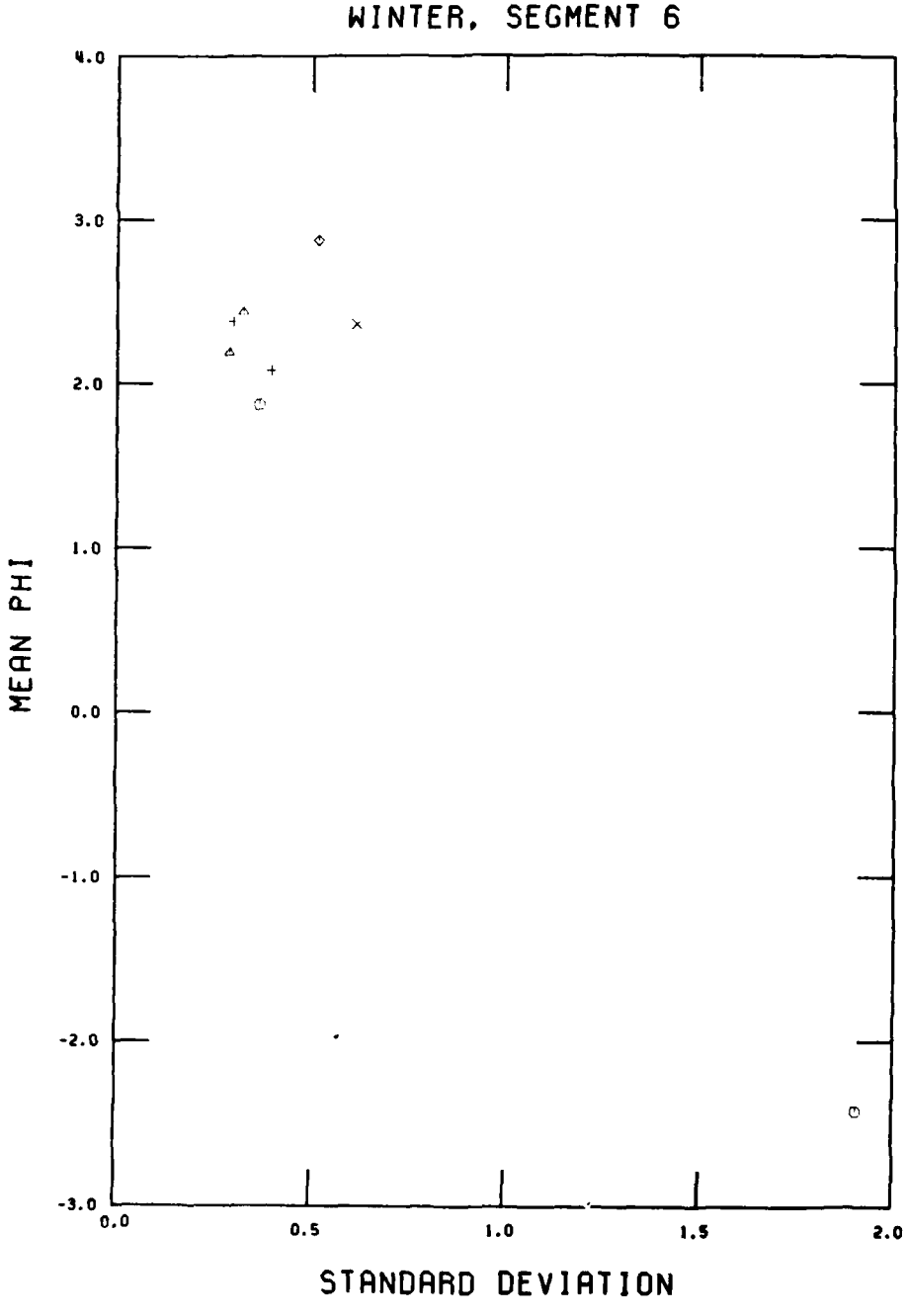
WINTER, SEGMENT 6
4.0
3.0
2.0
1.0
0.0
-1.0
-2.0
-3.0
MEAN PHI
0.0
0.5
1.0
1.5
2.0
STANDARD DEVIATION

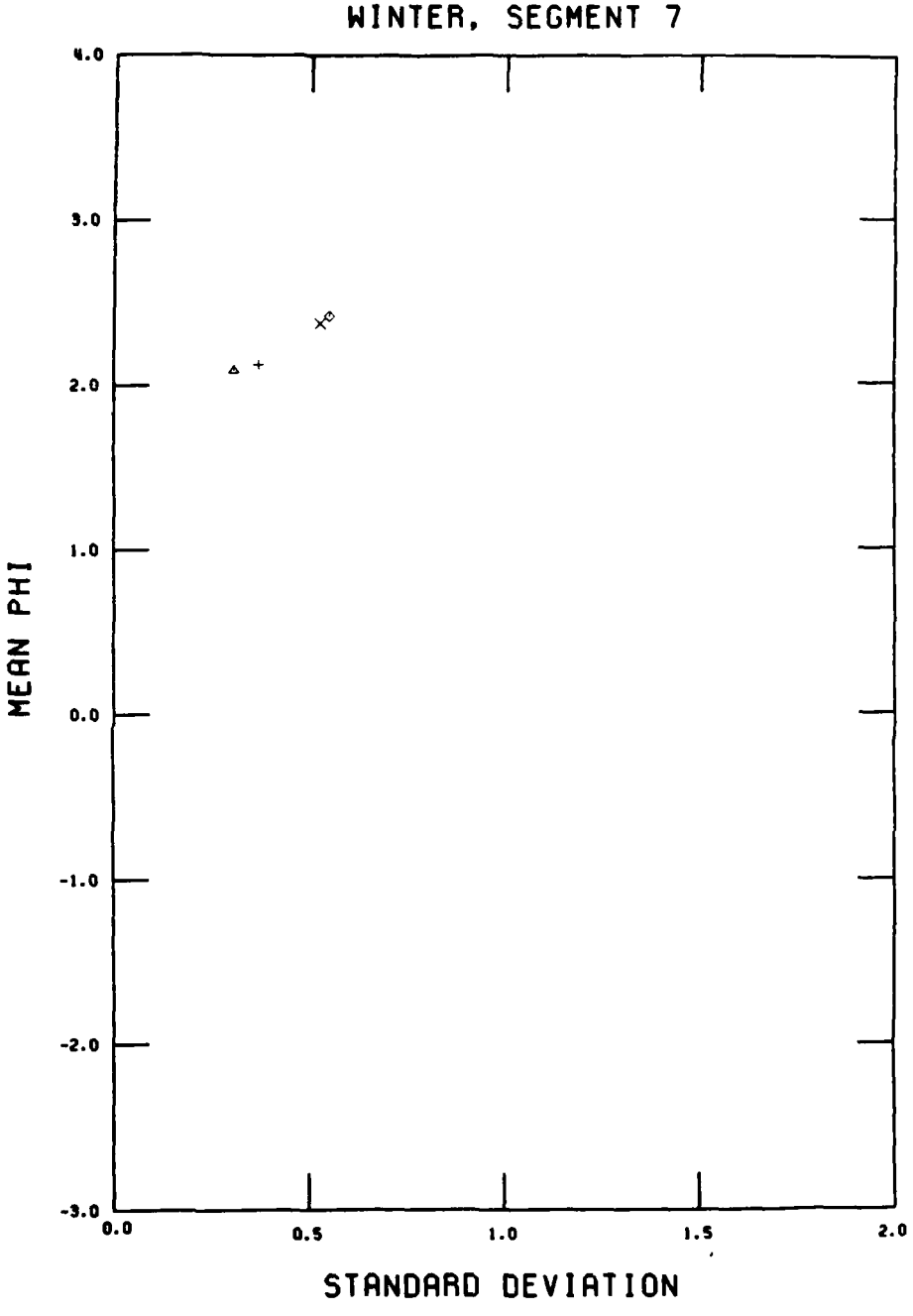
WINTER, SEGMENT 7
4.0
3.0
2.0
1.0
0.0
-1.0
-2.0
-3.0
MEAN PHI
0.0
0.5
1.0
1.5
2.0
STANDARD DEVIATION

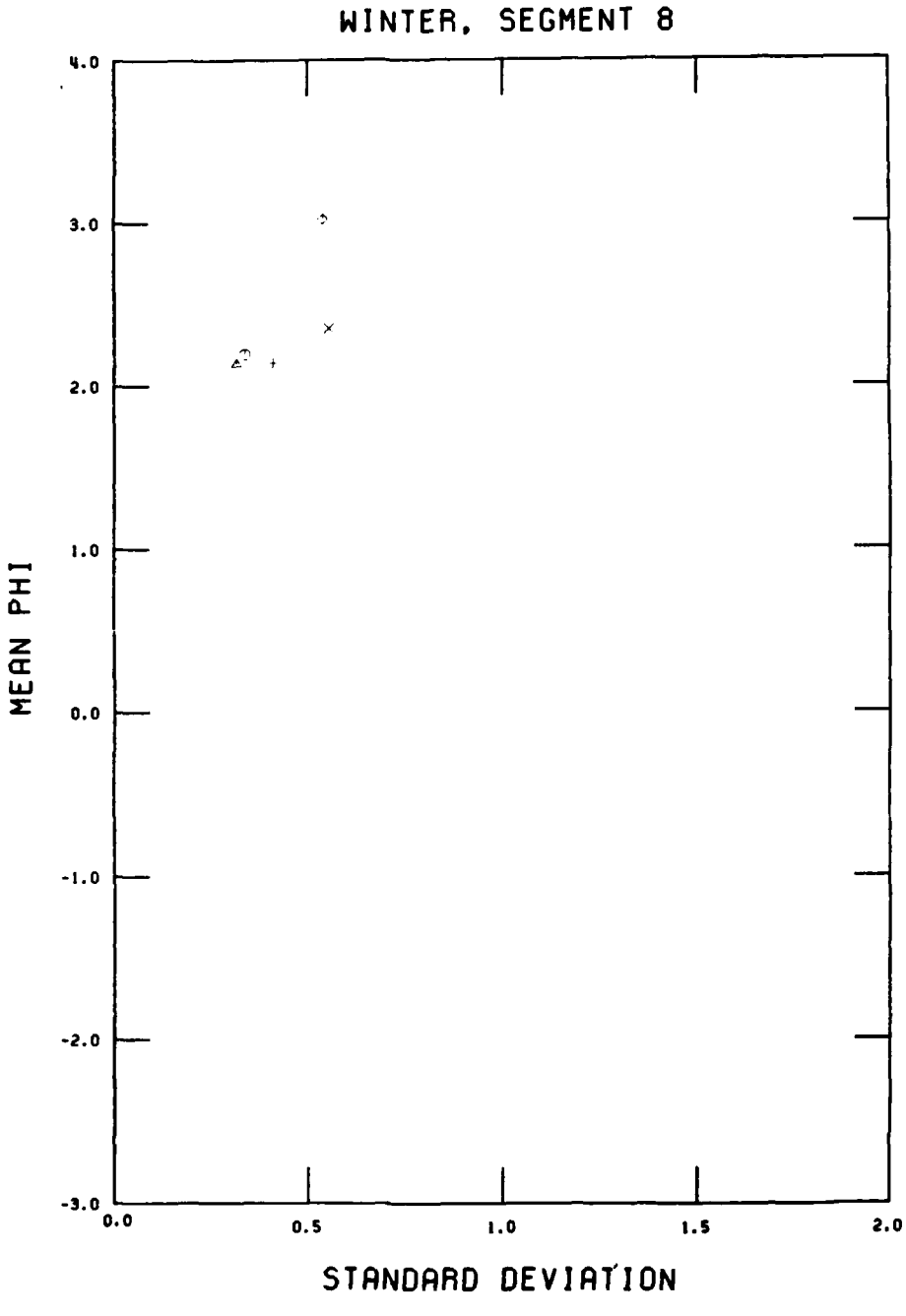
WINTER, SEGMENT 8
4.0
3.0
2.0
1.0
0.0
-1.0
-2.0
-3.0
MEAN PHI
0.0
0.5
1.0
1.5
2.0
STANDARD DEVIATION

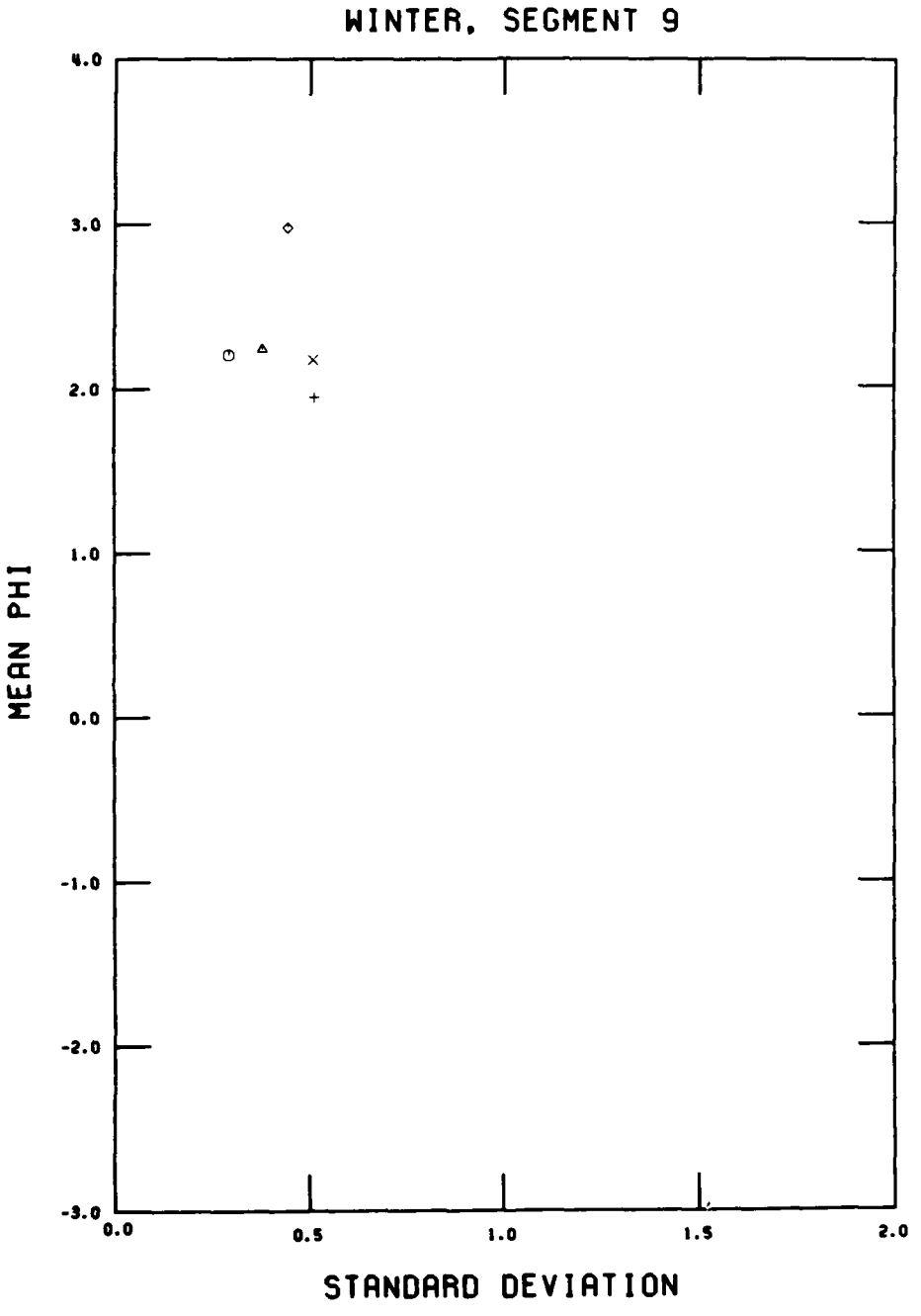
WINTER, SEGMENT 9
4.0
3.0
2.0
1.0
0.0
-1.0
-2.0
-3.0
MEAN PHI
0.0
0.5
1.0
1.5
2.0
STANDARD DEVIATION

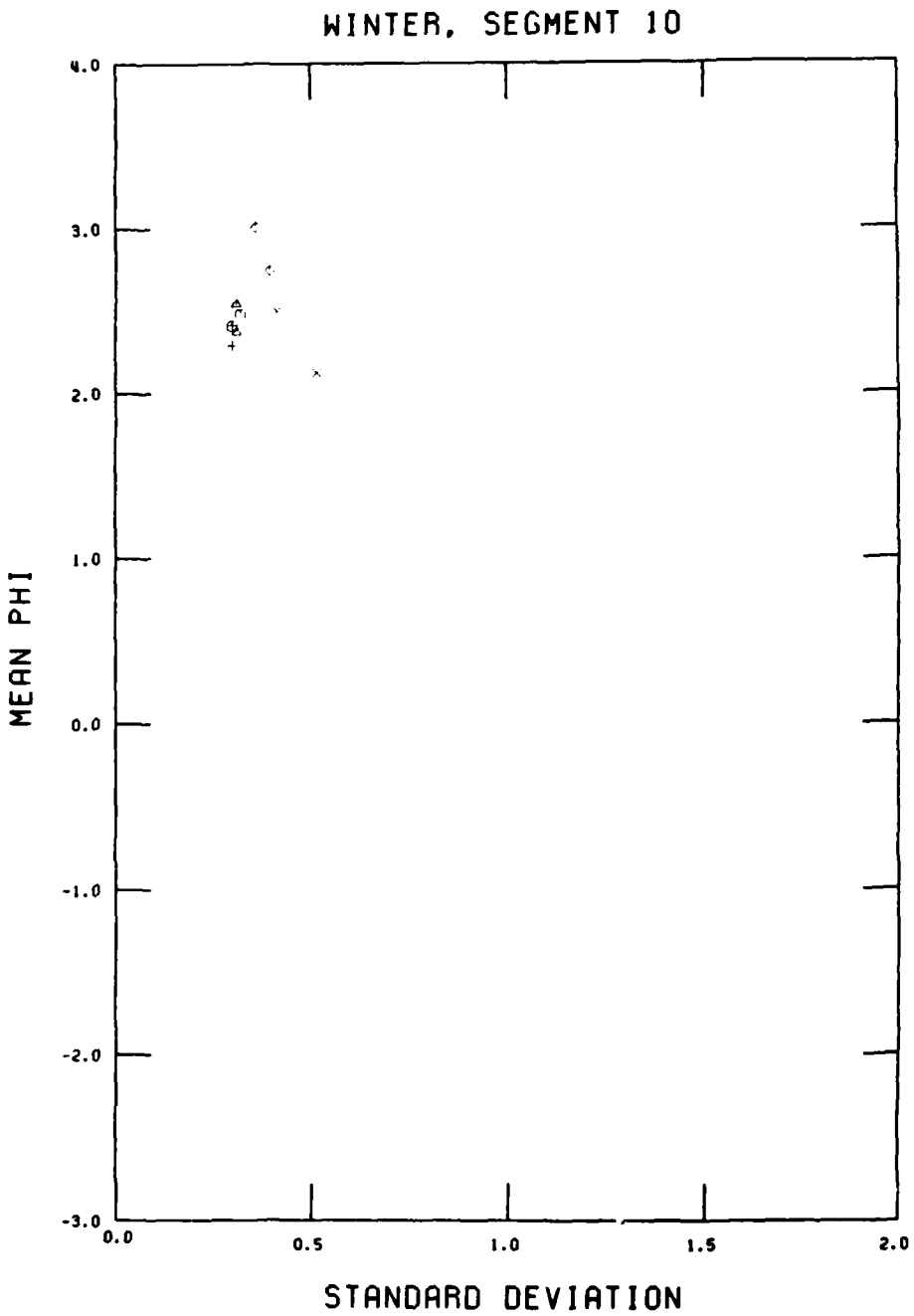
WINTER, SEGMENT 10
MEAN PHI
4.0
3.0
2.0
1.0
0.0
-1.0
-2.0
-3.0
0.0
0.5
1.0
1.5
2.0
STANDARD DEVIATION

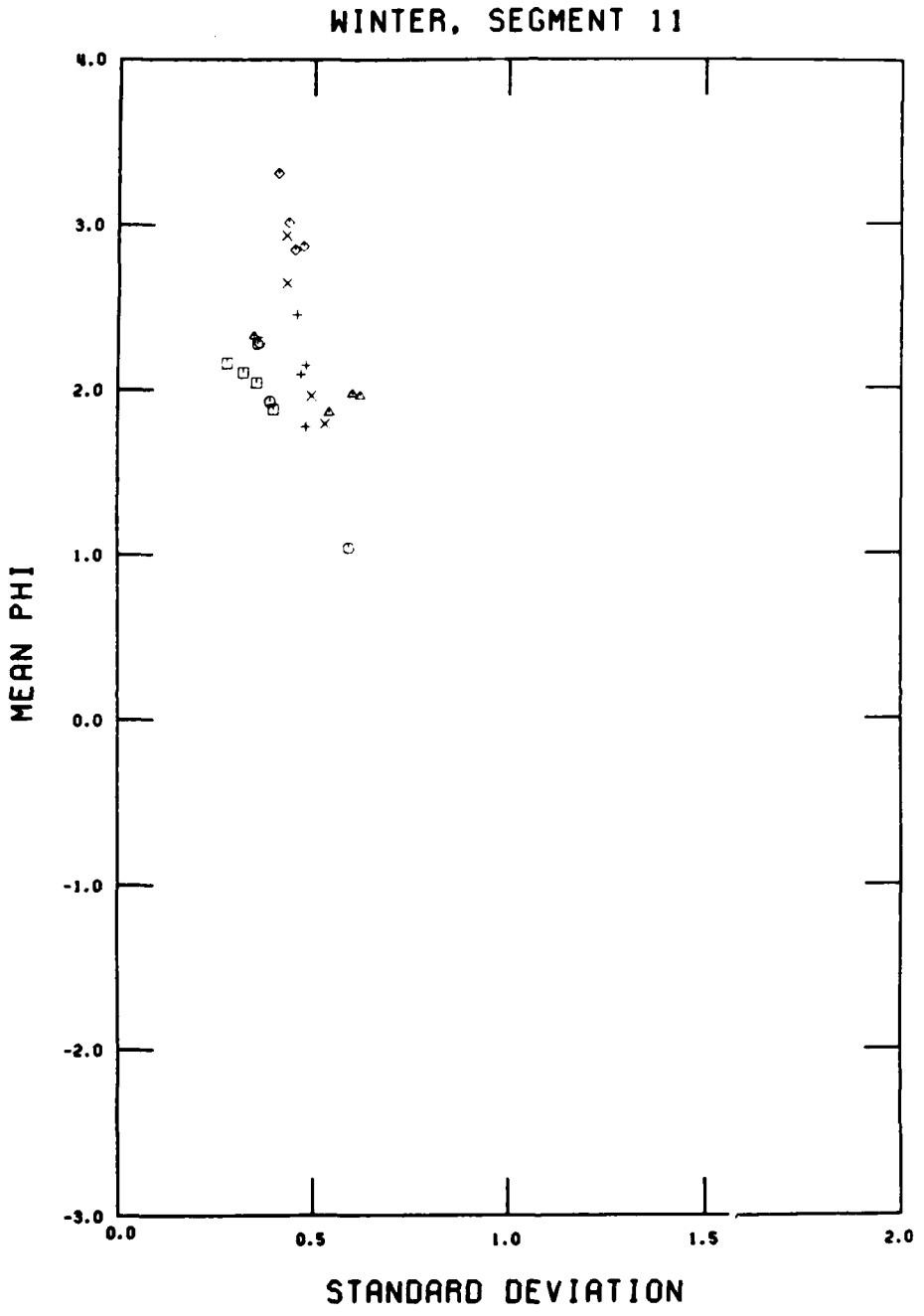
WINTER, SEGMENT 11
4.0
3.0
2.0
1.0
0.0
-1.0
-2.0
-3.0
MEAN PHI
0.0
0.5
1.0
1.5
2.0
STANDARD DEVIATION

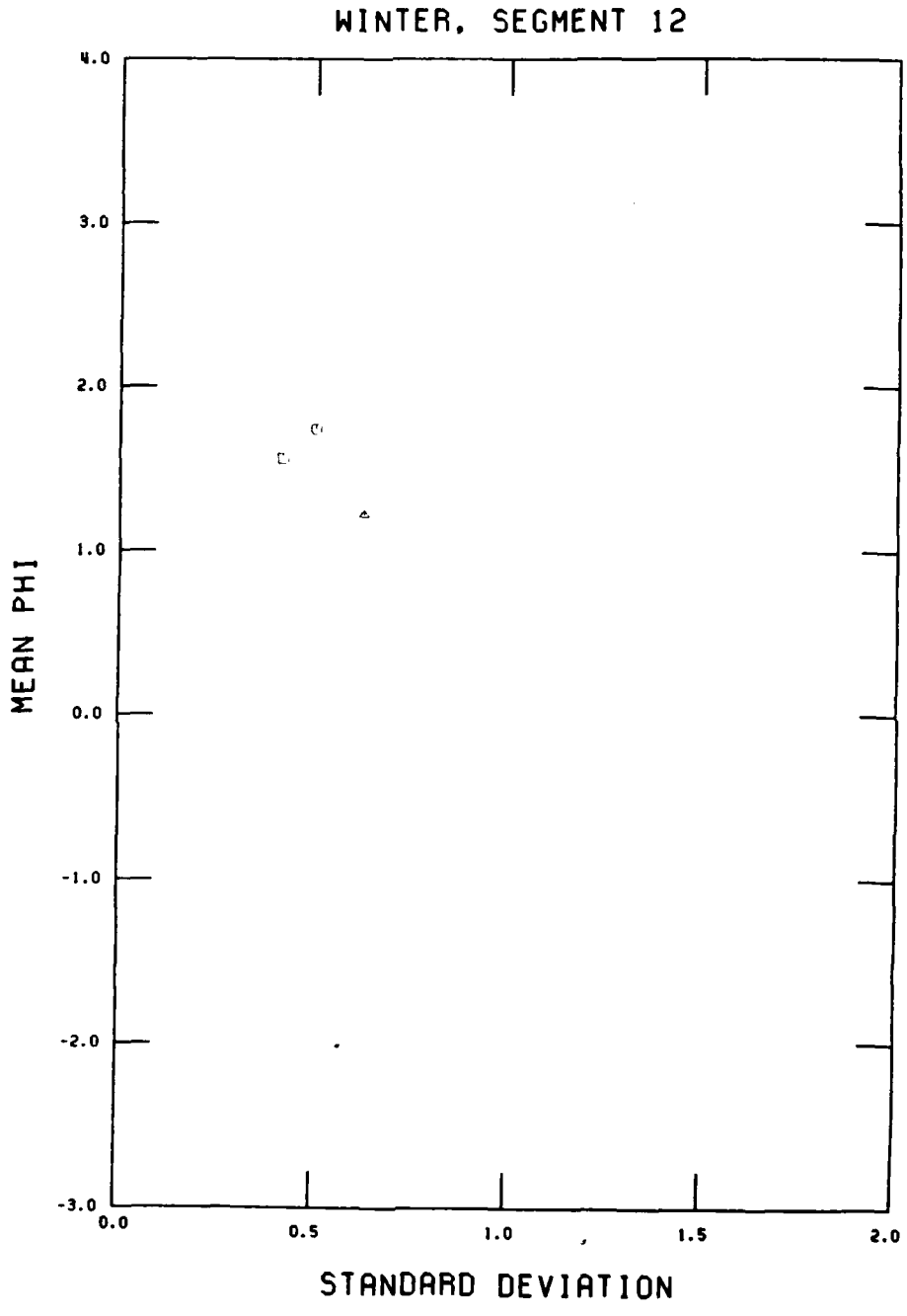
WINTER, SEGMENT 12
4.0
3.0
2.0
1.0
0.0
-1.0
-2.0
-3.0
MEAN PHI
0.0
0.5
1.0
1.5
2.0
STANDARD DEVIATION

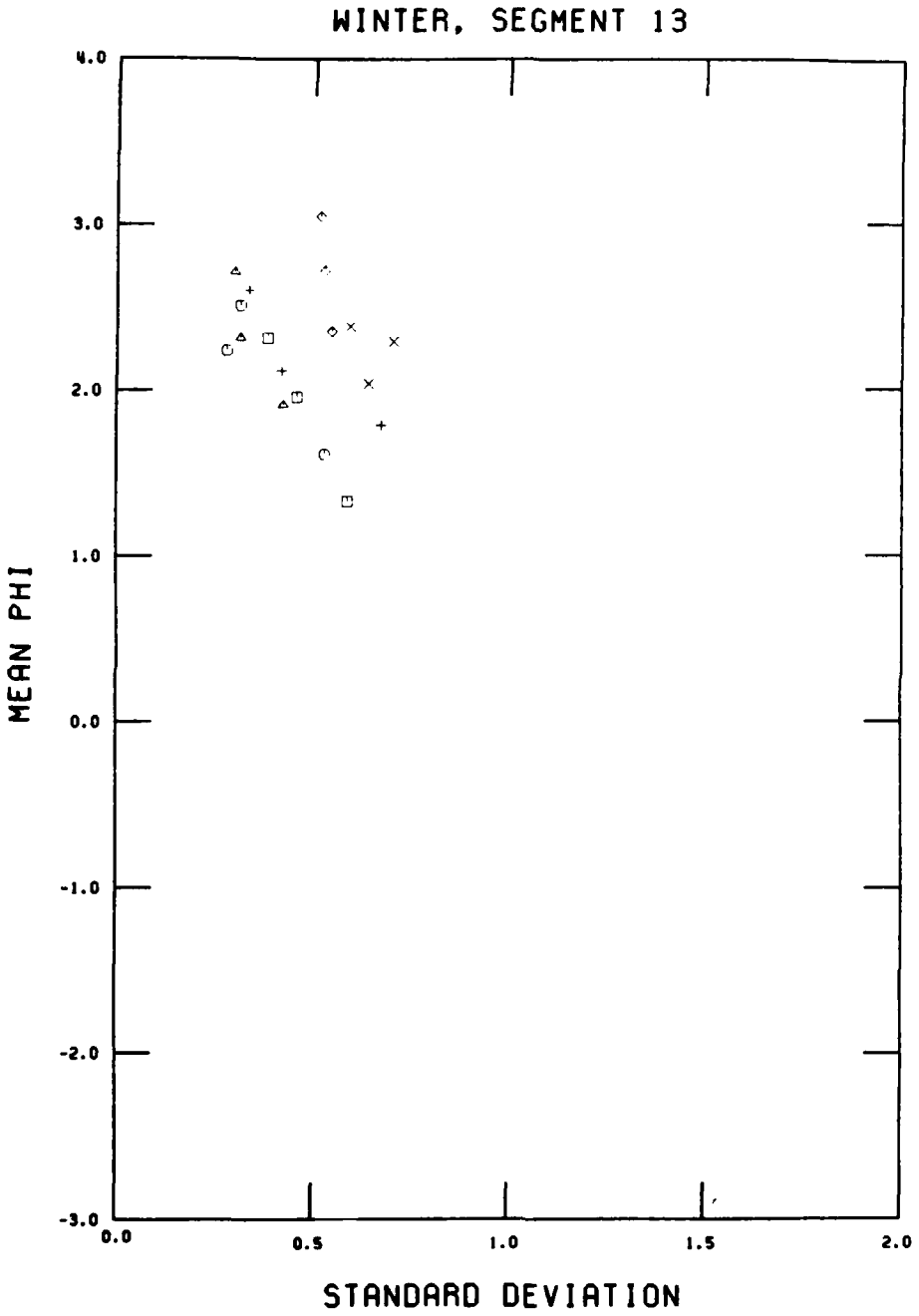
WINTER, SEGMENT 13
4.0
3.0
2.0
1.0
0.0
-1.0
-2.0
-3.0
MEAN PHI
0.0
0.5
1.0
1.5
2.0
STANDARD DEVIATION

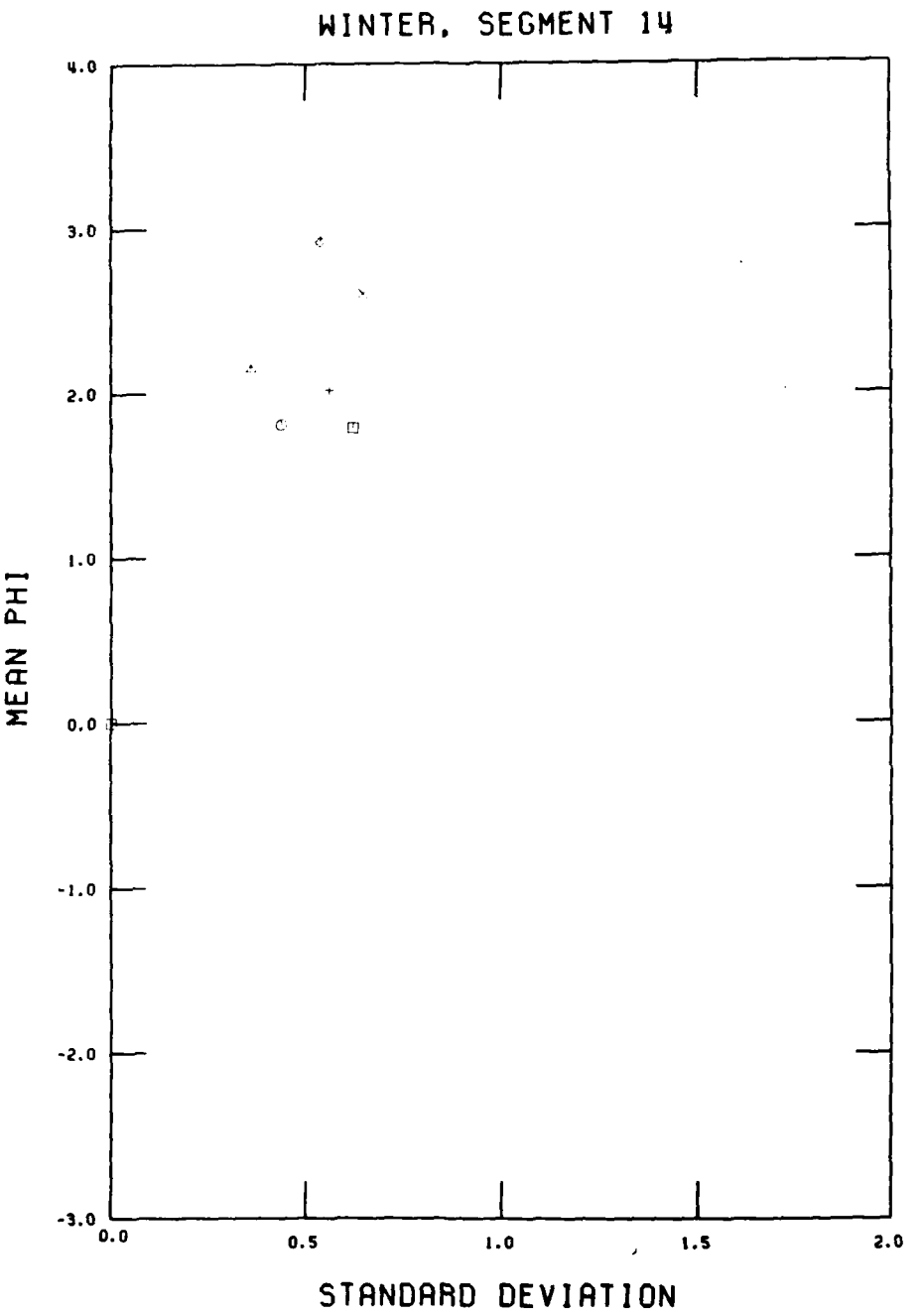
WINTER, SEGMENT 14
MEAN PHI
4.0
3.0
2.0
1.0
0.0
-1.0
-2.0
-3.0
0.0
0.5
1.0
1.5
2.0
STANDARD DEVIATION

Appendix E Bivariate plots of mean phi versus phi skewness for the end-of-winter regional data set by littoral segment. Symbols are the same as for Appendix A.

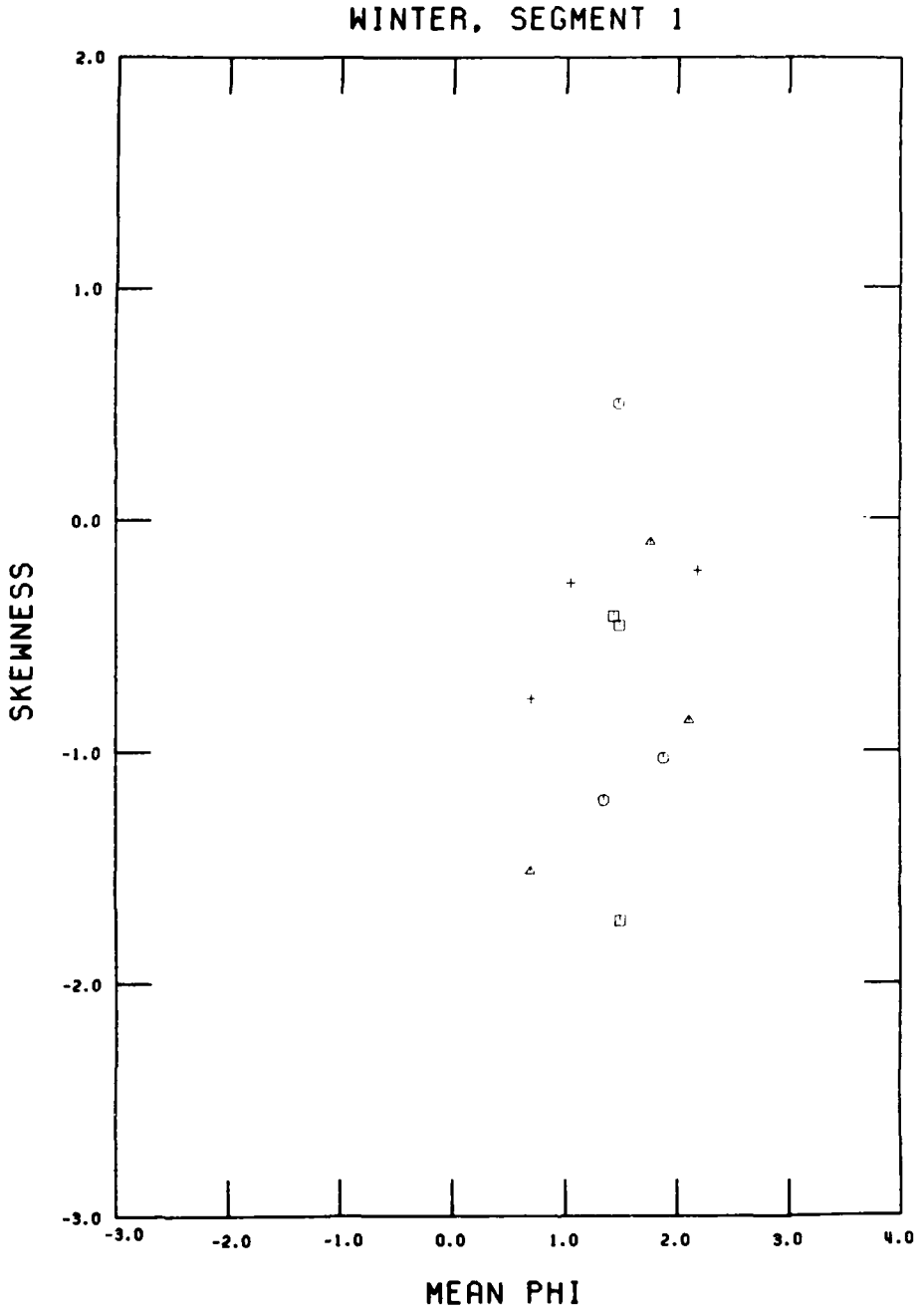
WINTER, SEGMENT 1
SKEWNESS
MEAN PHI
2.0
1.0
0.0
-1.0
-2.0
-3.0
-3.0
-2.0
-1.0
0.0
1.0
2.0
3.0
4.0

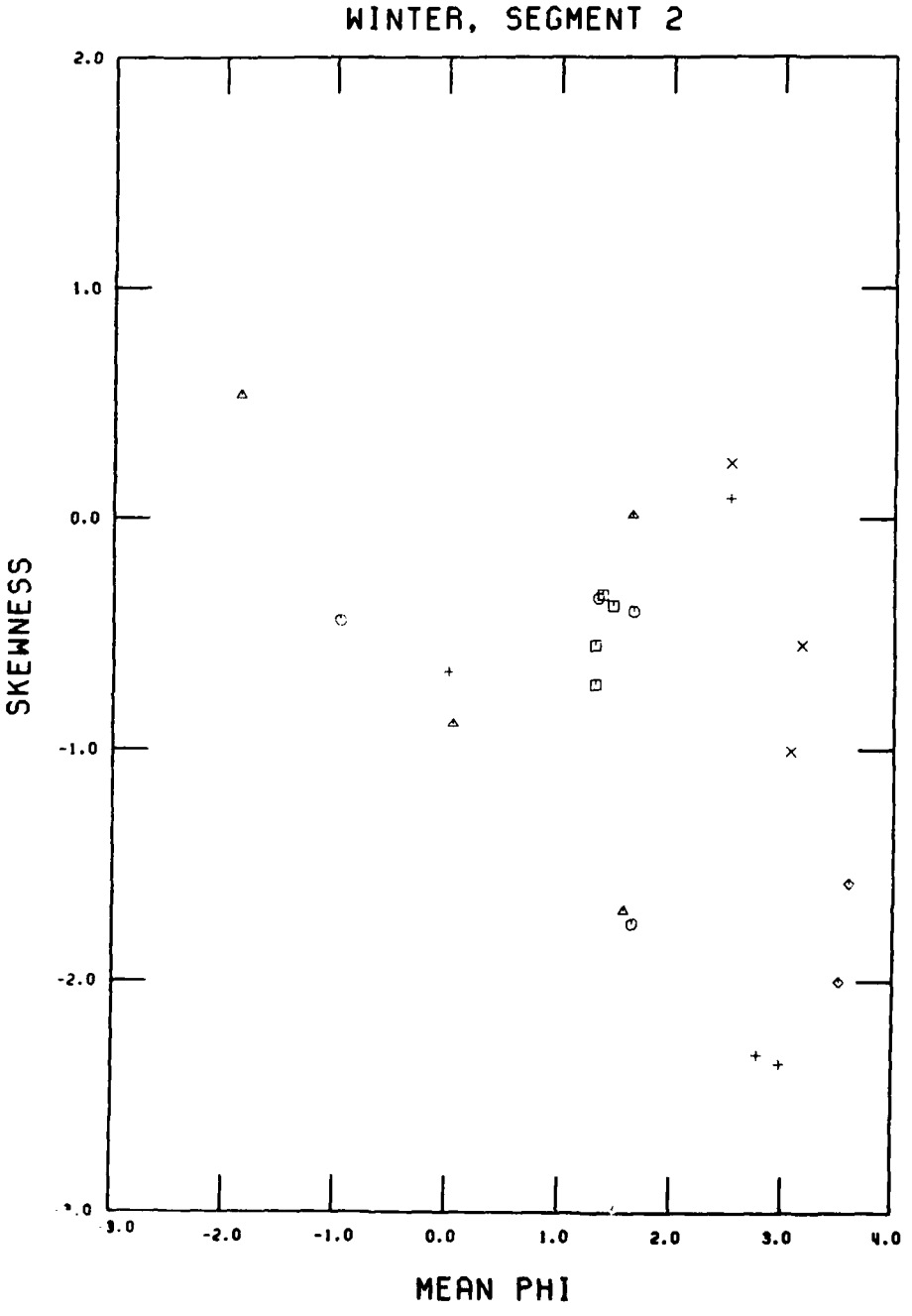
WINTER, SEGMENT 2
SKEWNESS
MEAN PHI
2.0
1.0
0.0
-1.0
-2.0
-3.0
-2.0
-1.0
0.0
1.0
2.0
3.0
4.0

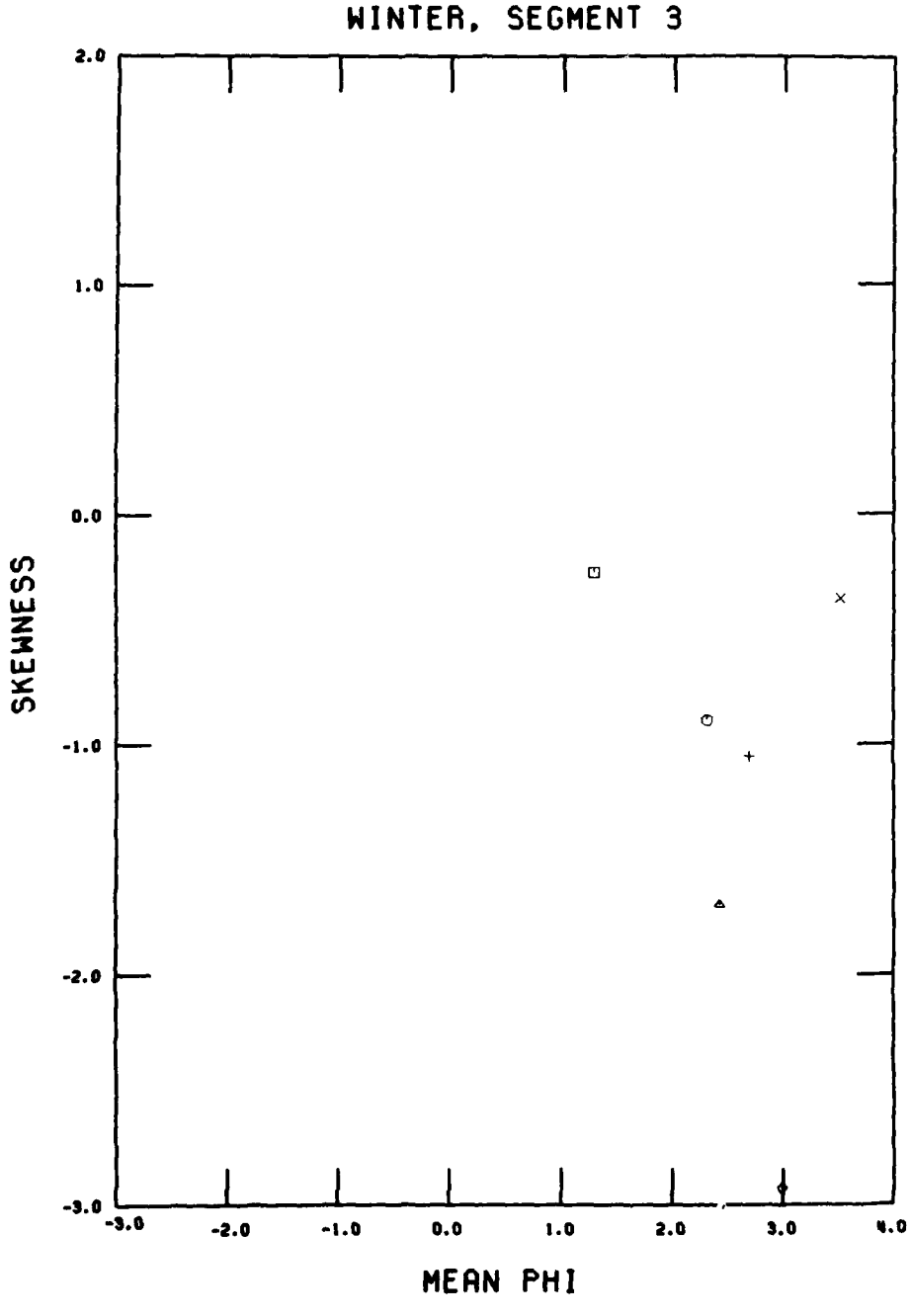
WINTER, SEGMENT 3
SKEWNESS
MEAN PHI
2.0
1.0
0.0
-1.0
-2.0
-3.0
-3.0
-2.0
-1.0
0.0
1.0
2.0
3.0
4.0

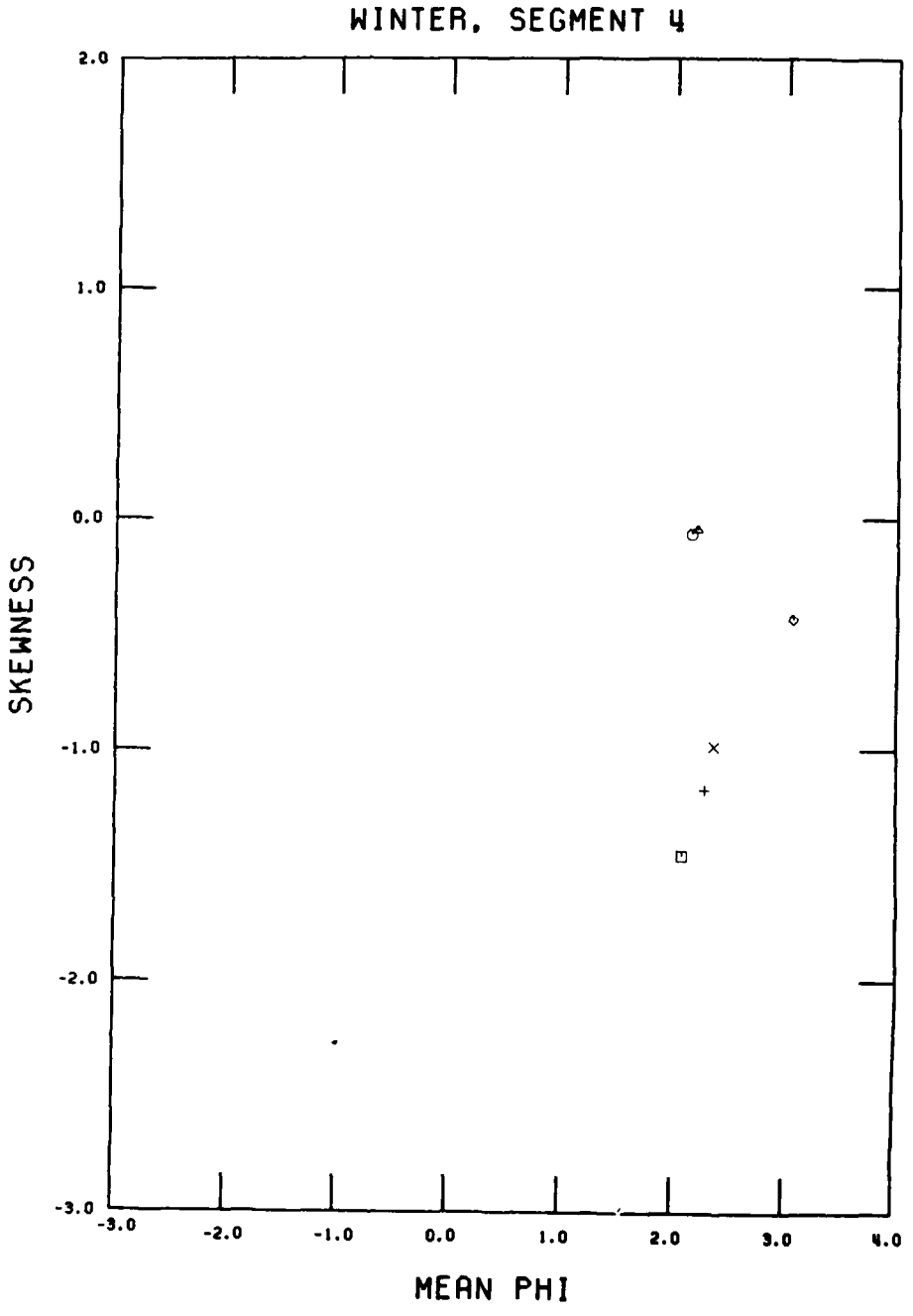
WINTER, SEGMENT 4
SKEWNESS
MEAN PHI
2.0
1.0
0.0
-1.0
-2.0
-3.0
-3.0
-2.0
-1.0
0.0
1.0
2.0
3.0
4.0

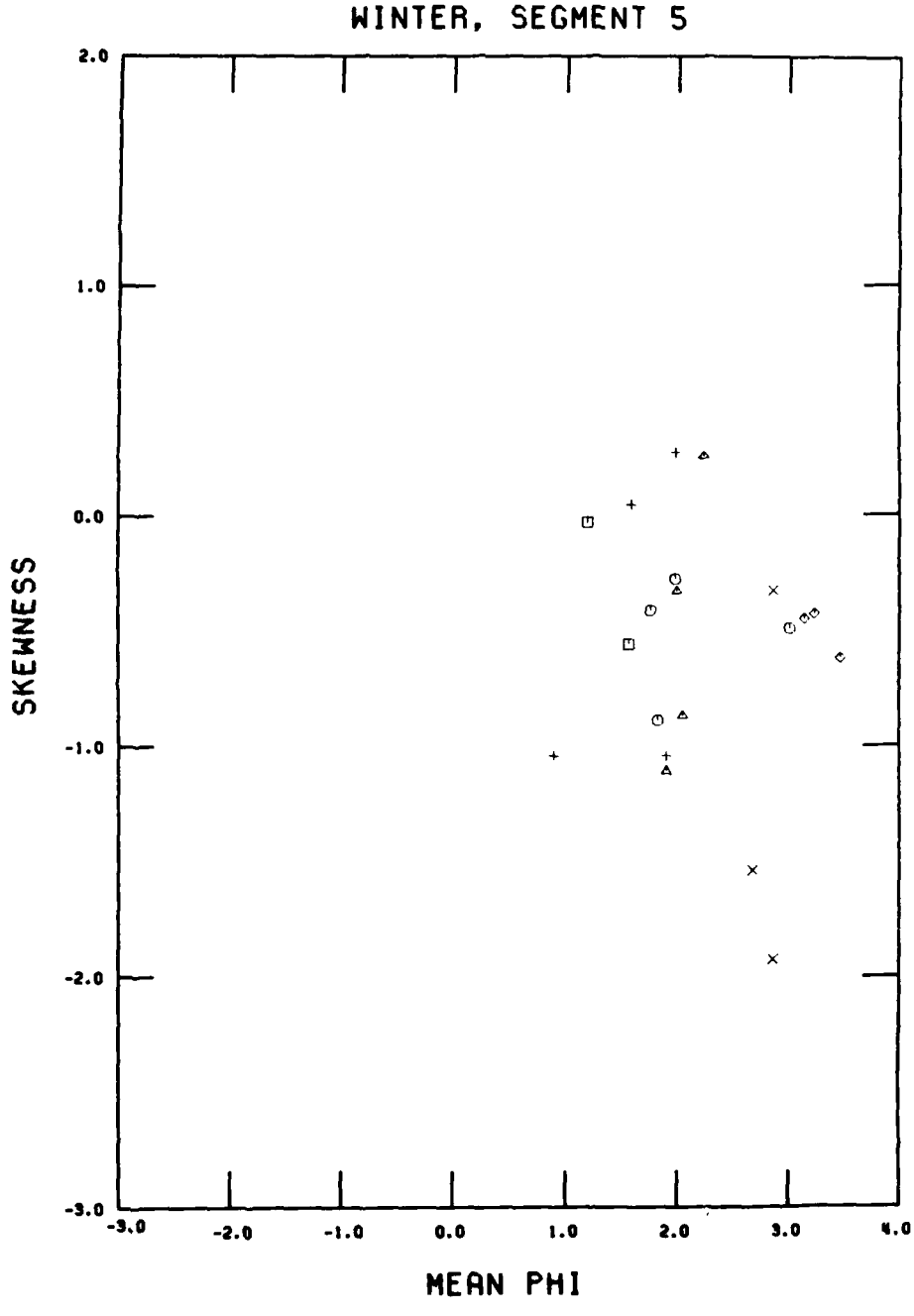
WINTER, SEGMENT 5
SKEWNESS
MEAN PHI
2.0
1.0
0.0
-1.0
-2.0
-3.0
-3.0
-2.0
-1.0
0.0
1.0
2.0
3.0
4.0

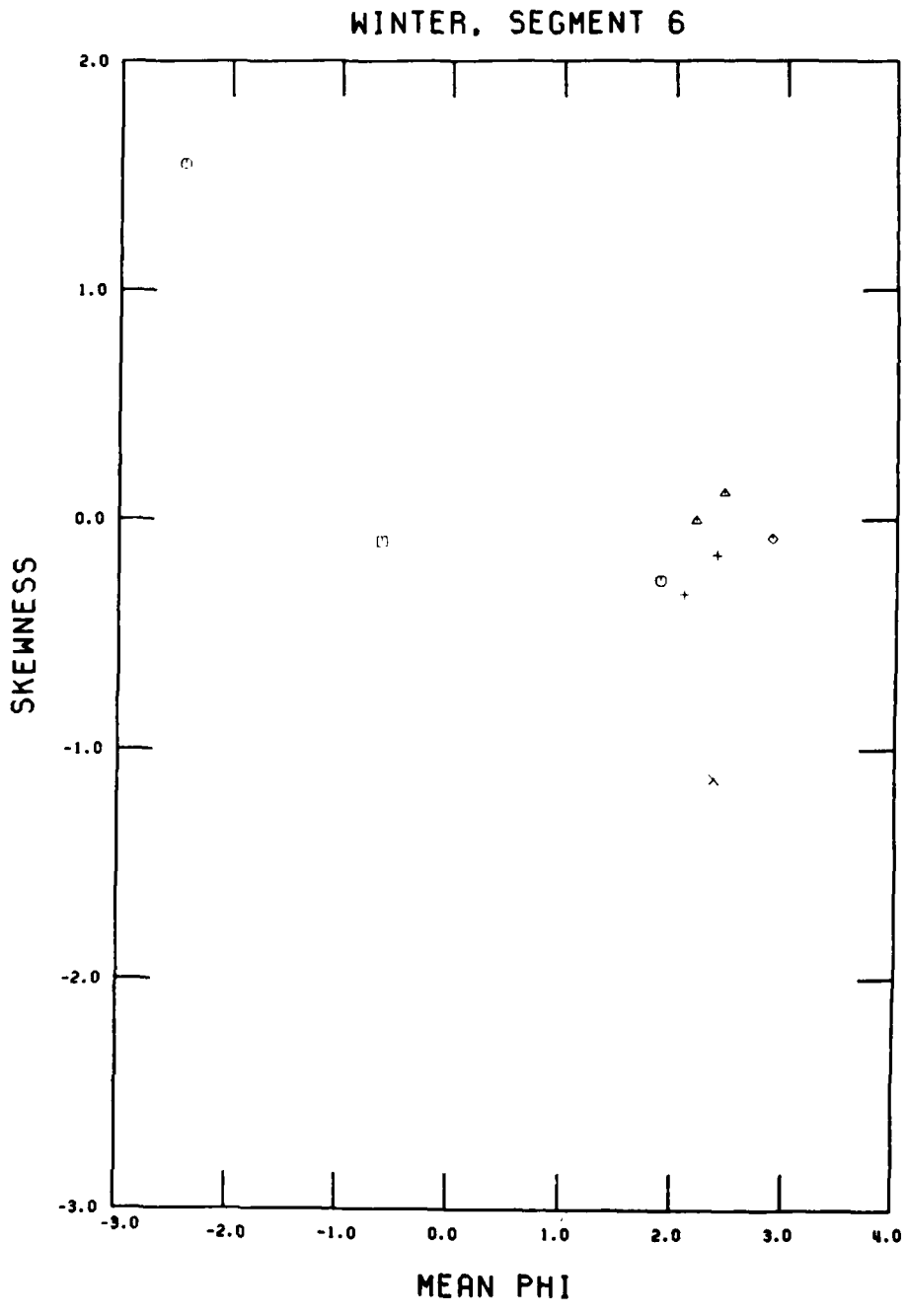
WINTER, SEGMENT 6
SKEWNESS
MEAN PHI
2.0
1.0
0.0
-1.0
-2.0
-3.0
-3.0
-2.0
-1.0
0.0
1.0
2.0
3.0
4.0

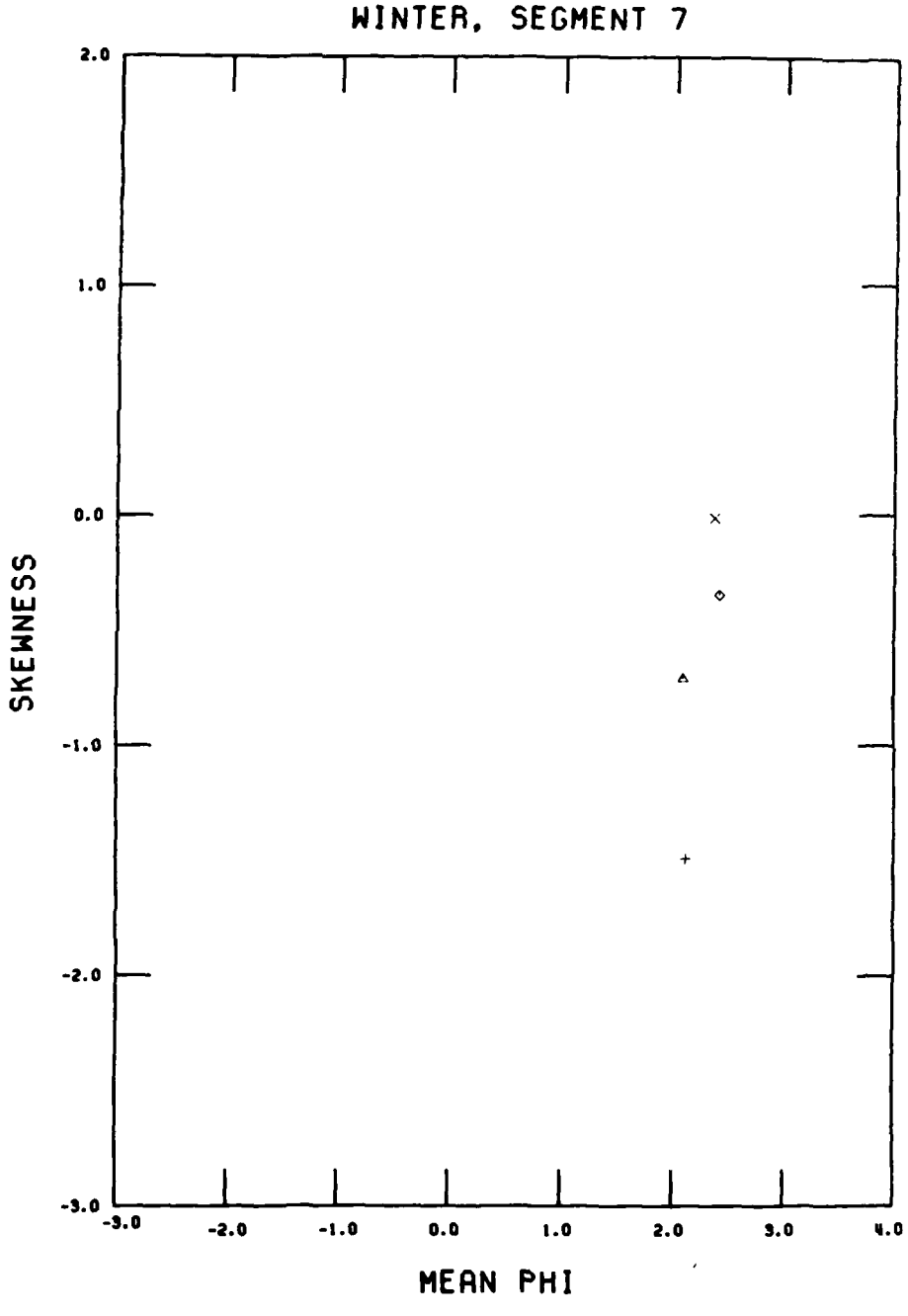
WINTER, SEGMENT 7
2.0
1.0
0.0
-1.0
-2.0
-3.0
SKEWNESS
-3.0
-2.0
-1.0
0.0
1.0
2.0
3.0
4.0
MEAN PHI

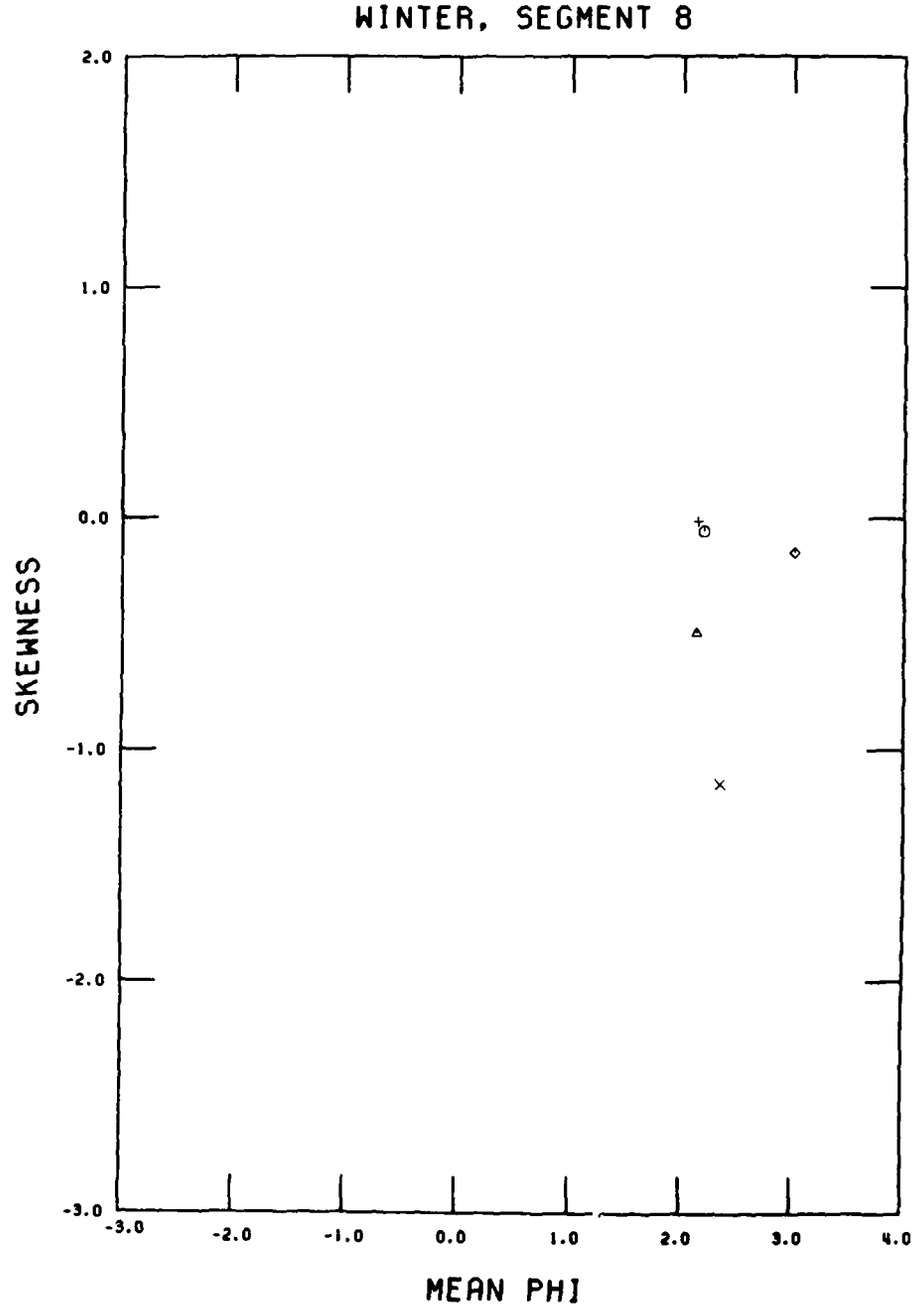
WINTER, SEGMENT 8
2.0
1.0
0.0
-1.0
-2.0
-3.0
SKEWNESS
-3.0
-2.0
-1.0
0.0
1.0
2.0
3.0
4.0
MEAN PHI

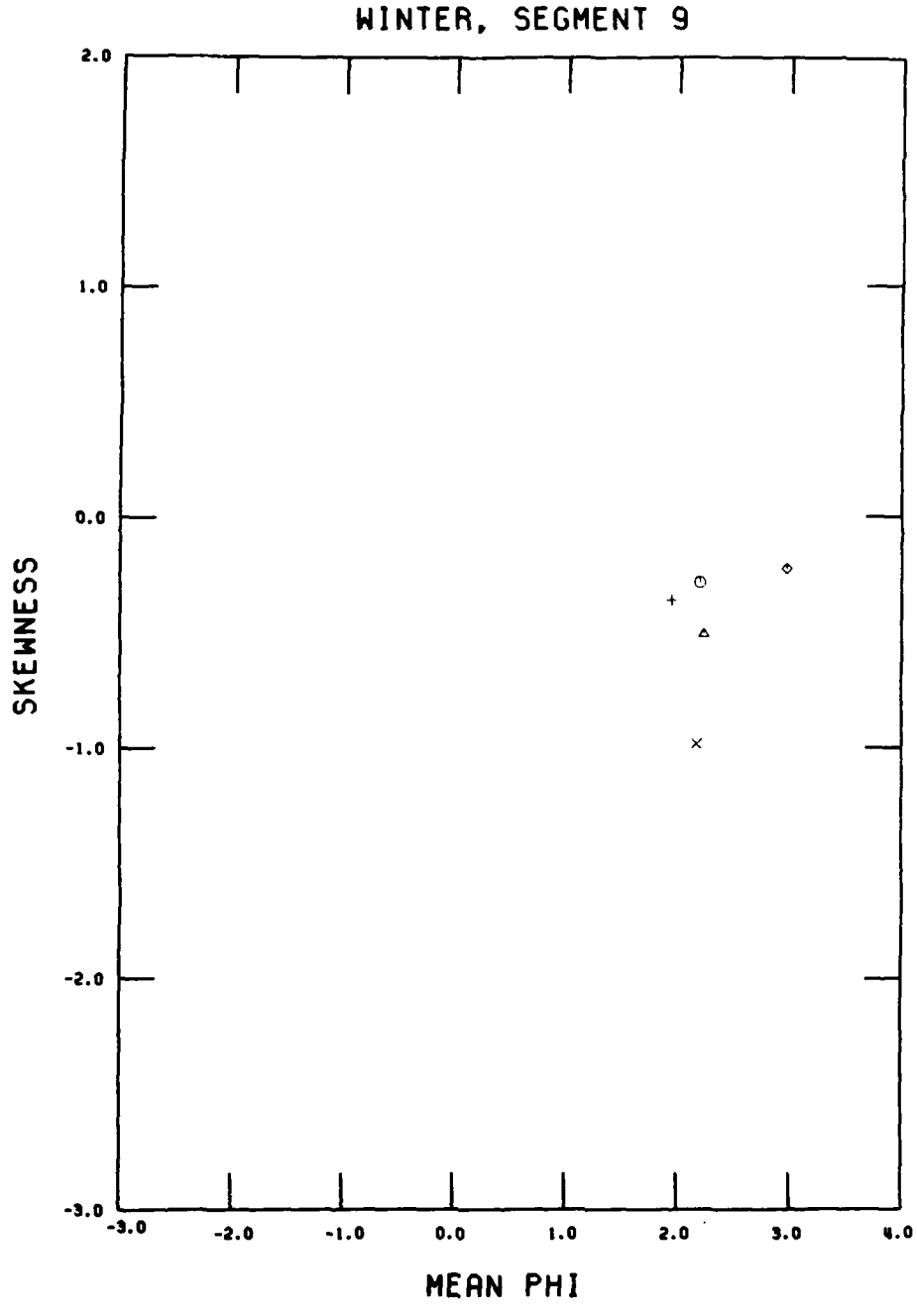
WINTER, SEGMENT 9
SKEWNESS
MEAN PHI
2.0
1.0
0.0
-1.0
-2.0
-3.0
-3.0
-2.0
-1.0
0.0
1.0
2.0
3.0
4.0

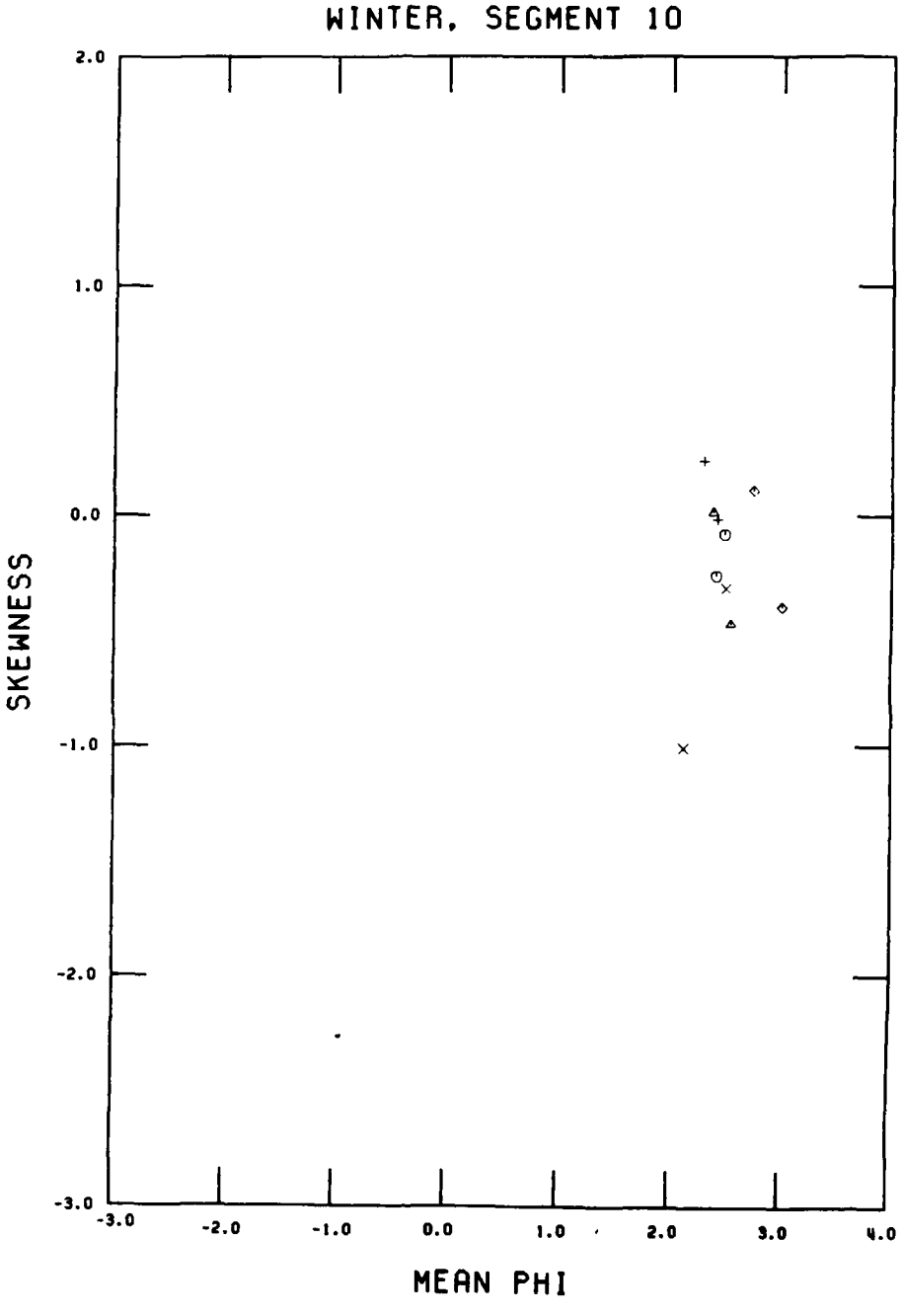
WINTER, SEGMENT 10
2.0
1.0
0.0
-1.0
-2.0
-3.0
SKEWNESS
-3.0
-2.0
-1.0
0.0
1.0
2.0
3.0
4.0
MEAN PHI

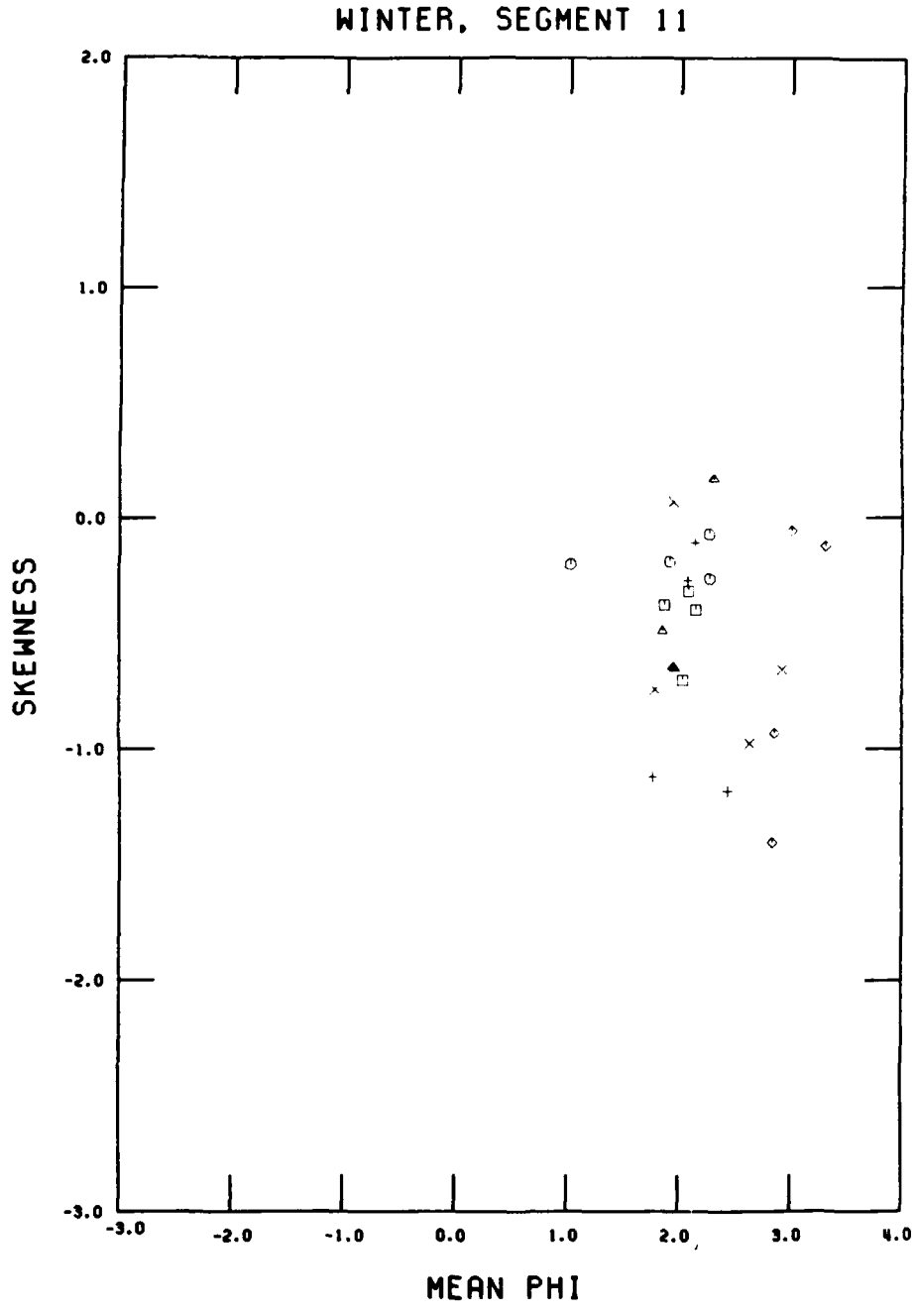
WINTER, SEGMENT 11
SKEWNESS
MEAN PHI
2.0
1.0
0.0
-1.0
-2.0
-3.0
-3.0
-2.0
-1.0
0.0
1.0
2.0
3.0
4.0

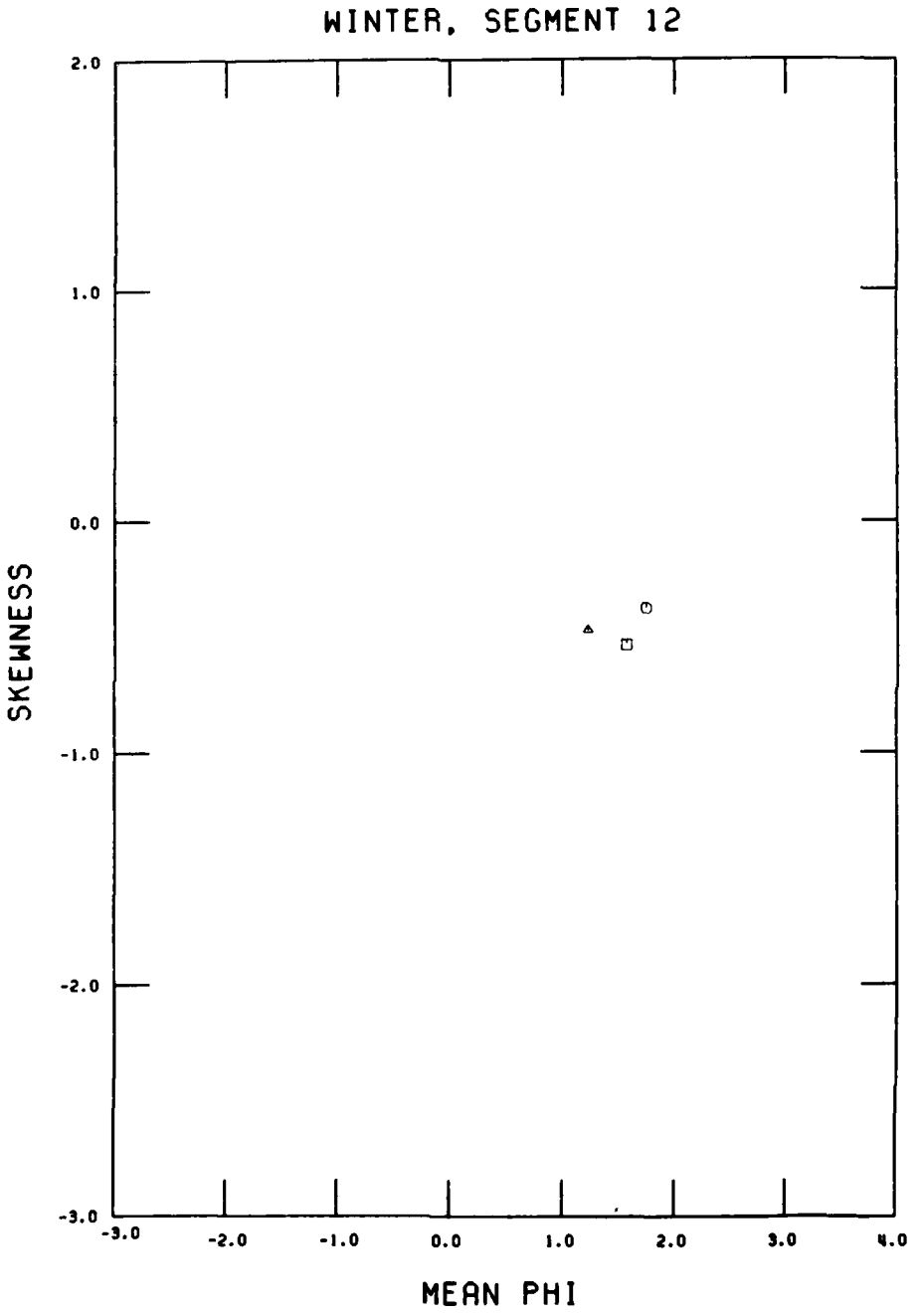
WINTER, SEGMENT 12
SKEWNESS
MEAN PHI
2.0
1.0
0.0
-1.0
-2.0
-3.0
-3.0
-2.0
-1.0
0.0
1.0
2.0
3.0
4.0

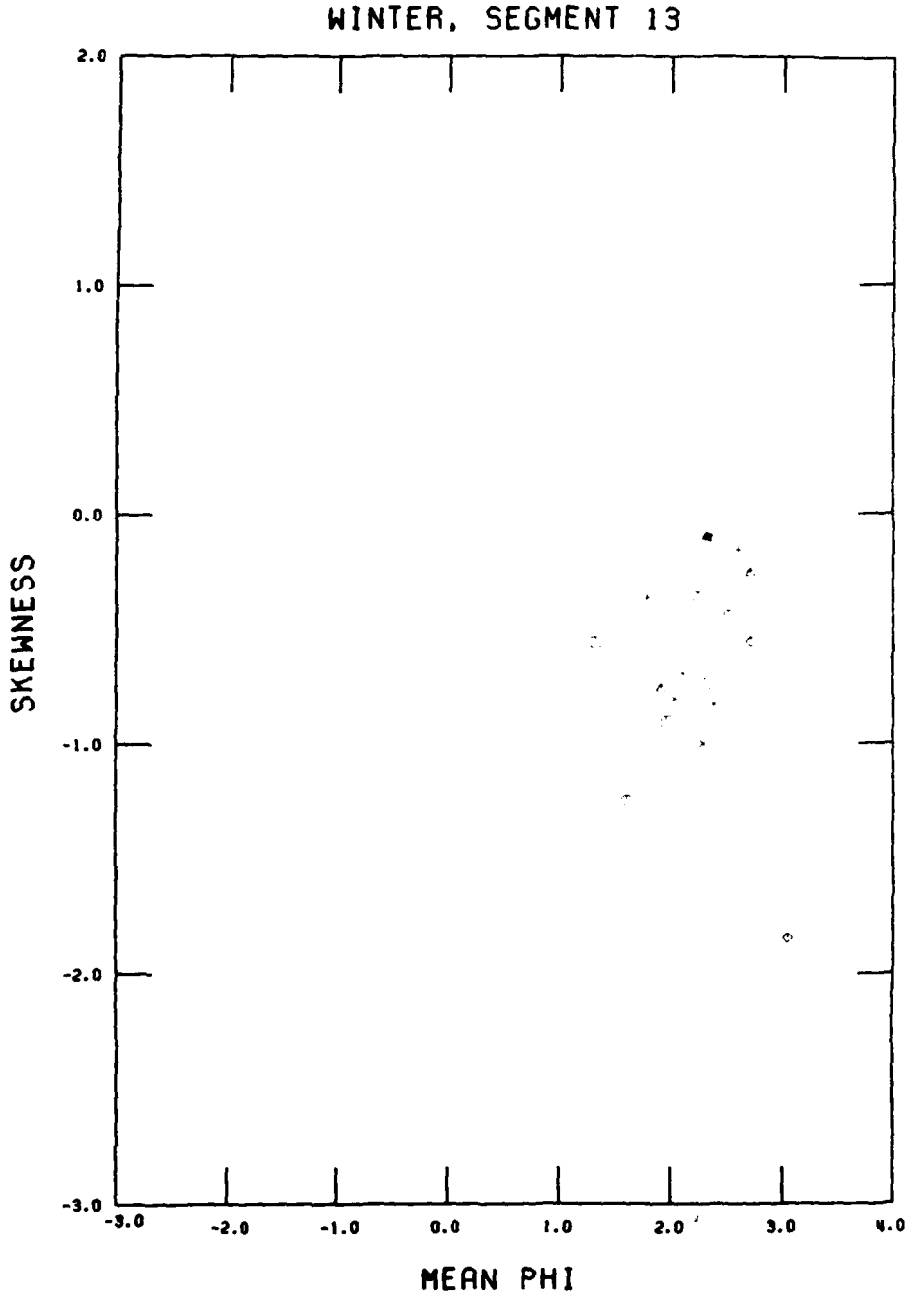
WINTER, SEGMENT 13
2.0
1.0
0.0
-1.0
-2.0
-3.0
SKEWNESS
-3.0
-2.0
-1.0
0.0
1.0
2.0
3.0
4.0
MEAN PHI

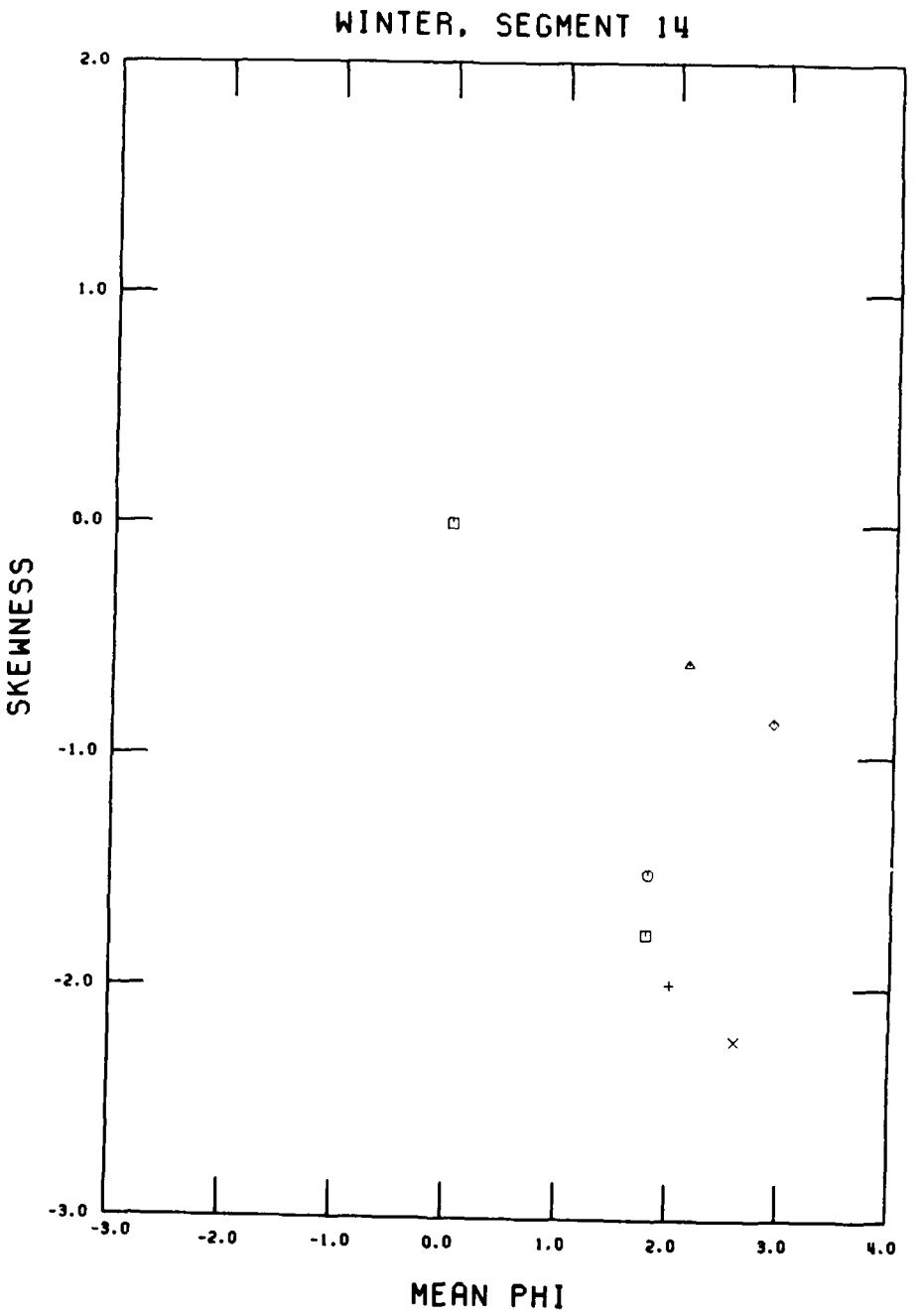
WINTER, SEGMENT 14
SKEWNESS
MEAN PHI
2.0
1.0
0.0
-1.0
-2.0
-3.0
-3.0
-2.0
-1.0
0.0
1.0
2.0
3.0
4.0

Appendix F Bivariate plots of phi standard deviation versus phi skewness for the end-of-winter regional data set by littoral segment. Symbols are the same as for Appendix A.

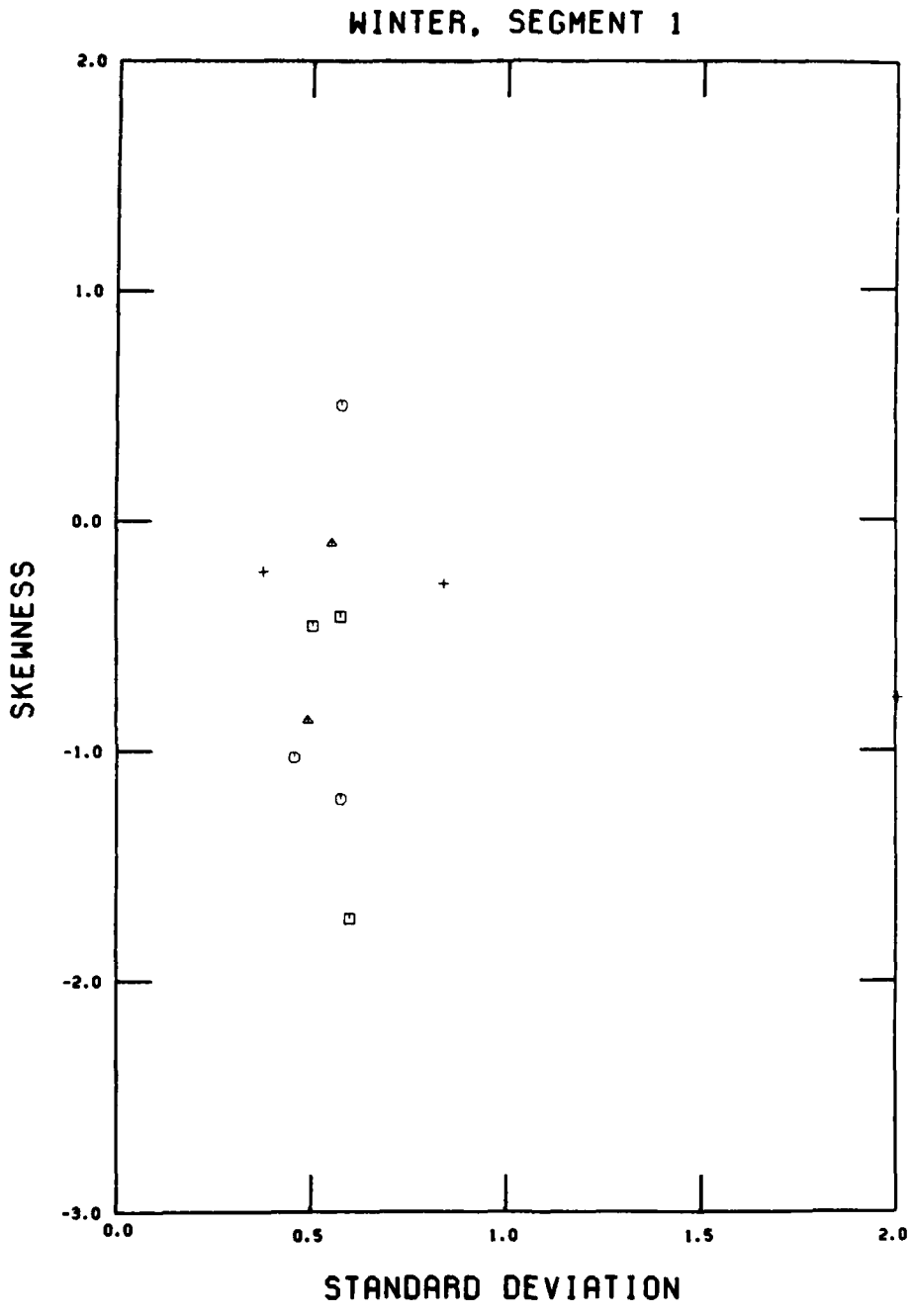
WINTER, SEGMENT 1
2.0
1.0
0.0
-1.0
-2.0
-3.0
SKEWNESS
0.0
0.5
1.0
1.5
2.0
STANDARD DEVIATION

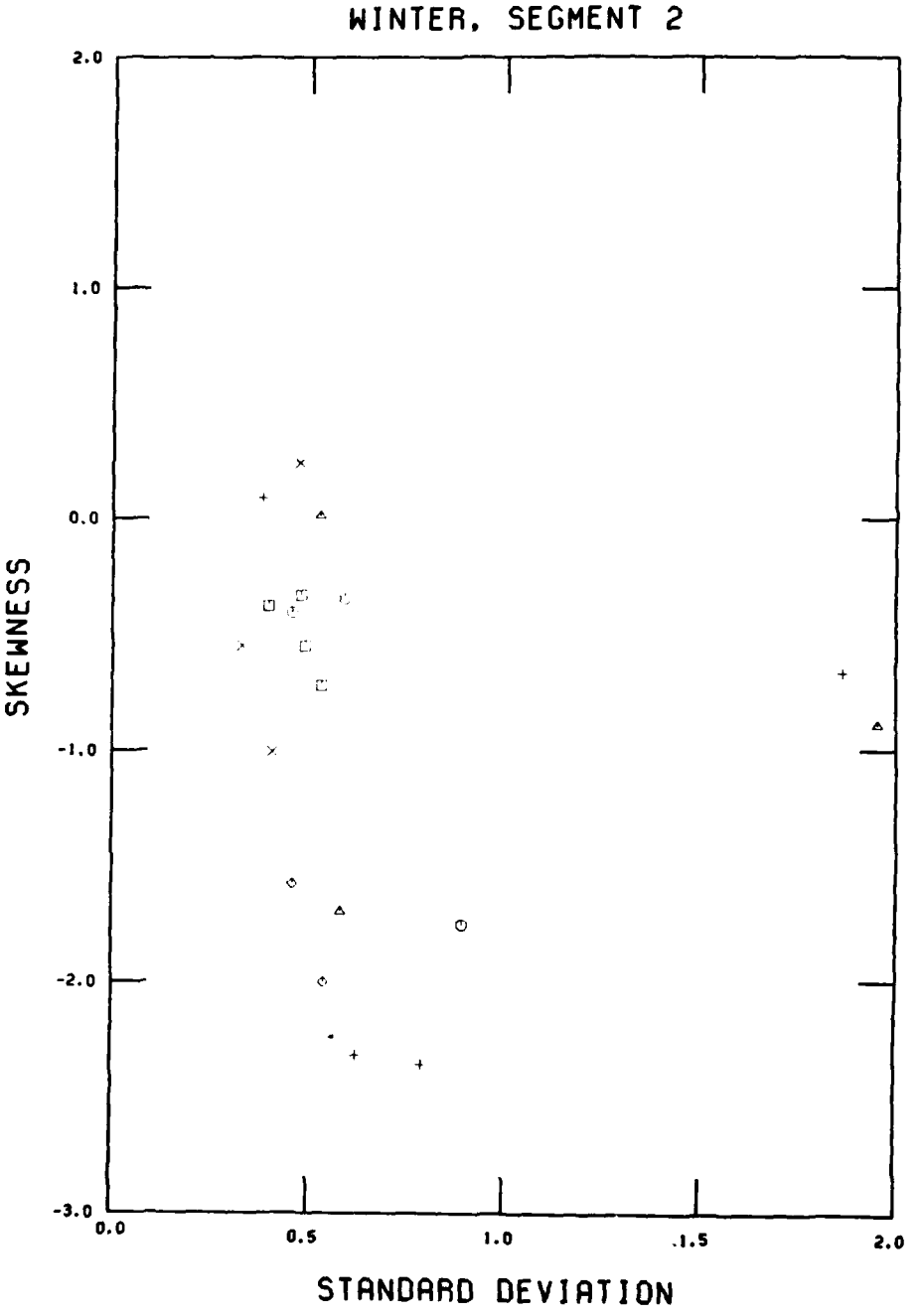
WINTER, SEGMENT 2
2.0
1.0
0.0
-1.0
-2.0
-3.0
SKEWNESS
0.0
0.5
1.0
1.5
2.0
STANDARD DEVIATION

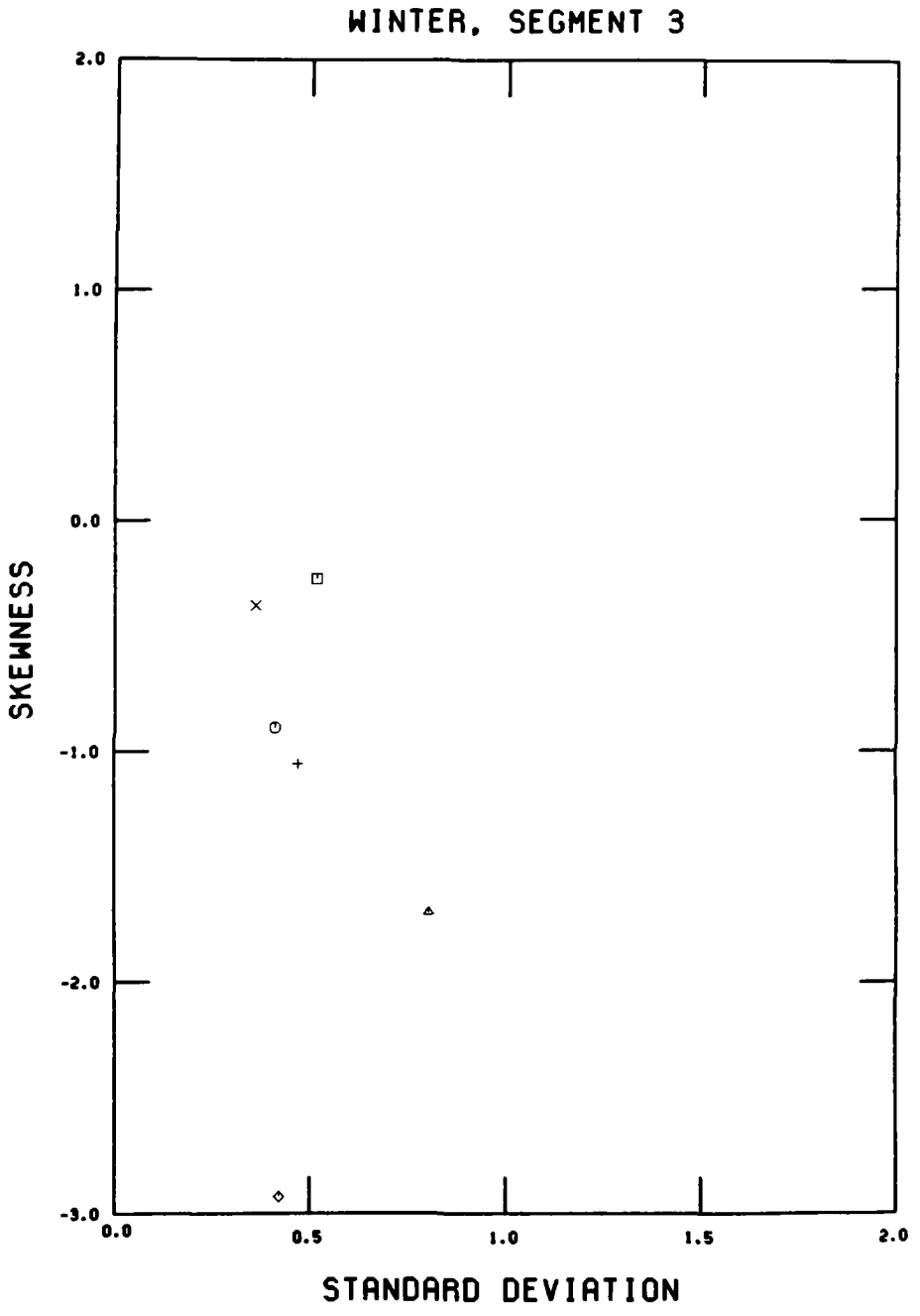
WINTER, SEGMENT 3
2.0
1.0
0.0
-1.0
-2.0
-3.0
SKEWNESS
0.0
0.5
1.0
1.5
2.0
STANDARD DEVIATION

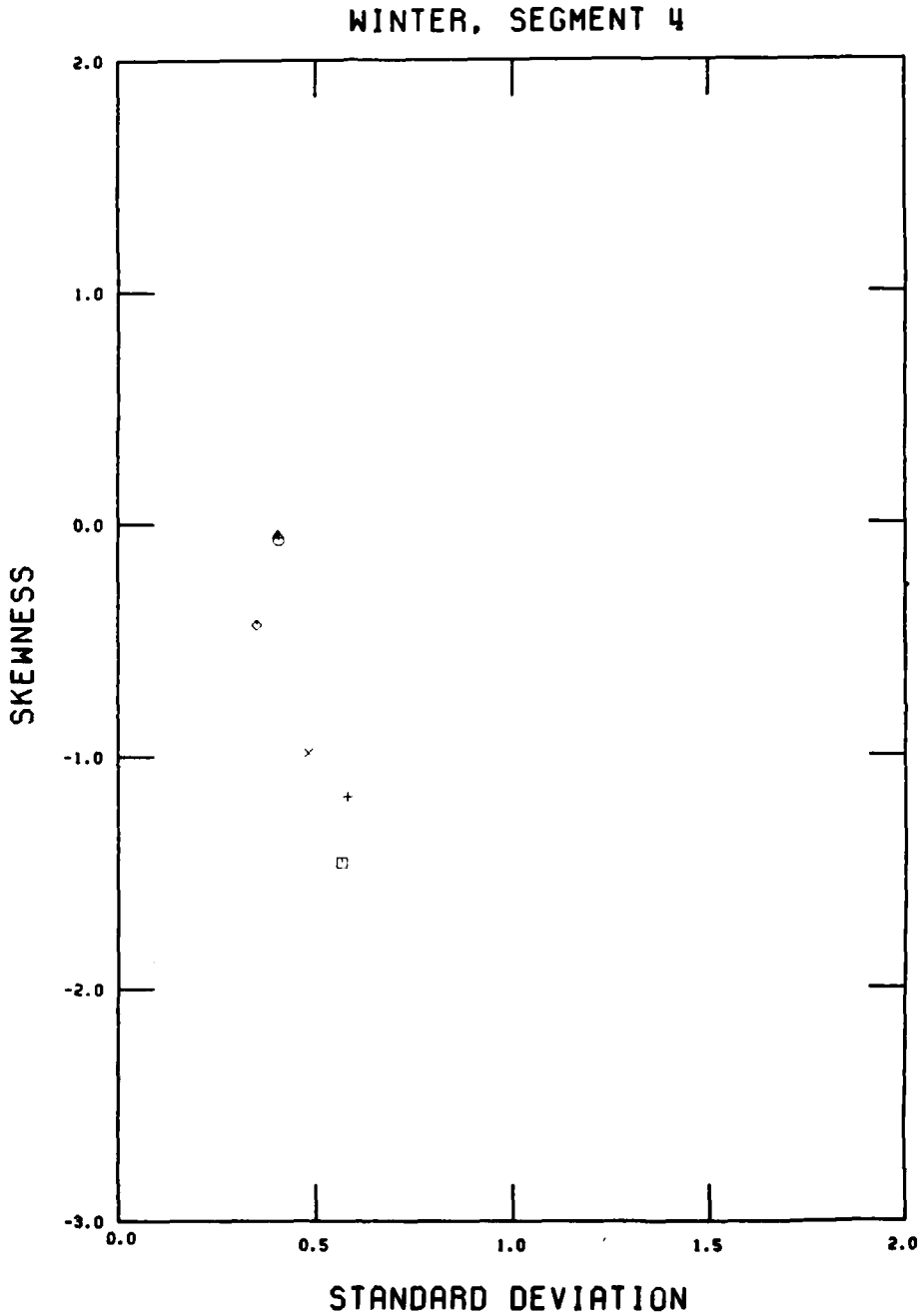
WINTER, SEGMENT 4
2.0
1.0
0.0
-1.0
-2.0
-3.0
SKEWNESS
0.0
0.5
1.0
1.5
2.0
STANDARD DEVIATION

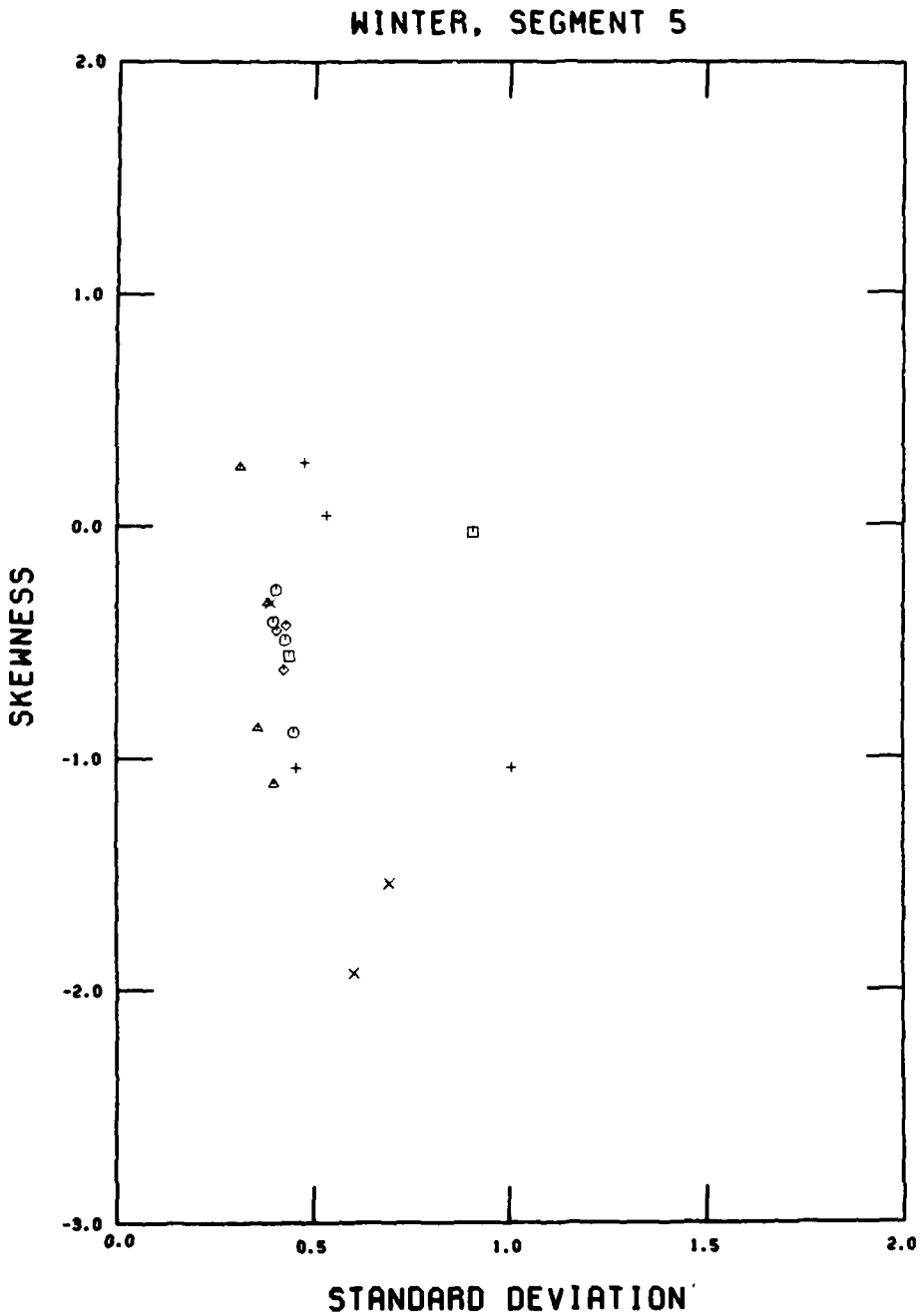
WINTER, SEGMENT 5
2.0
1.0
0.0
-1.0
-2.0
-3.0
SKEWNESS
0.0
0.5
1.0
1.5
2.0
STANDARD DEVIATION

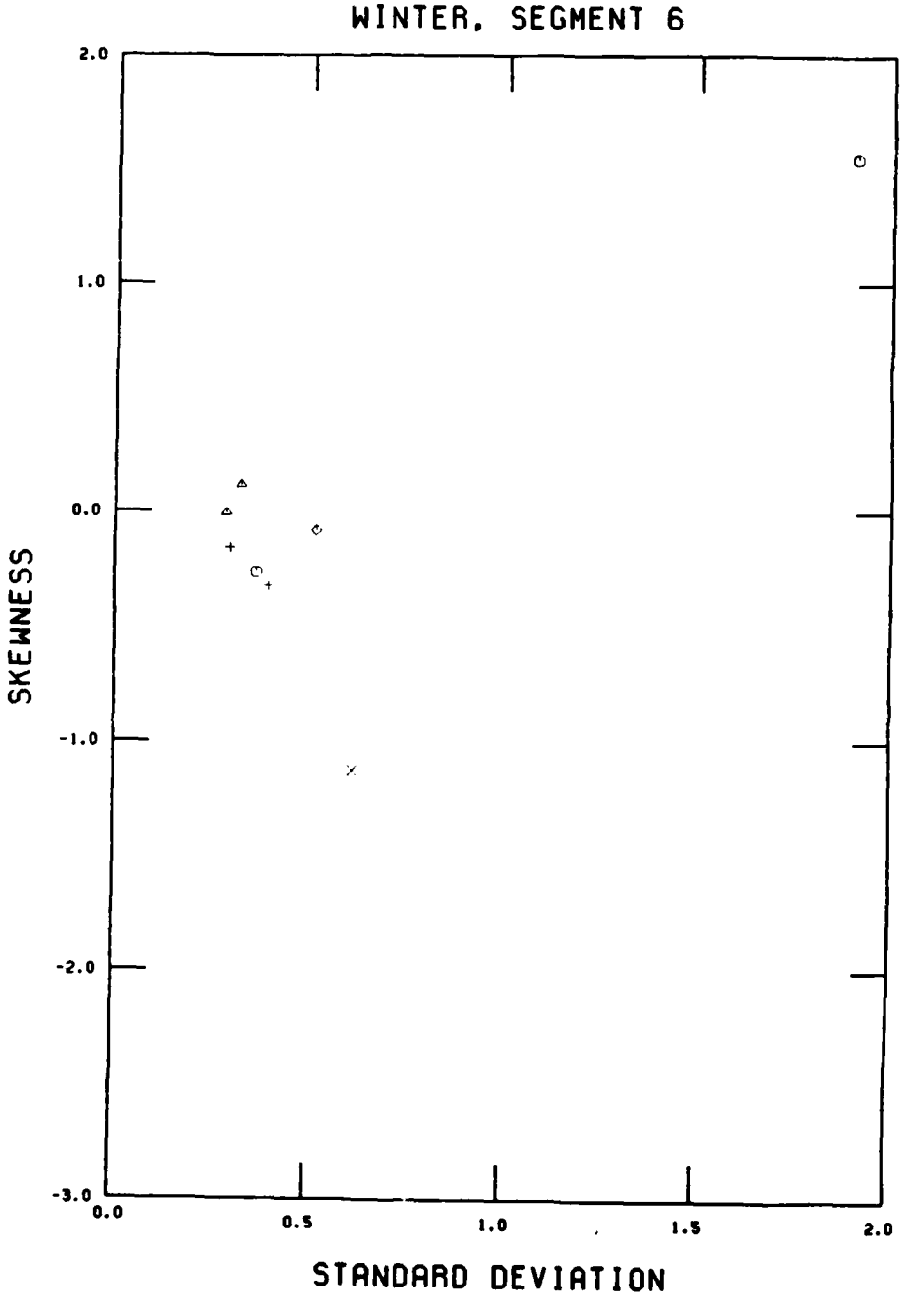
WINTER, SEGMENT 6
2.0
1.0
0.0
-1.0
-2.0
-3.0
SKEWNESS
0.0
0.5
1.0
1.5
2.0
STANDARD DEVIATION

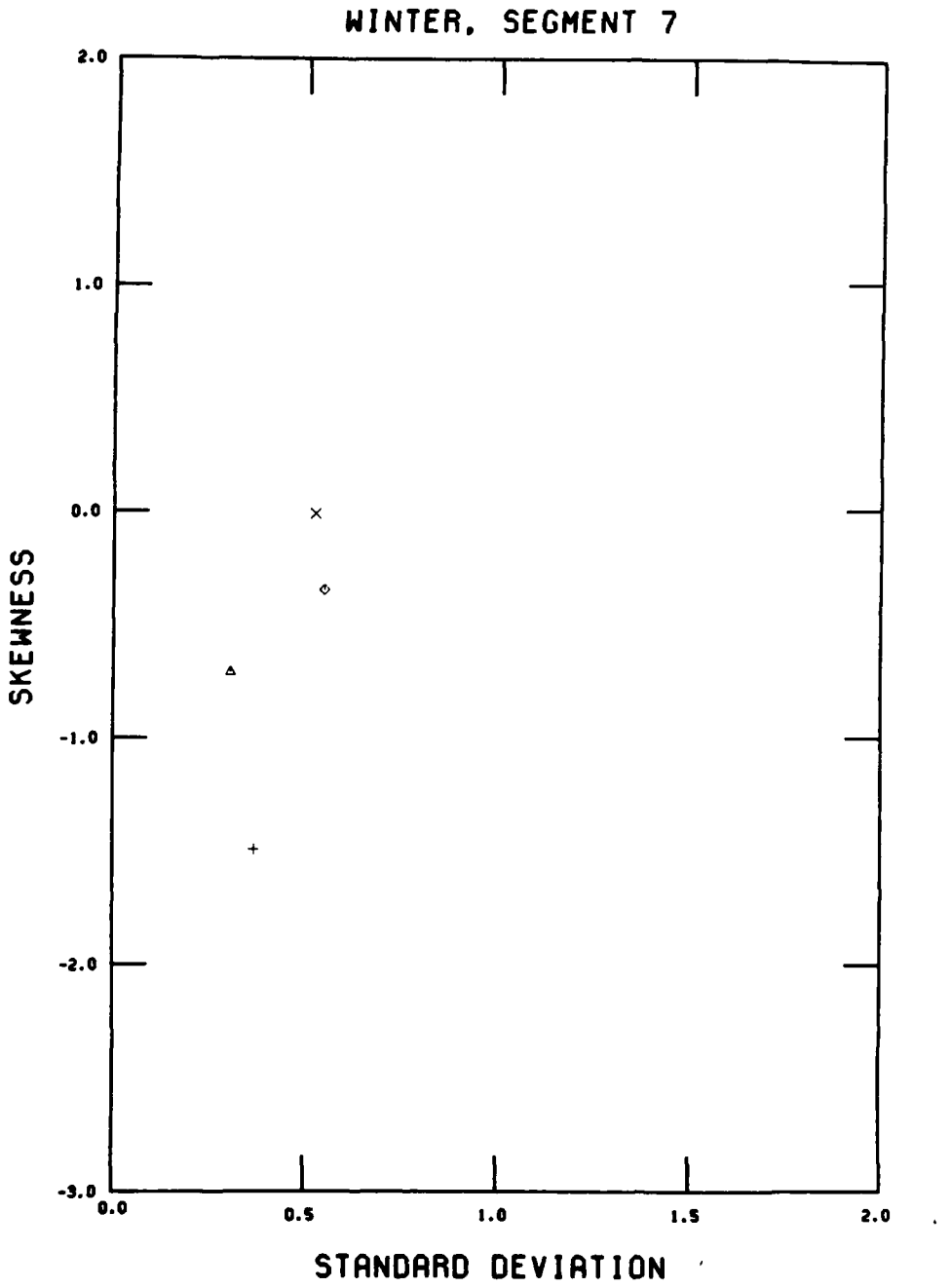
WINTER, SEGMENT 7
2.0
1.0
0.0
-1.0
-2.0
-3.0
SKEWNESS
0.0
0.5
1.0
1.5
2.0
STANDARD DEVIATION

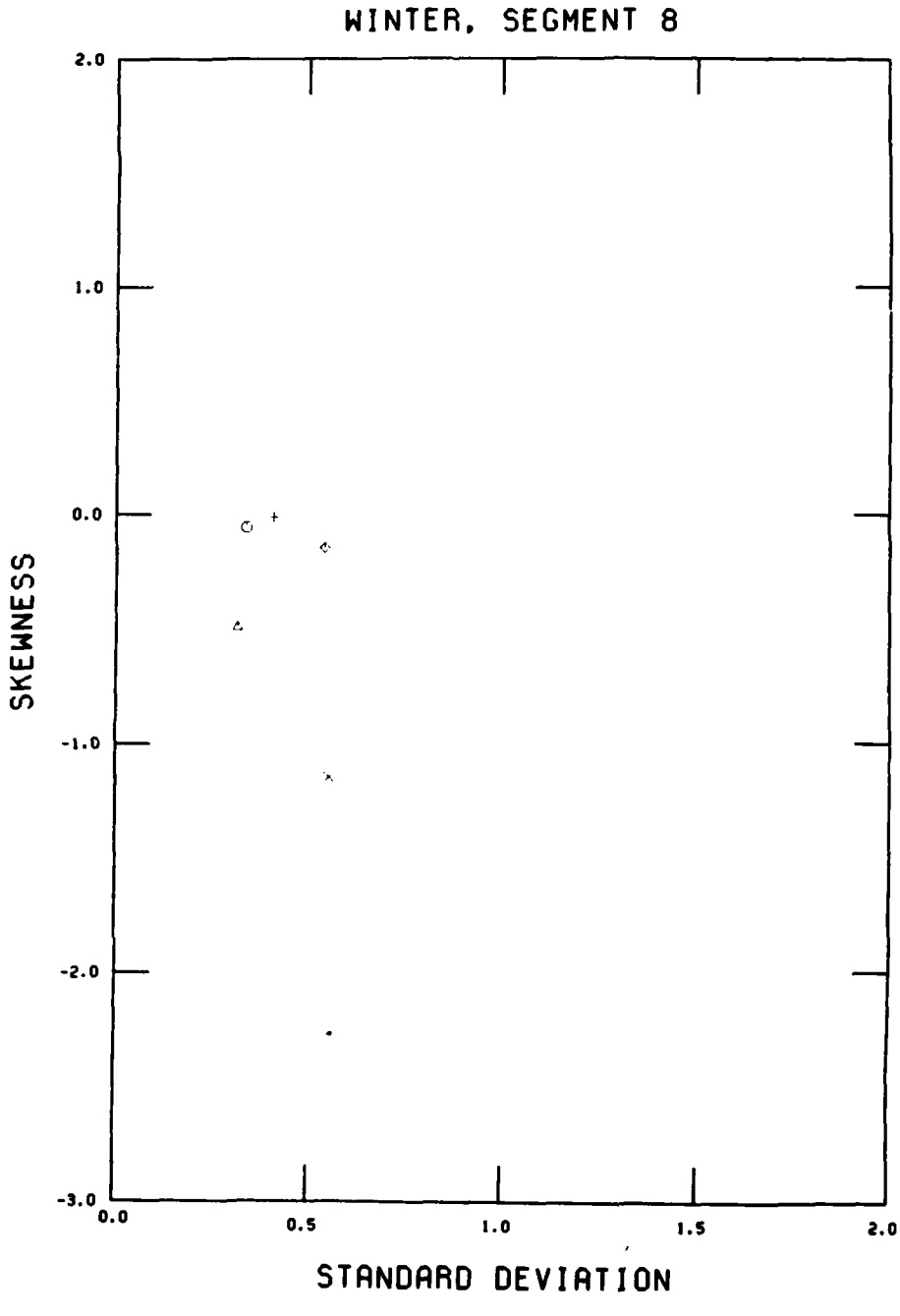
WINTER, SEGMENT 8
2.0
1.0
0.0
-1.0
-2.0
-3.0
SKEWNESS
0.0
0.5
1.0
1.5
2.0
STANDARD DEVIATION

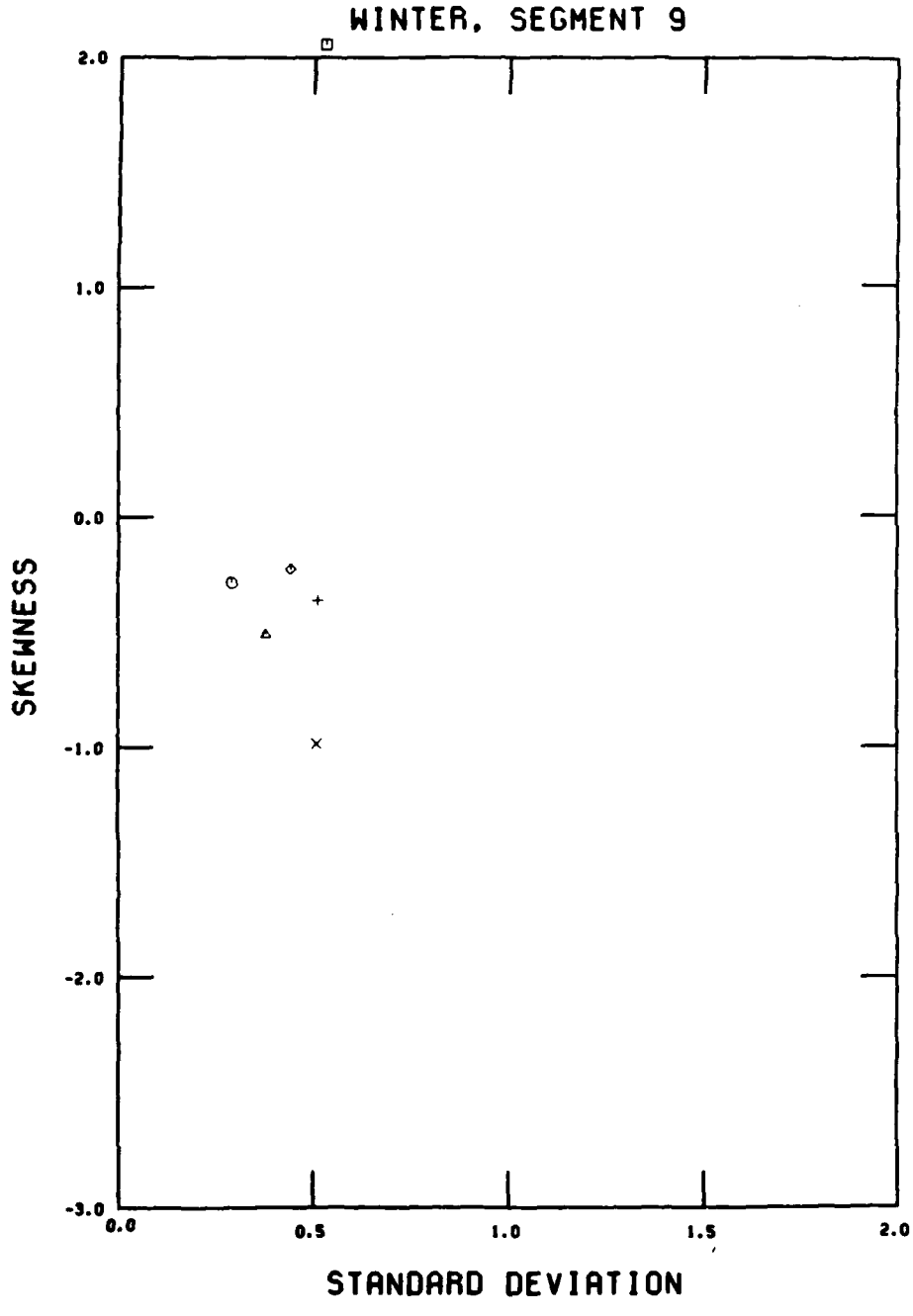
WINTER, SEGMENT 9
2.0
1.0
0.0
-1.0
-2.0
-3.0
SKEWNESS
0.0
0.5
1.0
1.5
2.0
STANDARD DEVIATION

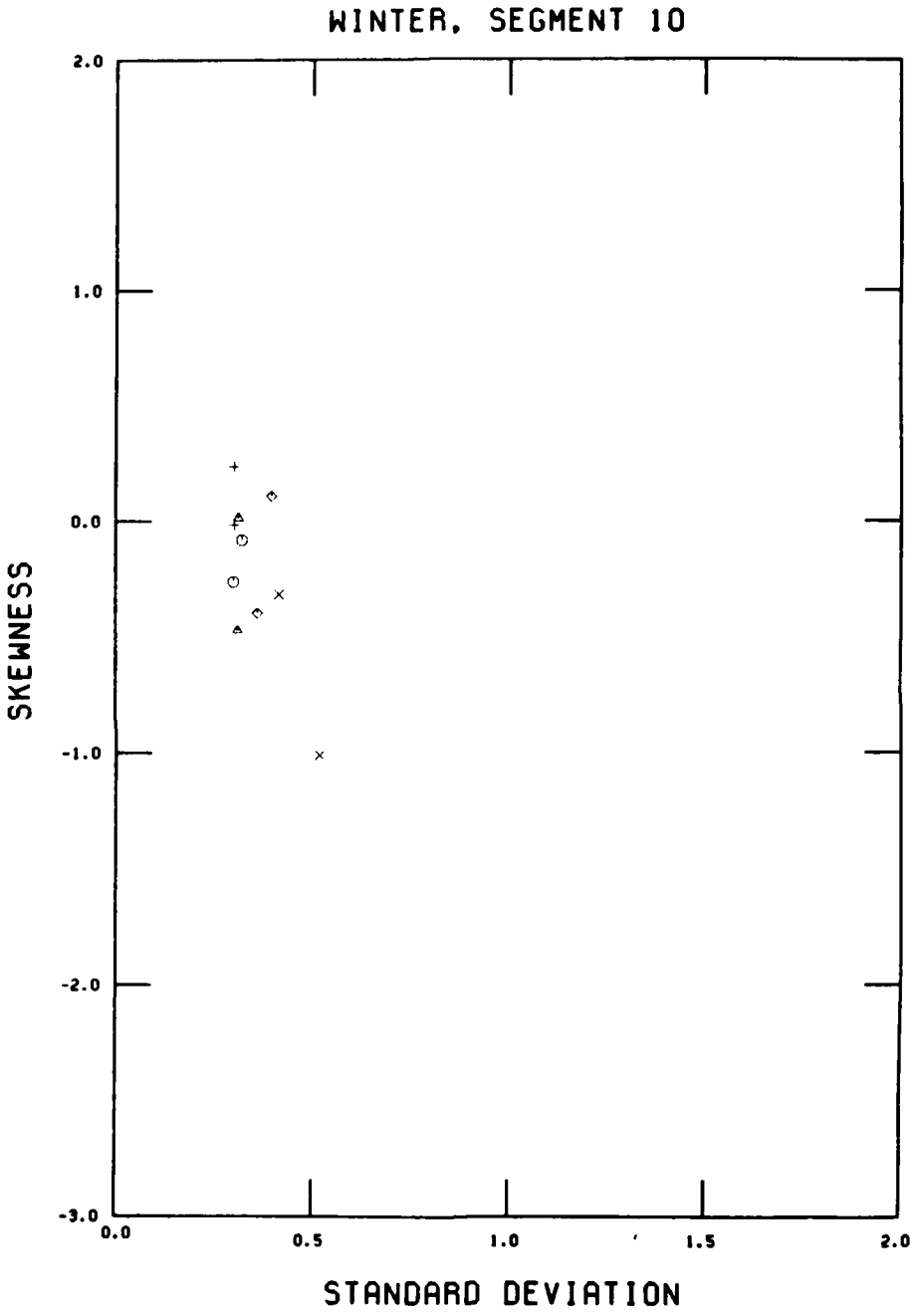
WINTER, SEGMENT 10
2.0
1.0
0.0
-1.0
-2.0
-3.0
SKEWNESS
0.0
0.5
1.0
1.5
2.0
STANDARD DEVIATION

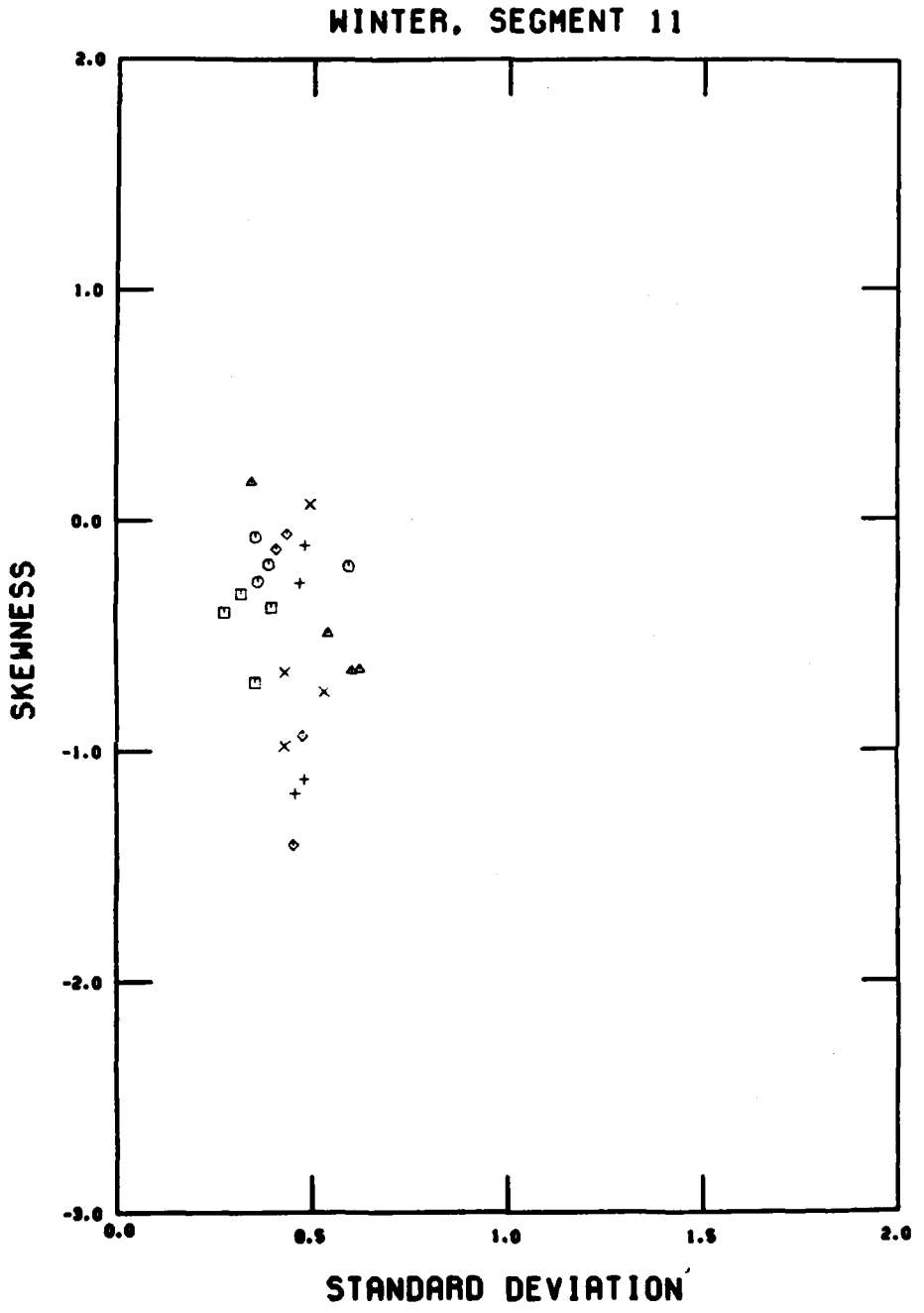
WINTER, SEGMENT 11
2.0
1.0
0.0
-1.0
-2.0
-3.0
SKEWNESS
0.0
0.5
1.0
1.5
2.0
STANDARD DEVIATION

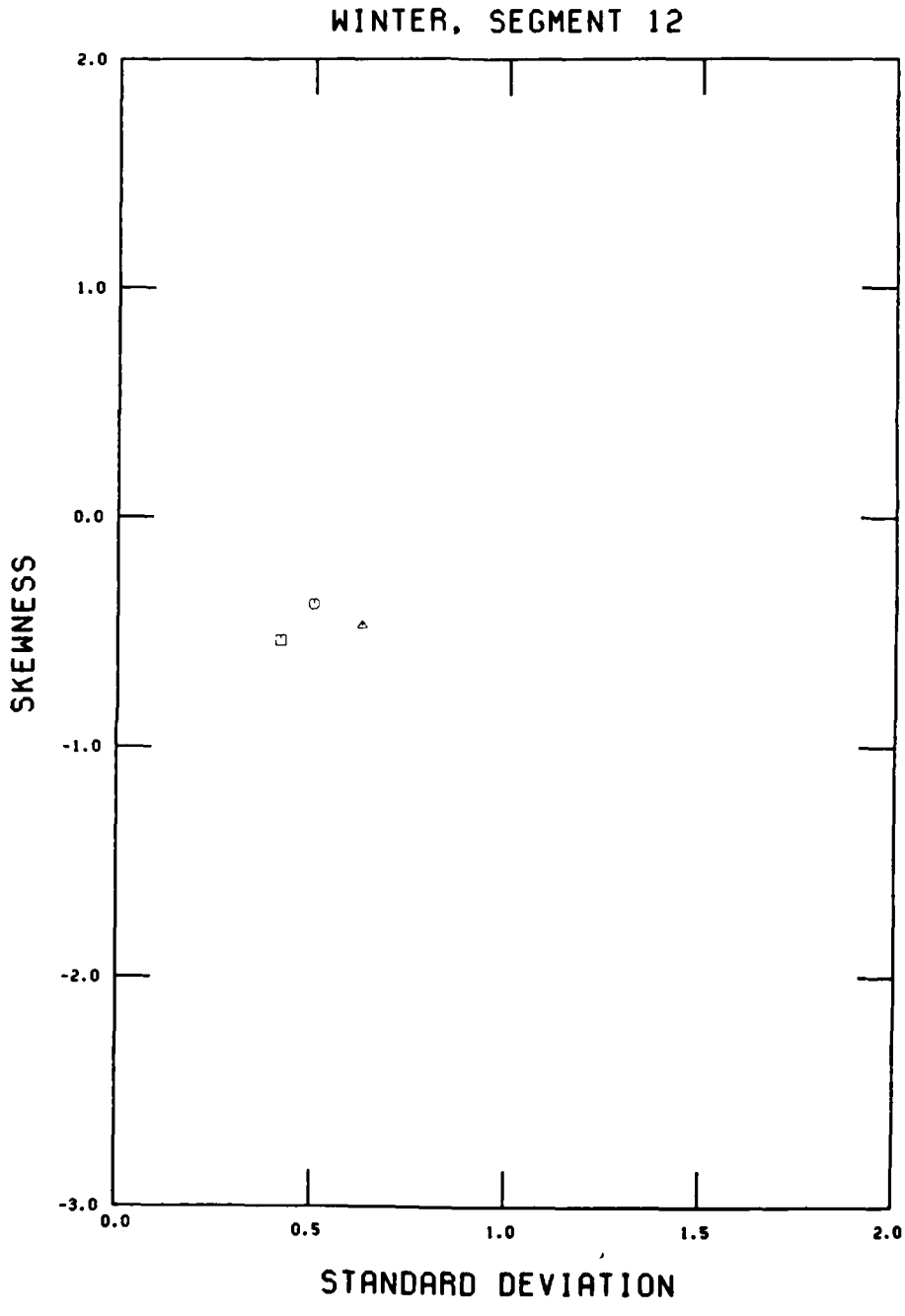
WINTER, SEGMENT 12
2.0
1.0
0.0
-1.0
-2.0
-3.0
SKEWNESS
0.0
0.5
1.0
1.5
2.0
STANDARD DEVIATION

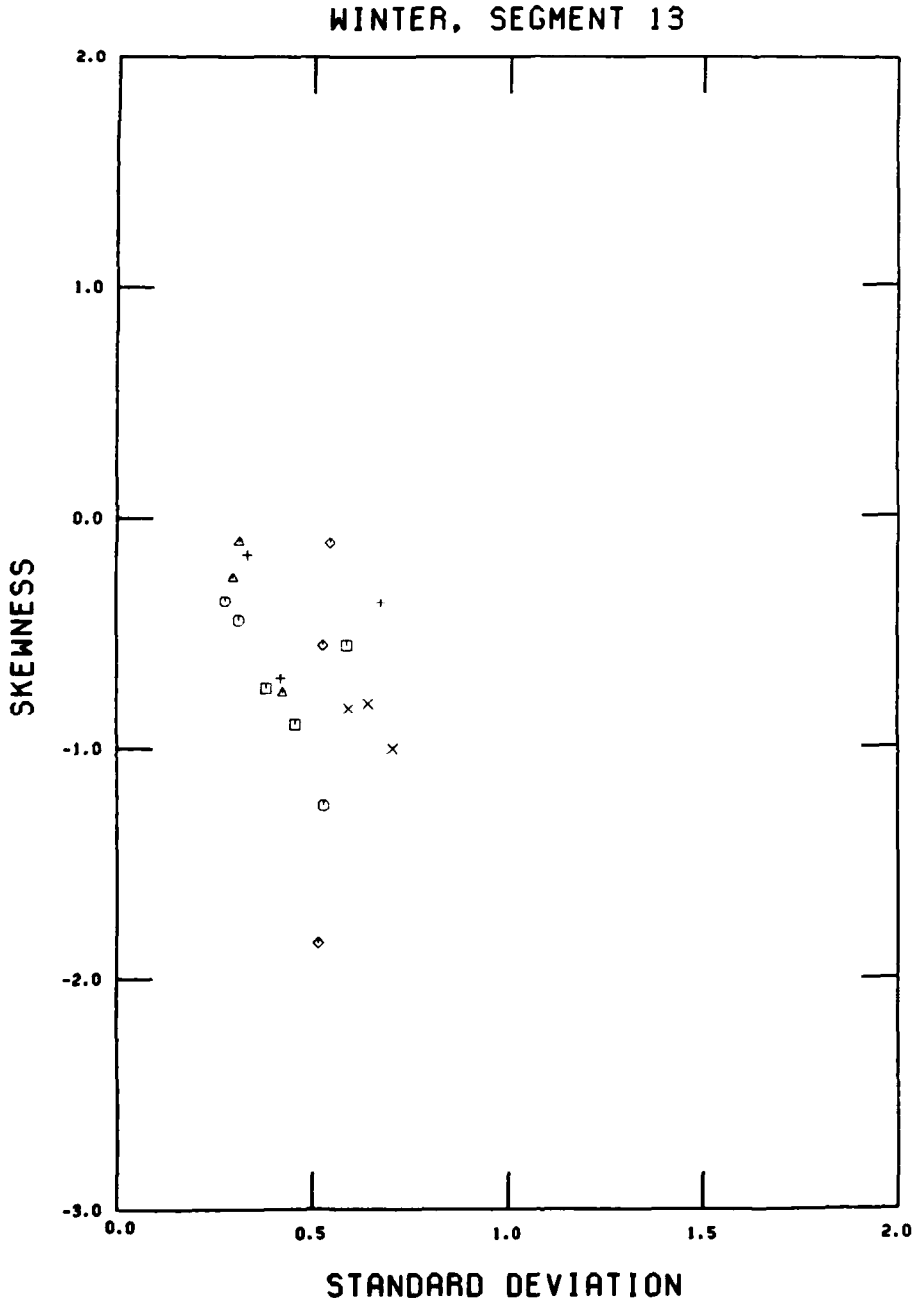
WINTER, SEGMENT 13
2.0
1.0
0.0
-1.0
-2.0
-3.0
SKEWNESS
0.0
0.5
1.0
1.5
2.0
STANDARD DEVIATION

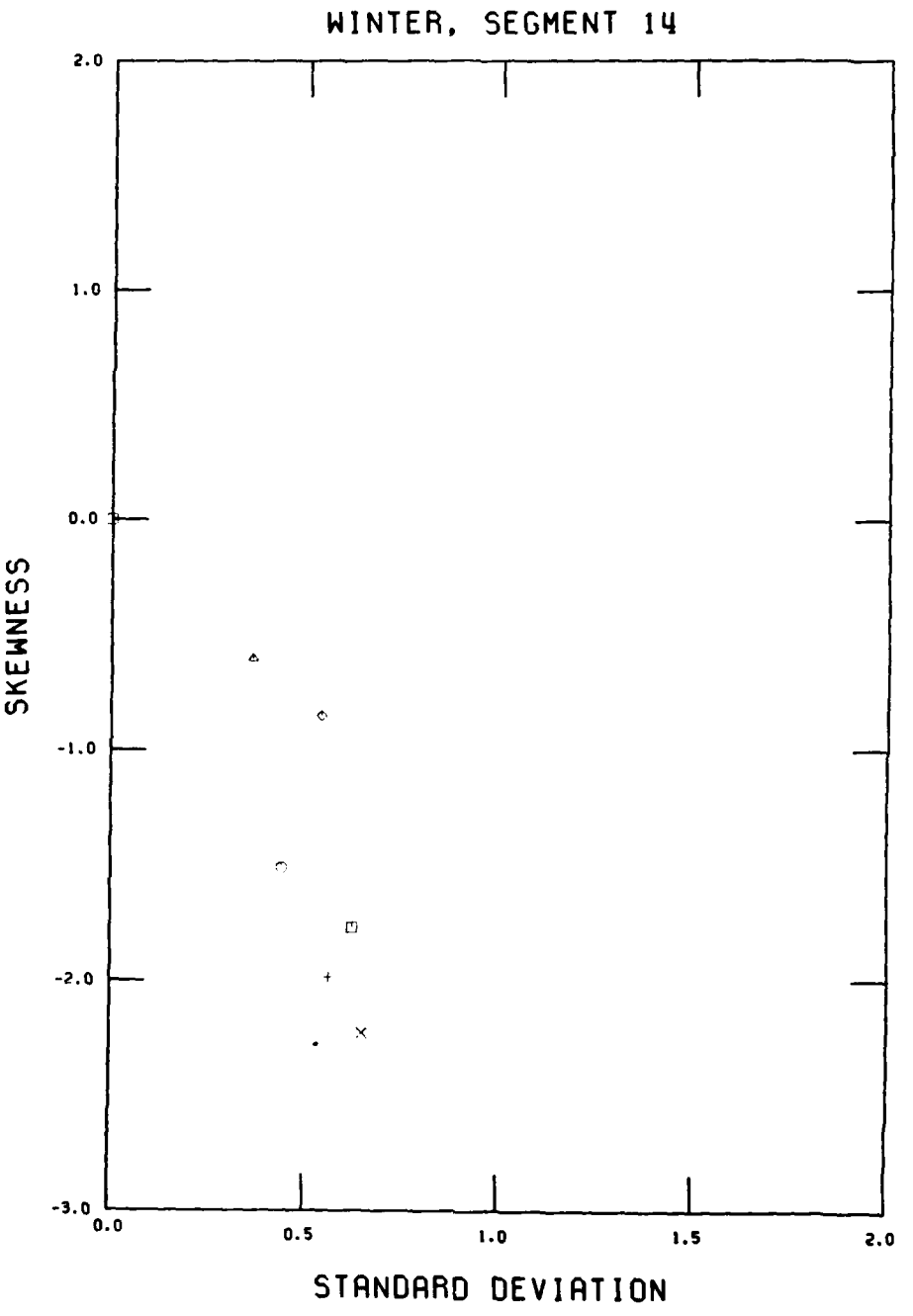
WINTER, SEGMENT 14
2.0
1.0
0.0
-1.0
-2.0
-3.0
SKEWNESS
0.0
0.5
1.0
1.5
2.0
STANDARD DEVIATION

END

DATE
FILMED

6-86